STATISTICAL MONITORING OF DISCRETE AND NONPARAMETRIC STATISTICS WITH EXACT RUN LENGTH PROPERTIES

Athens University of Economics and Business
Department of Statistics

A Thesis
by
THEDOROS D. PERDIKIS

A thesis submitted in fulfilment of the requirements for the degree of
DOCTOR OF PHILOSOPHY

Supervisor

Stelios Psarakis	Department of Statistics, Athens University of Economics & Business

Thesis committee

Philippe Castagliola	Nantes Université & LS2N UMR CNRS 6004
Petros Maravelakis	Department of Business Administration, University of Piraeus

External examination committee

Giovanni Celano	Department of Civil Engineering and Architecture, University of Catania
Alex Karagrigoriou	Department of Statistics & Actuarial-Financial Mathematics, University of the Aegean
Panagiotis Tsiamyrtzis	Department of Mechanical Engineering, Politecnico di Milano and Department of Statistics, Athens University of Economics & Business
Athanasios N. Yannacopoulos	Department of Statistics, Athens University of Economics & Business

ACKNOWLEDGMENTS

Firstly, I would like to express my most sincere gratitude and appreciation to my advisor Prof. Stelios Psarakis. He has invested a great amount of time and effort in providing guidance throughout the duration of this PhD project. Without his continuous encouragement, patience, and input this thesis would have never materialised. As far as I am concerned, he is the main reason that kept me focused on writing my thesis. Special thanks are due to my co-advisors Prof. Philippe Castagliola and Prof. Petros Maravelakis for their invaluable support during the last four years. Their feedback has helped me in ways that includes and goes beyond becoming a good researcher. Prof. Castagliola gave me the opportunity to visit him at his University and work with him. During the period that I spent there as an Erasmus PHD student I was able to write a significant part of my thesis. Moreover, Prof. Maravelakis during all these years providing me with his help for all the questions and concerns that I had. I would also like to thank all members of the external examination committee: Prof. Tsiamyrtzis, Prof. Celano, Prof. Yannacopoulos and Prof. Karagrigoriou for reviewing this work and for their suggestions to improve it. Finally, I would like to thank my father Dimitris and my mother Aggeliki for their endless love and support, and for helping me to achieve my goals.

DEDICATION

To Theodoros P. Papadakis

ABSTRACT

The current thesis is mainly focused on the design of Univariate nonparametric schemes for monitoring shifts in the process location or scale parameter. Enhanced and robust methodologies are provided which guarantee the chart's optimal and most important reliable statistical performance. In particular, first a short literature review is presented about existing parametric and nonparametric control charts. Additionally, two enhanced distribution-free control charts based on the Sign statistic are introduced, for monitoring shifts in the process location or scale parameter of interest. For each scheme, an extensive numerical analysis is conducted in order to provide to the reader a detailed presentation about each chart's statistical performance. Moreover, we introduce two distribution-free control charts based on the Wilxocon Signed Rank statistic and a simple methodology for the determination of the general distribution of the Wilxocon Signed Rank statistic is provided. Finally, for each proposed scheme, its statistical performance is examined and guidelines to practitioners are given regarding its optimal design. Finally, some concluding remarks and discussion for future work are stated.

TABLE OF CONTENTS

LIST OF FIGURES

LIST OF TABLES

Chapter 1

General introduction to Statistical Process Control

Introduction

In the world of business, quality improvement is of high importance for the manufacturing industries. Due to the fact that the competition in the globamarket is strong, industries are interested in measuring their products's characteristics as a variable using continuous measurements, such as length or content. The quality characteristics should reach a desired value (target value), relative to specifications. These target values are bounded by a range of values that are believed to be sufficiently close to the target value without affecting the process when the quality characteristic of the product is in this range. Statistical process control (SPC), is a valuable process, using statistical methods for monitoring and controlling the process performance. SPC techniques are employed to examine specific parts of a process and detect changes in process performance. One of the major tools of the statistical process control are the control charts. They are an on-line process monitoring technique whose purpose is to quickly detect shifts in the mean or in the variance of the process. It is worth mentioning that SPC techniques are being widely used not only in industrial and manufacturing fields but also in chemical and pharmaceutical applications. Additionally, they can be also used in Medicine in order to monitor a patient's treatment results. Consequently, SPC is a growing field of research where statistical methods are applied and give to the practitioners the capability, using graphical methods (charts), to check at each sampling point if the parameter of interest is in control.

It is well acknowledged in the literature (see e.g. Montgomery (2020)) that standard control charts usage involves two phases, phase I and phase II. During phase I, using a set of process

data, a retrospective analysis is conducted and trial control limits are constructed in order to determine if the process has been in control over the period of time where the data were collected and to see if reliable control limits can be established to monitor future production. As Montgomery (2020) states: control charts in phase I, primarily assist operating personnel in bringing the process into a state of statistical control. During phase II the control chart is used to monitor the process by comparing the sample statistic for each successive sample as it is drawn from the process to the control limits. In particular, during phase II, the control chart is used in order to detect shifts in the mean or in the variance by comparing the sample statistic for each successive sample as it is drawn from the process to the control limits. If the value of the statistic falls in between the control limits the process is considered to be in control. Otherwise an out of control signal is given and possible causes of this signal are investigated.

Depending on the parameter of interest, the number of characteristics to be monitored or their design phase, control charts can be divided into several categories as presented in Figure 1.1. In particular, the main categorization relies on the number of characteristics to be monitored. For instance, when practitioners want to monitor a single characteristic of a product, a *univariate* scheme is used. On the other hand, in cases where more than one characterising is needed to be monitored the use of a *multivariate* control chart is desired. Moreover, usually, conventional control charts for process monitoring are *Fixed Sampling Rate* (FSR) control charts based on taking samples of fixed size (n_0) with a fixed sampling interval (h_0) between samples. In variable sampling rate (VSR) control charts the sampling rate is varied as a function of the data from the process, based on the idea that the sampling rate should be increased when there is an indication of a potential shift in the process, and decreased when there is no indication of a problem with the process. A control chart is considered *adaptive* if at least one of the parameters i.e sample size, sampling interval, control limit, is allowed to change in real time during process monitoring. In order to design an adaptive control chart besides the sample size, sampling interval and control limits a warning limit (w) needs to be defined. The warning limit identifies a decision rule for switching from one value of the design parameter to another. In general, the type of control chart that is the optimal choice for monitoring a process, depends on the type of the characteristic to monitored. As a consequence, over the past decades, there is a plethora of schemes introduced into the literature focusing on monitoring shifts in the process mean or variability (in the univariate or multivariate case respectively). Moreover, in many industries, the quality of processes or products can be characterized by a *profile* that describes a relationship between a response variable and one or more explanatory variables. A change in the profile relationship may indicate a change in the quality characteristic of interest. Most of the work on

profile monitoring has been in the case where the profile can be sufficiently represented by a simple linear regression model. However, in many applications the simple linear regression model is not sufficient to represent the shape of a profile, so more complicated methods are needed. For all the categories mentioned above extensive literature reviews can be found in Bersimis et al. (2007), Castagliola et al. (2011), Nomikos and MacGregor (1995), Perdikis and Psarakis (2019), Woodall (2007).

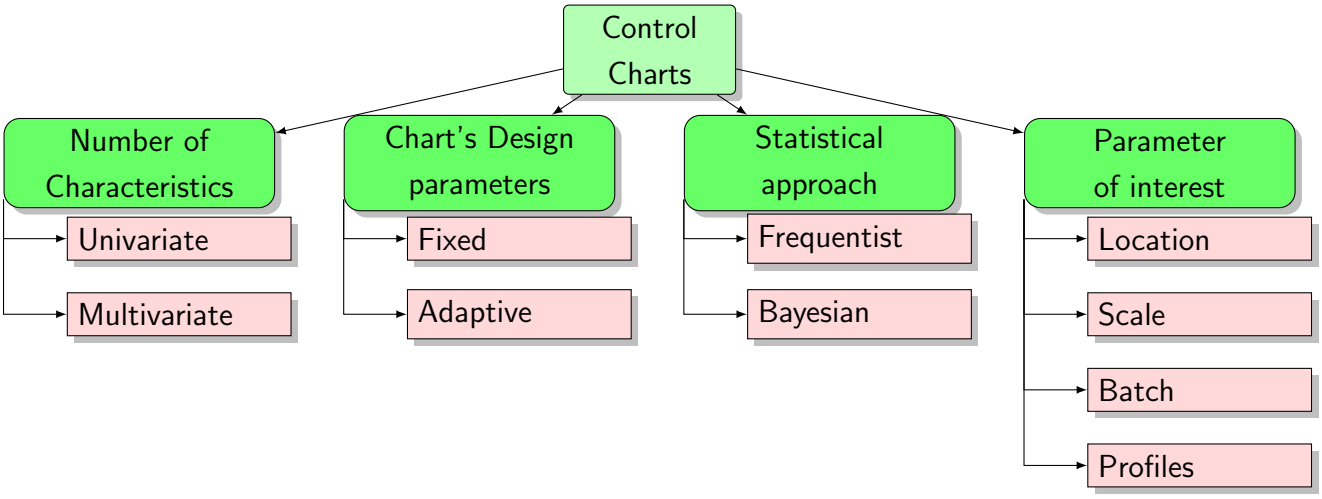

Figure 1.1: Control chart categories

1.1 Conventional control charts assuming Normality

Control charts have been widely used in manufacturing industries, as a powerful tool for the on-line monitoring of a process. Shewhart (1926) is considered as the pioneer of control charts, introducing schemes capable of monitoring relative large shifts in the process mean ($\bar{X}$ chart) or the variability (R and S charts). It has been shown that a conventional Shewhart control chart is preferable in detecting large shifts in the process mean. When shifts of small magnitude occur in the process parameters, Cumulative Sum (CUSUM, see Page (1954)) or Exponentially Weighted Moving Averge (EWMA, see Roberts (1959)) charts are preferable due to their superiority in early shift detection. redIn order to avoid any confusion, it should be clarified the fact that in this current thesis we are investigating a chart's performance in terms of persistent shifts instead of transient shifts.

Additionally, the schemes mentioned above are based on the assumption that the observations, collected at each sampling point, are random variables following a known distribution. This class of schemes are called as parametric/conventional control charts. It should be noted that, this work, is mainly focusing on the design of improved EWMA charts. As a result, before we begin to any new suggestions it is wise to review first the conventional $\bar{X}$ and EWMA charts.

1.1.1 The Shewhart $\bar{X}$ chart

Charting statistic and Control limits: In the early $1930's$, Shewhart (1926) introduced the control chart in which at each sampling point a sample of size n is collected, and the corresponding value of the $\bar{X}$ statistic is computed and plotted. With reference to the Phase II implementation of the control chart, at each sampling point a subgroup $\{X_{t,1}, X_{t,2}, \ldots, X_{t,n}\}$ of size n is collected at time $t = 1, 2, \ldots$. Each $X_{t,j}, j = 1, 2, \ldots, n$ are independently identically distributed normal random variables with parameters (μ_0, σ_0). Additionally, let $\bar{X}_t$ be the sample mean calculated at each time t. The Upper (UCL) and Lower (LCL) control limits are computed through the in-control distribution of the $\bar{X}$ statistic as:

$$\begin{aligned} \text{UCL} &= \text{E}(\bar{X}) + Z_{\alpha/2}\text{V}(\bar{X}), \\ \text{LCL} &= \text{E}(\bar{X}) - Z_{\alpha/2}\text{V}(\bar{X}), \end{aligned}$$

where α is a probability to be defined. Under the assumption of Normality, for the in-control case the above expressions can are expressed as:

$$\begin{aligned} \text{UCL} &= \mu_0 + Z_{\alpha/2}\sigma_0/\sqrt{n}, \\ \text{LCL} &= \mu_0 - Z_{\alpha/2}\sigma_0/\sqrt{n}. \end{aligned}$$

Run Length properties: The RL (Run Length) properties of the $\bar{X}$ control chart are determined by the random variable L defined as "*the number of plotted points until the t-th value falls outside the control limits*". As a consequence, the variable L follows a Geometric distribution and the Average Run Length (ARL), is computed as:

$$\text{ARL} = \frac{1}{\alpha}.$$

When the process is in-control (i.e. $\mu = \mu_0$) then α equals to:

$$\alpha = \mathrm{P}(\bar{X} \leq \mathrm{LCL} \text{ or } \bar{X} \geq \mathrm{UCL} | \mu = \mu_0),$$

and corresponds to the Type I error probability. The ARL is called as the in-control ARL (denoted as ARL_0) referring to *"the average number of plotted points until the t-th value falls outside the control limits given the process is in-control"*. Similarly, when the process is out-of-control (i.e. $\mu = \mu_1$) then

$$\mathrm{ARL} = \frac{1}{1-\beta}.$$

where

$$\beta = \mathrm{P}(\mathrm{LCL} \leq \bar{X} \leq \mathrm{UCL} | \mu = \mu_1),$$

corresponds to the Type II error probability. The ARL then is called as the out-of-control ARL (denoted as ARL_1) referring to *"the average number of plotted points until the t-th value outside the control limits given the process is out-of-control"*.

During the design phase of a control chart, practitioners need to find the proper values of the design parameters (for instance the corresponding control limits) in order to satisfy that the in-control ARL will be a relative large number (usually $\mathrm{ARL}_0 = 370.4$). In the case of the standard $\bar{X}$ chart $\alpha = 0.0027$.

1.1.2 The Exponentially weighted moving average control chart

The Exponentially weighted moving average control chart (EWMA-$\bar{X}$ chart) has been introduced into the literature by Roberts (1959). In particular, the EWMA-$\bar{X}$ control chart, was originally designed as a scheme capable of monitoring shifts in the process mean (μ). The characteristic of this control chart, is that in contrast to the conventional Shewhart $\bar{X}$ chart, it can detect a mean shift faster due to the fact that, at each sampling point, it takes into account previous measurements.

The two-sided EWMA-$\bar{X}$ chart: The charting statistic for the two-sided EWMA-$\bar{X}$ chart is defined by the following recursive formula:

$$Z_t = \lambda \bar{X}_t + (1-\lambda) Z_{t-1}, Z_0 = \mathrm{E}_0(\bar{X}_t). \tag{1.1}$$

where $(0 \leq \lambda \leq 1)$ is a parameter to be fixed called as the smoothing parameter. In particular, the value of λ defines the level of the past "information" which is being taken into account. Values close to zero assign more information to past data. Clearly, when $\lambda = 1$

the above statistic is consistent with the traditional $\bar{X}$ chart. For a better understanding of the operation of the charting statistic let us considered the following example.

- Suppose that at time $t = 1$, the sample $\{X_{1,1}, X_{1,2}, \ldots, X_{1,n}\}$ of size n is collected with corresponding sample mean $\bar{X}_1$. Then the charting statistic equals to

$$Z_1 = \lambda \bar{X}_1 + (1 - \lambda) Z_0.$$

- At time $t = 2$, the sample $\{X_{2,1}, X_{2,2}, \ldots, X_{2,n}\}$ of size n is collected with corresponding sample mean $\bar{X}_2$. Then the charting statistic equals to

$$\begin{aligned} Z_2 =& \lambda \bar{X}_2 + (1 - \lambda) Z_1 = \lambda \bar{X}_2 + (1 - \lambda)(\lambda \bar{X}_1 + (1 - \lambda) Z_0) \\ =& (1 - \lambda)^2 Z_0 + \lambda (1 - \lambda)^0 \bar{X}_2 + \lambda (1 - \lambda)^1 \bar{X}_1. \\ & \vdots \end{aligned}$$

- At time t, the sample $\{X_{t,1}, X_{t,2}, \ldots, X_{t,n}\}$ of size n is collected with corresponding sample mean $\bar{X}_t$. Then the charting statistic equals to

$$Z_t = (1 - \lambda)^t Z_0 + \lambda \sum_{j=0}^{t-1} (1 - \lambda)^j \bar{X}_{t-j}.$$

Similarly with the design of a conventional control chart, an out-of-control signal is given if at time t, the charting statistic Z_t defined in (1.1) exceeds the lower LCL or the upper UCL control limits defined as

$$\text{UCL} = \text{E}_0(Z_t) + K \sqrt{\text{V}_0(Z_t)}$$

$$\text{LCL} = \text{E}_0(Z_t) - K \sqrt{\text{V}_0(Z_t)}.$$

where K is a parameter to be determined. Moreover, $\text{E}_0(Z_t)$ and $\text{V}_0(Z_t)$ are the in-control mean and variance of Z_t. For the computation of the in-control mean of Z_t, assuming

$\mathrm{E}(Z_0) = \mu_0$ we have:

$$\begin{aligned}
\mathrm{E}_0(Z_t) =&(1-\lambda)^t \mathrm{E}_0(Z_0) + \lambda \sum_{j=0}^{t-1} (1-\lambda)^j \mathrm{E}_0(\bar{X}_{t-j}) \\
=&(1-\lambda)^t \mu_0 + \lambda \mu_0 \frac{1-(1-\lambda)^t}{\lambda} \\
=&(1-\lambda)^t \mu_0 + \mu_0 - (1-\lambda)^t \mu_0 \\
=&\mu_0. \qquad (1.2)
\end{aligned}$$

Similarly, for the in-control variance assuming $\mathrm{V}_0(\bar{X}_{t-j}) = \frac{\sigma_0^2}{n}$ we have :

$$\begin{aligned}
\mathrm{V}_0(Z_t) =&(1-\lambda)^{2t} \mathrm{V}_0(Z_0) + \lambda^2 \sum_{j=0}^{t-1} (1-\lambda)^{2j} \mathrm{V}_0(\bar{X}_{t-j}) \\
=&(1-\lambda)^{2t} \mathrm{V}_0(Z_0) + \lambda^2 \frac{\sigma_0^2}{n} \left(\frac{1-(1-\lambda)^{2t}}{\lambda(2-\lambda)} \right).
\end{aligned}$$

Finally, assuming that $Z_0 = \mu_0$ the above expression can be simplified as:

$$\mathrm{V}_0(Z_t) = \left(\frac{\lambda}{2-\lambda} \right) \frac{\sigma_0^2}{n} (1-(1-\lambda)^{2t}). \qquad (1.3)$$

Alternately, if we consider Z_0 as a random variable with mean $\mathrm{E}_0(Z_0) = \mu_0$ and variance $\mathrm{V}_0(Z_0) = \frac{\sigma_0^2}{n}$ the in-control variance of Z_0 is defined as:

$$\mathrm{V}_0(Z_t) = \frac{\sigma_0^2}{n} \left(\frac{\lambda + 2(1-\lambda)^{2t+1}}{2-\lambda} \right). \qquad (1.4)$$

It can be noticed that the variance of the series $Z_1, Z_2, \ldots, Z_t, \ldots$, when $t \to +\infty$, $\lim \mathrm{V}_0(Z_t) = \frac{\lambda}{2-\lambda} \frac{\sigma_0^2}{n}$. For instance, using the expressions presented in (1.2) and (1.3) the corresponding UCL, LCL values are computed and plotted in Figure (1.2) for $\lambda = 0.2, K = 2.7, n = 5$,v$\sigma_0 = 1$,$\mu_0 = 0$ and $t = 1, 2, \ldots, 25$. It can be clearly seen, that after the 20-th sampling point the control limits become steady. As a consequence, it usually recommended the use of the "steady-state" control limits :

$$\mathrm{UCL} = \mu_0 + K \sqrt{\frac{\lambda}{2-\lambda} \frac{\sigma_0^2}{n}}$$

$$\mathrm{LCL} = \mu_0 - K \sqrt{\frac{\lambda}{2-\lambda} \frac{\sigma_0^2}{n}}.$$

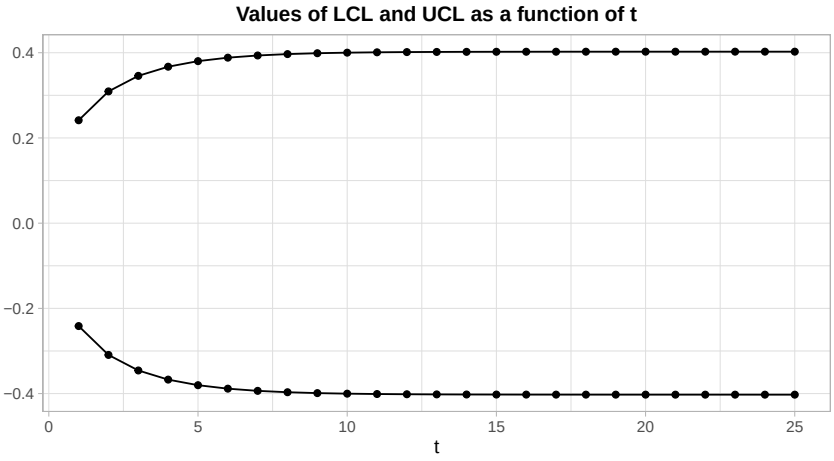

Figure 1.2: Values of UCL (upper line) and LCL (lower line) as a function of t

The upper-sided EWMA-$\bar{X}$ chart: In cases where practitioners has the desire of monitoring only increases in the process characteristic of interest (or know *a-priori* that only increases might happen in the process), upper-sided control charts are an efficient alternative and perform better for detecting increases in the process characteristic. In particular, for an upper-sided control chart only the corresponding upper control limit needs to de defined, along with the central line (CL which corresponds to the restart case). The upper-sided EWMA-$\bar{X}$ chart is defined by the following recursive formula:

$$Z_t = \max(\mathrm{E}_0(\bar{X}_t), \lambda\bar{X}_t + (1-\lambda)Z_{t-1}), Z_0 = \mathrm{E}_0(\bar{X}_t), \tag{1.5}$$

with a fixed asymptotic upper control limit and central line defined as:

$$\begin{aligned}\mathrm{UCL} =& \mu_0 + K_1\sqrt{\frac{\lambda}{2-\lambda}\frac{\sigma_0^2}{n}}.\\ \mathrm{CL} =& \mu_0,\end{aligned}$$

Similarly, with the two-sided case, K_1 is a parameter to be determined.

1.1.2.1 RL properties of the EWMA-$\bar{X}$ chart

Similarly with the design of a Shewhart control chart, the performance of the two-sided EWMA-$\bar{X}$ chart is evaluated in terms of its RL distribution. Concerning two-sided control schemes, RL is defined as the number of samples until the statistic plotted on a control chart

crosses for the first time one of the control limits.

RL ***properties of the two-sided EWMA-$\bar{X}$ chart***: In most existing parametric phase II EWMA charts their RL properties are obtained through the standard approach proposed by Brook and Evans (1972). In particular they proved that the RL distribution of a EWMA-type scheme can be considered as a Discrete Phase-type (DPH) random variable of parameters $(\mathbf{Q}, \mathbf{q})$. In particular, it is assumed that the operation of a EWMA-$\bar{X}$ control chart can be well represented by a discrete-time Markov chain where the interval $[\text{LCL}, \text{UCL}]$ is divided into $2m+1$ subintervals $(H_j - \Delta, H_j + \Delta)$, $j = \{-m, \ldots, 0, \ldots m\}$ of width $2\Delta = \frac{\text{UCL}-\text{LCL}}{2m+1}$. Moreover, let $H_j = \frac{\text{LCL}+\text{UCL}}{2} + 2j\Delta$ be the midpoint of state $j = \{-m, \ldots, 0, \ldots, m\}$. The transition probability matrix $\mathbf{P}$ of the EWMA-$\bar{X}$ chart is defined as:

$$\mathbf{P} = \begin{pmatrix} \mathbf{Q} & \mathbf{r} \\ \mathbf{0}^\intercal & 1 \end{pmatrix} = \begin{pmatrix} Q_{-m,-m} & \ldots & Q_{-m,-1} & Q_{-m,0} & Q_{-m,1} & \ldots & Q_{-m,m} & r_{-m} \\ \vdots & \vdots & \vdots & \vdots & \vdots & \vdots & \vdots & \\ Q_{-1,-m} & \ldots & Q_{-1,-1} & Q_{-1,0} & Q_{-1,1} & \ldots & Q_{-1,m} & r_{-1} \\ Q_{0,-m} & \ldots & Q_{0,-1} & Q_{0,0} & Q_{0,1} & \ldots & Q_{0,m} & r_0 \\ Q_{1,-m} & \ldots & Q_{1,-1} & Q_{1,0} & Q_{1,1} & \ldots & Q_{1,m} & r_1 \\ \vdots & \vdots & \vdots & \vdots & \vdots & \vdots & \vdots & \\ Q_{m,-m} & \ldots & Q_{m,-1} & Q_{m,0} & Q_{m,1} & \ldots & Q_{m1,m} & r_m \\ 0 & \ldots & 0 & 0 & 0 & \ldots & 0 & 1 \end{pmatrix}$$

where $\mathbf{Q}$ is the $(2m+1, 2m+1)$ matrix of transient probabilities, $\mathbf{0}^\intercal = (0, 0, \ldots, 0)$ and $\mathbf{r} = \mathbf{1} - \mathbf{Q1}$. Moreover, let $\mathbf{q} = (q_{-m}, \ldots, q_0, \ldots, q_m)^\intercal$ be the $(2m+1, 1)$ vector of initial probabilities associated with the $2m+1$ transient states which contains the probabilities that the Markov chain starts in a given state. For the two-sided EWMA-$\bar{X}$ chart without the head-start feature being considered (i.e $Z_0 = \text{E}_0(\bar{X}_t)$), it is assumed that $q_0 = 1$ and $q_i = 0$ for $i \neq 0$. Finally, the transient probabilities, $Q_{j,k}$ are obtained as:

$$\begin{aligned} Q_{j,k} &= \text{P}(Z_t \text{ is in state } k | Z_{t-1} \text{ is in state } j) \\ &= \text{P}(H_k - \Delta \leq Z_t \leq H_k + \Delta | Z_{t-1} = H_j). \end{aligned} \tag{1.6}$$

By substituting the definition of the charting statistic, defined in (1.1), into (1.6) the

transient probabilities, $Q_{j,k}$ are equal:

$$\begin{aligned}
Q_{j,k} &= \mathrm{P}\left(H_k - \Delta \leq \lambda \bar{X}_t + (1-\lambda) Z_{t-1} \leq H_k + \Delta \middle| \, Z_{t-1} = H_j\right) \\
&= \mathrm{P}\left(H_k - \Delta \leq \lambda \bar{X}_t + (1-\lambda) H_j \leq H_k + \Delta\right) \\
&= \mathrm{P}\left(\frac{H_k - \Delta - (1-\lambda) H_j}{\lambda} \leq \bar{X}_t \leq \frac{H_k + \Delta - (1-\lambda) H_j}{\lambda}\right) \\
&= F_{\bar{X}_t}\left(\frac{H_k + \Delta - (1-\lambda) H_j}{\lambda} | n, \mu_{\bar{X}_t}, \sigma_{\bar{X}_t}, \delta\right) - F_{\bar{X}_t}\left(\frac{H_k - \Delta - (1-\lambda) H_j}{\lambda} | n, \mu_{\bar{X}_t}, \sigma_{\bar{X}_t}, \delta\right).
\end{aligned}$$

where $\mu_{\bar{X}_t} = \mu_0, \sigma_{\bar{X}_t} = \frac{\sigma_0}{\sqrt{n}}$ and $F_{\bar{X}_t}$ is the c.d.f. of the $\bar{X}_t$ defined as:

$$F_{\bar{X}_t}(x | n, \mu_{\bar{X}_t}, \sigma_{\bar{X}_t}, \delta) = F_{\mathrm{N}}\left(\frac{x - \mu_{\bar{X}_t}}{\sigma_{\bar{X}_t}} - \delta\right)$$

with $F_{\mathrm{N}}(\ldots)$ be the c.d.f of the standard Normal distribution with mean zero and variance equal to 1. The parameter δ accounts for the shift magnitude in the process mean. In particular is defined through the expression $\mu_1 = \mu_0 + \delta\sigma_0$, where μ_1 is the process mean when a shift occurs. It is clear that when $\delta = 0$ we are refereeing to the in-control case (i.e the ARL_0) and when $\delta \neq 0$ we are refereeing to the out-of-control case (i.e the ARL_1).

The p.m.f. $f_{\mathrm{RL}}(t|\mathbf{Q}, \mathbf{q})$ and the c.d.f.$F_{\mathrm{RL}}(t|\mathbf{Q}, \mathbf{q})$ of RL are defined for $t = \{1, 2, \ldots, \}$ and they are respectively, equal to (see, for instance Neuts (1981) or Latouche and Ramaswami (1999)):

$$\begin{aligned}
f_{\mathrm{RL}}(t|\mathbf{Q}, \mathbf{q}) &= \mathbf{q}^{\intercal} \mathbf{Q}^{t-1} \mathbf{r}, \\
F_{\mathrm{RL}}(t|\mathbf{Q}, \mathbf{q}) &= 1 - \mathbf{q}^{\intercal} \mathbf{Q}^{t-1} \mathbf{1}.
\end{aligned}$$

The determination of the mean and standard deviation of RL can be derived through some simple computations based on the factorial moment formula, $\nu_i = \mathrm{E}\left(\mathrm{RL}(\mathrm{RL}-1)\ldots,(\mathrm{RL}-i+1)\right)$ of order $i \geq 1$ defined as:

$$\nu_i = i! \mathbf{q}^{\intercal} (\mathbf{I} - \mathbf{Q})^{-i} \mathbf{Q}^{i-1} \mathbf{1}.$$

For $i = 1, 2$ the first two factorial moments ν_1 and ν_2 of order 1 and 2 respectively are:

$$\begin{aligned}
\nu_1 &= \mathbf{q}^{\intercal} (\mathbf{I} - \mathbf{Q})^{-1} \mathbf{1} \\
\nu_2 &= 2\mathbf{q}^{\intercal} (\mathbf{I} - \mathbf{Q})^{-2} \mathbf{Q} \mathbf{1}.
\end{aligned}$$

Finally, since $\mathrm{V}(\mathrm{RL}) = \mathrm{E}(\mathrm{RL}^2) - (\mathrm{E}(\mathrm{RL}))^2$ and $\nu_2 = \mathrm{E}(\mathrm{RL}(\mathrm{RL}-1)) = \mathrm{E}(\mathrm{RL}^2) - \mathrm{E}(\mathrm{RL})$ the mean and standard deviation of RL equal:

$$\begin{aligned} \mathrm{E}(\mathrm{RL}) &= \nu_1 \\ \mathrm{SDRL}(\mathrm{RL}) &= \sqrt{\nu_2 - \nu_1^2 + \nu_1}. \end{aligned}$$

When the number $2m+1$ of subintervals is sufficiently large (say $2m+1 \approx 200$), the approach of Brook and Evans (1972) provides an effective method that allows the Average Run Length (ARL) and the Standard Deviation Run Length (SDRL) of *continuous* statistics to be accurately evaluated by using the following classical formulas from the theory of Markov chains

$$\mathrm{ARL} = \mathbf{q}^{\intercal}(\mathbf{I} - \mathbf{Q})^{-1}\mathbf{1}, \tag{1.7}$$

$$\mathrm{SDRL} = \sqrt{2\mathbf{q}^{\intercal}(\mathbf{I} - \mathbf{Q})^{-2}\mathbf{Q}\mathbf{1} + \mathrm{ARL}(1 - \mathrm{ARL})}. \tag{1.8}$$

RL ***properties of the upper-sided EWMA-$\bar{X}$ chart*** : In order to obtain the zero-state ARL and SDRL of the one-sided EWMA-$\bar{X}$ control chart, similarly with the two-sided case, the standard approach proposed by Brook and Evans (1972) is used with some small modifications. Specifically, the interval $[\mathrm{CL}, \mathrm{UCL}]$ is divided into $m+1$ subintervals of width $\Delta = \frac{\mathrm{UCL}}{2m}$. Moreover, let $H_j = (2j-1)\Delta$ be the midpoint of state $j = \{1, \ldots, m\}$. The transient state $i = 0$ corresponds to the "restart state" feature of the chart (due to the presence of the $\max(\ldots)$ in the charting statistic defined in (1.5)). This state is represented by the value $H_0 = 0$. Finally, the transition probability matrix $\mathbf{P}$ is defined as:

$$\mathbf{P} = \begin{pmatrix} \mathbf{Q} & \mathbf{r} \\ \mathbf{0}^{\intercal} & 1 \end{pmatrix} = \begin{pmatrix} Q_{0,0} & Q_{0,1} & \ldots & Q_{0,m-1} & Q_{0,m} & r_0 \\ Q_{1,0} & Q_{1,1} & \ldots & Q_{1,m-1} & Q_{1,m} & r_1 \\ \vdots & \vdots & \ddots & \vdots & \vdots & \vdots \\ Q_{m,0} & Q_{m,1} & \ldots & Q_{m,m-1} & Q_{m,m} & r_m \\ 0 & 0 & \ldots & 0 & 0 & 1 \end{pmatrix}$$

where $\mathbf{Q}$ is the $(m+1, m+1)$ matrix of transient probabilities, $\mathbf{0}^{\intercal} = (0, 0, \ldots, 0)$ and $\mathbf{r} = \mathbf{1} - \mathbf{Q}\mathbf{1}$. In addition, the transient probabilities, $Q_{k,j}$ will be computed as:

- if $j = 0$,

$$Q_{k,0} = F_{\bar{X}_t}\left(-\frac{(1-\lambda)H_k}{\lambda} | n, \mu_{\bar{X}_t}, \sigma_{\bar{X}_t}, \delta\right).$$

- if $j = 1, 2, \ldots, m$,

$$Q_{k,j} = F_{\bar{X}_t}\left(\frac{H_i + \Delta - (1-\lambda)H_k}{\lambda}|n, \mu_{\bar{X}_t}, \sigma_{\bar{X}_t}, \delta\right) - F_{\bar{X}_t}\left(\frac{H_i - \Delta - (1-\lambda)H_k}{\lambda}|\mu_{\bar{X}_t}, \sigma_{\bar{X}_t}, \delta\right). \tag{1.9}$$

Finally, let $\mathbf{q} = (q_0, q_1, \ldots, q_m)^\intercal$ be the $(m+1, 1)$ vector of initial probabilities associated with the $m+1$ transient states. In our case, we assume $\mathbf{q} = (1, 0, \ldots, 0)^\intercal$, i.e. the initial state corresponds to the "restart state".

1.1.2.2 Reliability of the Brook and Evans method in the chart's RL properties

Generally, in conventional parametric EWMA control charts for monitoring measurement data from a continuous distribution as the number of subintervals (i.e. $2m + 1$) increases the method proposed by Brook and Evans (1972) is known to be a reliable approximation of the chart's RL properties. In Table 1.1, several in-and out-of-control pairs of (ARL, SDRL) are reported as a function of the number of subintervals $2m + 1 = \{51, 61, \ldots, 201\}$ for the two-sided EWMA-$\bar{X}$ chart. It can be clearly seen that the number of subintervals does not affect the ARL, or the SDRL of the two-sided EWMA-$\bar{X}$ chart. Similarly, for the upper-sided case, from Table 1.2 we may conclude that its RL properties also remain unaffected by the number of subintervals.

Table 1.1: In- and out-of-control pairs of (ARL, SDRL) values for the two-sided EWMA-$\bar{X}$ chart as a function of $2m+1 = \{51, 61, \ldots 201\}$.

$(n = 1, \lambda = 0.2, K = 2.7)$			
$2m+1$	$\delta = 0$	$\delta = 0.5$	$\delta = 1$
51	(236.6,232.6)	(29.3,24.5)	(8.8,5.2)
61	(236.9,233.5)	(29.3,24.5)	(8.8,5.2)
71	(237.1,233.2)	(29.3,24.5)	(8.8,5.2)
81	(237.3,233.3)	(29.3,24.5)	(8.8,5.2)
91	(237.3,233.4)	(29.3,24.5)	(8.8,5.2)
101	(237.4,233.5)	(29.3,24.5)	(8.8,5.2)
111	(237.5,233.5)	(29.3,24.5)	(8.8,5.2)
121	(237.5,233.6)	(29.3,24.5)	(8.8,5.2)
131	(237.5,233.6)	(29.3,24.5)	(8.8,5.2)
141	(237.6,233.6)	(29.3,24.5)	(8.8,5.2)
151	(237.6,233.6)	(29.3,24.5)	(8.8,5.2)
161	(237.6,233.6)	(29.3,24.5)	(8.8,5.2)
171	(237.6,233.7)	(29.3,24.5)	(8.8,5.2)
181	(237.6,233.7)	(29.3,24.5)	(8.8,5.2)
191	(237.6,233.7)	(29.3,24.5)	(8.8,5.2)
201	(237.6,233.7)	(29.3,24.5)	(8.8,5.2)

Table 1.2: In- and out-of-control pairs of (ARL, SDRL) values for the upper-sided EWMA-$\bar{X}$ chart as a function of $2m + 1 = \{51, 61, \ldots 201\}$.

$(n = 1, \lambda = 0.2, K = 2.7)$			
m	$\delta = 0$	$\delta = 0.5$	$\delta = 1$
50	(311.4,306.7)	(27.7,23.1)	(8.7,5.1)
60	(311.5,306.8)	(27.7,23.1)	(8.7,5.1)
70	(311.6,306.9)	(27.7,23.1)	(8.7,5.1)
80	(311.6,307.1)	(27.7,23.1)	(8.7,5.1)
90	(311.6,307.1)	(27.7,23.1)	(8.7,5.1)
100	(311.7,307.1)	(27.7,23.1)	(8.7,5.1)
110	(311.7,307.1)	(27.7,23.1)	(8.7,5.1)
120	(311.7,307.1)	(27.7,23.1)	(8.7,5.1)
130	(311.7,307.1)	(27.7,23.1)	(8.7,5.1)
140	(311.7,307.1)	(27.7,23.1)	(8.7,5.1)
150	(311.7,307.1)	(27.7,23.1)	(8.7,5.1)
160	(311.7,307.1)	(27.7,23.1)	(8.7,5.1)
170	(311.7,307.1)	(27.7,23.1)	(8.7,5.1)
180	(311.7,307.1)	(27.7,23.1)	(8.7,5.1)
190	(311.7,307.1)	(27.7,23.1)	(8.7,5.1)
200	(311.7,307.1)	(27.7,23.1)	(8.7,5.1)

1.1.3 The Cumulative Sum Control Chart

Another efficient memory-type scheme capable of monitoring small shifts in the process mean is the Cumulative Sum (CUSUM-$\bar{X}$) control chart introduced by Page (1954). At each sampling point, t, a normally distributed sample is collected and its corresponding sample mean $\bar{X}_t$ is computed. The charting statistics of the CUSUM-$\bar{X}$ chart are then computed as:

$$Y_t^+ = \max\{0, \bar{X}_t - (\mu_0 + k) + Y_{t-1}^+\}$$
$$Y_t^- = \max\{0, (\mu_0 - k) - \bar{X}_t + Y_{t-1}^-\}$$

where k is a parameter to be fixed called as the reference value. Finally an out-of-control signal is given if:

$$\max(Y_t^+, Y_t^-) > H$$

where H is the control limit coefficient which satisfies the in-control ARL equals to a pre-defined value, ARL_0. In general, for the determination of the optimal value of H and the chart's out-of-control performance, the method of Brook and Evans (1972) is used based on a similar design as for the EWMA-$\bar{X}$ chart regarding the computation of the midpoints at each subinterval.

1.2 Parametric versus non-parametric approach

In general, in the design of conventional control charts as the ones mentioned above, it is assumed that the distribution of the observations collected over time is known, with the most common choice being that of normal distribution. However, in practice, either the assumption of, say, normal distribution is violated or practitioners do not want to use a specific distribution model for their process. As a result, designing schemes capable of monitoring shifts in the process without any knowledge of the observations' underlying distribution, have drawn the researchers' attention and led to nonparametric (or distribution-free) control charts. Over the past decades there is a growing amount of publications related with the design of distribution-free control charts for monitoring shifts in the process. In particular, the work of Chakraborti et al. (2001) is considered as the first general framework regarding the design and operation of distribution-free control charts. Additionally, recent extensions of nonparametric Shewhart, EWMA and CUSUM control charts can be found in Chakraborti and Graham (2019), Triantafyllou and Ram (2021b), Triantafyllou and Ram (2021a). In Figure 1.3, several publications related with univariate distribution-free control charts are illustrated (blue dots) across the past three decades (red dashed lines). For instance, during the 90's, Amin and Searcy (1991) and Amin et al. (1995) introduced the use of nonparametric tests (such as the Sign and the Wilcoxon Signed Rank statistics) in the design of distributions-free EWMA and CUSUM charts for monitoring the process location parameters (for instance the median or any other quantile of interest). Similarly Hackl and Ledolter (1991) and Hackl and Ledolter (1992) presented two nonparametric EWMA control charts based on sequential ranks. Additionally, over the last decade, from Figure 1.3 it can be seen that, there is an increased number of publications introducing new nonparametric schemes for monitoring shifts in the process mean and dispersion. It is worth stretching that, using distribution-free control charts, for monitoring the process median for example, there is no need for any a-priori information of the in-control value of the process dispersion. On the other hand, in conventional parametric schemes such as the $\bar{X}$ chart, besides the

in-control value of the sample's mean, μ_0, the corresponding value of the in-control variance, σ_0, is needed. Fairly speaking, the use of nonparametric control charts may also have some drawbacks. For instance, their proper operation and ability for detecting a shift in the process parameter, require a sufficiently large number of data. Moreover, comparing with the parametric schemes, they are not useful in settings with short runs.

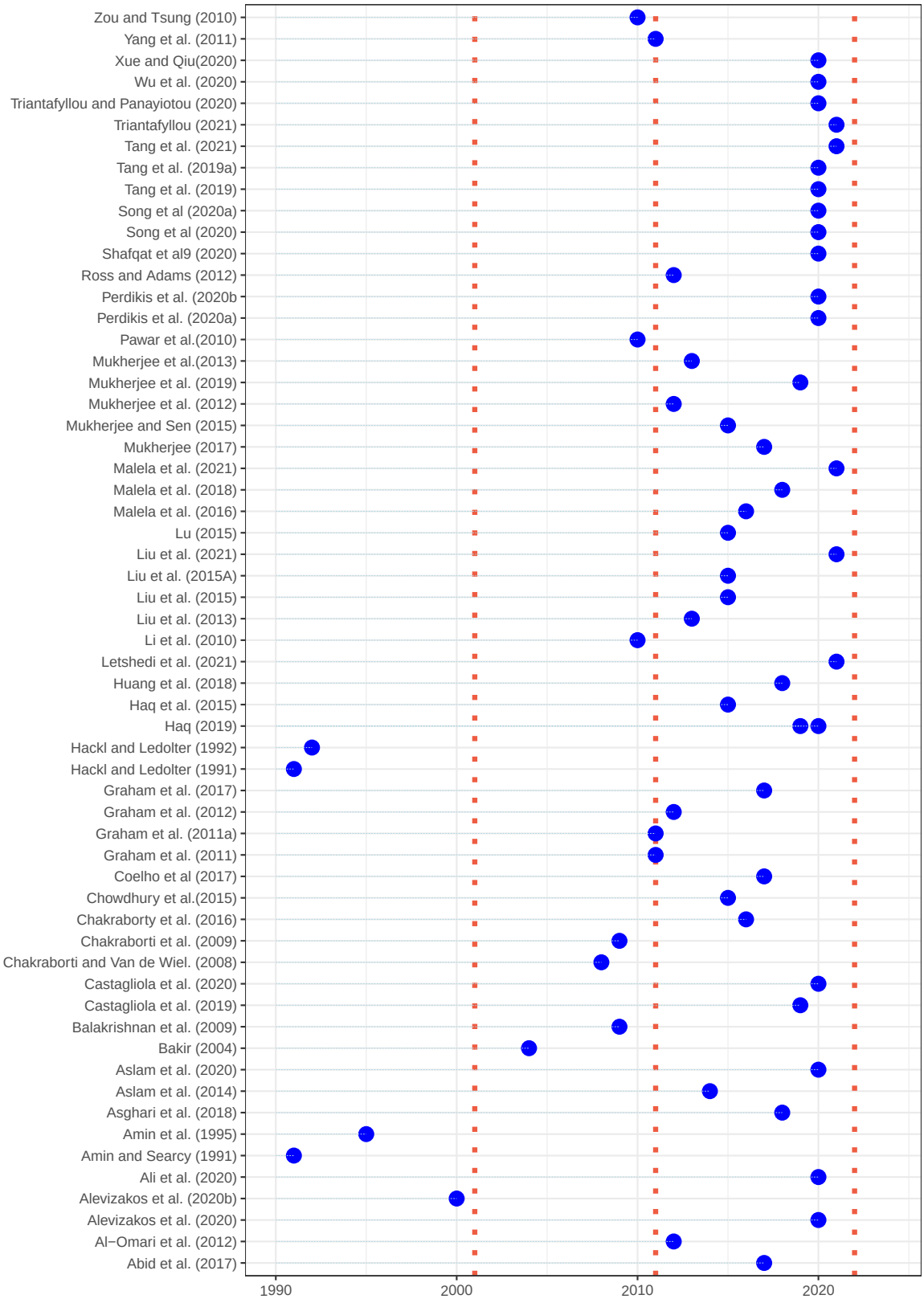

source: Chakraborti & Graham(2019),Triantafyllou & Ram(2020),

Figure 1.3: Univariate non-parametric control charts

1.3 State of the art

It is worth stretching that, regarding the design phase of an EWMA-type control chart a proper computation of its RL (Run length) properties is crucial. Specifically, for the determination of the design parameters λ (smoothing parameter) and K (control limit parameter) of an EWMA-type chart, a search algorithm needs to be run, for a particular shift in the process, in order to find the optimal pair (λ^*, K^*) which minimizes the out-of-control ARL, under the constraint $\text{ARL} = \text{ARL}_0$ where ARL_0 is a predefined value of the in-control ARL. In conventional EWMA-type schemes the RL properties are often obtained by using the Markov Chain approach of Brook and Evans presented in Brook and Evans (1972), which is based on a discretization of the control limits interval into a pre-specified number of subintervals. In the case of measurement data (usually assuming normality) as the number of subintervals increase, the method of Brook and Evans tends to give reliable approximations of the chart's RL properties. Generally, the nonparametric statistics (such as sign, Wilcoxon signed rank, etc.) used by the distribution-free schemes mentioned above, are defined on a discrete domain. When the standard continuous EWMA chart is applied to discrete data, a common technique in order to compute its RL properties is to use simulation-based techniques. The main disadvantage of this approach is that it leads to approximated results which depend on the number of runs.

In this work, we aim to present new enhanced formulas regarding the design of nonparametric EWMA charts based on the Sign and Wilcoxon signed rank statistics with *exact* and *robust* RL properties. In particular a combination of the approach of Brook and Evans (1972) and a Kernel-based method will be utilised to make the results unaffected by the number of subintervals. The rest of the current thesis is organised as follows: In Chapter 2, a short review regarding the original design of nonparametric Shewhart and EWMA charts is presented based on the Sign and the Wilcoxon Signed Rank statistics. More specifically, their statistical design is presented and the robustness of their in- and out-of-control performance is investigated using the convetional method of Brook and Evans (1972). In Chapter 3, a modified version of the "classical" Sign EWMA chart is presented in which an enhanced approach is used for the exact determination of the chart's RL properties, while in Chapter 4, an examination of the proposed chart's performance is preformed under the presence of tied observations during the process monitoring. In particular, a simple solution is provided in which the distribution-free properties of the chart remain unaffected by the occurrence of ties. Additionally, in Chapter 5, a new nonparametric EWMA chart for monitoring the process dispersion is proposed which is based on a Sign-type statistic and its exact in- and out-of control properties are determined. Moreover, Chapters 6 and 7 are focusing on the design of EWMA control charts based on the Wilcoxon Signed Ranks statistic. More specifically, in

Chapter 6, an EWMA-type chart based on the Wilcoxon Signed Rank statistic is introduced in which the exact number of subintervals is determined leading into the exact determination of the chart's RL properties. In Chapter 7, The same approach used in Chapter 3 is applied to the corresponding EWMA chart based on the Wilcoxon Signed Rank statistic. Finally, in Chapter 8, some concluding remarks of this thesis are presented and suggestions for future works are discussed.

Chapter 2

Shewhart and EWMA control charts based on the Sign and Wilcoxon Signed Rank statistics

Introduction

Generally, the Sign or the Wilcoxon Signed Rank statistics have been extensively applied in the design of nonparametric schemes for monitoring shifts in the process location (as the process median or any quantile of interest). Due to their simplicity in design, schemes based on these statistics, are efficient tools that can successively detect shifts during the process monitoring. In this Chapter, a short revision regarding the theoretical properties of these statistics will be presented and their application in nonparametric Shewhart and EWMA charts will be revisited. Finally, a discussion will be made regarding the robustness of these charts and their optimal design.

2.1 Theoretical background of the Sign and Wilcoxon Signed Rank statistics

2.1.1 Distribution of the Sign statistic

The Sign test, is a simple nonparametric technique, for testing hypotheses about a location parameter, θ_0. Suppose that, at time $t = 1, 2, \ldots$, a subgroup $\{X_{t,1}, X_{t,2}, \ldots, X_{t,n}\}$ of size n following an unknown continuous distribution with c.d.f. $F_X(x|\theta)$ is collected where

θ is the location parameter of interest. The test statistic is computed as:

$$\mathrm{SN}_t = \sum_{j=1}^{n} S_{t,j}, \tag{2.1}$$

where $S_{t,j} = \mathrm{sign}(X_{t,j} - \theta_0)$ with sign(x) $= -1$, 0 or $+1$ if $x < 0, x = 0$ or -1 respectively. Moreover, let $\boldsymbol{p} = (p_{-1}, p_0, p_{+1})$ be the vector of probabilities:

$$\begin{aligned} p_{-1} &= \mathrm{P}(S_{t,j} = -1) = \mathrm{P}(X_{t,j} < \theta_0) = F_X(\theta_0|\theta), \\ p_0 &= \mathrm{P}(S_{t,j} = 0) = \mathrm{P}(X_{t,j} = \theta_0), \\ p_{+1} &= \mathrm{P}(S_{t,j} = +1) = \mathrm{P}(X_{t,j} > \theta_0) = 1 - F_X(\theta_0|\theta). \end{aligned}$$

It should be noted that the assumption of having samples from a *continuous* distribution, prevents to have tied pairs for $X_{t,j}$ and θ_0 and so, the event $S_{t,j} = 0$ is not possible to occur. As a consequence, $S_{t,j}$ can be either $+1$ or -1 and we have $p_0 = 0$ and $p_{-1} = 1 - p_{+1}$.

The theoretical properties of SN_t can be derived by taking into account that SN_t is defined on $\{-n, -n+2, \ldots, n-2, n\}$ and its distribution can be derived from the relationship

$$\mathrm{SN}_t = 2D_t - n \tag{2.2}$$

where D_t is the number of observations $\{X_{t,1}, X_{t,2}, ...X_{t,n}\}$ larger than θ_0. As a result, D_t is a binomial random variable with parameters n and success probability p_{+1}. Therefore, assuming that the location parameter of interest is the median we simply have $p_{+1} = \mathrm{P}(X_{t,j} > \theta_0)$. The c.d.f. $F_{\mathrm{SN}_t}(s|n, p_{+1})$ of SN_t is equal to

$$F_{\mathrm{SN}_t}(s|n, p_{+1}) = F_{\mathrm{Bin}}\left(\frac{n+s}{2}\Big|n, p_{+1}\right), \tag{2.3}$$

where $s \in \{-n, -n+2, \ldots, n-2, n\}$ and $F_{\mathrm{Bin}}(\ldots|n, p_{+1})$ is the c.d.f. of the binomial distribution which depends on the sample size n and p_{+1}.

Using the relationship between SN_t and D_t, the mean and variance of SN_t are equal to

$$\mathrm{E}(\mathrm{SN}_t) = 2\mathrm{E}(D_t) - n = 2np_{+1} - n, \tag{2.4}$$

$$\mathrm{V}(\mathrm{SN}_t) = 4\mathrm{V}(D_t) = 4np_{+1}(1 - p_{+1}). \tag{2.5}$$

Under the *null* hypothesis, since $p_{-1} = p_{+1} = 0.5$, the mean $\mathrm{E}_0(\mathrm{SN}_t)$ and variance $\mathrm{V}_0(\mathrm{SN}_t)$ of SN_t are simply defined as:

$$\mathrm{E}_0(\mathrm{SN}_t) = 0, \tag{2.6}$$

$$\mathrm{V}_0(\mathrm{SN}_t) = n. \tag{2.7}$$

2.1.2 Distribution of the Wilcoxon Signed Rank statistic

The Wilcoxon Signed Rank test statistic is one of the most commonly used nonparametric technique for testing hypotheses about a location parameter, θ_0. Suppose that at each sampling point a subgroup $\{X_{t,1}, X_{t,2}, \ldots, X_{t,n}\}$ of size n, following a continuous *symmetric* distribution, is collected at time $t = 1, 2, \ldots$. Let $L_{t,j} \in \{1, 2, \ldots, n\}$ denotes the rank of the absolute value of the differences $|X_{t,j} - \theta_0|, j = 1, 2, ..., n$ for subgroup $t = 1, 2, \ldots$. The usual test statistic is the sum of the SR_t defined as:

$$\mathrm{SR}_t = \sum_{j=1}^{n} \mathrm{sign}(X_{t,j} - \theta_0) L_{t,j}. \tag{2.8}$$

Due to the assumption that each sample follows a continuous distribution, the condition $X_{t,j} = \theta_0$, does not hold. Moreover, by definition, the SR_t statistic is defined on $\{-\frac{n(n+1)}{2}, -\frac{n(n+1)}{2} + 2, \ldots, \frac{n(n+1)}{2} - 2, \frac{n(n+1)}{2}\}$. It should be noted that the domain on which SR_t is defined contains zero only if $\frac{n(n+1)}{2}$ is an even integer.

Two equivalent test statistics linearly related to (2.8) can be considered as the sum of the corresponding positive ranks

$$\mathrm{SR}_t^+ = \sum_{j=1}^{n} r_{t,j}^+ L_{t,j}, \tag{2.9}$$

with

$$r_{t,j}^+ = \begin{cases} 1 & \text{if } X_{t,j} - \theta_0 > 0 \\ 0 & \text{if } X_{t,j} - \theta_0 < 0 \end{cases},$$

or the sum of the of the negative ranks

$$\mathrm{SR}_t^- = \sum_{j=1}^{n} r_{t,j}^- L_{t,j}, \tag{2.10}$$

with

$$r_{t,j}^- = \begin{cases} 1 & \text{if } X_{t,j} - \theta_0 < 0 \\ 0 & \text{if } X_{t,j} - \theta_0 > 0 \end{cases}.$$

It should be noted that since the sum of the statistics SR_t^- and SR_t^+ is just the sum of the numbers from 1 to n, they are related through the relation:

$$\mathrm{SR}_t^+ + \mathrm{SR}_t^- = \frac{n(n+1)}{2}.$$

Hence, the following relations between the statistics $\mathrm{SR}_t^+, \mathrm{SR}_t^-, \mathrm{SR}_t$ arise:

$$\mathrm{SR}_t^- = -\mathrm{SR}_t^+ + \frac{n(n+1)}{2}.$$

and

$$\mathrm{SR}_t = 2\mathrm{SR}_t^+ - \frac{n(n+1)}{2}. \tag{2.11}$$

Under the null hypothesis, the distributions of SR_t^+ and SR_t^- are the same, symmetric about $\frac{n(n+1)}{4}$ and ranging from 0 to $\frac{n(n+1)}{2}$. Moreover, the distribution of SR_t is symmetric about zero and ranges from $-\frac{n(n+1)}{2}$ to $\frac{n(n+1)}{2}$. Note that, the sum of the positive signed ranks (SR_t^+) defined in (2.9), is often called as the *null* distribution of Wilcoxon and under the null hypothesis its distribution is known. Finally, the distribution of SR_t, is usually derived through the distribution of SR_t^+ using the relation presented in (2.11).

2.1.3 Approaches for the Computation of the Null Distribution of SR_t^+

Generally, in schemes based on the Wilcoxon Signed Rank statistic, their Run Length properties have been investigated only under the in-control case. Regarding their out-of-control performance, it has been examined only based on a given distribution. As a consequence, the fact that the distribution of SR_t is determined only for the in-control case, makes it difficult to optimise the chart for detecting efficiently shifts of a specific magnitude. In the rest of this Section, after a brief review of existing methodologies on the determination of the SR_t^+ statistic, a new approach will be provided for the exact determination of the

general distribution of SR_t^+.

c.d.f. of SR_t^+ ***via a recursive formula***: The methodology regarding the computation of the null distribution of SR_t was originally presented by Wilcoxon (1947) through the computation of the p.m.f. (probability mass function), $f_{\mathrm{SR}_t^+}(s|n)$ of SR_t^+. More specifically, the p.m.f. of SR_t is computed by evaluating the number $N_{\mathrm{SR}_t^+}(s|n)$ of subsets of integers in $\{1,\ldots,n\}$ having a sum equal to $s \in \{0,1,\ldots,\frac{n(n+1)}{2}\}$ and by computing

$$f_{\mathrm{SR}_t^+}(s|n) = \frac{N_{\mathrm{SR}_t^+}(s|n)}{2^n}.$$

For a better understanding, let us consider an example where the p.m.f, $f_{\mathrm{SR}_t^+}(s|n)$ of SR_t^+ is computed for $n = 3$ (Table 2.1). With 2^3 possible patterns of signed ranks $\pm1, \pm2, \pm3$ and assuming that all differences are positive (i.e the signed ranks are $+1, +2$, and $+3$), the sum of the positive ranks is $\mathrm{SR}_t^+ = 6$. Since there is only one such configuration, then $N_{\mathrm{SR}_t^+}(6|3) = 3$. For the remaining cases we simply have:

- For $s = 0$ the only configuration that satisfies a sum equal to 0 is $(-1,-2,-3)$.
- For $s = 1$ the configuration that satisfies a sum equal to 1 is $(+1,-2,-3)$.
  $\vdots$
- For $s = 5$ the configuration that satisfies a sum equal to 1 is $(-1,+2,+3)$.

Table 2.1: Computation of the null p.m.f. of SR_t^+ for $n = 3$

s	$N_{SR_t^+}(s\|n)$	Configurations	$f_{SR_t^+}(s\|n)$
0	1	$(-1,-2,-3)$	$\frac{1}{8}$
1	1	$(+1,-2,-3)$	$\frac{1}{8}$
2	1	$(-1,+2,-3)$	$\frac{1}{8}$
3	2	$(+1,+2,-3),(-1,-2,+3)$	$\frac{2}{8}$
4	1	$(+1,-2,+3)$	$\frac{1}{8}$
5	1	$(-1,+2,+3)$	$\frac{1}{8}$
6	1	$(+1,+2,+3)$	$\frac{1}{8}$

Finally the c.d.f.(cummulative distribution function) will be simply computed as $F_{SR_t^+}(s|n) = \sum_{w=1}^{s} f_{SR_t^+}(w|n)$. Extended tables and critical values for large values on n have been derived by McCornack (1965) who proposed the use of the following recursive formula:

$$N_{SR_t^+}(s|n) = N_{SR_t^+}(s|n-1) + N_{SR_t^+}(s-n|n-1).$$

Normal approximation of SR_t^+ ***under the null hypothesis,*** H_0: Under the null hypothesis, H_0, assuming $\theta = \theta_0$ as the median of the process, by definition, we have that $P(X_{t,j} > \theta_0|\theta = \theta_0) = P(X_{t,j} < \theta_0|\theta = \theta_0) = p_0 = 0.5$. As a consequence we are interested in testing the hypothesis

$$H_0 : p = 0.5 \text{ vs } H_1 : p \neq 0.5.$$

Wilcoxon (1947) investigated the asymptotic properties of the SR_t^+ statistic and provided tables based on the Normal approximation for the signed-rank statistic. Bennett (1972) revised the asymptotic properties of the SR_t^+ statistic proving its asymptotically normality properties not only for the null but also for the alternative distribution.

It is well known into the literature that the statistic $SR_t^+ = \sum_{j=1}^{n} r_{t,j}^+ L_{t,j}$ can be expressed as

a linear combination of the ranks of the positive differences, $L_{t,j}$ and i.i.d random variables from a Bernoulli distribution $\psi_k \sim \text{Ber}(p)$ as:

$$\text{SR}_t^+ = \sum_{j=1}^{n} \psi_{t,j} L_{t,j}.$$

For the use of the Normal approximation the mean and variance of SR_t^+ need to be defined first. More specifically, for a given value of $p \in (0,1)$ and n the mean and variance are defined as:

$$\text{E}(\text{SR}_t^+) = \underbrace{\text{E}(\psi_{t,j})}_{p} \underbrace{\sum_{j=1}^{n} L_{t,j}}_{\frac{n(n+1)}{2}} = \frac{n(n+1)p}{2}, \tag{2.12}$$

and

$$\text{V}(\text{SR}_t^+) = \underbrace{\text{V}(\psi_{t,j})}_{pq} \underbrace{\sum_{k=1}^{n} L_{t,j}^2}_{\frac{n(n+1)(2n+1)}{6}} = \frac{n(n+1)(2n+1)pq}{6}, \tag{2.13}$$

with $q = 1 - p$. Under H_0, since $p = 0.5$, the mean and variance are obtained though the following expressions

$$\begin{aligned} \text{E}_{H_0}(\text{SR}_t^+) &= \frac{n(n+1)}{4}, \\ \text{V}_{H_0}(\text{SR}_t^+) &= \frac{n(n+1)(2n+1)}{24}. \end{aligned} \tag{2.14}$$

Finally, under H_0, for $s \in \{0, 1, \ldots, \frac{n(n+1)}{2}\}$, the c.d.f $F_{\text{SR}^+}(s|n,p)$ of SR_t^*, which will be depend on the sample size n and p, can be replaced by its Normal approximation as (see, Wilcoxon (1947) :

$$F_{\text{SR}^+}(s|n, 0.5) \simeq F_{\text{N}} \left(\frac{s + 0.5 - \text{E}_{H_0}(\text{SR}_t^+)}{\sqrt{\text{V}_{H_0}(\text{SR}_t^+)}} \right)$$

where $F_{\text{N}}(\ldots)$ is the c.d.f. of the standard Normal, distribution, $N(0,1)$. It has been proven that, for a sufficient large sample size ($n > 30$), this approximation works efficiently, for $p \in (0,1)$. In particular, it tends to be more accurate as $p \simeq 0.5$ and less accurate as $p \to 0$ or $p \to 1$.

As for the computation of the p.m.f. $f_{\text{SR}_t^+}(s|n, 0.5)$ of SR_t^+,under H_0, it is computed

though its c.d.f. as:

$$f_{\mathrm{SR}^+}(s|n, 0.5) = F_{\mathrm{SR}^+}(s|n, 0.5) - F_{\mathrm{SR}^+}(s-1|n, 0.5).$$

p.g.f. of SR_t^+ ***under*** H_0 : Another efficient and accurate method is to derive the null distribution of SR_t^+ through its p.g.f. (probability generating function). By definition, in the random sample $\{X_1, X_2, \ldots, X_n\}$, the variable whose rank is j contributes either 0 or j to SR_t^+. Under the null hypothesis, both of those have probability $p = \frac{1}{2}$. Then the SR_t^+ statistic presented in (2.9) can be rewritten as:

$$\mathrm{SR}_t^+ = \sum_{j=1}^{n} w_j \tag{2.15}$$

where w_j is a characteristic function defined as:

$$w_j = \begin{cases} j & \text{if } X_{t,j} - \theta_0 > 0 \\ 0 & \text{otherwise} \end{cases}.$$

The p.g.f of each w_j is defined as

$$\mathbb{P}_{w_j}(\omega) = E(\omega^{w_j}) = \frac{1}{2}\omega^0 + \frac{1}{2}\omega^j = \frac{1+\omega^j}{2}. \tag{2.16}$$

Additionally, due to the independence of w_j's, the p.g.f of SR_t^+ under the null hypothesis is computed as:

$$\mathbb{P}_{\mathrm{SR}_t^+}(\omega) = \mathbb{P}_{w_1}(\omega) \ldots \mathbb{P}_{w_n}(\omega) = \frac{1}{2^n} \prod_{j=1}^{n} (1+\omega^j). \tag{2.17}$$

Finally, expanding the above product the coefficient of ω^j corresponds to $\mathrm{P}(\mathrm{SR}_t^+ = j)$, $j = \{0, 1, \ldots \frac{n(n+1)}{2}\}$. For a better understanding, an example for $n = 6$ is provided. In particular, following the above steps, the p.g.f. of SR_t^+ is computed as:

$$\begin{aligned}\mathbb{P}_{\mathrm{SR}_t^+}(\omega) = &= \frac{1}{64}(1+\omega^1)(1+\omega^2)(1+\omega^3)(1+\omega^4)(1+\omega^5)(1+\omega^6)\\ &=\frac{1}{64}\big(1+\omega+\omega^2+2\omega^3+2\omega^4+3\omega^5+4\omega^6+4\omega^7\\ &+4\omega^8+5\omega^9+5\omega^{10}+5\omega^{11}+5\omega^{12}+4\omega^{13}\\ &+4\omega^{14}+4\omega^{15}+3\omega^{16}+2\omega^{17}+2\omega^{18}+\omega^{19}+\omega^{20}+\omega^{21}\big),\end{aligned}$$

and the p.m.f. of of SR_t^+ under H_0, $f_{\mathrm{SR}^+}(s|n=6,p=0.5)$ is obtained as:

- For $s=0$ the p.m.f of SR_t^+ is equal to $f_{\mathrm{SR}^+}(s|6,0.5)=\frac{1}{64}$ which corresponds to the coefficient of ω^0).
- For $s=1$ the p.m.f of SR_t^+ is equal to $f_{\mathrm{SR}^+}(s|6,0.5)=\frac{1}{64}$ which corresponds to the coefficient of ω^1).

  ⋮

  ⋮
- For $s=10$ the p.m.f of SR_t^+ is equal to $f_{\mathrm{SR}^+}(s|6,0.5)=\frac{5}{64}$ which corresponds to the coefficient of ω^{10}).
- For $s=11$ the p.m.f of SR_t^+ is equal to $f_{\mathrm{SR}^+}(s|6,0.5)=\frac{5}{64}$ which corresponds to the coefficient of ω^1).

  ⋮

  ⋮
- For $s=20$ the p.m.f of SR_t^+ is equal to $f_{\mathrm{SR}^+}(s|6,0.5)=\frac{1}{64}$ which corresponds to the coefficient of ω^{20})
- For $s=21$ the p.m.f of SR_t^+ is equal to $f_{\mathrm{SR}^+}(s|6,0.5)=\frac{1}{64}$ which corresponds to the coefficient of ω^{21})

2.2 The Shewhart Sign control chart

The nonparametric Shewhart control chart based on the a sign statistic (to be denoted as S-SN chart) has been originally introduced by Amin et al. (1995). Suppose that, at each sampling point $t=1,2,\ldots$, a subgroup $\{X_{t,1},X_{t,2},\ldots,X_{t,n}\}$ of size n following an

unknown continuous distribution with c.d.f. $F_X(x|\theta)$ is collected where θ is the location parameter to be monitored. If $\theta = \theta_0$ the process is declared as in-control and, if $\theta = \theta_1$, the process is declared as out-of-control. Generally, in nonparametric schemes, the parameter θ is considered as the median of the process, but theoretically it can be considered as any percentile of interest. As a result, at each time t, the statistic $\mathrm{SN}_t = \sum_{j=1}^{n} S_{t,j}$ is computed and plotted. The signal rule for the phase II implementation of a two-sided S-SN chart is that an out-of-control signal is given if $\mathrm{SN}_t \notin [-C_l, C_l]$ where C_l is the control limit coefficient to be fixed, defined in $\{1, 2 \ldots, n\}$. Similarly, for an upper-sided control chart, an out-of-control signal is given if $\mathrm{SN}_t \geq C_l'$ and for a lower-sided if $\mathrm{SN}_t \leq -C_l'$.

2.2.1 Performance and Run Length properties

Similarly with most of the conventional phase II control charts (parametric or not) the RL properties of the S-SN chart are computed through the type-II error probability β. In particular, the computation of the ARL values of the two-sided S-SN chart is computed through the type-II error probability β as:

$$\mathrm{ARL} = \frac{1}{1-\beta}$$

where

$$\beta = \mathrm{P}(-C_l < \mathrm{SN}_t < C_l|\theta) = \mathrm{P}(-C_l < \mathrm{SN}_t \leq C_l - 1|\theta),$$

which can be rewritten in terms of the binomial distribution as:

$$\beta = F_{\mathrm{Bin}}\left(\frac{n+s}{2} - 1\Big|n, p_{+1}\right) - F_{\mathrm{Bin}}\left(\frac{n+s}{2}\Big|n, p_{+1}\right),$$

where $p_{+1} = 1 - F_X(\theta_0|\theta)$. It is clear that when $\theta = \theta_0$ we are referring to the in-control case while when $\theta = \theta_1$ we are referring to the out-of-control.

Regarding the design phase of nonparametric Shewhart charts, due to the discrete nature of the statistics to be monitored, it is not always possible to be designed with a corresponding ARL_0 value be exactly equal to the desired one. In Table 2.2 several ARL_0 values for the S-SN chart are presented for different combinations of (n, C_l). It can be seen that for $n < 15$, there is no candidate value for C_l that guarantees an ARL_0 value close 370 or 500. Generally, when the sample size increases, it is possible to find a value of C_l which will give a corresponding ARL_0 value close to 370.4. It is worth stretching that, during the design phase of the S-SN chart, for moderate or even large sample sizes, there might be cases for which the ARL_0 values are far from the desired ones. For example, when $n = 20, 25, 30$ the corresponding "optimal" ARL_0 values are $388, 400.98, 300.58$. Similarly, for $n = 40, 45, 50$ the corresponding ARL_0 values are $450.16, 406.69, 384.29$. Practically speaking, of course choosing a value of C which gives an $ARL_0 = 450.16$ will provide to practitioners a nonparametric chart capable of monitoring large shifts in the process median. However, it will not be fairly comparable with other schemes with corresponding $ARL_0 \approx 370.4$ or $ARL_0 \approx 500$.

Table 2.2: pairs of (ARL_0, C_l) for different sample sizes $n = \{5, 10, \ldots, 50\}$

Sample Size									
5	10	15	20	25	30	35	40	45	50
(1,1)	(1,1)	(1,1)	(1,1)	(1,1)	(1,1)	(1,1)	(1,1)	(1,1)	(1,1)
(1.45,2)	(1.33,2)	(1.24,2)	(1.21,2)	(1.18,2)	(1.17,2)	(1.15,2)	(1.14,2)	(1.13,2)	(1.13,2)
(2.67,3)	(1.82,3)	(1.65,3)	(1.51,3)	(1.45,3)	(1.39,3)	(1.36,3)	(1.32,3)	(1.31,3)	(1.28,3)
(4.57,4)	(2.91,4)	(2.2,4)	(1.99,4)	(1.79,4)	(1.71,4)	(1.62,4)	(1.57,4)	(1.52,4)	(1.49,4)
(16,5)	(4.41,5)	(3.31,5)	(2.61,5)	(2.36,5)	(2.11,5)	(2,5)	(1.88,5)	(1.81,5)	(1.74,5)
	(9.14,6)	(4.76,6)	(3.8,6)	(3.06,6)	(2.77,6)	(2.47,6)	(2.33,6)	(2.17,6)	(2.08,6)
	(15.28,7)	(8.44,7)	(5.28,7)	(4.36,7)	(3.56,7)	(3.22,7)	(2.87,7)	(2.69,7)	(2.49,7)
	(85.33,9)	(28.44,9)	(12.76,9)	(9.28,9)	(6.68,9)	(5.7,9)	(4.74,9)	(4.3,9)	(3.81,9)
	(512,10)	(47.01,10)	(24.16,10)	(13.24,10)	(10.13,10)	(7.55,10)	(6.5,10)	(5.44,10)	(4.93,10)
		(135.4,11)	(37.59,11)	(23.1,11)	(14.13,11)	(11.17,11)	(8.53,11)	(7.4,11)	(6.22,11)
		(239.18,12)	(84.62,12)	(34.53,12)	(23.38,12)	(15.33,12)	(12.39,12)	(9.63,12)	(8.41,12)
		(>1000,>13)	(138.94,13)	(68.34,13)	(33.96,13)	(24.41,13)	(16.78,13)	(13.8,13)	(10.88,13)
			(388.07,14)	(106.89,14)	(62.02,14)	(34.7,14)	(25.99,14)	(18.49,14)	(15.41,14)
			(671.3,15)	(245.26,15)	(93.69,15)	(59.97,15)	(36.32,15)	(28.01,15)	(20.46,15)
				(400.98,16)	(191.47,16)	(88.25,16)	(60.28,16)	(38.62,16)	(30.45,16)
				(>1000,>17)	(300.58,17)	(167,17)	(86.9,17)	(62.13,17)	(41.51,17)
					(698.86,18)	(254.25,18)	(155.6,18)	(88.09,18)	(65.16,18)
					(>1000,>19)	(532.42,19)	(231.27,19)	(151.31,19)	(91.13,19)
						(838.05,20)	(450.16,20)	(220.56,20)	(151.5,20)
						(>1000,>21)	(689.42,21)	(406.69,21)	(217.33,21)
								(609.2,22)	(384.29,22)
									(565.23,23)
									(>1000,>24)

2.3 The EWMA control chart based on the Sign statistic

Graham et al. (2011a) introduced a new nonparametric two-sided EWMA chart based on the Sign statistic and, using the Markov-Chain approach of Brook and Evans (1972), they obtained its optimal design parameters and investigated its out-of-control performance under several distributions.

The two-sided EWMA Sign chart: Suppose that, at each sampling point $t = 1, 2, \ldots$, a subgroup $\{X_{t,1}, X_{t,2}, \ldots, X_{t,n}\}$ of size n following an unknown continuous distribution is collected where θ is the median of the distribution. The two-sided EWMA chart (2-SN EWMA chart) based on the Sign statistic is defined by the following formula:

$$Z_t = \lambda \mathrm{SN}_t + (1-\lambda) Z_{t-1}, Z_0 = \mathrm{E}_0(\mathrm{SN}_t), \tag{2.18}$$

where $\mathrm{E}_0(\mathrm{SN}_t)$ is the in-control expectance of SN_t. The asymptotic upper and lower control limits of the two-sided SN EWMA chart are obtained by using the following classical formulas

$$\begin{aligned}
\mathrm{LCL} &= \mathrm{E}_0(\mathrm{SN}_t) - K\sqrt{\mathrm{V}_0(\mathrm{SN}_t)} \times \sqrt{\frac{\lambda}{2-\lambda}}, \\
\mathrm{UCL} &= \mathrm{E}_0(\mathrm{SN}_t) + K\sqrt{\mathrm{V}_0(\mathrm{SN}_t)} \times \sqrt{\frac{\lambda}{2-\lambda}}.
\end{aligned}$$

If we consider the in-control values $\mathrm{E}_0(\mathrm{SN}_t)$ and $\mathrm{V}_0(\mathrm{SN}_t)$ as presented in (2.6) and (2.7) the asymptotic upper and lower control limits simply reduce to

$$\begin{aligned}
\mathrm{LCL} &= -K\sqrt{\frac{n\lambda}{2-\lambda}}, \\
\mathrm{UCL} &= K\sqrt{\frac{n\lambda}{2-\lambda}}.
\end{aligned}$$

The upper-sided EWMA Sign chart: The plotting statistic of the upper-sided EWMA chart based on the Sign statistic (SN EWMA chart) is defined by the following formula:

$$Z_t = \max(\mathrm{E}_0(\mathrm{SN}_t), \lambda \mathrm{SN}_t + (1-\lambda) Z_{t-1}), Z_0 = \mathrm{E}_0(\mathrm{SN}_t), \tag{2.19}$$

with asymptotic upper and lower control limits defined as:

$$\begin{aligned} \text{LCL} &= 0 \\ \text{UCL} &= K_1\sqrt{\frac{n\lambda}{2-\lambda}}. \end{aligned}$$

2.3.1 Performance

Generally, in most existing phase II EWMA charts (parametric or not) their RL properties are derived through the standard method of Brook and Evans (1972). As a consequence, the RL properties of the two-sided 2-SN EWMA chart are obtained as presented in Chapter 1 (see, Section 1.1.2.1) with the only difference that the transient probabilities are computed as:

$$Q_{j,k} = F_{\text{SN}_t}\left(\frac{H_k + \Delta - (1-\lambda)H_j}{\lambda}|n, p_{+1}\right) - F_{\text{SN}_t}\left(\frac{H_k - \Delta - (1-\lambda)H_j}{\lambda}|n, p_{+1}\right), \quad (2.20)$$

where $F_{\text{SN}_t}(x|n, p_{+1})$ is the c.d.f. of SN_t as defined in equation (2.3). Similarly, for the upper-sided EWMA chart the transient probabilities, $Q_{k,j}$ are computed as:

- if $j = 0$,

$$Q_{k,0} = F_{\text{SN}_t}\left(-\frac{(1-\lambda)H_k}{\lambda}|n, p_{+1}\right).$$

- if $j = 1, 2, \ldots, m$,

$$Q_{k,j} = F_{\text{SN}_t}\left(\frac{H_i + \Delta - (1-\lambda)H_k}{\lambda}|n, p_{+1}\right) - F_{\text{SN}_t}\left(\frac{H_i - \Delta - (1-\lambda)H_k}{\lambda}|n, p_{+1}\right). \quad (2.21)$$

In order to examine the efficiency of the Brook and Evans (1972) method used for the computation of the RL properties of the two- and upper-sided EWMA Sign charts, in Table 2.3 several pairs of in-control (ARL, SDRL) values are presented, as a function of the number of subintervals $2m + 1$, for the 2-SN EWMA chart (top) and the SN EWMA chart (bottom) for different sample sizes. The corresponding ARL_0 values are plotted as a function of the number of subintervals in Figure 2.1 (two-sided) and Figure 2.2 (upper-sided). In particular, in these plots, the red dashed lines correspond to the simulated ARL_0 values obtained through a Monte Carlo simulation of 10^6 runs. From Table 2.3 it can be concluded that, the in-control ARL and SDRL values are strongly affected by the number of subintervals. For instance:

- For the two-sided case, when $n = 8$, the ARL_0 values vary from 376 to 418. Additionally, for the same case, the SDRL_0 values vary from 371.5 to 413.5.
- Similarly, for the upper-sided case when $n = 17$, the ARL_0 values fluctuate from 478.7 to 500.8. and the SDRL_0 values vary from 471.5 to 495.7.

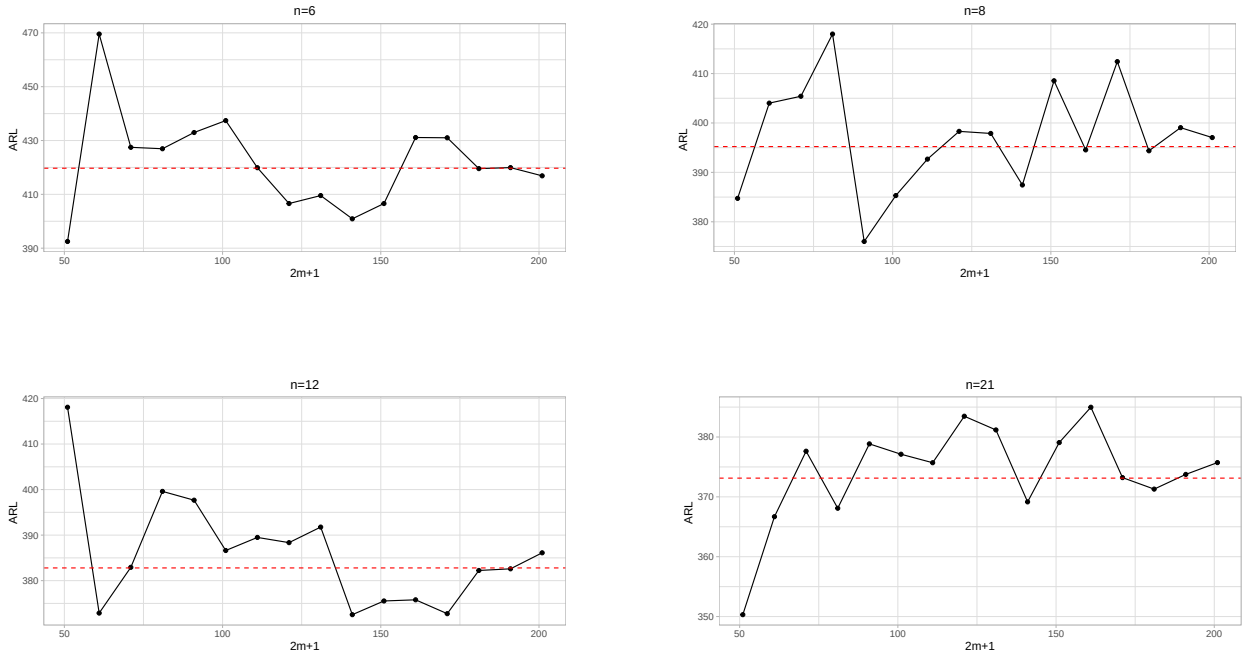

Figure 2.1: ARL_0 (plain lines) as a function of the number of sub-intervals $2m + 1 \in \{51, 61, \ldots, 201\}$ for the 2-SN EWMA chart with parameters $(\lambda = 0.2, K = 2.85)$ and $n \in \{6, 8, 12, 21\}$ using the standard Markov Chain method

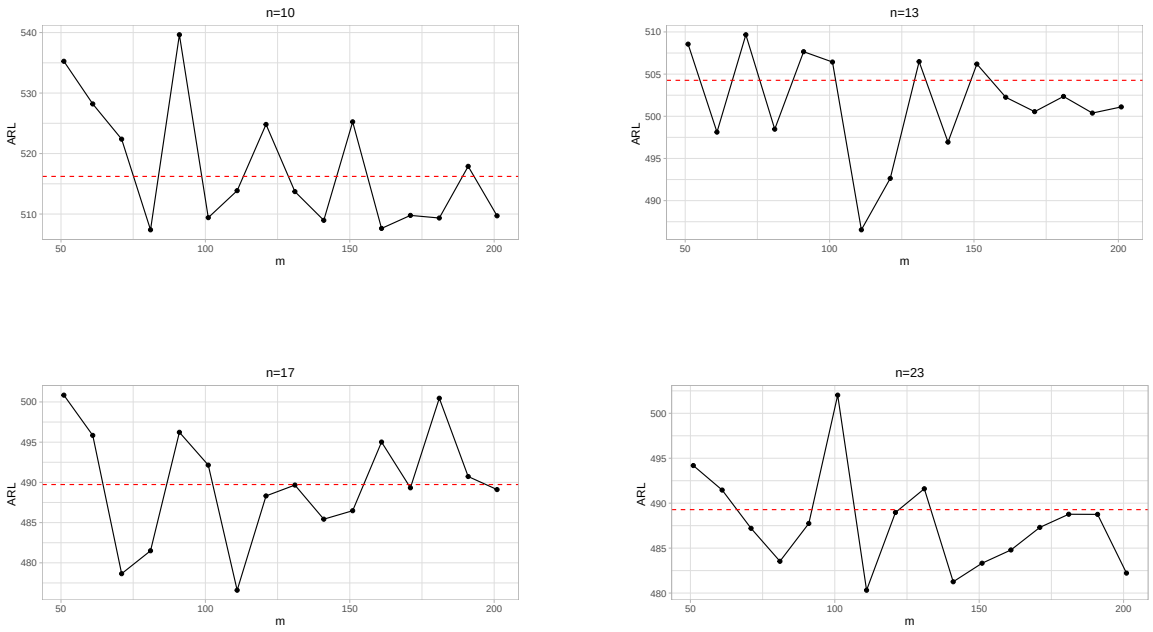

Figure 2.2: ARL_0 (plain lines) in function of the number of sub-intervals $m \in \{50, 60, \ldots, 200\}$ for the SN EWMA chart with parameters $(\lambda = 0.2, K_1 = 2.85)$ and $n \in \{10, 13, 17, 23\}$ using the standard Markov Chain method

In general, as the number of sub-intervals increases, the results tend to be more "steady", but still, as it can be seen, there are cases where the results differ significantly from the ones obtained using simulations. An immediate consequence of these results is that it is almost impossible to "optimize" (i.e. find optimal pairs (λ, K) or (λ, K_1)) the Sign EWMA chart (upper- or two-sided) if ARL_0 values are computed using the standard Markov Chain method of Brook and Evans (1972). Therefore, a more efficient technique is needed for the exact and robust determination of ARL values regardless the number of subintervals,the sample size, n or the pair of the design parameters.

Table 2.3: pair of $(\mathrm{ARL}_0, \mathrm{SDRL}_0)$ values as a function of the number of subintervals for the 2-SN EWMA chart (top) and the SN EWMA chart (bottom) for different sample sizes.

$(\mathrm{ARL}_0, \mathrm{SDRL}_0)$ values for the 2-SN EWMA chart for $(\lambda, K) = (0.2, 2.85)$				
$2m+1$	$n=6$	$n=8$	$n=12$	$n=21$
51	(392.5,387.9)	(384.7,380.4)	(418.1,413.5)	(350.3,346.1)
61	(469.6,464.6)	(404,399.5)	(372.9,368.5)	(366.7,362.4)
71	(427.5,422.8)	(405.4,401)	(382.9,378.5)	(377.6,373.3)
81	(426.9,422.3)	(418,413.5)	(399.6,395.2)	(368.1,363.7)
91	(433,428.4)	(376,371.5)	(397.7,393.2)	(378.9,374.5)
101	(437.4,432.8)	(385.3,380.8)	(386.6,382.2)	(377.1,372.8)
111	(419.9,415.3)	(392.7,388.2)	(389.5,385)	(375.7,371.4)
121	(406.6,401.9)	(398.3,393.8)	(388.3,383.9)	(383.5,379.1)
131	(409.5,405)	(397.9,393.3)	(391.8,387.3)	(381.2,376.9)
141	(400.9,396.3)	(387.4,382.9)	(372.5,368.1)	(369.2,364.8)
151	(406.6,401.9)	(408.5,403.9)	(375.5,371.1)	(379.1,374.7)
161	(431.1,426.5)	(394.6,390)	(375.8,371.4)	(385,380.6)
171	(431,426.4)	(412.4,407.8)	(372.7,368.4)	(373.2,368.9)
181	(419.6,414.9)	(394.4,389.8)	(382.2,377.8)	(371.3,367)
191	(419.9,415.3)	(399.1,394.4)	(382.6,378.2)	(373.8,369.4)
201	(416.9,412.3)	(397,392.5)	(386.1,381.6)	(375.7,371.4)

$(\mathrm{ARL}_0, \mathrm{SDRL}_0)$ values for the SN EWMA chart $(\lambda, K_1) = (0.2, 2.85)$				
m	$n=10$	$n=13$	$n=17$	$n=23$
50	(535.3,530)	(508.6,503.4)	(500.8,495.7)	(494.2,489.2)
60	(528.2,522.9)	(498.1,493)	(495.8,490.8)	(491.5,486.4)
70	(522.4,517.1)	(509.7,504.5)	(478.7,473.6)	(487.2,482.2)
80	(507.4,502.2)	(498.5,493.4)	(481.5,476.4)	(483.5,478.5)
90	(539.6,534.4)	(507.7,502.5)	(496.2,491.2)	(487.7,482.7)
100	(509.4,504.2)	(506.4,501.3)	(492.1,487.1)	(502,497)
110	(513.9,508.7)	(486.5,481.4)	(476.6,471.5)	(480.3,475.3)
120	(524.8,519.6)	(492.6,487.5)	(488.3,483.3)	(489,483.9)
130	(513.7,508.5)	(506.5,501.3)	(489.7,484.6)	(491.6,486.6)
140	(509,503.7)	(496.9,491.8)	(485.4,480.4)	(481.3,476.3)
150	(525.2,520)	(506.2,501.1)	(486.5,481.4)	(483.3,478.3)
160	(507.6,502.4)	(502.3,497.1)	(495,489.9)	(484.8,479.8)
170	(509.8,504.6)	(500.5,495.4)	(489.3,484.3)	(487.3,482.3)
180	(509.3,504.1)	(502.4,497.2)	(500.5,495.4)	(488.8,483.7)
190	(517.9,512.6)	(500.4,495.2)	(490.7,485.7)	(488.8,483.7)
200	(509.7,504.5)	(501.1,496)	(489.1,484)	(482.2,477.2)

2.4 The Shewhart chart based on Wilcoxon Signed Rank statistic

Bakir (2004) introduced a non-parametric Shewhart-type control chart based on the Wilcoxon signed rank statistic (S-WSR chart). Following the same notation presented in section (2.1.2), at each sampling point a subgroup $\{X_{t,1}, X_{t,2}, \ldots, X_{t,n}\}$ of size n, following a continuous *symmetric* distribution, is collected at time $t = 1, 2, \ldots$. At each sampling

point the test statistic $\mathrm{SR}_t = \sum_{j=1}^{n} \mathrm{sign}(X_{t,j} - \theta_0) L_{t,j}$ is computed and plotted. The signal rule for the phase II implementation of a two-sided S-WSR chart is that an out-of-control signal is given if $\mathrm{SR}_t \notin (-C', C')$ where C' is a pre-defined control limit coefficient, $C' \in \left\{1, 2, \ldots, \frac{n(n+1)}{2}\right\}$. Additionally, for a upper-sided control chart an out-of-control signal is given if $\mathrm{SR}_t \geq C$ and for a lower-sided if $\mathrm{SR}_t \leq -C^*$. where $C, C^* \in \left\{1, 2, \ldots, \frac{n(n+1)}{2}\right\}$

2.4.1 Performance and Run Length properties

According to Bakir (2004), the RL properties of the upper-sided, lower-sided and two-sided S-WSR chart are defined respectively by the random variables L^+, L^- and L, as:

$$L^+ = \min\{\mathrm{t};\ \mathrm{SR}_t \geq C\ \}$$

$$L^- = \min\{\mathrm{t};\ \mathrm{SR}_t \leq -C^*\ \}$$

$$L = \min\{\mathrm{t};\ \mathrm{SR}_t \leq -C' \text{ or } \mathrm{SR}_t \geq C'\ \}$$

Since, each one of the run lengths L^+, L^- and L follows a Geometric distribution with parameters $\alpha^+ = \mathrm{P}(\mathrm{SR}_t \geq C)$, $\alpha^- = \mathrm{P}(\mathrm{SR}_t \leq -C^*)$ and $\alpha = \mathrm{P}(\mathrm{SR}_t \leq -C' \text{ or } \mathrm{SR}_t \geq C'$) respectively, the ARL, ARL^-, and ARL^+ of the upper-, lower- and the two-sided S-WSR chart are computed as:

$$\mathrm{ARL}^+ = \frac{1}{\alpha^+}$$

$$\mathrm{ARL}^- = \frac{1}{\alpha^-}$$

$$\mathrm{ARL} = \frac{1}{\alpha}$$

In particular, for the computation of the in-control ARL^+ value of the upper-sided S-WSR chart (to be denoted as ARL_0^+) the Type I error, α^+ is computed as:

$$\begin{aligned}\alpha^+ &= \mathrm{P}(\mathrm{SR}_t \geq C | \theta = \theta_0) = 1 - \mathrm{P}(\mathrm{SR}_t < C | \theta = \theta_0) \\ &= 1 - \mathrm{P}(\mathrm{SR}_t \leq C - 1 | \theta = \theta_0) = 1 - F_{\mathrm{SR}_t}(C - 1 | n, p = 0.5)\end{aligned}$$

where $F_{\mathrm{SR}_t}(s|n, p = 0.5)$, $s \in \{-\frac{n(n+1)}{2}, -\frac{n(n+1)}{2} + 2, \ldots, \frac{n(n+1)}{2} - 2, \frac{n(n+1)}{2}\}$ is the c.d.f of SR_t under the in-control case (i.e. when $\theta = \theta_0$) and can be derived through the relation presented in (2.11) as:

$$F_{\mathrm{SR}_t}(s|n, p = 0.5) = F_{\mathrm{SR}_t^+}\left(\frac{s + \frac{n(n+1)}{2}}{2}|n, p = 0.5)\right).$$

Then the ARL^+ of the upper-sided S-WSR chart is finally computed as:

$$\mathrm{ARL}^+ = \frac{1}{\alpha^+} = 1 - F_{\mathrm{SR}_t}(C - 1|n, p = 0.5)$$

Similarly for the lower-sided S-WSR chart we have:

$$\mathrm{ARL}_0^- = \frac{1}{a^-} = \frac{1}{\mathrm{P}(\mathrm{SR}_t \leq C^*|\theta = \theta_0)} = \frac{1}{1 - F_{\mathrm{SR}_t}(C^*|n, p = 0.5)}$$

Finally, concerning the computation of the in-control ARL for the two-sided case, is computed as (see, Bakir (2004)):

$$\mathrm{ARL}_0 = \frac{\mathrm{ARL}_0^+}{2}.$$

Regarding the value of the control limit coefficient C, it is chosen accordingly to satisfy the condition that the corresponding in-control value ARL_0 will be equal to a fixed constant(say 370.4).

Bakir (2004) studied the chart's RL properties verifying its in-control distribution-free properties. He provided several in-control ARL_0^+ for given values of $n = \{8, 10\}$ and C (see Table 2.4). Regarding the out-of-control case, he examined the chart's performance under different scenarios of given symmetric distributions.

Table 2.4: Values of ARL_0^+ in subgroups of size n (presented in Bakir (2004), Table 2.)

$n = 8$			$n = 10$		
C	ARL_0^+	α^+	C	ARL_0^+	α^+
18	8.00	0.12500	25	8.60	0.11621
20	10.24	0.09766	27	10.34	0.09668
22	13.47	0.07422	29	12.49	0.08008
24	18.26	0.05469	31	15.28	0.06543
26	25.60	0.03906	33	18.96	0.05273
28	36.57	0.02734	35	23.81	0.04199
30	51.20	0.01953	37	31.03	0.03223
32	85.33	0.01172	39	40.96	0.02441
34	128.00	0.00781	41	53.89	0.01855
36	256.00	0.00391	43	73.146	0.01367
> 36	∞	0.00	45	102.40	0.00977
			47	146.29	0.00684
			49	204.80	0.00488
			51	341.33	0.00293
			53	512.00	0.00195
			55	1024.00	0.00098
			> 55	∞	0.00

It should be noted that, in the design of the upper-sided S-WSR chart (or similarly for the lower- or the two-sided cases) is not possible to find a value for C which guarantees a corresponding value to be exactly equal to the desired ARL_0^+ (say $ARL_0^+ = 370.4$). As a consequence, during the design phase of the control chart, a value for C is chosen in order to give an ARL_0^+ value as close as possible to the desired one. Generally, for relative large samples, it may be possible to find a proper value of C which gives a corresponding ARL_0^+ value relative close to the desired value, but even so, from Table 2.4 it can be seen that for $n = 10$, assuming 370.4 as the desired in-control, the closest value is $ARL_0^+ = 341.33$ for $C = 51$ which is practically far from 370.4. As, a consequence, it is not always possible to obtain the chart's optimal design parameters in order to perform fair comparisons with other schemes. Additionally, the determination of the chart's out-of-control performance is made through simulations for a given distribution. In fact, in almost all existing schemes based on the Wilcoxon Signed Rank statistic, their out-of-control performance is examined through

simulations.

2.4.2 The S-WSR chart with exact RL properties

As it has been already mentioned in previous Sections, over the last two decades there is a large amount of publications related with distribution-free control charts based on the Wilcoxon signed rank statistic. However, the determination of their out-of-control performance is examined via simulation-based techniques for a given distribution. As a consequence, practitioners may not always be sure about the chart's *exact* out-of-control performance.

In this Section, we aim to provide an answer to the question "What is the distribution of SR_t^+ *in general*". More specifically, following the notation presented in section 2.1.2, the p.m.f. of SR_t^+ will be depend on n and $p = P(X_{t,j} > \theta_0|\theta)$, $p \in (0,1)$ and will be denoted as $f_{SR_t^+}(s|n,p)$. With respect to the Phase II implementation of the control chart, when the process is in-control, assuming θ as the median of the process we have that $P(X_{t,j} > \theta_0|\theta = \theta_0) = P(X_{t,j} < \theta_0|\theta = \theta_0) = p_0 = 0.5$. On the other hand, let $p_1 = P(X_{t,j} > \theta_0|\theta = \theta_1) = 1 - F_X(\theta_0|\theta_1)$ be defined as the probability of having an observation larger than θ_0 when the process runs out-of-control with median $\theta = \theta_1$. Note that, a value of p_1 close to $p_0 = 0.5$ corresponds to a "small" shift from θ_0 to θ_1 while, a value of p_1 close to 0 or 1 corresponds to a "large" shift from θ_0 to θ_1.

2.4.2.1 RL properties of the S-WSR chart

The question that needs to be answered first is "What is p.m.f. of the Wilcoxon Signed Rank statistic when $p = p_1 \neq p_0$?", or at least, " How can we approximate it well ?". In order to give an answer to these questions, two approaches will be presented and their efficiency will be tested. In particular, first the efficiency of the Normal approximation, presented in Section 2.1.2, for the general distribution of SR_t^+ will be tested. Moreover, the design of control schemes based on Signed Ranks in which the *general* distribution of SR_t^+ will be derived through the p.g.f. of SR_t^+ not only under H_0 but also for the alternative hypothesis.

RL ***properties of the S-WSR chart using the Normal approximation***: As it was presented in Section 2.1.2, Wilcoxon (1947) investigated the asymptotic properties of the SR_t^+ statistic under H_0. Similarly, Bennett (1972) proved the asymptotic properties of SR_t^+ not only under H_0 but also for the alternative, H_1. In particular, the c.d.f. of SR^+ for $p \in (0,1)$ and $s \in \{0,1,\ldots,\frac{n(n+1)}{2}\}$ can be replaced by its normal approximation as :

$$F_{\mathrm{SR}^+}(s|n,p) \simeq F_{\mathrm{N}}\left(\frac{s+0.5-\mathrm{E}(\mathrm{SR}_t^+)}{\sqrt{\mathrm{V}(\mathrm{SR}_t^+)}}\right).$$

Moreover, by substituting the definition of the mean and variance of SR_t^+presented in (2.14) we have:

$$F_{\mathrm{SR}^+}(s|n,p) \simeq F_{\mathrm{N}}\left(\frac{s+0.5-\frac{n(n+1)p}{2})}{\sqrt{\frac{n(n+1)(2n+1)pq}{6}}}\right).$$

In terms of the theoretical properties of the distribution of SR_t^+, the Normal approximation provides reliable results, especially as n increases. However, practically speaking, for the design of a control chart, the primary goal is to make sure that an approximation of SR^+ will provide a robust approximation to the corresponding chart's RL properties. Taking as an example the upper-sided S-WSR chart, in Figure 2.3 the corresponding ARL^+ values are plotted for different combinations of $n = \{10, 15, 20\}$ and C (blue dashed lines) when the Normal approximation is being used. Additionally, the red dashed lines correspond to the results obtained through Monte-Carlo simulation in which the SR_t^+ statistic was simulated from the exact null distribution of SR_t^+. It can be clearly seen that even though the Normal approximation is an efficient way to approximate the distribution of SR_t^+, for the computation of the chart's RL properties of the control chart the approximation is not accurate enough.

For a better understanding of why these large differences in the ARL_0^+ values might occur, it will be very useful to compare the in-control RL properties of the upper-sided S-WSR chart when using the exact null distribution of SR_t (entitled as Exact SR_t) v.s. using the Normal approximation (entitled as Normal Approximation). In Table 2.5 some in-control ARL^+ values are presented for different combinations of n and the control limit coefficient C using the exact null distribution of SR_t and the Normal approximation. Moreover, for each case, the corresponding probabilities p^+ are reported along with their absolute differences between the two cases (entitled as "abs of p^+'s"). From Table 2.5, it can be seen that, at each case, even though the absolute errors of p^+ are small (i.e. the Normal approximation works efficiently), the corresponding values of the $\mathrm{ARL}_0^+ = \frac{1}{p^+}$ are quite sensitive to these small differences. For instance, when $n = 20$ and $C = 136$ the absolute difference between the exact and the approximated probabilities p^+ is 0.004. However, regarding the corresponding

ARL_0^+ value, using the Normal approximation we get $ARL_0^+ = 115.5$ while the true value of ARL_0^+ is 211.96. Consequently, the Normal approximation does not guarantee reliable in-control RL properties for the control chart making it useless for the general approximation or the chart's RL properties.

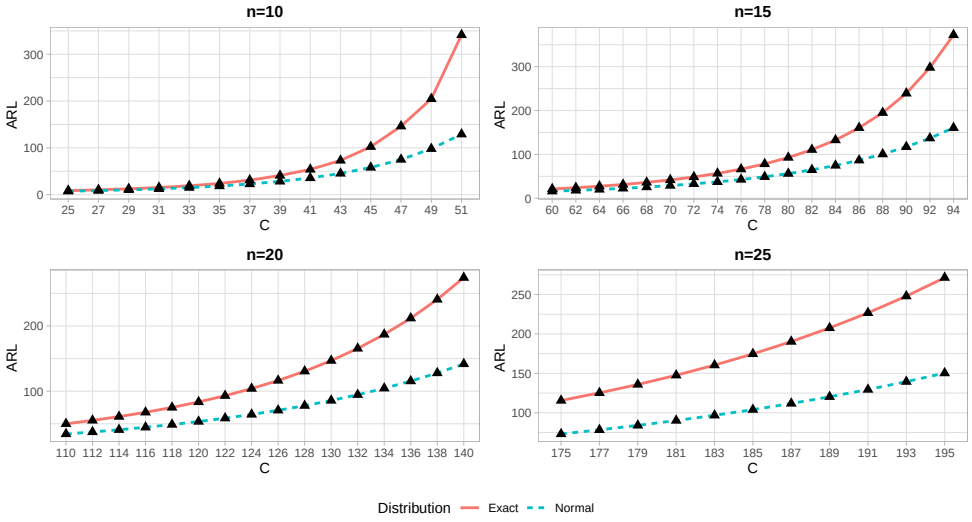

Figure 2.3: Comparisons for ARL_0^+ values between the exact and approximated distribution of SR_t

Table 2.5: Comparisons for ARL_0^+ values between the exact and approximated distribution of SR_t

$n = 10$

	Exact SR_t		Normal Aproximation		
C	ARL^+	p^+	ARL^+	p^+	abs of p^+'s
37	31.03	0.03223	22.79	0.04388	0.01165
39	40.96	0.02441	28.40	0.03521	0.01079
41	53.89	0.01855	35.73	0.02799	0.00944
43	73.14	0.01367	45.35	0.02205	0.00838
45	102.40	0.00977	58.09	0.01721	0.00745
47	146.29	0.00684	75.12	0.01331	0.00648
49	204.80	0.00488	98.04	0.01020	0.00532
51	341.33	0.00293	129.15	0.00774	0.00481

$n = 15$

	Exact SR_t		Normal Aproximation		
C	ARL^+	p^+	ARL^+	p^+	abs of p^+'s
80	92.83	0.01077	56.17	0.01780	0.00703
82	110.70	0.00903	64.70	0.01545	0.00642
84	132.66	0.00754	74.74	0.01338	0.00584
86	160.63	0.00623	86.59	0.01155	0.00532
88	195.04	0.00513	100.61	0.00994	0.00481
90	239.18	0.00418	117.24	0.00853	0.00435
92	297.89	0.00336	137.01	0.00730	0.00394
94	372.36	0.00269	160.60	0.00623	0.00354

$n = 20$

	Exact SR_t		Normal Aproximation		
C	ARL^+	p^+	ARL^+	p^+	abs of p^+'s
120	83.50	0.01198	53.46	0.01870	0.00673
122	93.09	0.01074	58.61	0.01706	0.00632
124	103.98	0.00962	64.33	0.01554	0.00593
126	116.40	0.00859	70.70	0.01414	0.00555
128	130.61	0.00766	77.80	0.01285	0.00520
132	165.57	0.00604	94.56	0.01058	0.00454
134	187.11	0.00534	104.44	0.00957	0.00423
136	211.96	0.00472	115.50	0.00866	0.00394
138	240.71	0.00415	127.90	0.00782	0.00366
140	274.13	0.00365	141.81	0.00705	0.00340

$n = 25$

	Exact SR_t		Normal Aproximation		
C	ARL^+	p^+	ARL^+	p^+	abs of p^+'s
175	115.52	0.00866	73.10	0.01368	0.00502
177	125.21	0.00799	78.33	0.01277	0.00478
179	135.85	0.00736	83.99	0.01191	0.00454
181	147.55	0.00678	90.12	0.01110	0.00432
183	160.43	0.00623	96.76	0.01033	0.00410
185	174.62	0.00573	103.96	0.00962	0.00389
187	190.28	0.00526	111.77	0.00895	0.00369
189	207.57	0.00482	120.24	0.00832	0.00350
191	226.69	0.00441	129.43	0.00773	0.00331
193	247.86	0.00403	139.43	0.00717	0.00314
195	271.33	0.00369	150.29	0.00665	0.00297

2.4.2.2 The general distribution of SR_t^+ through the p.g.f. of SR_t^+

So far we saw that even though the Normal approximation is an efficient way to approximate the distribution of SR_t^+, it does not provide reliable results in the computation of the RL properties of a control chart based on the Wilcoxon signed ranks statistic. In this section a simple method for the *exact* computation of the general distribution of SR_t^+ will be provided not only for the null but also for the alternative hypothesis. As illustrated in 2.1.2 existing methodologies for computing the distribution of SR_t^+ only focus on the in-control case. Computing the p.m.f. of SR_t^+ (exactly, without any approximation) under the *alternative* hypothesis (i.e. $p \neq 0.5$) is more tricky. The solution that has been opted to, consists in evaluating firstly the p.g.f. $G_{SR_t^+}(\omega)$ of SR_t^+ as (see Bennett (1972))

$$G_{SR_t^+}(\omega) = \prod_{i=1}^{n}(p\omega^i + q), \tag{2.22}$$

where $q = 1 - p$ and to obtain the p.m.f. $f_{SR_t^+}(s|n,p)$ of SR_t^+ by differentiating $G_{SR_t^+}(\omega)$, s times, at $\omega = 0$, using the formula

$$f_{SR_t^+}(s|n,p) = \frac{1}{s!}G^{(s)}_{SR_t^+}(\omega)\bigg|_{\omega=0},$$

where $G^{(s)}_{SR_t^+}(\omega)$ is the s^{th} derivative of $G_{SR_t^+}(\omega)$. As $G_{SR_t^+}(\omega)$ is a polynomial of degree $\frac{n(n+1)}{2}$ then, for $s \in \{0, 1, \ldots, \frac{n(n+1)}{2}\}$, $G^{(s)}_{SR_t^+}(\omega)$ is a polynomial of degree $\frac{n(n+1)}{2} - s$ and we can write

$$\frac{1}{s!}G^{(s)}_{SR_t^+}(\omega) = \sum_{j=0}^{\frac{n(n+1)}{2}-s} c_{s,j}w^j,$$

where $c_{s,j}$ is the coefficient of degree j corresponding to the polynomial $\frac{1}{s!}G^{(s)}_{SR_t^+}(\omega)$. For a better understanding of this approach let us consider the following example with $n = 4$ and $p = 0.2$. In this case $SR_t^+ \in \{0, 1, \ldots, 10\}$ and we have

- $\frac{1}{0!}G_{SR_t^+}(\omega) = 0.0016\omega^{10} + 0.0064\omega^9 + 0.0064\omega^8 + 0.032\omega^7 + 0.032\omega^6 + 0.0512\omega^5 + 0.128\omega^4 + 0.128\omega^3 + 0.1024\omega^2 + 0.1024\omega + 0.4096$. The coefficients $c_{0,j}$ are listed in the first row (for $s = 0$) of Table 2.6. Replacing $\omega = 0$ in this polynomial gives $f_{SR_t^+}(0|4, 0.2) = 0.4096$.

- Now, if we evaluate the first derivative, we have $\frac{1}{1!}G^{(1)}_{SR_t^+}(\omega) = 0.016\omega^9 + 0.0576\omega^8 + 0.0512\omega^7 + 0.224\omega^6 + 0.192\omega^5 + 0.256\omega^4 + 0.512\omega^3 + 0.384\omega^2 + 0.2048\omega + 0.1024$. The coefficients $c_{1,j}$ are listed in the second row (for $s = 1$) of Table 2.6. Replacing $\omega = 0$ in this polynomial gives $f_{SR_t^+}(1|4, 0.2) = 0.1024$.

$\vdots$

- If we evaluate the 9^{th} derivative, we have $\frac{1}{9!}G^{(9)}_{\text{SR}^+_t}(\omega) = 0.016\omega + 0.0064$. The coefficients $c_{9,j}$ are listed in the row corresponding for $s = 9$ of Table 2.6. Replacing $\omega = 0$ in this polynomial gives $f_{\text{SR}^+_t}(9|4, 0.2) = 0.0064$. A final derivative gives $\frac{1}{10!}G^{(10)}_{\text{SR}^+_t}(\omega) = 0.0016$ and we have $f_{\text{SR}^+_t}(10|4, 0.2) = 0.0016$.

Because polynomials can be efficiently coded as vectors of coefficients, fast arithmetic operations (addition, multiplication and power) and derivation can be efficiently implemented (as in Matlab for instance) and the evaluation of $f_{\text{SR}^+_t}(s|n, p)$ can be obtained in a very fast way. Equivalently, the p.m.f of SR^+_tcan be simply obtained by expanding the product in (2.22) as showed in Section 2.1.3. It should be noted that this method can also be applied when $p = 0.5$, i.e. for the null hypothesis case. As a consequence, this approach is effective and guarantees the exact determination of the RL properties of the S-WSR chart.

Table 2.6: Computation of the p.m.f. of SR^+_t for $n = 4$ and $p = 0.2$

s	$c_{s,10}$	$c_{s,9}$	$c_{s,8}$	$c_{s,7}$	$c_{s,6}$	$c_{s,5}$	$c_{s,4}$	$c_{s,3}$	$c_{s,2}$	$c_{s,1}$	$c_{s,0}$	$f_{\text{SR}^+_t}(s\|4, 0.2)$
0	0.0016	0.0064	0.0064	0.0320	0.0320	0.0512	0.1280	0.1280	0.1024	0.1024	0.4096	0.4096
1	-	0.0160	0.0576	0.0512	0.2240	0.1920	0.2560	0.5120	0.3840	0.2048	0.1024	0.1024
2	-	-	0.0720	0.2304	0.1792	0.6720	0.4800	0.5120	0.7680	0.3840	0.1024	0.1024
3	-	-	-	0.1920	0.5376	0.3584	1.1200	0.6400	0.5120	0.5120	0.1280	0.1280
4	-	-	-	-	0.3360	0.8064	0.4480	1.1200	0.4800	0.2560	0.1280	0.1280
5	-	-	-	-	-	0.4032	0.8064	0.3584	0.6720	0.1920	0.0512	0.0512
6	-	-	-	-	-	-	0.3360	0.5376	0.1792	0.2240	0.0320	0.0320
7	-	-	-	-	-	-	-	0.1920	0.2304	0.0512	0.0320	0.0320
8	-	-	-	-	-	-	-	-	0.0720	0.0576	0.0064	0.0064
9	-	-	-	-	-	-	-	-	-	0.0160	0.0064	0.0064
10	-	-	-	-	-	-	-	-	-	-	0.0016	0.0016

2.4.2.3 Exact performance of the S-WSR chart

Since an efficient and robust methodology for the computation of the general distribution of SR_t has been provided, practitioners are now capable of designing a scheme based on the statistic with exact in- and out-of-control RL properties without any prior knowledge for the sample's underlying distribution.

As shown in Section 2.4, the in-control average run length of the upper-sided S-WSR chart is computed as:

$$\text{ARL}^+_0 = \frac{1}{\alpha^+}$$

where the Type I error, α^+ is:

$$\alpha^+ = \mathrm{P}(\mathrm{SR}_t \geq C|\theta = \theta_0) = 1 - F_{\mathrm{SR}_t}(C-1|n, p = 0.5).$$

Similarly,the out-of-control average run length of the upper-sided S-WSR chart is computed as:

$$\mathrm{ARL}_1^+ = \frac{1}{1-\beta^+}$$

where the Type II error, β^+ is:

$$\beta^+ = \mathrm{P}(\mathrm{SR}_t < C|\theta = \theta_1) = 1 - F_{\mathrm{SR}_t}(C-1|n, p = p_1).$$

In Table 2.7 the *exact* distribution-free in- and out-of-control performance of the upper-sided S-WSR chart is presented for different values of the sample size n. Generally, in practice, for the desired in-control ARL_0^+ close to values like 200, 370 or 500 are preferable. So, for sample size n, the corresponding C values are presented with the corresponding in-control ARL^+ to be as close as possible to the above values. Note that, the corresponding in-control ARL_0 values and the false alarm rate probabilities (α_0) of the symmetric two-sided S-WSR chart can be obtained through the relations $\mathrm{ARL}_0 = \frac{\mathrm{ARL}_0^+}{2}$ and $\alpha_0 = 2\alpha_0^+$.

Table 2.7: In- and out-of-control ARL performance of the upper-sided S-WSR chart

	p									
C	0.5	0.55	0.6	0.65	0.7	0.75	0.8	0.85	0.9	0.95
					($n = 8$)					
32	85.33	45.30	25.52	15.11	9.34	5.99	3.97	2.71	1.90	1.36
34	127.99	65.68	35.72	20.40	12.14	7.49	4.77	3.12	2.09	1.43
36	255.97	119.42	59.54	31.38	17.35	9.99	5.96	3.67	2.32	1.51
					($n = 10$)					
50	204.79	95.73	48.01	25.57	14.34	8.41	5.14	3.25	2.13	1.44
52	341.30	149.75	70.88	35.76	19.06	10.65	6.21	3.75	2.35	1.51
54	511.93	217.14	99.23	48.28	24.78	13.32	7.45	4.32	2.58	1.59
					($n = 12$)					
64	215.58	94.25	44.78	22.86	12.43	7.16	4.35	2.78	1.87	1.33
66	292.58	124.61	57.69	28.70	15.20	8.52	5.03	3.12	2.03	1.39
68	409.62	168.00	75.18	36.23	18.63	10.15	5.82	3.50	2.21	1.45
					($n = 15$)					
90	239.17	93.91	40.77	19.33	9.93	5.49	3.26	2.09	1.45	1.12
92	297.87	114.68	48.87	22.76	11.48	6.24	3.64	2.28	1.55	1.16
94	372.33	140.46	58.70	26.82	13.28	7.08	4.05	2.49	1.66	1.21
					($n = 18$)					
120	260.03	93.24	37.70	16.96	8.42	4.58	2.74	1.80	1.31	1.07
122	304.06	107.23	42.65	18.88	9.22	4.94	2.90	1.87	1.34	1.08
124	357.08	123.82	48.44	21.10	10.13	5.34	3.08	1.95	1.37	1.09
					($n = 25$)					
200	326.42	95.78	33.15	13.32	6.16	3.26	1.98	1.38	1.11	1.01
202	358.64	104.01	35.59	14.14	6.46	3.38	2.03	1.40	1.11	1.01
204	394.52	113.08	38.26	15.03	6.79	3.52	2.08	1.42	1.12	1.01

It is worth stretching that, even though the S-WSR chart can be theoretically used with a relatively small sample size, it is practically impossible to design it in order to guarantee an acceptable and relative large in-control ARL_0 say $\text{ARL}_0 > 200$. In Table 2.8 some in-control ARL^+ values for the positive-sided S-WSR chart are presented for $n = \{5, 6, \ldots, 10\}$. For instance it can be seen that, when $n = 5$, the largest feasible in-control ARL^+ is obtained

for $C = 15$ and equals to $\text{ARL}_0^+ = 32$. Similarly, when $n = 7$, the largest feasible in-control ARL^+ is obtained for $C = 28$ and equals to $\text{ARL}_0^+ = 128$. As a general guidance to practitioners, they are advised to use the S-WSR chart for moderate to large values of the sample size.

Table 2.8: ARL_0^+ values for small sample sizes

(ARL_0^+, C)			
$n = 5$	$n = 6$	$n = 7$	$n = 8$
(6.40, 9)	(12.80, 15)	(25.60, 22)	(51.20, 30)
(6.40, 10)	(12.80, 16)	(25.60, 23)	(51.20, 31)
(10.67, 11)	(21.33, 17)	(42.67, 24)	(85.33, 32)
(16.00, 13)	(32.00, 19)	(64.00 ,26)	(127.99, 34)
(32.00, 15)	(64.00, 21)	(128.00, 28)	(255.97, 36)
$(\infty, > 15)$	$(\infty, > 21)$	$(\infty, > 28)$	$(\infty, > 36)$

2.5 The EWMA chart based on the Wilcoxon Signed Rank statistic

Graham et al. (2011b) introduced a new nonparametric two-sided EWMA chart based on the Wilcoxon Signed Rank statistic. Using the Markov-Chain approach of Brook and Evans (1972) they computed its in-control Run Length properties and obtained its optimal design parameters. Concerning its out-of-control performance they performed a Monte Carlo simulation under several symmetric distributions and different shifts in the process median. In this Section, we will revisit the design and practical implementation of the EWMA chart based on Signed Ranks as it was originally introduced by Graham et al. (2011b) along with its in- and out-of-control Run Length properties. The only difference will be that, similarly with the WSR Shewhart chart, the chart's out-of-control performance, will be computed exactly without any assumption of the sample's underlying distribution.

The two-sided EWMA chart based on Signed Ranks: Suppose that at each sampling point a subgroup $\{X_{t,1}, X_{t,2}, \ldots, X_{t,n}\}$ of size n, following a continuous *symmetric* distribution, is collected at time $t = 1, 2, \ldots$. The two-sided EWMA chart based on Signed Ranks (2-WSR EWMA chart) is defined by the following recursive formula:

$$Z_t = \lambda \mathrm{SR}_t + (1-\lambda) Z_{t-1}, Z_0 = \mathrm{E}_0(\mathrm{SR}_t). \tag{2.23}$$

Similarly with the design of the conventional parametric EWMA chart the asymptotic upper and lower control limits for the 2-WSR EWMA chart are defined as:

$$\mathrm{UCL} = \mathrm{E}_0(\mathrm{SR}_t) + K\sqrt{\mathrm{V}_0(\mathrm{SR}_t)} \times \sqrt{\frac{\lambda}{2-\lambda}}.$$

$$\mathrm{LCL} = \mathrm{E}_0(\mathrm{SR}_t) - K\sqrt{\mathrm{V}_0(\mathrm{SR}_t)} \times \sqrt{\frac{\lambda}{2-\lambda}}.$$

where $\mathrm{E}_0(\mathrm{SR}_t)$ and $\mathrm{V}_0(\mathrm{SR}_t)$ are the in-control mean and variance of SR_t. Using the relationship between SR_t and SR_t^+, presented in (2.11), the in-control expected value and variance of SR_t are equal to:

$$\mathrm{E}_0(\mathrm{SR}_t) = \mathrm{E}_0\left(2\mathrm{SR}_t^+ + \frac{n(n+1)}{2}\right) = \frac{n(n+1)(2p_0-1)}{2}, \tag{2.24}$$

$$\mathrm{V}_0(\mathrm{SR}_t) = \mathrm{V}_0\left(2\mathrm{SR}_t^+ + \frac{n(n+1)}{2}\right) = \frac{2n(n+1)(2p_0-1)}{3}, \tag{2.25}$$

where p_0 is the in control value. If we assume that θ is the median (i.e. $p_0 = 0.5$) we simply have $\mathrm{E}_0(\mathrm{SR}_t) = 0$ and $\mathrm{V}_0(\mathrm{SR}_t) = \frac{n(n+1)(2n+1)}{6}$. As a consequence, the in-control limits are simply reduced:

$$\mathrm{UCL} = +K\sqrt{\frac{\lambda}{2-\lambda}\frac{n(n+1)(2n+1)}{6}}. \tag{2.26}$$

$$\mathrm{LCL} = -K\sqrt{\frac{\lambda}{2-\lambda}\frac{n(n+1)(2n+1)}{6}}. \tag{2.27}$$

It should be noted that, as it will be shown hereafter the two-sided WSR EWMA chart, besides monitoring the median, can be also used for monitoring any percentile defined on

$p_0 \in (0, 1)$.

The upper-sided EWMA chart based on Signed Ranks: For the upper-sided EWMA chart based on Signed Ranks (WSR EWMA chart) the charting statistic is defined by the following recursive formula:

$$Z_t = \max(\mathrm{E}_0(\mathrm{SR}_t), \lambda \mathrm{SR}_t + (1-\lambda) Z_{t-1}), Z_0 = \mathrm{E}_0(\mathrm{SR}_t),$$

with a fixed asymptotic upper control limit and central line defined as:

$$\begin{aligned} \mathrm{UCL} =& \mathrm{E}_0(\mathrm{SR}_t) + K_1 \sqrt{\mathrm{V}_0(\mathrm{SR}_t)} \times \sqrt{\frac{\lambda}{2-\lambda}}. \\ \mathrm{CL} =& \mathrm{E}_0(\mathrm{SR}_t). \end{aligned}$$

Finally, assuming θ_0 as the in-control value of the process median (i.e $\mathrm{E}(\mathrm{SR}_t) = 0$ and $\mathrm{V}(\mathrm{SR}_t^+) = \frac{n(n+1)(2n+1)}{6}$) the above expressions are simply reduced as:

$$\begin{aligned} \mathrm{UCL} =& + K_1 \sqrt{\frac{\lambda}{2-\lambda} \frac{n(n+1)(2n+1)}{6}}. \\ \mathrm{CL} =& 0. \end{aligned}$$

As a Phase II practical implementation of the operation of the 2-WSR EWMA chart the following example is provided. Suppose that a practitioner is interested in monitoring a shift in the process median $\theta_0 = 5$ (i.e $p_0 = 0.5$) in the phase II sample of 10 subgroups of size $n = 10$ listed in Table 2.9. Additionally, the values of the charting statistic Z_t at each time t, are plotted in Figure 2.4. For illustrative purposes the chart parameters are set to $\lambda = 0.2, K = 2.7$ and $Z_t = 0$. Since $p_0 = 0.5$, the upper, UCL, and lower, LCL control limits will be symmetric around zero (CL = 0) and will be computed thought the expressions presented in equations (2.26) and (2.27). The computation of the charting statistic, Z_t defined in (2.23) will be:

- For $t = 1$ we have $\mathrm{SR}_1 = \sum_{k=1}^{10} \mathrm{sign}(X_{1,k} - 5) L_{1,k} = 5$. The corresponding value for the charting statistic is $Z_1 = 0.2 \times (5) + 0.8 \times 0 = 1$.
- For $t = 2$ we have $\mathrm{SR}_2 = \sum_{k=1}^{10} \mathrm{sign}(X_{2,k} - 5) L_{2,k} = 25$. The corresponding value for the charting statistic is $Z_2 = 0.2 \times (25) + 0.8 \times 1 = 5.80$.

  ⋮

- For $t = 10$ we have $\mathrm{SR}_{10} = \sum_{k=1}^{10} \mathrm{sign}(X_{10,k} - 5)L_{10,k} = 31$. The corresponding value for the charting statistic is $Z_{10} = 0.2 \times (31) + 0.8 \times (-5.64) = 1.69$.

Table 2.9: Illustrative example for the operation of the 2WSR-EWMA chart

	$X_{t,k}$									
n	1	2	3	4	5	6	7	8	9	10
1	5.87	5.98	5.28	5.17	4.88	6.00	7.95	4.97	4.71	7.55
2	5.45	6.55	5.80	4.47	4.69	3.22	4.05	4.99	5.72	4.19
3	4.85	5.32	4.94	5.22	4.34	6.09	4.23	4.65	4.79	3.55
4	4.48	5.43	3.61	6.04	3.82	4.49	5.27	3.94	4.20	5.57
5	5.04	6.14	5.64	5.90	6.37	5.03	4.61	5.15	3.70	5.83
6	3.89	4.57	6.26	5.56	4.74	6.60	5.41	4.98	3.86	5.33
7	3.89	5.56	3.45	4.68	4.12	4.56	3.86	5.11	5.87	6.84
8	5.13	4.40	5.04	4.75	5.54	2.24	4.66	5.32	4.53	6.01
9	6.11	4.77	4.80	5.26	4.56	4.03	4.39	5.81	5.19	5.23
10	6.88	4.84	5.94	3.64	5.16	4.31	5.43	5.21	5.03	6.33
Z_t	1.00	5.80	6.04	6.23	1.19	-1.25	-4.00	-1.80	-5.64	1.69
SR_t	5	25	7	7	-19	-11	-15	7	-21	31

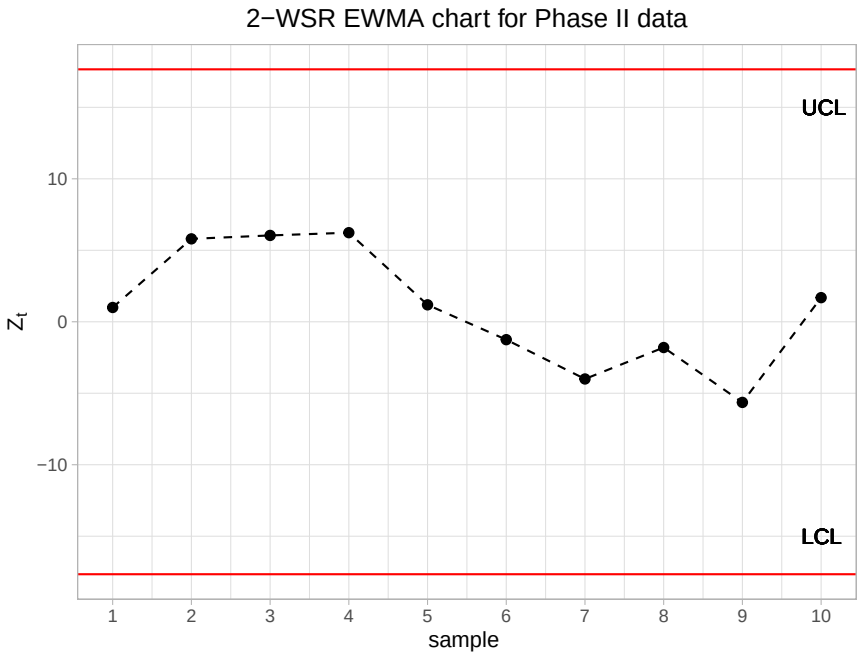

Figure 2.4: Illustrative example for the 2-WSR EWMA chart for the Phase II data listed in Table 2.9

2.5.1 RL properties of the two- and upper-sided WSR EWMA chart

Following the same approach used for the conventional parametric EWMA chart presented in Section 1.1.2.1, the transition probability matrix $\mathbf{P}$ of the 2-WSR EWMA chart is the same with the only difference that the transient probabilities, $Q_{j,k}$ are obtained as:

$$\begin{aligned} Q_{j,k} &= \mathrm{P}(Z_t \text{ is in state } k | Z_{t-1} \text{ is in state } j) \\ &= \mathrm{P}(H_k - \Delta \leq Z_t \leq H_k - \Delta | Z_{t-1} = H_j). \end{aligned} \tag{2.28}$$

By substituting the definition of the charting statistic, defined in (2.23), into (2.28) the

transient probabilities, $Q_{j,k}$ are equal:

$$\begin{aligned} Q_{j,k} &= \mathrm{P}\left(H_k - \Delta \leq \lambda \mathrm{SR}_t + (1-\lambda) Z_{t-1} \leq H_k + \Delta \middle| \, Z_{t-1} = H_j\right) \\ &= \mathrm{P}\left(H_k - \Delta \leq \lambda \mathrm{SR}_t + (1-\lambda) H_j \leq H_k + \Delta\right) \\ &= \mathrm{P}\left(\frac{H_k - \Delta - (1-\lambda)H_j}{\lambda} \leq \mathrm{SR}_t \leq \frac{H_k + \Delta - (1-\lambda)H_j}{\lambda}\right) \\ &= F_{\mathrm{SR}_t}\left(\frac{H_k + \Delta - (1-\lambda)H_j}{\lambda} | n, p_1\right) - F_{\mathrm{SR}_t}\left(\frac{H_k - \Delta - (1-\lambda)H_j}{\lambda} | n, p_1\right). \end{aligned}$$

Regarding the computation of $f_{\mathrm{SR}_t}(x|n, p_1)$, the method introduced in Section 2.4.2.2 will be used, in which the *general* distribution of SR_t is computed through the p.g.f. of SR_t^+ without any knowledge of the underlying distribution. It is worth stretching that in existing EWMA nonparamtetric control charts based on the Wilcoxon Signed Rank statistic the out-of-control performance is examined for a given distribution. On the other hand, the use of this method provides the capability of computing the chart's RL properties without any knowledge of the underlying distribution.

As a consequence, the transient probabilities, $Q_{j,k}$ of the 2-WSR EWMA chart for a given sample size, n and shift $p_1 \in (0, 1)$, are defined as:

$$\begin{aligned} &F_{\mathrm{SR}_t^+}\left(\frac{1}{2}\left(\frac{H_k + \Delta - (1-\lambda)H_j}{\lambda} + \frac{n(n+1)}{2}\right) \middle| n, p_1\right) - \\ &F_{\mathrm{SR}_t^+}\left(\frac{1}{2}\left(\frac{H_k - \Delta - (1-\lambda)H_j}{\lambda} + \frac{n(n+1)}{2}\right) \middle| n, p_1\right) \end{aligned} \tag{2.29}$$

Finally, The ARL and SDRL values of the WSR EWMA control chart, similarly with the upper-sided case presented in Section 1.1.2.1, are computed via the standard approach proposed by Brook and Evans (1972). The only difference will be in the computation of the transient probabilities where:

- if $j = 0$,

$$Q_{k,0} = F_{\mathrm{SR}_t}\left(-\frac{(1-\lambda)H_k}{\lambda} | n, p_1\right).$$

- if $j = 1, 2, \ldots, m$,

$$Q_{k,j} = F_{\mathrm{SR}_t}\left(\frac{H_i + \Delta - (1-\lambda)H_k}{\lambda}|n, p_1\right) - F_{\mathrm{SR}_t}\left(\frac{H_i - \Delta - (1-\lambda)H_k}{\lambda}|n, p_1\right). \tag{2.30}$$

2.5.2 Reliability of the Brook and Evans method in the chart's RL properties

The two-sided case: In order to examine the efficiency of the standard method of Brook and Evans (1972), for computing the RL properties of a EWMA chart based on the Wilcoxon signed rank statistic, in Figure 2.5 (plain lines) some in control ARL values are presented for $n = \{5, 7, 11, 14\}$ and $2m + 1 = \{51, 61, \ldots, 251\}$ with parameters $\lambda = 0.2$, $K = 2.85$. The values for λ and K have been randomly selected since in practice, for EWMA schemes, it is recommended to set $\lambda \approx 0.2$ and $K \approx 3$. Moreover, for each case, the corresponding ARL values, computed through a Monte Carlo simulation of 10^6 iterations, are reported (dotted lines). As it was previously stated, in conventional parametric EWMA control charts, setting the number of subintervals $2m+1 \approx 200$ yields to a reliable approximation of the chart's RL properties. However, from Figure 2.5, it can be seen that in the content of a nonparametric EWMA chart based on the Wilcoxon signed rank statistic the ARL_0 values are affected by the number of subintervals $2m + 1$. In particular, from Figure 2.5 we may conclude that:

- When $n = 5$, the in control ARL values vary from 468.9 to 509.0 and the corresponding simulated value is 494.8.
- When $n = 7$, the in control ARL values vary from 435.2 to 458.0 and the corresponding simulated value is 450.7.
- When $n = 11$, the in control ARL values vary from 404.2 to 415.0 and the corresponding simulated value is 413.7.
- When $n = 14$, the in control ARL values vary from 384.3 to 416.1 and the corresponding simulated value is 401.8.

Additionally, from Figure 2.6 it can be seen that, as expected, the exact same pattern occurs for the corresponding SDRL values also. More specifically:

- When $n = 5$, the in control SDRL values vary from 463.9 to 503.8 and the corresponding simulated value is 494.2.
- When $n = 7$, the in control SDRL values vary from 430.4 to 453.18 and the corresponding simulated value is 445.6.

- When $n = 11$, the in control SDRL values vary from 399.6 to 410.4 and the corresponding simulated value is 409.9.
- When $n = 14$, the in control SDRL values vary from 379.8 to 411.5 and the corresponding simulated value is 393.4.

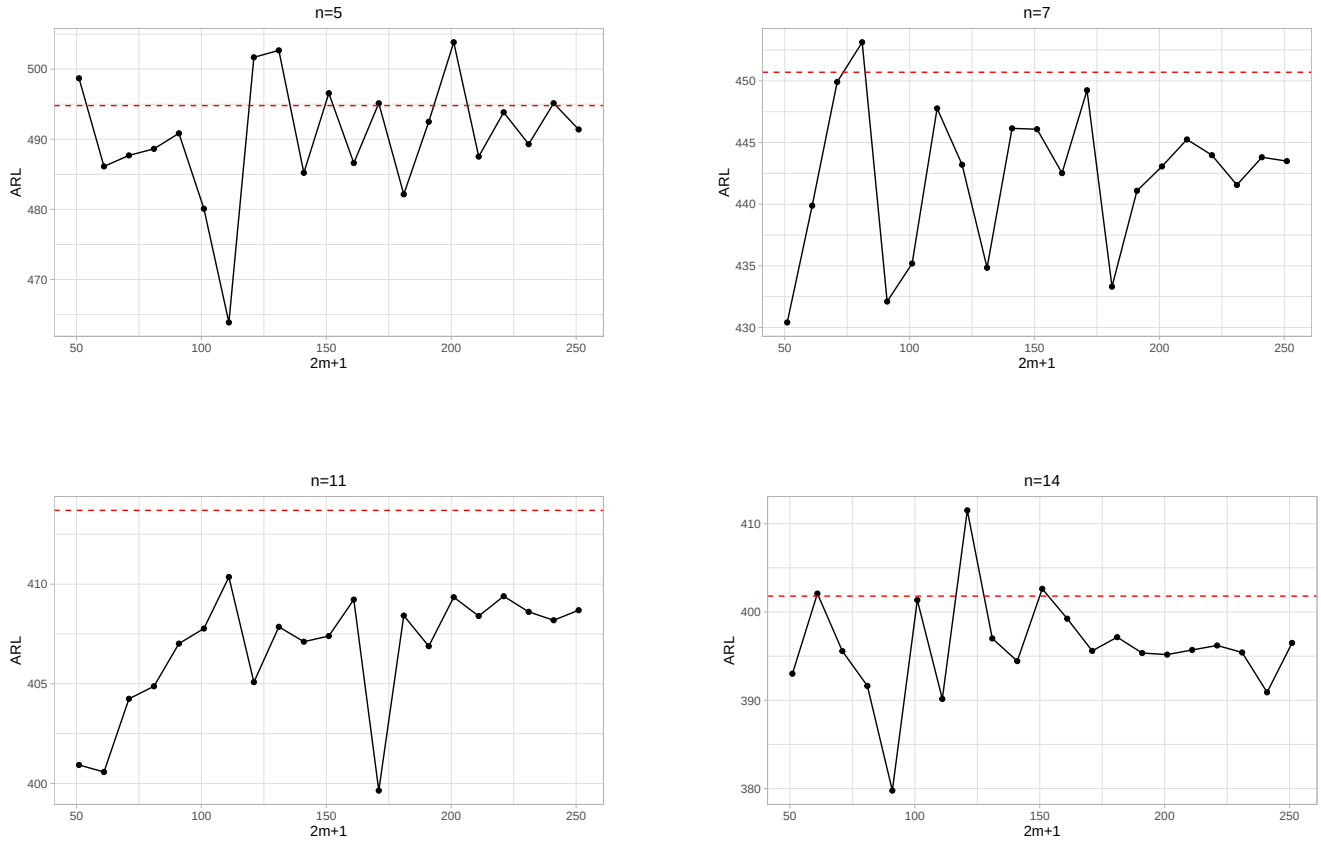

Figure 2.5: ARL_0 (plain lines) in function of the number of sub-intervals $2m + 1 \in \{51, 61, \ldots, 251\}$ for the 2- WSR EWMA chart with parameters $(\lambda = 0.2, K = 2.85)$ and $n \in \{5, 7, 11, 14\}$ using the standard Markov Chain method

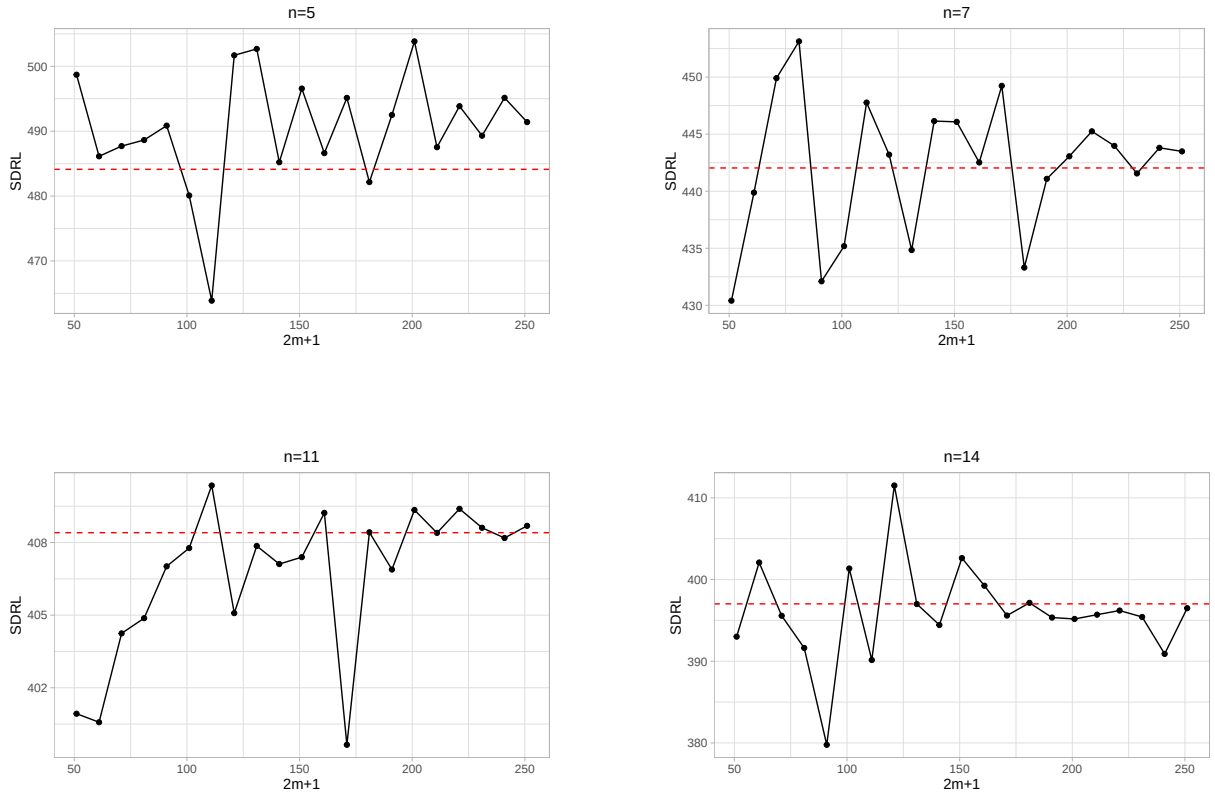

Figure 2.6: SDRL_0 (plain lines) in function of the number of sub-intervals $2m+1 \in \{51, 61, \ldots, 251\}$ for the 2- WSR EWMA chart with parameters $(\lambda = 0.2, K = 2.85)$ and $n \in \{5, 7, 11, 14\}$ using the standard Markov Chain method

The upper-sided case: Similarly with the two-sided case the efficiency of the standard method of Brook and Evans (1972), for the upper-sided WSR EWMA chart is tested. In Figure 2.7 some in-control ARL values are presented for $n = \{5, 10, 15, 20\}$ and $m = \{50, 60, \ldots, 200\}$ with parameters $\lambda = 0.2$, $K_1 = 2.75$. From Figure 2.7 we may conclude that the in-control ARL values are highly affected by the number of subintervals m. For instance, when $n = 15$, the in control ARL values vary from 293.4 to 535.5 and the corresponding simulated value is 494.8. Similarly, when $n = 20$, the in control ARL values vary from 342.4 to 382.6 and the corresponding simulated value is 374.8. We can see that comparing with the two-sided case the differences are way much larger.

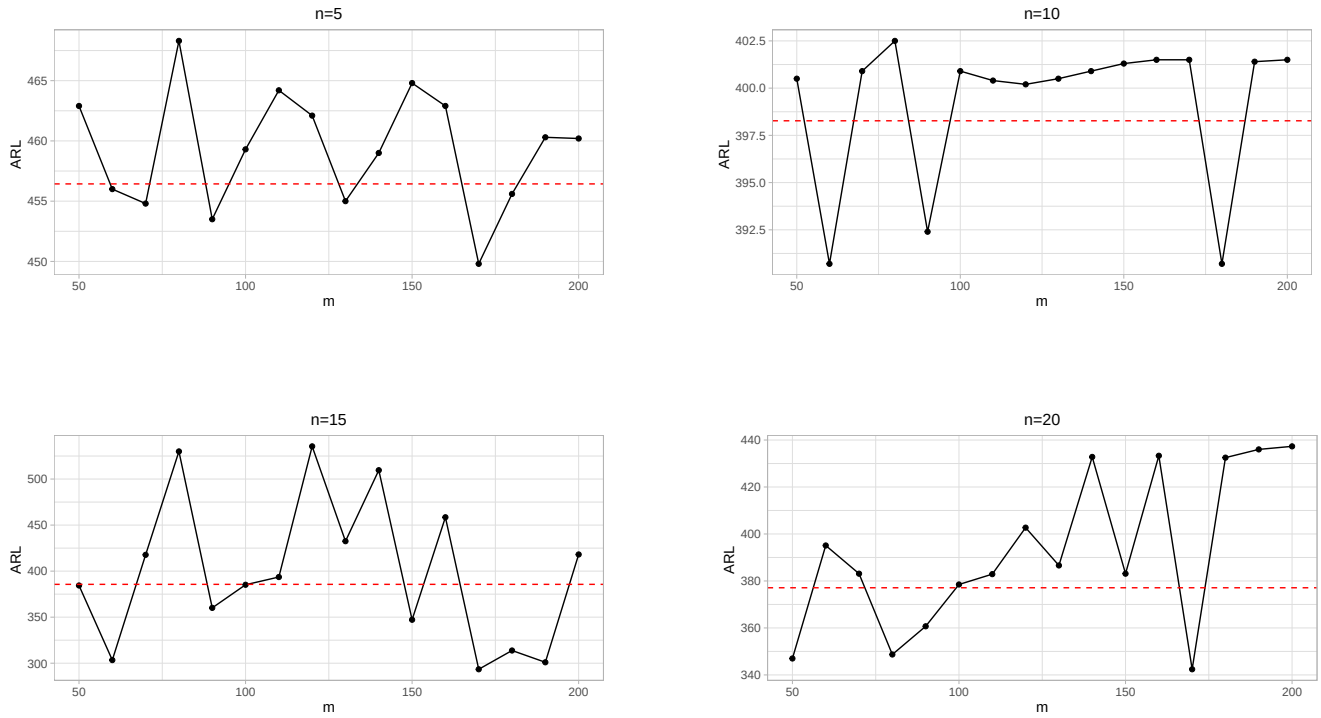

Figure 2.7: ARL_0 values in function of the number of sub-intervals $m \in \{50, 60, \ldots, 250\}$ for the WSR EWMA chart with parameters $(\lambda = 0.2, K_1 = 2.75)$ and $n \in \{5, 10, 15, 20\}$ using the standard Markov Chain method

2.6 Conclusions

As it has been highlighted so far, the conventional method of Brook and Evans (1972) is an efficient tool regarding the determination of the RL properties of a phase II parametric control chart. However, it has been proven that, when it is applied to nonparametric EWMA charts, there might be cases where the chart's RL properties are affected by the number of subintervals. As a consequence, the practitioners, during the design phase of the control chart, might not be able to properly optimized. The main motivation of this thesis is to propose schemes in which their RL properties are obtained through robust and simple methodologies in order to remain unaffected by the number of subintervals. In the rest of this work, efficient and simple approaches will be provided in which the ARL values (not only for the in-control but also for the out-of-control cases) are no longer affected by the number of sub-intervals and become rapidly stable.

Chapter 3

EWMA charts based on the Sign statistic with exact run length properties

Introduction

So far, it has been proved that the standard method of Brook and Evans (1972) is a robust technique for computing the RL properties of a conventional parametric EWMA chart. On the other hand, in the previous Chapter, it was highlighted the fact that when a nonparametric statistic, such as the Sign statistic, is considered, the chart's corresponding ARL and SDRL values might be affected by the number of subintervals. As a consequence, there might be cases where it is impossible to derive the chart's optimal deign parameters which will guarantee its optimal performance in terms of the ARL and SDRL metrics.

Recently, Wu et al. (2020) proposed a distribution-free EWMA-TBEA (Time Between Events and Amplitude) control chart where they introduced a new approach called as the "continuousify" method in which the values of the initial discrete random variables are transformed into continuous ones based on weighted Gaussian Kernels. As a result, since the Markov chain of Brook and Evans (1972) performs well in the case of continuous random variables, Wu et al. (2020) showed that the above method yields robust results without the need of setting large values for the number sub-intervals used in the Markov chain. In the rest of this Chapter, the"continuousify" method will be applied to the nonparametric EWMA chart based on the Sign statistic which, as it will be proven hereafter, yields to reliable results and the exact determination of the chart's in- and out-of-control RL properties. Parts of this Chapter have been published in Perdikis et al. (2021c).

3.1 A short review on the Kernel estimation method

The KDE (Kernel Density Estimation), originally introduced from the idea of Rosenblatt and Parzen (Parzen (1962)) dedicated to density estimation, is a very efficient technique being widely used for the estimation of the p.d.f. or the c.d.f. of random variables. (Wand and Jones (1994), Silverman (1986))

The Rosenblatt-Parzen Kernel estimator for the p.d.f. is:

$$\hat{f}(x) = \frac{1}{nh} \sum_{i=1}^{n} K\left(\frac{x - u_i}{h}\right), \tag{3.1}$$

where $\mathbf{u} = (u_1, u_2, \ldots, u_n)$ is the random sample from the population with unknown density function $f(x)$ of size n. The parameter h controls the smoothness of the estimator. Note that, for every Kernel function, the following conditions must hold:

- $K(x)$ is non-negative: $K(x) \geq 0$.
- $K(x)$ is symmetric: $K(x) = K(-x)$.

In addition $K(x)$ should be centered around zero with finite variance, i.e.:

$$\begin{aligned}
&\int_{\Omega} K(x)dx = 1, \\
&\int_{\Omega} xK(x)dx = 0, \\
&\int_{\Omega} x^2 K(x)dx = k_2 > 0.
\end{aligned}$$

Similarly, the Nadaraya Kernel estimator for the c.d.f. is defined as follows:

$$\hat{F}(x) = \frac{1}{n} \sum_{i=1}^{n} \int_{-\infty}^{\frac{x-u_i}{h}} K(y)dy = \frac{1}{n} \sum_{i=1}^{n} W\left(\frac{x - u_i}{h}\right), \tag{3.2}$$

where $W(x) = \int_{-\infty}^{t} K(t)dt$. According to Silverman (1986), the most popular metric, used as a measure of accuracy is the MISE (Mean Integrated Squared Error) expressed as:

$$\text{MISE}(\hat{f}(x)) = \int_{\forall x} MSE(\hat{f}(x))dx,$$

where $\text{MSE}(\hat{f}(x)) = \text{E}(\hat{f}(x) - f(x))^2$ is the mean squared error term. As shown in Parzen (1962) the optimal value of the parameter h can be obtained through the minimization of

the AMISE (approximated MISE):

$$\text{AMISE}(\hat{f}(x)) = \frac{1}{4}h^4 k_2^2 \int_{\forall x} (f^{(2)}(x))^2 dx + \frac{1}{nh}\int_{\forall t} K^2(t)dt.$$

Moreover, Parzen (1962) showed that the optimal value of h_a obtained by minimizing the AMISE is:

$$h_a = k_2^{-\frac{2}{5}} \left(\int_{\forall t} K^2(t)dt\right)^{\frac{1}{5}} \left(\int_{\forall x} (f^{(2)}(x))^2 dx\right)^{-\frac{1}{5}} n^{-\frac{1}{5}}.$$

In case where the density function of the observed data is unknown (as a consequence $f^{(2)}(x)$ is unknown) Rahman et al. (1995) proposed the following estimation:

$$\hat{f^{(2)}} = \frac{1}{nh}\sum_{i=1}^{n} K^{(2)}\left(\frac{x-u_i}{h}\right).$$

Alternately, a general class of density estimators, (or equivalently for c.d.f. Kernel estimation) can be defined in terms of a normalised sample, $\zeta_1, \zeta_2, \ldots, \zeta_n$ ($\sum_{i=1}^{n}\zeta_i = 1$) carrying a weight attached to the observations:

$$\hat{f}(x) = \frac{1}{nh}\sum_{i=1}^{n}\zeta_i K\left(\frac{x-u_i}{h}\right) \tag{3.3}$$

$$\hat{F}(x) = \frac{1}{n}\sum_{i=1}^{n}\zeta_i W\left(\frac{x-u_i}{h}\right) \tag{3.4}$$

3.1.1 The use of the "continuousified" method in SPC

Wu et al. (2020) proposed that any discrete random variable, X, can be well-presented by a new *continuous* one, X^* as a mixture of Normal distributions Y_t^* where, for each $\psi_t \in \Psi$,

$Y_t^* \sim N(\psi_t, h)$ the corresponding p.d.f. $f_{X^*}(x|\boldsymbol{\theta})$ and c.d.f. $F_{X^*}(x|\boldsymbol{\theta})$ of X_t^* is computed as:

$$f_{X^*}(x|\boldsymbol{\theta}) = \sum_{\psi \in \Psi} f_X(\psi|\boldsymbol{\theta}) f_{\mathrm{N}}(x|\psi, h), \tag{3.5}$$

$$F_{X^*}(x|\boldsymbol{\theta}) = \sum_{\psi \in \Psi} f_X(\psi|\boldsymbol{\theta}) F_{\mathrm{N}}(x|\psi, h), \tag{3.6}$$

For illustration purposes and a better understanding of the "continuousify"method the following example is considered. Suppose that X is an discrete random variable, defined in $\{-1, 0, 1\}$ with corresponding p.m.f. $f_X(x)$:

$$f_X(x) = \begin{cases} \frac{1}{4}, & \text{if } x = -1 \\ \frac{1}{4}, & \text{if } x = 0 \\ \frac{1}{2}, & \text{if } x = 1 \end{cases}.$$

Then according to Wu et al. (2020), X can be well-presented by a new *continuous* random variable, X^* as a mixture of Normal distributions as:

$$X^* = \begin{cases} Y_{-1}^*, & \text{if } X = -1 \\ Y_0^*, & \text{if } X = 0 \\ Y_1^*, & \text{if } X = 1 \end{cases}.$$

where $Y_{-1}^* \sim \mathrm{N}(-1, h)$, $Y_0^* \sim \mathrm{N}(0, h)$ and $Y_1^* \sim \mathrm{N}(1, h)$ Additionally, the parameter h is a fixed value called as the "continuousify" parameter.

Then the p.d.f and c.d.f of the transformed variable X^* are computed as:

$$f_{X^*}(x|h) = w_{-1} f_{\mathrm{N}}(x| - 1, h) + w_0 f_{\mathrm{N}}(x|0, h) + w_1 f_{\mathrm{N}}(x|1, h),$$

$$F_{X^*}(x|h) = w_{-1} F_{\mathrm{N}}(x|0, h) + w_0 F_{\mathrm{N}}(x|0, h) + w_1 F_{\mathrm{N}}(x|1, h),$$

with weights $w_{-1} = \frac{1}{4}$,$w_0 = \frac{1}{4}$ and $w_1 = \frac{1}{2}$, corresponding to the probabilities of $f_X(x|h), x \in \{-1, 0, 1\}$.

3.2 The "continuousified" two-sided SN EWMA chart

3.2.1 Theoretical properties of the new transformed variable

For the proposed scheme based on the Sign statistic, since the domain in which SN_t is defined is $\Psi = \{-n, -n+2, \ldots, n-2, n\}$, the statistic SN_t will be transformed into a new *continuous* one denoted as SN_t^*:

$$\mathrm{SN}_t^* = \begin{cases} \text{Generate from } \mathrm{N}(-n, h), & \text{if } \mathrm{SN}_t = -n \\ \text{Generate from } \mathrm{N}(-n+2, h), & \text{if } \mathrm{SN}_t = -n+2 \\ \vdots & \vdots \\ \text{Generate from } \mathrm{N}(0, h), & \text{if } \mathrm{SN}_t = 0 \\ \vdots & \vdots \\ \text{Generate from } \mathrm{N}(n-2, h), & \text{if } \mathrm{SN}_t = n-2 \\ \text{Generate from } \mathrm{N}(n, h), & \text{if } \mathrm{SN}_t = n \end{cases}.$$

The computation of the p.d.f. $f_{\mathrm{SN}_t^*}(s|n, p_{+1})$ and c.d.f. $F_{\mathrm{SN}_t^*}(s|n, p_{+1})$ of the new transformed statistic, SN_t^* defined for $s \in \Psi$ will be obtained as:

$$f_{\mathrm{SN}_t^*}(s|n, p_{+1}) = \sum_{\psi \in \Psi} f_{\mathrm{Bin}}\left(\frac{\psi + n}{2}|n, p_{+1}\right) f_{\mathrm{N}}(s|\psi, h), \tag{3.7}$$

$$F_{\mathrm{SN}_t^*}(s|n, p_{+1}) = \sum_{\psi \in \Psi} f_{\mathrm{Bin}}\left(\frac{\psi + n}{2}|n, p_{+1}\right) F_{\mathrm{N}}(s|\psi, h), \tag{3.8}$$

3.2.2 Charting statistic and control limits

Following the same design with the conventional two-sided EWMA chart, the charting statistic of the "continuousified" two-sided SN EWMA (denoted as 2C-SN EWMA chart) will be defined as:

$$Z_t^* = \lambda \mathrm{SN}_t^* + (1-\lambda) Z_{t-1}^*, Z_0^* = \mathrm{E}_0(\mathrm{SN}_t^*), \tag{3.9}$$

with fixed asymptotic control limits:

$$\mathrm{LCL} = \mathrm{E}_0(\mathrm{SN}_t^*) - K\sqrt{\mathrm{SN}(\mathrm{SN}_t^*)} \times \sqrt{\frac{\lambda}{2-\lambda}}. \tag{3.10}$$

$$\text{UCL} = \text{E}_0(\text{SN}_t^*) + K\sqrt{\text{V}_0(\text{SN}_t^*)} \times \sqrt{\frac{\lambda}{2-\lambda}}. \tag{3.11}$$

The mean $\text{E}(\text{SN}_t^*)$ and variance $\text{V}(\text{SN}_t^*)$ of SN_t^* are equal to:

$$\begin{aligned} \text{E}(\text{SN}_t^*) &= \text{E}(\text{SN}_t), \\ \text{V}(\text{SN}_t^*) &= \text{V}(\text{SN}_t) + h^2. \end{aligned} \tag{3.12}$$

More specifically, let $\text{E}_N(X) = \mu$ and $\text{V}_N(X) = h^2$ denote the mean and variance of a random variable, X, from a Normal distribution. Then the mean of SN_t^*, is computed as:

$$\begin{aligned} \text{E}(\text{SN}_t^*) &= \int_{-\infty}^{\infty} s \times f_{\text{SN}_t^*}(s|n, p_{+1})ds \\ &= \int_{-\infty}^{\infty} s \times \sum_{\psi\in\Psi} f_{\text{Bin}}\left(\frac{\psi+n}{2}|n, p_{+1}\right) \times f_{\text{N}}(s|\psi, h)ds \\ &= \sum_{\psi\in\Psi}\left[f_{\text{Bin}}\left(\frac{\psi+n}{2}|n, p_{+1}\right) \times \int_{-\infty}^{\infty} s \times f_{\text{N}}(s|\psi, h)ds\right] \\ &= \sum_{\psi\in\Psi}\left[f_{\text{Bin}}\left(\frac{\psi+n}{2}|n, p_{+1}\right) \times \text{E}_N(s)\right] \\ &= \sum_{\psi\in\Psi}\left[f_{\text{Bin}}\left(\frac{\psi+n}{2}|n, p_{+1}\right) \times \psi\right] \\ &= \text{E}(\text{SN}) \end{aligned}$$

Similarly, using the fact that $\text{E}(\text{SN}_t^*) = \text{E}(\text{SN})$ the variance of SN_t^* is computed as:

$$
\begin{aligned}
\mathrm{V}(\mathrm{SN}_t^*) &= \mathrm{E}\left(\mathrm{SN}_t^*\right)^2 - \left(\mathrm{E}(\mathrm{SN}_t^*)\right)^2 \\
&= \int_{-\infty}^{\infty} s^2 \times f_{\mathrm{SN}_t^*}(s|n,p_1)ds - \left(\mathrm{E}(\mathrm{SN}_t^*)\right)^2 \\
&= \int_{-\infty}^{\infty} s^2 \times \sum_{\psi\in\Psi}\left[f_{\mathrm{SN}_t}\left(\frac{\psi+n}{2}|n,p_{+1}\right) \times f_{\mathrm{N}}(s|\psi,h)\right]ds - \left(\mathrm{E}(\mathrm{SN}_t)\right)^2 \\
&= \sum_{\psi\in\Psi}\left[f_{\mathrm{Bin}}\left(\frac{\psi+n}{2}|n,p_{+1}\right) \times \int_{-\infty}^{\infty} s^2 \times f_{\mathrm{N}}(s|\psi,h)ds\right] - \left(\mathrm{E}(\mathrm{SN}_t)\right)^2 \\
&= \sum_{\psi\in\Psi}\left[f_{\mathrm{Bin}}\left(\frac{\psi+n}{2}|n,p_{+1}\right) \times \mathrm{E}_N(s^2)\right] - \left(\mathrm{E}(\mathrm{SN}_t)\right)^2 \\
&= \sum_{\psi\in\Psi}\left[f_{\mathrm{Bin}}\left(\frac{\psi+n}{2}|n,p_{+1}\right) \times \left(\mathrm{V}_N(s) + (\mathrm{E}_N(s))^2\right)\right] - \left(\mathrm{E}(\mathrm{SN}_t)\right)^2 \\
&= \sum_{\psi\in\Psi}\left[f_{\mathrm{Bin}}\left(\frac{\psi+n}{2}|n,p_{+1}\right) \times \left(h^2+\psi^2\right)\right] - \left(\mathrm{E}(\mathrm{SN}_t)\right)^2 \\
&= h^2 \times \sum_{\psi\in\Psi} f_{\mathrm{Bin}}\left(\frac{\psi+n}{2}|n,p_{+1}\right) + \sum_{\psi\in\Psi}\psi^2 \times f_{\mathrm{Bin}}\left(\frac{\psi+n}{2}|n,p_{+1}\right) - \left(\mathrm{E}(\mathrm{SN}_t)\right)^2 \\
&= h^2 + \mathrm{E}\left(\mathrm{SN}_t\right)^2 - \left(\mathrm{E}(\mathrm{SN}_t)\right)^2 \\
&= h^2 + \mathrm{V}(\mathrm{SN}_t).
\end{aligned}
$$

It can be clearly seen that the expressions in (3.12) are obtained regardless the nonparametric statistic being used. As a consequence, the "continuousified" method is applicable to *any* nonparametric statistic. Finally, for the in-control case (i.e. for $p_0 = 0.5$, assuming θ as the process median. the in-control mean and variance of SN_t^* will be:

$$
\begin{aligned}
\mathrm{E}(\mathrm{SN}_t^*) &= 0, \\
\mathrm{V}(\mathrm{SN}_t^*) &= n + h^2.
\end{aligned} \tag{3.13}
$$

For illustrative purposes regarding the computation of the charting statistic of the proposed chart, a random generated dataset of $t = 5$ subgroups of size $n = 10$ is provided in Table 3.1. The values of the design parameters, $(\lambda, K, h) = (0.2, 2.85, 0.2)$, have been randomly chosen just for illustration purposes. Finally, the charting statistic Z_t^* is plotted in Figure 3.1.

- For $t = 1$ we have $\mathrm{SN}_1 = -2$. The corresponding value for SN_1^* is computed by

generating a $\mathrm{N}(-2, 0.2)$ random variable $Y_1 = -1.953$. The value of the charting statistic is $Z_1^* = 0.2 \times Y_1 + 0.8 \times 0 = -0.391$.

- For $t = 2$ we have $\mathrm{SN}_2 = 4$. The corresponding value for SN_2^* is computed by generating a $\mathrm{N}(4, 0.2)$ random variable $Y_2 = 3.792$. The value of the charting statistic is $Z_2^* = 0.2 \times Y_2 + 0.8 \times (-0.391) = 0.446$.
  $\vdots$

- For $t = 10$ we have $\mathrm{SN}_{10} = -4$. The corresponding value for SN_{10}^* is computed by generating a $\mathrm{N}(-4, 0.2)$ random variable $Y_{10} = -4.131$. The value of the charting statistic is $Z_{10}^* = 0.2 \times Y_{10} + 0.8 \times (1.296)) = 0.211$.

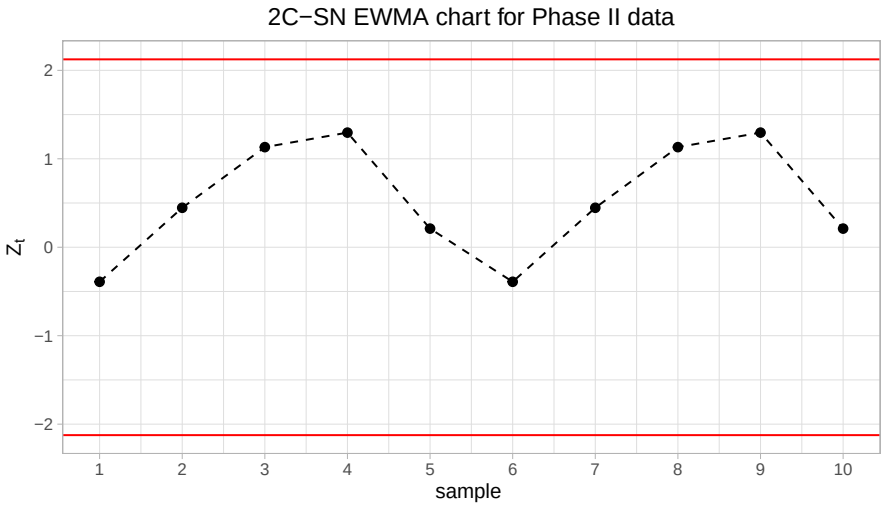

Figure 3.1: Illustrative example for the 2C-SN EWMA chart for the Phase II data listed in Table 3.1

Table 3.1: Illustrative example for the 2C-SN EWMA chart

	$X_{t,k}$				
n	1	2	3	4	5
1	4.021	5.539	6.061	5.287	3.082
2	4.257	6.795	5.856	4.105	5.579
3	5.015	4.767	5.767	5.123	4.047
4	5.092	5.194	4.549	4.927	4.049
5	3.463	5.677	5.615	5.475	4.954
6	3.899	5.166	5.896	5.051	3.986
7	5.220	5.260	4.536	5.534	2.978
8	5.708	4.169	5.540	4.047	3.408
9	4.769	4.925	5.627	3.055	6.139
10	4.111	5.973	3.813	6.222	6.974
SN_t	-2	4	4	2	-4
SN_t^*	-1.953	3.792	3.875	1.953	-4.131
Z_t^*	-0.391	0.446	1.132	1.296	0.211

3.2.3 Run Length properties and efficiency

In order to obtain the RL properties of the two-sided 2C-SN EWMA control chart, the standard discrete-time Markov chain approach of Brook and Evans (1972) presented in Section 2.3.1 will be used with the only difference that the p.m.f. of SN_t will be replaced by the p.d.f. of SN_t^* in the computation of the transient probabilities $Q_{k,i}$ as:

$$F_{SN_t^*}\left(\frac{H_k+\Delta-(1-\lambda)H_j}{\lambda}\middle|n,p_1\right)-F_{SN_t^*}\left(\frac{H_k-\Delta-(1-\lambda)H_j}{\lambda}\middle|n,p_1\right). \tag{3.14}$$

It should be pointed out that even though the operations of this chart requires random numbers to be generated, its Run Length properties (ARL, SDRL, ...), are obtained directly through the distribution of the SN_t^* with the exact Markov chain method shown above without the need of performing any simulations. This fact has also mentioned by Wu et al. (2020).

In order to show the efficiency of the "continuousify" method, Table 3.2 presents some in-control ARL values of the 2-SN EWMA (without "continuousify") and 2C-SN EWMA (with "continuousify") charts for $\lambda = 0.2$, $K = 2.85$ for several combinations of (n, p_0). In

Table 3.2, the value $h = 0.2$ has been fixed but, as it will be highlighted in the next Section, the results are are not significantly affected by this choice. Additionally, even though the value of K is fixed as it will be shown hereafter the following results are consistent regardless the value of K. Based on the results in Table 3.2 we draw the following conclusions:

- As it has has been already shown in Figure 2.1, the ARL_0 values obtained without "continuousify" (i.e. the 2-SN EWMA chart) strongly fluctuate depending on the value of $2m+1$. Clearly, they do not exhibit any monotonic convergence. For instance, when $n = 6$, the in control ARL values obtained without "continuousify" range from 392.5 to 469.6 (see, Table 3.2). Of course, we may argue with the fact that, by considering a really large number of subintervals and a large sample size, the results, obtained by the classical method of Brook and Evans (1972), will eventually converge. However, for small to moderate sample sizes, there is not guarantee that the same will happen and most important the computational cost is significantly increased.

- On the contrary, for $2m + 1 \geq 101$, the ARL values obtained with the "continuousify" method (i.e. the 2C-SN EWMA chart) exhibit a *strong* stability and they seem to converge rapidly to a reliable value. Even for $2m + 1 = 101$ the results obtained with the "continuousify" approach are very reliable. For instance, using the same case when $n = 6$, the ARL_0 values obtained with "continuousify" converge rapidly to 419. As a consequence, we are able to compute the chart's ARL_0 value eliminating the effect of ties an most important minimizing the computational cost during the chart's optimization.

We have also computed the ARL values of the 2-WSR EWMA chart using 10^6 Monte-Carlo simulation runs (see bottom of Table 3.2). What can be seen is that the in-control ARL values obtained with the "continuousify" method are almost the same or just a bit larger to the ones obtained using simulations. Additionally, as expected, the same pattern occurs for the corresponding SDRL values.

Based on the results presented so far, for randomly selected values of the design parameters (λ, K) the superiority of the "continuousify" method was verified when is being used in a nonparametric two-sided EWMA scheme based on the Sign statistic. It has been proven that the continuous transformation of the discrete statistic (such as the Sign statistic) combined with the standard method of the Brook and Evans (1972) makes the in-control ARL values steady and unaffected by the number of subinterval, even when $2m + 1 \approx 101$. The rest of this Chapter will be focused to an extensive sensitivity analysis, regarding the performance and reliability of the "continuousify" method when is used in the two-sided Sign EWMA charts.

Table 3.2: Comparison of ARL values for the two-sided 2-SN EWMA (without "continuousify") and two-sided 2C-SN EWMA (with "continuousify" and $h = 0.2$) chart when $\lambda = 0.2$ and $K = 2.85$

	$(n = 6, p_{+1} = 0.5)$		$(n = 12, p_{+1} = 0.5)$		$(n = 21, p_{+1} = 0.5)$		$(n = 23, p_{+1} = 0.5)$	
$2m+1$	2-SN EWMA	2C-SN EWMA	2-SN EWMA	2C-SN EWMA	2-SN EWMA	2C-SN EWMA	2-SN EWMA	2C-SN EWMA
51	(392.5,387.9)	(416.5,411.9)	(418.1,413.5)	(382.6,378.1)	(350.3,346.1)	(367.1,362.7)	(376.3,372)	(371.6,367.3)
61	(469.6,464.6)	(417.4,412.8)	(372.9,368.5)	(382.6,378.2)	(366.7,362.4)	(372.2,367.8)	(383.9,379.6)	(371.5,367.1)
71	(427.5,422.8)	(418,413.3)	(382.9,378.5)	(383.1,378.6)	(377.6,373.3)	(372.3,368)	(359,354.8)	(371.4,367.1)
81	(426.9,422.3)	(418.3,413.7)	(399.6,395.2)	(383.4,379)	(368.1,363.7)	(372.9,368.6)	(381.1,376.8)	(372.4,368.1)
91	(433,428.4)	(418.5,413.9)	(397.7,393.2)	(383.6,379.2)	(378.9,374.5)	(373.1,368.8)	(375.1,370.7)	(372.7,368.4)
101	(437.4,432.8)	(418.7,414.1)	(386.6,382.2)	(383.8,379.4)	(377.1,372.8)	(373.3,368.9)	(376.8,372.4)	(372.8,368.4)
111	(419.9,415.3)	(418.8,414.2)	(389.5,385)	(383.9,379.5)	(375.7,371.4)	(373.4,369.1)	(368,363.7)	(372.9,368.5)
121	(406.6,401.9)	(418.9,414.3)	(388.3,383.9)	(384,379.6)	(383.5,379.1)	(373.5,369.1)	(377.2,372.9)	(373,368.6)
131	(409.5,405)	(419,414.4)	(391.8,387.3)	(384.1,379.6)	(381.2,376.9)	(373.5,369.2)	(370.7,366.4)	(373,368.7)
141	(400.9,396.3)	(419.1,414.4)	(372.5,368.1)	(384.1,379.7)	(369.2,364.8)	(373.6,369.3)	(381.7,377.4)	(373.1,368.8)
151	(406.6,401.9)	(419.1,414.5)	(375.5,371.1)	(384.2,379.8)	(379.1,374.7)	(373.6,369.3)	(373.7,369.3)	(373.1,368.8)
161	(431.1,426.5)	(419.2,414.5)	(375.8,371.4)	(384.2,379.8)	(385,380.6)	(373.7,369.3)	(372.9,368.6)	(373.2,368.8)
171	(431,426.4)	(419.2,414.6)	(372.7,368.4)	(384.2,379.8)	(373.2,368.9)	(373.7,369.4)	(376.9,372.5)	(373.2,368.9)
181	(419.6,414.9)	(419.2,414.6)	(382.2,377.8)	(384.3,379.8)	(371.3,367)	(373.7,369.4)	(372.8,368.5)	(373.2,368.9)
191	(419.9,415.3)	(419.3,414.6)	(382.6,378.2)	(384.3,379.9)	(373.8,369.4)	(373.8,369.4)	(371.7,367.3)	(373.2,368.9)
201	(416.9,412.3)	(419.3,414.6)	(386.1,381.6)	(384.3,379.9)	(375.7,371.4)	(373.8,369.4)	(369.5,365.2)	(373.3,368.9)
sim	**(418.7, 414.5**)		**(384.0,379.9)**		**(373.6 ,368.8)**		**(372.0 ,378.4)**	
	$(n = 6, p_{+1} = 0.52)$		$(n = 12, p_{+1} = 0.55)$		$(n = 21, p_{+1} = 0.53)$		$(n = 23, p{+}1 = 0.52)$	
$2m+1$	2-SN EWMA	2C-SN EWMA	2-SN EWMA	2C-SN EWMA	2-SN EWMA	2C-SN EWMA	2-SN EWMA	2C-SN EWMA
51	(300.9,295.9)	(318.4,313.3)	(77.3,71.5)	(73.3,67.7)	(101.2,95.7)	(104.6,99.1)	(172.3,167)	(170.7,165.4)
61	(354.8,349.5)	(318.9,313.9)	(71.7,66.1)	(73.3,67.6)	(104.4,98.9)	(105.5,100)	(174.9,169.6)	(170.5,165.2)
71	(325.7,320.6)	(319.3,314.2)	(73.1,67.5)	(73.3,67.6)	(107,101.5)	(105.5,100)	(165.7,160.5)	(170.5,165.2)
81	(325.2,320.1)	(319.5,314.4)	(74.9,69.2)	(73.3,67.7)	(104.3,98.7)	(105.6,100.1)	(173.8,168.5)	(170.8,165.5)
91	(329.6,324.6)	(319.6,314.6)	(74.6,68.9)	(73.3,67.7)	(106.7,101.1)	(105.6,100.1)	(171.5,166.2)	(170.9,165.6)
101	(333,328)	(319.7,314.7)	(73.5,67.8)	(73.3,67.7)	(106.1,100.6)	(105.7,100.1)	(172.1,166.8)	(170.9,165.6)
111	(319.2,314.2)	(319.8,314.8)	(73.7,68)	(73.3,67.7)	(106.1,100.5)	(105.7,100.1)	(169.2,163.9)	(170.9,165.6)
121	(310.5,305.4)	(319.9,314.8)	(73.9,68.2)	(73.4,67.7)	(107.6,102.1)	(105.7,100.2)	(172.5,167.2)	(170.9,165.7)
131	(312.6,307.6)	(319.9,314.9)	(73.7,68)	(73.4,67.7)	(107.3,101.8)	(105.7,100.2)	(169.7,164.4)	(171,165.7)
141	(306.7,301.7)	(320,314.9)	(71.5,65.9)	(73.4,67.7)	(104.7,99.2)	(105.7,100.2)	(174.1,168.8)	(171,165.7)
151	(310.5,305.4)	(320,314.9)	(72,66.4)	(73.4,67.7)	(106.5,100.9)	(105.7,100.2)	(171,165.7)	(171,165.7)
161	(327.8,322.8)	(320,315)	(72.2,66.6)	(73.4,67.7)	(107.8,102.3)	(105.7,100.2)	(170.6,165.3)	(171,165.7)
171	(327.8,322.8)	(320,315)	(71.8,66.2)	(73.4,67.7)	(105.5,99.9)	(105.7,100.2)	(172.3,166.9)	(171,165.7)
181	(319.9,314.8)	(320.1,315)	(72.8,67.1)	(73.4,67.7)	(105.2,99.6)	(105.7,100.2)	(170.8,165.5)	(171,165.7)
191	(320.1,315)	(320.1,315)	(73,67.3)	(73.4,67.7)	(105.3,99.7)	(105.7,100.2)	(170.2,164.9)	(171,165.7)
201	(317.9,312.9)	(320.1,315)	(73.4,67.7)	(73.4,67.7)	(105.9,100.4)	(105.7,100.2)	(169.8,164.5)	(171,165.7)
sim	**(317.5,312.7)**		**(73.1,66.7)**		**(104.9,99.4)**		**(170.6,164.4)**	

3.2.4 Sensitivity analysis

Based on the results presented so far, it is clear that the "continuousify" method is a great improvement in the computation of the RL properties of a nonparametric EWMA control chart based on the Sign statistic. In this Section, the stability, and the advantages that the "continuousify" method provides will be highlighted, focussing on the:

- Effect of the chart parameters (λ, K, h) and the desired value for ARL_0.
- Effect of the shift magnitude p_1.
- Effect of the Kernel density estimation method.
- Effect of the in-control value of p_{+1}.

3.2.4.1 Effect of the chart parameters (λ, K, h) and the desired value of ARL_0

In should be noted that, in the computations performed so far, the smoothing parameter h was fixed and equal to 0.2. Generally, in Kernel density estimation methods, the optimal value of h is usually obtained through optimization procedures as presented in Section 3.1. In Table 3.3 for different combinations of n, p_{+1} and $h = \{0.1, 0.15, 0.2, 0.25, 0.3\}$ the corresponding in-control ARL values are presented as a function of the number of subintervals. For each case, the chart's parameters λ, K are chosen in order to give a desired $\text{ARL}_0 = 370.4$. From Table 3.3 it can be seen that the value of h does not affect the results. In particular, when h is neither too small or too large the results the same. As a consequence, setting the value of $h \approx 0.2$ is a reasonable choice to consider.

During the design phase of an EWMA chart, practitioners need to find a combination of the parameters λ, K which will give a corresponding in control $\text{ARL}(K, \lambda, p_0) = \text{ARL}_0$ where ARL_0 is a predefined fixed constant. In practice, the desired value of the in-control ARL is set to be equal (or at least really close) to relative large values such as 200, 370.4, or 500. In Table 3.4 comparisons between the two-sided 2-SN EWMA (without "continuousify") and two-sided 2C-SN EWMA (with "continuousify" and $\sigma = 0.2$) charts are presented when the desired fixed ARL_0 values are 200, 370.4 and 500. It can be seen that for $\text{ARL}_0 = 200$ there are no significant differences between the two approaches. For, $\text{ARL}_0 = 370.4$ or $\text{ARL}_0 = 500$ from Table 3.4 we see that by considering a small numbers of subintervals the results obtained by the standard approach of Brook and Evans fluctuate.

Table 3.3: ARL values of the 2C-SN EWMA chart for $\lambda = 0.2$, $K = 2.85$ and for fixed values of $h = \{0.1, 0.15, \ldots, 0.3\}$ and different values of n

	$(n, p_{+1}) = (5, 0.5)$					$(n, p_{+1}) = (8, 0.5)$					$(n, p_{+1}) = (11, 0.5)$				
	h					h					h				
$2m+1$	0.1	0.15	0.2	0.25	0.3	0.1	0.15	0.2	0.25	0.3	0.1	0.15	0.2	0.25	0.3
51	416.1	420.4	420.6	420.1	419.6	392.0	393.2	393.6	393.9	394.1	369.7	382.7	388.3	389.3	388.9
61	424.6	422.3	421.7	421.2	420.6	393.1	394.0	394.4	394.7	395.0	395.2	392.2	391.0	390.3	389.6
71	422.9	422.9	422.3	421.8	421.3	395.0	394.7	394.9	395.2	395.5	392.8	392.0	391.4	390.7	390.0
81	423.8	423.3	422.7	422.2	421.7	394.8	395.0	395.3	395.6	395.9	392.4	392.1	391.6	390.9	390.2
91	424.1	423.6	423.0	422.5	421.9	395.0	395.3	395.5	395.8	396.1	392.0	392.3	391.8	391.1	390.4
101	424.3	423.8	423.2	422.7	422.1	395.3	395.4	395.7	396.0	396.2	393.4	392.4	391.9	391.2	390.6
111	424.5	423.9	423.4	422.8	422.3	395.4	395.6	395.8	396.1	396.4	392.9	392.5	392.0	391.3	390.7
121	424.6	424.0	423.5	423.0	422.4	395.5	395.7	395.9	396.2	396.5	392.9	392.6	392.0	391.4	390.7
131	424.7	424.1	423.6	423.1	422.5	395.6	395.8	396.0	396.3	396.6	393.0	392.7	392.1	391.5	390.8
141	424.8	424.2	423.7	423.1	422.6	395.6	395.8	396.1	396.3	396.6	393.1	392.7	392.1	391.5	390.9
151	424.8	424.3	423.7	423.2	422.6	395.7	395.9	396.1	396.4	396.6	393.1	392.7	392.2	391.6	390.9
161	424.9	424.3	423.8	423.2	422.7	395.7	395.9	396.1	396.4	396.7	393.1	392.8	392.2	391.6	390.9
171	424.9	424.4	423.8	423.3	422.7	395.7	395.9	396.2	396.5	396.7	393.1	392.8	392.2	391.6	390.9
181	424.9	424.4	423.8	423.3	422.8	395.8	395.9	396.2	396.5	396.8	393.2	392.8	392.2	391.6	391.0
191	425.0	424.4	423.9	423.3	422.8	395.8	396.0	396.2	396.5	396.8	393.2	392.8	392.3	391.6	391.0
201	425.0	424.4	423.9	423.4	422.8	395.8	396.0	396.2	396.5	396.8	393.2	392.8	392.3	391.7	391.0

	$(n, p_{+1}) = (13, 0.6)$					$(n, p_{+1}) = (15, 0.55)$					$(n, p_{+1}) = (20, 0.52)$				
	h					h					h				
$2m+1$	0.1	0.15	0.2	0.25	0.3	0.1	0.15	0.2	0.25	0.3	0.1	0.15	0.2	0.25	0.3
51	17.7	17.8	17.8	17.9	17.9	59.4	59.4	59.4	59.5	59.6	179.4	182.2	183.9	184.9	185.3
61	17.8	17.8	17.9	17.9	17.9	58.9	59.2	59.4	59.5	59.6	185.9	185.7	185.7	185.7	185.7
71	17.9	17.9	17.9	17.9	17.9	59.3	59.3	59.4	59.5	59.6	184.0	185.1	185.6	185.8	185.8
81	17.8	17.8	17.9	17.9	17.9	59.2	59.3	59.4	59.5	59.6	185.6	185.7	185.8	185.8	185.9
91	17.8	17.8	17.9	17.9	17.9	59.4	59.3	59.4	59.5	59.7	185.5	185.8	185.8	185.9	185.9
101	17.8	17.8	17.9	17.9	17.9	59.3	59.3	59.4	59.5	59.7	186.5	185.9	185.9	185.9	186.0
111	17.8	17.8	17.9	17.9	17.9	59.3	59.3	59.4	59.5	59.7	185.8	185.9	185.9	186.0	186.0
121	17.8	17.8	17.9	17.9	17.9	59.3	59.3	59.4	59.5	59.7	186.0	185.9	185.9	186.0	186.0
131	17.8	17.8	17.9	17.9	17.9	59.3	59.3	59.4	59.5	59.7	185.8	185.9	186.0	186.0	186.1
141	17.8	17.8	17.9	17.9	17.9	59.3	59.4	59.4	59.5	59.7	185.9	185.9	186.0	186.0	186.1
151	17.8	17.8	17.9	17.9	17.9	59.3	59.4	59.4	59.5	59.7	185.8	185.9	186.0	186.0	186.1
161	17.8	17.8	17.9	17.9	17.9	59.3	59.4	59.4	59.5	59.7	185.9	186.0	186.0	186.0	186.1
171	17.8	17.8	17.9	17.9	17.9	59.3	59.4	59.4	59.5	59.7	185.9	186.0	186.0	186.0	186.1
181	17.8	17.8	17.9	17.9	17.9	59.3	59.4	59.4	59.5	59.7	185.9	186.0	186.0	186.1	186.1
191	17.8	17.8	17.9	17.9	17.9	59.3	59.4	59.4	59.5	59.7	185.9	186.0	186.0	186.1	186.1
201	17.8	17.8	17.9	17.9	17.9	59.3	59.4	59.4	59.5	59.7	185.9	186.0	186.0	186.1	186.1

Table 3.4: Comparison of in control ARL values for the two-sided 2-SN EWMA (without "continuousify") and two-sided 2C-SN EWMA (with "continuousify" and $h = 0.2$) for several desired ARL_0 values

(In-control ARL values for the 2-SN EWMA and 2C-SN EWMA charts for desired $ARL_0 = 200$)

	$(n, \lambda, K) = (5, 0.2, 2.6014)$		$(n, \lambda, K) = (8, 0.2, 2.6114)$		$(n, \lambda, K) = (9, 0.2, 2.6130)$		$(n, \lambda, K) = (11, 0.2, 2.6143)$	
$2m+1$	2-SN EWMA	2C-SN EWMA	2-SN EWMA	2C-SN EWMA	2-SN EWMA	2C-SN EWMA	2-SN EWMA	2C-SN EWMA
51	218.2	199.0	209.7	199.2	192.8	199.0	206.4	199.4
71	200.0	199.5	187.0	199.6	201.5	199.6	203.1	199.7
91	206.3	199.7	201.5	199.8	204.0	199.8	210.5	199.8
111	192.0	199.8	197.0	199.9	197.9	199.9	197.6	199.9
131	201.6	199.9	198.2	199.9	205.1	199.9	198.6	199.9
151	201.4	199.9	199.0	200.0	200.0	200.0	198.4	200.0
171	196.8	200.0	200.9	200.0	196.1	200.0	198.8	200.0
191	198.8	200.0	200.5	200.0	196.0	200.0	203.4	200.0
201	198.0	200.0	197.2	200.0	201.6	200.0	201.6	200.0

(In-control ARL values for the 2-SN EWMA and 2C-SN EWMA charts for desired $ARL_0 = 370.4$)

	$(n, \lambda, K) = (5, 0.2, 2.8074)$		$(n, \lambda, K) = (8, 0.2, 2.8276)$		$(n, \lambda, K) = (9, 0.2, 2.8252)$		$(n, \lambda, K) = (11, 0.2, 2.8306)$	
$2m+1$	2-SN EWMA	2C-SN EWMA	2-SN EWMA	2C-SN EWMA	2-SN EWMA	2C-SN EWMA	2-SN EWMA	2C-SN EWMA
51	327.1	367.7	381.0	368.1	387.3	368.4	351.9	367.4
71	375.9	369.1	382.8	369.2	352.0	369.4	372.9	369.6
91	366.1	369.7	368.8	369.8	355.5	369.9	361.3	369.9
111	359.2	370.0	370.6	370.0	357.3	370.1	378.1	370.1
131	367.8	370.2	387.8	370.2	366.4	370.2	367.0	370.2
151	382.0	370.3	366.7	370.3	363.2	370.3	384.8	370.3
171	365.7	370.3	367.7	370.3	377.6	370.3	373.4	370.4
191	374.8	370.4	367.0	370.4	381.0	370.4	362.4	370.4
201	362.0	370.4	371.4	370.4	369.5	370.4	369.4	370.4

(In-control ARL values for the 2-SN EWMA and 2C-SN EWMA charts for desired $ARL_0 = 500$)

	$(n, \lambda, K) = (5, 0.2, 2.85)$		$(n, \lambda, K) = (7, 0.2, 2.882)$		$((n, \lambda, K) = (9, 0.2, 2.89)$		$(n, \lambda, K) = (11, 0.2, 2.910)$	
$2m+1$	2-SN EWMA	2C-SN EWMA	2-SN EWMA	2C-SN EWMA	2-SN EWMA	2C-SN EWMA	2-SN EWMA	2C-SN EWMA
51	579.0	495.6	525.2	495.9	473.3	497.0	587.5	497.7
71	527.0	497.8	528.6	498.0	548.8	498.5	491.3	498.3
91	516.0	498.7	515.2	498.8	498.1	499.1	525.0	499.0
111	519.9	499.2	521.3	499.2	512.6	499.4	484.9	499.4
131	524.1	499.4	532.0	499.5	501.4	499.6	496.9	499.6
151	492.2	499.6	487.1	499.6	500.5	499.7	501.4	499.7
171	508.7	499.7	493.3	499.7	502.8	499.8	491.2	499.8
191	502.4	499.8	494.2	499.8	501.9	499.9	508.7	499.9
201	506.4	499.8	491.6	499.9	502.7	499.9	498.5	499.9

3.2.4.2 Effect of the shift magnitude p_1

As it was presented above, the in-control ARL values of the 2-SN EWMA chart are significantly affected by the number of subintervals. For the investigation of the out-of-control performance of the "continuousify"method two types of scenarios will be investigated. The first one account for large shifts in the process (Table 3.5), while the second one for small shifts in the process median (Table 3.6). From Table 3.5 it can be seen that minor differences exist for $p_1 > 0.6$. Nevertheless, since we proved that for the in-control case the results are different, practitioners may not be sure about the true out-of-control performance of the chart in term of its RL properties. On the other hand, when we have a small shift $p_1 \approx 0.5$, from Table 3.6, we can observe that for small sample sizes and small number of subintervals the results fluctuate. For example, for $n = 5$ and $p_1 = 0.52$ the ARL_1 values range from 305.1 to 341.7. On the other hand, for the same case, using the "continuousify"method the corresponding ARL_1 values become steady really soon even when $2m + 1 \approx 101$.

Table 3.5: l ARL_1 values for the two-sided 2-SN EWMA (without "continuousify") for large shifts

	$n = 8$				$n = 11$				$n = 15$			
$2m+1$	$p_{+1} = 0.55$	$p_{+1} = 0.6$	$p_{+1} = 0.65$	$p_{+1} = 0.7$	$p_{+1} = 0.55$	$p_{+1} = 0.6$	$p_{+1} = 0.64$	$p_{+1} = 0.7$	$p_{+1} = 0.55$	$p_{+1} = 0.6$	$p_{+1} = 0.65$	$p_{+1} = 0.7$
51	102.9	28.6	13.0	7.9	76.0	20.5	9.7	6.1	58.6	15.4	7.6	5.0
61	105.4	28.9	13.1	7.9	84.5	21.8	10.1	6.3	59.7	15.5	7.6	4.9
71	106.7	29.3	13.2	7.9	81.9	21.4	10.0	6.2	59.0	15.4	7.6	4.9
81	108.0	29.4	13.2	8.0	80.6	21.2	9.9	6.2	58.7	15.4	7.6	4.9
91	100.5	28.1	12.8	7.8	80.2	21.1	9.9	6.2	60.2	15.6	7.7	5.0
101	102.7	28.5	13.0	7.9	85.1	21.9	10.1	6.3	59.3	15.5	7.6	5.0
111	103.6	28.6	13.0	7.9	80.2	21.1	9.9	6.2	58.7	15.4	7.6	4.9
121	105.1	29.0	13.1	7.9	80.7	21.2	9.9	6.2	59.7	15.5	7.6	4.9
131	104.4	28.8	13.1	7.9	79.3	21.0	9.9	6.2	58.6	15.4	7.6	4.9
141	102.8	28.6	13.0	7.9	79.9	21.1	9.9	6.2	60.2	15.6	7.6	5.0
151	106.8	29.3	13.2	8.0	80.3	21.1	9.9	6.2	58.5	15.3	7.6	4.9
161	104.3	28.8	13.1	7.9	78.8	20.9	9.8	6.2	59.5	15.5	7.6	5.0
171	107.6	29.4	13.3	8.0	79.7	21.1	9.9	6.2	59.0	15.4	7.6	4.9
181	104.3	28.8	13.1	7.9	79.9	21.1	9.9	6.2	59.6	15.5	7.6	5.0
191	104.8	28.9	13.1	7.9	80.6	21.2	9.9	6.2	58.0	15.3	7.5	4.9
201	104.7	28.9	13.1	7.9	79.7	21.0	9.9	6.2	59.1	15.4	7.6	5.0

	$n = 20$				$n = 12$				$n = 16$			
$2m+1$	$p_{+1} = 0.55$	$p_{+1} = 0.6$	$p_{+1} = 0.65$	$p_{+1} = 0.7$	$p_{+1} = 0.55$	$p_{+1} = 0.6$	$p_{+1} = 0.64$	$p_{+1} = 0.7$	$p_{+1} = 0.55$	$p_{+1} = 0.6$	$p_{+1} = 0.65$	$p_{+1} = 0.7$
51	43.6	11.7	6.0	4.0	77.3	19.9	9.4	5.9	56.8	14.7	7.3	4.8
61	45.7	12.0	6.1	4.1	71.7	19.0	9.1	5.8	62.1	15.4	7.5	4.9
71	44.8	11.8	6.1	4.1	73.1	19.2	9.1	5.8	57.4	14.8	7.3	4.8
81	45.7	12.0	6.1	4.1	74.9	19.4	9.2	5.8	55.2	14.5	7.2	4.7
91	45.2	11.9	6.1	4.1	74.6	19.4	9.2	5.8	54.3	14.3	7.2	4.7
101	45.5	11.9	6.1	4.1	73.5	19.3	9.2	5.8	55.8	14.6	7.2	4.7
111	45.3	11.9	6.1	4.1	73.7	19.3	9.2	5.8	56.4	14.6	7.2	4.7
121	46.0	12.0	6.1	4.1	73.9	19.4	9.2	5.8	55.3	14.5	7.2	4.7
131	45.1	11.9	6.1	4.1	73.7	19.3	9.2	5.8	56.9	14.7	7.3	4.7
141	44.9	11.8	6.1	4.1	71.5	19.0	9.1	5.8	57.0	14.7	7.3	4.7
151	44.6	11.8	6.1	4.1	72.0	19.0	9.1	5.8	56.0	14.6	7.2	4.7
161	45.1	11.9	6.1	4.1	72.2	19.1	9.1	5.8	56.2	14.6	7.3	4.7
171	45.2	11.9	6.1	4.1	71.8	19.0	9.1	5.8	56.2	14.6	7.2	4.7
181	45.2	11.9	6.1	4.1	72.8	19.1	9.1	5.8	56.5	14.7	7.3	4.7
191	45.1	11.9	6.1	4.1	73.0	19.2	9.1	5.8	56.2	14.6	7.3	4.7
201	45.3	11.9	6.1	4.1	73.4	19.3	9.2	5.8	55.7	14.5	7.2	4.7

Table 3.6: Comparison of in control ARL values for the two-sided SN EWMA (without "continuousify") and two-sided C-SN EWMA (with "continuousify" and $\sigma = 0.2$) using $(\lambda, K) = (0.2, 2.85)$ for different (n, p_{+1}) combinations.

	$(n, p_{+1}) = (5, 0.52)$		$(n, p_{+1}) = (5, 0.53)$		$(n, p_{+1}) = (5, 0.54)$		$(n, p_{+1}) = (5, 0.55)$	
$2m+1$	2-SN EWMA	2C-SN EWMA	2-SN EWMA	2C-SN EWMA	2-SN EWMA	2C-SN EWMA	2-SN EWMA	2C-SN EWMA
51	305.3	334.2	243.0	264.3	187.6	202.9	143.9	154.8
71	317.5	335.4	251.2	265.2	192.9	203.5	147.3	155.2
91	346.9	335.8	272.8	265.5	208.2	203.7	158.1	155.3
111	339.1	336.1	267.3	265.6	204.5	203.8	155.6	155.4
131	328.1	336.2	259.1	265.7	198.6	203.9	151.4	155.4
151	319.7	336.3	253.1	265.8	194.5	203.9	148.5	155.4
171	335.1	336.4	264.4	265.8	202.5	203.9	154.2	155.5
191	341.7	336.4	269.2	265.9	206.0	203.9	156.6	155.5
201	338.4	336.4	267.1	265.9	204.6	203.9	155.9	155.5
	$(n, p_{+1}) = (15, 0.52)$		$(n, p_{+1}) = (15, 0.53)$		$(n, p_{+1}) = (15, 0.54)$		$(n, p_{+1}) = (15, 0.55)$	
$2m+1$	2-SN EWMA	2C-SN EWMA	2-SN EWMA	2C-SN EWMA	2-SN EWMA	2C-SN EWMA	2-SN EWMA	2C-SN EWMA
51	210.2	213.9	133.6	264.3	86.6	87.9	58.6	59.4
71	212.5	214.2	134.8	265.2	87.3	87.9	59.0	59.4
91	218.9	214.4	138.4	265.5	89.3	88.0	60.2	59.4
111	211.3	214.5	134.1	265.6	86.9	88.0	58.7	59.4
131	210.6	214.6	133.7	265.7	86.6	88.0	58.6	59.4
151	210.4	214.6	133.5	265.8	86.5	88.0	58.5	59.4
171	213.3	214.7	135.2	265.8	87.4	88.0	59.0	59.4
191	207.8	214.7	132.1	265.9	85.7	88.0	58.0	59.4
201	213.6	214.7	135.4	265.9	87.5	88.0	59.1	59.4
	$(n, p_1) = (20, 0.52)$		$(n, p_1) = (20, 0.53)$		$(n, p_1) = (20, 0.54)$		$(n, p_1) = (20, 0.55)$	
$2m+1$	2-SN EWMA	2C-SN EWMA	2-SN EWMA	2C-SN EWMA	2-SN EWMA	2C-SN EWMA	2-SN EWMA	2C-SN EWMA
51	174.7	183.9	104.7	109.4	65.6	68.1	43.6	45.0
71	183.7	185.6	109.1	110.2	67.8	68.5	44.8	45.2
91	185.8	185.9	110.2	110.4	68.4	68.5	45.2	45.3
111	186.3	185.9	110.5	110.4	68.6	68.6	45.3	45.3
131	185.2	186.0	109.9	110.4	68.3	68.6	45.1	45.3
151	182.3	186.0	108.4	110.4	67.4	68.6	44.6	45.3
171	186.0	186.0	110.4	110.4	68.5	68.6	45.2	45.3
191	185.3	186.0	110.0	110.4	68.3	68.6	45.1	45.3
201	186.3	186.0	110.6	110.4	68.7	68.6	45.3	45.3

3.2.4.3 Effect of the Kernel density estimation

Following the approach of Wu et al. (2020) the distribution / kernel used for transforming the discrete random variable SN_t into a continuous one, is chosen to be the Normal (ψ, h) distribution (see (3.5) and (3.6)) which can be simply derived from the $N(0, 1)$ distribution

by a straightforward standardization. More specifically. For the Gaussian kernel we have

$$K_{\text{Nor}}(x) = \frac{1}{\sqrt{2\pi}} e^{-\frac{x^2}{2}}$$

where $\text{E}(K_{\text{Nor}}) = 0$, $\text{V}(K_{\text{Nor}}) = 1$. The corresponding Kernel density function for SN_t is defined as:

$$f(s|n, p_{+1}) = \frac{1}{h} \sum_{k=-n}^{n} w_k K_{\text{Nor}} \left(\frac{s-k}{h} \right) = \frac{1}{h} \sum_{k=n}^{n} w_k f_{\text{N}} \left(\frac{s-k}{h} | 0, 1 \right)$$

where $w_k = f_{\text{Bin}}(\frac{k+n}{2}|n, p_{+1})$, $s \in \mathbb{R}$, $k = \{-n, -n+2, \ldots, n-2, n\}$ and h is the bandwidth. A legitimate question is what happens to the previous results concerning the 2C-SN EWMA chart if the normal kernel used in (3.5) and (3.6) is replaced by another continuous one? Are the ARL values obtained by this modification different from what has been obtained with the normal kernel? Therefore, the goal is to investigate the impact of the choice of the kernel on the ARL values of the 2C-SN EWMA chart if (3.5) and (3.6) are replaced by

$$\begin{aligned} f_{\text{SN}_t^*}(s|n, p_{+1}) &= \sum_{\psi \in \Psi} f_{\text{Bin}} \left(\frac{\psi + n}{2} | n, p_{+1} \right) f_K \left(\frac{s-\psi}{h} \right) \\ F_{\text{SN}_t^*}(s|n, p_{+1}) &= \sum_{\psi \in \Psi} f_{\text{Bin}} \left(\frac{\psi + n}{2} | n, p_{+1} \right) F_K \left(\frac{s-\psi}{h} \right), \end{aligned}$$

where $f_K(\dots)$ and $F_K(\dots)$ are the p.d.f. and c.d.f. of a continuous kernel as the ones listed in Table 3.7.

Table 3.7: Some continuous kernels

Kernel	Domain	$K(x)$	$\int xK(x)dx$	$\int x^2K(x)dx$
Parabolic	$[-1,1]$	$\frac{3}{4}(1-x^2)$	0	$\frac{1}{5}$
Biweight	$[-1,1]$	$\frac{15}{16}(1-x^2)^2$	0	$\frac{1}{7}$
Triweight	$[-1,1]$	$\frac{35}{32}(1-x^2)^3$	0	$\frac{1}{9}$
Cosine	$[-1,1]$	$\frac{\pi}{4}\cos(x\frac{\pi}{2})$	0	$1-\frac{8}{\pi^2}$
Normal	$(-\infty,\infty)$	$\frac{e^{-x^2/2}}{\sqrt{2\pi}}$	0	1

In general, for illustration and fair comparison purposes, it is helpful to consider the standardised version of the above Kernels. In particular, if the probability density exists for all values of the complete parameter set, then the density (as a function of the scale parameter, s) satisfies:

$$f_s(x) = \frac{1}{s} f_Z\left(\frac{x}{s}\right),$$

where $f_Z(\ldots)$ is the density of a standardized version of the Kernel density.

Let $f(x)$ be the kernel with support $|x| \leq 1$ and variance h^2. If we set $s = \sqrt{\sigma}$ then the kernel with unit variance $f_z(z)$ will be defined as:

$$f_Z(z) = sf(sz), |z| \leq \frac{1}{s}$$

with corresponding c.d.f $F_z(z) = \int_{\frac{1}{s}}^{z} f_z(t)dt$.

Let us consider the simplest density Kernel estimation technique based on the Uniform Kernel, $f(x) = \frac{1}{2}$ for $|x| \leq 1$ with variance $h^2 = \frac{1}{3}$. If we set $s = \frac{1}{\sqrt{3}}$ then the p.d.f with unit variance, $f_z(z)$, will be defined as:

$$f_z(z) = \frac{1}{2\sqrt{3}}, |z| \leq \sqrt{3},$$

then $\int_{-\sqrt{3}}^{\sqrt{3}} f_z(z)dz = 1$ with unit variance:

- $\int_{-\sqrt{3}}^{\sqrt{3}} f_z(z)dz = \int_{-\sqrt{3}}^{\sqrt{3}} \frac{1}{2\sqrt{3}}dz = \frac{1}{2\sqrt{3}}z\Big|_{-\sqrt{3}}^{\sqrt{3}} = \frac{1}{2\sqrt{3}}2\sqrt{3} = 1$
- $\int_{-\sqrt{3}}^{\sqrt{3}} z^2 f_z(z)dz = \int_{-\sqrt{3}}^{\sqrt{3}} z^2 \frac{1}{2\sqrt{3}}dz = \frac{1}{2\sqrt{3}}\frac{z^3}{3}\Big|_{-\sqrt{3}}^{\sqrt{3}} = \frac{1}{2\sqrt{3}}\frac{2(\sqrt{3})^3}{3} = \frac{2(\sqrt{3})^2}{2\cdot 3} = 1$

Similarly, for the parabolic Kernel $f(x) = \frac{3}{4}(1-x^2)$ with $|x| \leq 1$ and $h^2 = \frac{1}{5}$, if we set $s = \frac{1}{\sqrt{5}}$ then the p.d.f. with unit variance will be defined as:

$$f_z(z) = \frac{3}{4\sqrt{5}}\left(1 - \frac{1}{5}z^2\right), |z| \leq \sqrt{5},$$

and the c.d.f will be computed as:

$$\begin{aligned}
F_z(z) &= \int_{-\sqrt{5}}^{z} f_z(t)dt = \int_{-\sqrt{5}}^{z} \frac{3}{4\sqrt{5}}\left(1 - \frac{1}{5}t^2\right)dt = \int_{-\sqrt{5}}^{z} \frac{3}{4\sqrt{5}}dt - \int_{-\sqrt{5}}^{z} \frac{3}{4\sqrt{5}}\frac{t^2}{5}dt \\
&= \frac{3}{4\sqrt{5}}t\Big|_{-\sqrt{5}}^{z} - \frac{1}{4\cdot 5\sqrt{5}}t^3\Big|_{-\sqrt{5}}^{z} = \frac{3}{4\sqrt{5}}\left(z + \sqrt{5}\right) - \frac{1}{4\cdot 5\sqrt{5}}\left(z^3 + (\sqrt{5})^3\right) \\
&= \frac{3z}{4\sqrt{5}} + \frac{3\sqrt{5}}{4\sqrt{5}} - \frac{z^3}{4\cdot 5\sqrt{5}} - \frac{(\sqrt{5})^3}{4\cdot 5\sqrt{5}} = \frac{3z}{4\sqrt{5}} + \frac{3}{4} - \frac{z^3}{4\cdot 5\sqrt{5}} - \frac{1}{4} \\
&= \frac{3z}{4\sqrt{5}} - \frac{z^3}{4\cdot 5\sqrt{5}} + \frac{1}{2}.
\end{aligned}$$

Finally, the c.d.f if defined as:

$$F_z(z) = \begin{cases} 0 & \text{if } z < -\sqrt{5} \\ \frac{3z}{4\sqrt{5}} - \frac{z^3}{4\cdot 5\sqrt{5}} + \frac{1}{2} & \text{if } |z| < \sqrt{5} \\ 1 & \text{if } z > \sqrt{5} \end{cases}.$$

For the remaining Kernels presented above, their corresponding *standardised* version is presented in Table 3.8. In order to examine if the choice of the Kernel function for the computation of the p.d.f. and c.d.f. of SN_t^* affects the performance of the 2C-SN EWMA chart, for each standardised Kernel listed in Table 3.8 and for different values for the sample size and the desired ARL_0, the corresponding in-control ARL_0 are computed and listed in Table 3.9. From the results presented in Table 3.9 we may conclude that regardless the

desired ARL_0 value the performance of the "continuousified" method in the 2C-SN EWMA chart is the same regardless the Kernel density being used. In particular, for $2m+1 > 101$ the corresponding ARL_0 values are exactly the same. Only some minor differences in the first decimal point are occurred for $2m+1 < 101$, but practically speaking they are not significant.

Table 3.8: *standardized* continuous kernels

Kernel	Domain	$K(x)$
Parabolic	$[-\sqrt{5}, \sqrt{5}]$	$\frac{3}{4\sqrt{5}}\left(1-\frac{1}{5}x^2\right)$
Biweight	$[-\sqrt{7}, \sqrt{7}]$	$\frac{15}{16\sqrt{7}}(1-\frac{x^2}{7})^2$
Triweight	$[-3, 3]$	$\frac{35}{96}\left(1-\frac{x^6}{3^6}-\frac{3x^2}{9}+\frac{3x^4}{3^4}\right)$
Cosine	$\left[-\frac{1}{\sqrt{1-\frac{8}{\pi^2}}}, \frac{1}{\sqrt{1-\frac{8}{\pi^2}}}\right]$	$\sqrt{\frac{\pi^2}{16}-\frac{1}{2}}\cos\left(\sqrt{\frac{\pi^2x^2}{4}-2x^2}\right)$
Normal	$(-\infty, \infty)$	$\frac{e^{-x^2/2}}{\sqrt{2\pi}}$

Table 3.9: ARL values of the 2C-SN EWMA chart for $\sigma = 0.2$, $n \in \{5, 8, 9\}$ for the standardised kernels listed in Table 3.7

(In-control ARL values the 2C-SN EWMA charts for desired $\text{ARL}_0 = 370.4$)

	$(n, \lambda, K) = (5, 0.2, 2.807)$					$(n, \lambda, K) = (8, 0.2, 2.827)$					$(n, \lambda, K) = (9, 0.2, 2.825)$				
$2m+1$	Parabolic	Biweight	Cosine	Triweight	Normal	Parabolic	Biweight	Cosine	Triweight	Normal	Parabolic	Biweight	Cosine	Triweight	Normal
51	366.8	367.3	366.9	367.6	367.7	367.5	367.7	367.6	367.8	368.1	368.3	368.4	368.3	368.4	368.4
61	368.7	368.6	368.6	368.6	368.6	368.8	368.8	368.7	368.8	368.8	369.2	369.1	369.2	369.1	369.0
71	369.1	369.1	369.1	369.1	369.1	369.5	369.3	369.4	369.3	369.2	369.2	369.4	369.3	369.4	369.4
81	369.4	369.4	369.4	369.4	369.5	369.5	369.6	369.5	369.6	369.5	369.3	369.6	369.4	369.7	369.7
91	369.5	369.6	369.5	369.7	369.7	369.8	369.8	369.8	369.8	369.8	370.0	369.9	370.1	369.9	369.9
101	369.8	369.8	369.8	369.8	369.9	369.9	369.9	369.9	369.9	369.9	370.2	370.0	370.1	370.0	370.0
111	369.9	369.9	369.9	370.0	370.0	370.0	370.0	370.0	370.0	370.0	370.1	370.1	370.1	370.1	370.1
121	370.1	370.1	370.1	370.1	370.1	370.1	370.1	370.1	370.1	370.1	370.1	370.1	370.1	370.1	370.2
131	370.1	370.1	370.1	370.1	370.2	370.2	370.2	370.2	370.2	370.2	370.2	370.2	370.2	370.2	370.2
141	370.2	370.2	370.2	370.2	370.2	370.3	370.2	370.3	370.2	370.2	370.2	370.2	370.2	370.2	370.3
151	370.2	370.2	370.2	370.2	370.3	370.3	370.3	370.3	370.3	370.3	370.3	370.3	370.3	370.3	370.3
161	370.3	370.3	370.2	370.3	370.3	370.3	370.3	370.3	370.3	370.3	370.3	370.3	370.3	370.3	370.3
171	370.3	370.3	370.3	370.3	370.3	370.3	370.4	370.3	370.3	370.3	370.3	370.3	370.3	370.3	370.3
181	370.3	370.3	370.3	370.3	370.4	370.4	370.4	370.4	370.4	370.4	370.4	370.3	370.4	370.4	370.4
191	370.3	370.4	370.3	370.4	370.4	370.4	370.4	370.4	370.4	370.4	370.3	370.4	370.3	370.4	370.4
201	370.4	370.4	370.4	370.4	370.4	370.4	370.4	370.4	370.4	370.4	370.4	370.4	370.4	370.4	370.4

(In-control ARL values for the 2C-SN EWMA charts for desired $\text{ARL}_0 = 500$)

	$(n, \lambda, K) = (5, 0.2, 2.900)$					$(n, \lambda, K) = (8, 0.2, 2.925)$					$(n, \lambda, K) = (9, 0.2, 2.922)$				
$2m+1$	Parabolic	Biweight	Cosine	Triweight	Normal	Parabolic	Biweight	Cosine	Triweight	Normal	Parabolic	Biweight	Cosine	Triweight	Normal
51	496.9	496.1	496.6	495.9	495.6	496.4	496.2	496.4	496.1	495.9	497.0	497.1	497.1	497.0	497.0
61	496.6	497.0	496.9	497.0	497.0	497.4	497.3	497.4	497.2	497.2	497.9	497.9	497.9	497.9	498.0
71	497.5	497.7	497.5	497.8	497.8	498.0	498.0	497.9	498.0	498.0	499.2	498.6	499.0	498.5	498.5
81	498.2	498.3	498.2	498.3	498.4	498.3	498.4	498.4	498.5	498.5	499.3	498.8	499.1	498.8	498.9
91	498.7	498.7	498.7	498.7	498.7	498.6	498.7	498.6	498.8	498.8	498.9	498.9	498.9	499.0	499.1
101	498.9	499.0	498.9	499.0	499.0	499.4	499.1	499.3	499.1	499.1	499.1	499.1	499.1	499.1	499.3
111	499.1	499.1	499.1	499.2	499.2	499.2	499.3	499.3	499.3	499.2	499.2	499.3	499.2	499.3	499.4
121	499.4	499.3	499.3	499.3	499.3	499.2	499.4	499.2	499.4	499.4	499.3	499.4	499.3	499.4	499.5
131	499.5	499.4	499.5	499.4	499.4	499.6	499.5	499.5	499.5	499.5	499.3	499.4	499.3	499.5	499.6
141	499.5	499.5	499.5	499.5	499.5	499.6	499.6	499.6	499.6	499.6	499.4	499.5	499.4	499.6	499.7
151	499.6	499.6	499.6	499.6	499.6	499.6	499.7	499.6	499.6	499.6	499.4	499.6	499.4	499.6	499.7
161	499.6	499.7	499.6	499.7	499.7	499.7	499.7	499.7	499.7	499.7	499.5	499.6	499.6	499.6	499.8
171	499.7	499.7	499.7	499.7	499.7	499.8	499.8	499.8	499.8	499.7	499.6	499.6	499.6	499.7	499.8
181	499.7	499.8	499.7	499.8	499.8	499.8	499.8	499.8	499.8	499.8	499.6	499.7	499.6	499.7	499.8
191	499.8	499.8	499.8	499.8	499.8	499.9	499.8	499.9	499.8	499.8	499.6	499.7	499.6	499.7	499.9
201	499.8	499.8	499.8	499.8	499.8	499.8	499.9	499.9	499.9	499.9	499.7	499.7	499.7	499.8	499.9

3.2.4.4 Effect of the in-control value of p_{+1}

Generally, in nonparametric charts, when the shift in the process characteristic, θ_0, is expressed in terms of p_{+1}, it is possible to design a chart (Shewhart-type or EWMA-type) capable of detecting shifts for every quantile (or percentile) of interest. In particular, considering that we are interested in monitoring shifts in the 3^{rd} quantile, the in-control value of p_{+1} will be equal to $p_{+1} = 0.75$. As a consequence, from equations (2.6) and (2.7) the corresponding in-control mean and variance of SN_t^* will be equal to:

$$\mathrm{E}_0(\mathrm{SN}_t^*) = 2n\frac{1}{3} - n = \frac{n}{3}, \tag{3.15}$$

$$\mathrm{V}_0(\mathrm{SN}_t^*) = 4n\frac{1}{3}(1 - \frac{1}{3}) = \frac{8n}{9}. \tag{3.16}$$

Finally, the charting statistic and the control limits of the 2C-SN EWMA chart will be adjusted as:

$$Z_t^* = \lambda \mathrm{SN}_t^* + (1-\lambda)Z_{t-1}^*, Z_0^* = \mathrm{E}_0(\mathrm{SN}_t^*) = \frac{n}{3},$$

with fixed asymptotic control limits:

$$\mathrm{UCL}^* = \frac{n}{3} + K\sqrt{\frac{\lambda}{2-\lambda}\left(\frac{8n}{9} + h^2\right)}.$$

$$\mathrm{LCL}^* = \frac{n}{3} - K\sqrt{\frac{\lambda}{2-\lambda}\left(\frac{8n}{9} + h^2\right)}.$$

Similarly, for any in-control value of $p_{+1} \in (0,1)$, practitioners can design a scheme, capable of monitoring any percentile of interest. In order to examine the stability of the in-control ARL with and without the "continuousify" method, 4 cases regarding the in-control value of p_{+1} are considered. In Figure 3.2 the corresponding in-control ARL values for the two-sided 2-SN EWMA (without "continuousify") and two-sided 2C-SN EWMA (with "continuousify" and $h = 0.2$), for monitoring the different percentiles of interest, $p_{+1} = \{0.65, 0.75, 0.85, 0.95\}$ are presented. From Figure 3.2 it can be concluded that regardless the in-control value of p_{+1} the "continuousify" method is a great improvement for the stability of the ARL_0 values for $2m + 1 \approx 101$.

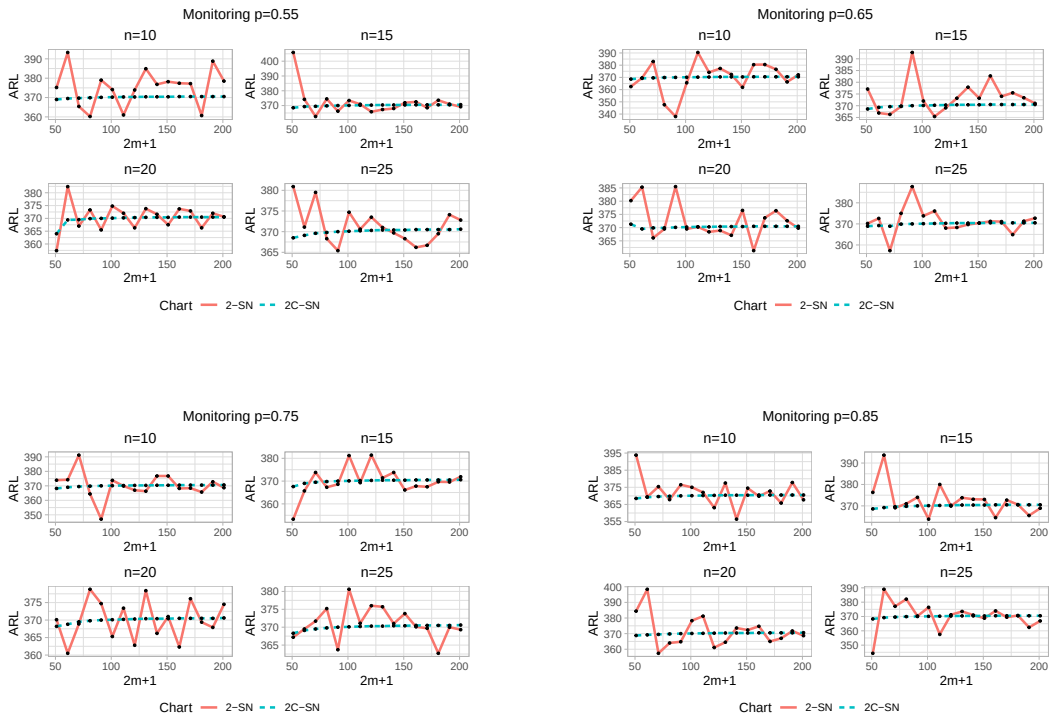

Figure 3.2: ARL_0 (plain lines) as a function of the number of sub-intervals $2m+1 \in \{51, 61, \ldots, 251\}$ for the 2-SN EWMA and 2C-SN EWMA charts for different values of the in-control p_{+1}

3.2.5 Optimal design of the 2C-SN EWMA chart

Regarding the optimal design parameters of the proposed scheme the next simple steps have been followed:

- *Step 1*: Set the number of subintervals $2m+1$, the in-control value of p_{+1} and the desired ARL_0.
- *Step 2*: For a specified set of values $\lambda \in (0, 1)$ find the corresponding K that gives an in-control $\mathrm{ARL} = \mathrm{ARL}_0$
- *Step 3*: For all the possible optimal pair of (λ, K) obtained in *Step 2* for a specified shift $p_{+1} \in (0.5, 1)$ (assuming $p_{+1} = 0.5$ for the in-control case) find the combination of (λ, K) that give the minimum out-of-control ARL.

In particular, for step 2 (i.e the searching algorithm), the classical Regula–Falsi method was initialised. Through its simplicity, for a given value of λ, it is capable of finding the

corresponding value of K that gives an in-control ARL = ARL_0. This method is presented in algorithm 3.1 where arl_t is the desired in-control ARL value and h_1, h_2 are two initial values for K. During our computations, we saw that for $n \in \{5, 6, \ldots, 25\}$ and setting $h_1 \approx 2.5, h_2 = h_1 + 0.01$ this method is quite fast and it is not sensitive to the initial values of h_1, h_2. Nevertheless, we may argue with the fact that setting the initial values so close to each other it could be dangerous we suggest that setting $h_2 \approx h_1 + 0.05$ or $h_2 \approx h_1 + 0.1$ can be considered as a reasonable choice. It is worth streaking, that through the "continuousify" method, practitioners are capable of finding a value of K that gives a corresponding in-control ARL to be *exactly* equal to the desired one. Finally, in Table 3.10 the optimal pairs of (λ^*, K^*) for the two-sided 2C-SN EWMA chart are given, along with the corresponding ARL_1 values for different shifts magnitudes and sample sizes. As a result, when the parameter of interest to be monitored is the median, determining the desirable value for the sample size and choosing the appropriate pair of (λ, K) from Table 3.10 practitioners are capable of monitoring efficiently shifts in the process median. In cases where the shift magnitude is unknown, for monitoring small, moderate or large shift magnitudes, choosing the corresponding pair of (λ, K) for $p_{+1} \approx 0.5$, $p_{+1} \approx 0.7$ or $p_{+1} \approx 0.9$ can be considered as an efficient choice.

Algorithm 3.1 Computation of candidate combination of (λ, K) for the EWMA chart)

Define arl_t,λ,h_1,m,p_{+1}
$h_2 \rightarrow h_1 + 0.01$

for each λ **do**
  repeat
    $arl_1 \rightarrow \text{ARL0}(\lambda, h_1, m, p_{+1})$
    $arl_2 \rightarrow \text{ARL0}(\lambda, h_2, m, p_{+1})$
    $h_new \rightarrow h_2 + (arl_t - arl_2)\frac{(h2-h1)}{(arl_2-arl_1)}$
    $arl_1 \rightarrow arl_2$
    $h1 \rightarrow h_2$
    $h_2 \rightarrow h_new$
    $arl_2 \rightarrow ARL0(\lambda, h_2, m, p_{+1})$
  until $(|arl_t - arl_2| < 10^{-8})$
  Use as staring value,h_1, for the next iteration the newest value of h_2
end for

Table 3.10: Optimal combinations of (λ^*, K^*) for the two-sided 2C-SN EWMA chart along with the corresponding ARL_1 values.

	p_{+1}						
n	0.55	0.60	0.65	0.70	0.80	0.85	0.9
2	(0.02,2.138,135.61)	(0.02,2.138,57.65)	(0.04,2.41,33.49)	(0.06,2.54,22.2)	(0.12,2.693,11.97)	(0.16,2.719,9.3)	(0.195,2.72,7.43)
3	(0.02,2.14,106.54)	(0.03,2.304,44.087)	(0.055,2.509,25.13)	(0.085,2.62,16.48)	(0.15,2.737,8.72)	(0.19,2.769,6.81)	(0.31,2.757,5.38)
4	(0.02,2.138,89.04)	(0.035,2.363,36.21)	(0.065,2.57,20.38)	(0.1,2.682,13.26)	(0.185,2.775,7.01)	(0.215,2.783,5.46)	(0.33,2.798,4.32)
5	(0.02,2.138,77.25)	(0.04,2.407,31.03)	(0.08,2.621,17.3)	(0.12,2.726,11.18)	(0.215,2.814,5.89)	(0.345,2.815,4.59)	(0.455,2.799,3.46)
6	(0.02,2.137,68.74)	(0.05,2.489,27.27)	(0.09,2.661,15.11)	(0.135,2.746,9.76)	(0.27,2.844,5.06)	(0.295,2.848,3.91)	(0.315,2.849,3.13)
7	(0.02,2.137,62.29)	(0.055,2.513,24.44)	(0.1,2.69,13.46)	(0.145,2.771,8.67)	(0.33,2.857,4.53)	(0.37,2.861,3.48)	(0.38,2.862,2.81)
8	(0.02,2.137,57.2)	(0.06,2.548,22.2)	(0.11,2.709,12.19)	(0.175,2.805,7.82)	(0.285,2.863,4.09)	(0.36,2.866,3.18)	(0.4,2.865,2.56)
9	(0.025,2.229,53.03)	(0.065,2.572,20.38)	(0.12,2.736,11.15)	(0.18,2.811,7.16)	(0.345,2.881,3.72)	(0.38,2.882,2.91)	(0.715,2.838,2.19)
10	(0.025,2.231,49.47)	(0.07,2.594,18.88)	(0.135,2.76,10.29)	(0.195,2.83,6.6)	(0.375,2.887,3.45)	(0.66,2.866,2.65)	(0.67,2.865,1.94)
11	(0.025,2.228,46.48)	(0.075,2.616,17.61)	(0.135,2.763,9.58)	(0.205,2.835,6.14)	(0.525,2.894,3.22)	(0.545,2.893,2.4)	(0.565,2.891,1.87)
12	(0.03,2.303,43.85)	(0.08,2.632,16.53)	(0.145,2.781,8.96)	(0.23,2.856,5.73)	(0.47,2.902,2.98)	(0.485,2.9,2.3)	(0.505,2.898,1.84)
13	(0.03,2.3,41.57)	(0.085,2.652,15.57)	(0.165,2.802,8.44)	(0.24,2.866,5.39)	(0.435,2.908,2.8)	(0.745,2.889,2.05)	(0.77,2.885,1.5)
14	(0.03,2.303,39.55)	(0.095,2.68,14.74)	(0.16,2.802,7.98)	(0.26,2.873,5.1)	(0.595,2.91,2.65)	(0.625,2.907,1.95)	(0.645,2.905,1.49)
15	(0.035,2.36,37.73)	(0.095,2.683,14)	(0.17,2.811,7.57)	(0.25,2.874,4.84)	(0.535,2.915,2.49)	(0.555,2.914,1.89)	(0.56,2.914,1.49)
16	(0.035,2.362,36.1)	(0.1,2.696,13.35)	(0.18,2.824,7.2)	(0.27,2.884,4.6)	(0.48,2.921,2.38)	(0.78,2.91,1.77)	(0.8,2.91,1.33)
17	(0.035,2.361,34.65)	(0.105,2.708,12.76)	(0.19,2.836,6.87)	(0.28,2.888,4.4)	(0.65,2.921,2.25)	(0.69,2.918,1.64)	(0.71,2.916,1.26)
18	(0.04,2.411,33.3)	(0.11,2.721,12.22)	(0.195,2.838,6.59)	(0.285,2.894,4.21)	(0.59,2.926,2.13)	(0.59,2.926,1.62)	(0.95,2.874,1.27)
19	(0.04,2.411,32.07)	(0.115,2.73,11.74)	(0.2,2.846,6.32)	(0.34,2.913,4.03)	(0.51,2.931,2.09)	(0.8,2.924,1.56)	(0.815,2.925,1.21)
20	(0.04,2.411,30.96)	(0.12,2.743,11.29)	(0.22,2.861,6.07)	(0.305,2.903,3.89)	(0.69,2.93,1.94)	(0.72,2.928,1.43)	(0.73,2.928,1.14)

3.3 The "continuousified" upper-sided SN EWMA chart

The charting statistic of the "continuousified" upper-sided SN EWMA (denoted as C-SN EWMA chart) will be defined as:

$$Z_t^* = \max(0, \lambda \mathrm{SN}_t^* + (1-\lambda) Z_{t-1}^*), Z_0^* = \mathrm{E}_0(\mathrm{SN}_t^*),$$

with fixed upper asymptotic control limit:

$$\mathrm{UCL} = \mathrm{E}_0(\mathrm{SN}_t^*) + K_1 \sqrt{\mathrm{V}_0(\mathrm{SN}_t^*)} \times \sqrt{\frac{\lambda}{2-\lambda}}.$$

Assuming that θ_0 is the in-control value of the process median since $\mathrm{E}(\mathrm{SN}_t) = 0$ and $\mathrm{V}(\mathrm{SN}_t^*) = n$ the above expressions can be rewritten as:

$$\mathrm{UCL} = + K_1 \sqrt{\frac{\lambda}{2-\lambda}(n + h^2)}.$$

$$\mathrm{CL} = 0.$$

3.3.1 Run Length properties and efficiency of the C-SN EWMA chart

In order to obtain the RL properties of the upper-sided C-SN EWMA control chart, the standard discrete-time Markov chain approach of Brook and Evans (1972) presented in Section 2.3.1 will be used with, the only difference that the p.m.f. of SN_t will be replaced by the p.d.f. of SN_t^* in the computation of the transient probabilities $Q_{k,j}$ as:

- if $j = 0$,

$$Q_{k,0} = F_{\mathrm{SN}_t^*}\left(-\frac{(1-\lambda)H_k}{\lambda}|n, p_{+1}\right).$$

- if $j = 1, 2, \ldots, m$,

$$Q_{k,j} = F_{\mathrm{SN}_t^*}\left(\frac{H_j + \Delta - (1-\lambda)H_k}{\lambda}|n, p_{+1}\right) - F_{\mathrm{SN}_t^*}\left(\frac{H_j - \Delta - (1-\lambda)H_k}{\lambda}|n, p_{+1}\right). \tag{3.17}$$

Similarly, with the two-sided case in Table 3.11 several pairs of in control (ARL, SDRL) values are presented as a function of the number of subintervals between the upper-sided SN EWMA (without "continuousify") and upper-sided C-SN EWMA (with "continuousify" and $h = 0.2$) charts. It is clear that, as expected, the "continuousify" method yields to steady ARL and SDRL values regardless the number of the subintervals.

Table 3.11: Comparison of in-control (ARL, SDRL) values for the upper-sided SN EWMA (without "continuousify") and upper-sided C-SN EWMA (with "continuousify" and $h = 0.2$) chart when $\lambda = 0.2$ and $K_1 = 2.75$

	$(n = 5, p_{+1} = 0.5)$		$(n = 9, p_{+1} = 0.5)$		$(n = 12, p_{+1} = 0.5)$		$(n = 16, p_{+1} = 0.5)$	
m	SN EWMA	C-SN EWMA	SN EWMA	C-SN EWMA	SN EWMA	C-SN EWMA	SN EWMA	C-SN EWMA
50	(410.9,405.6)	(400.8,395.7)	(392,387)	(384.7,379.7)	(383.1,378.2)	(374.2,369.3)	(370.7,365.8)	(372,367.1)
60	(400.9,395.7)	(401.1,395.9)	(400.6,395.6)	(384.8,379.9)	(377.9,373)	(374.5,369.6)	(367.6,362.7)	(372.2,367.3)
70	(409,403.8)	(401.2,396)	(380.3,375.4)	(384.9,380)	(360.3,355.4)	(374.6,369.7)	(372,367.1)	(372.4,367.5)
80	(396.3,391.1)	(401.3,396.1)	(385.8,380.8)	(385,380)	(376,371.2)	(374.7,369.8)	(366.4,361.6)	(372.4,367.6)
90	(422,416.7)	(401.3,396.2)	(389.3,384.3)	(385,380.1)	(374.4,369.5)	(374.8,369.9)	(369.6,364.7)	(372.5,367.6)
100	(396.3,391.1)	(401.4,396.2)	(387.8,382.9)	(385.1,380.1)	(384.2,379.3)	(374.8,369.9)	(373.2,368.4)	(372.5,367.7)
110	(395.5,390.3)	(401.4,396.2)	(406.5,401.5)	(385.1,380.1)	(383,378.1)	(374.8,369.9)	(394.8,389.9)	(372.6,367.7)
120	(409,403.8)	(401.4,396.3)	(380.9,376)	(385.1,380.2)	(370.7,365.8)	(374.9,370)	(374.6,369.8)	(372.6,367.7)
130	(395.9,390.7)	(401.4,396.3)	(380.1,375.2)	(385.1,380.2)	(379.6,374.7)	(374.9,370)	(375.9,371)	(372.6,367.7)
140	(410.6,405.4)	(401.5,396.3)	(383.1,378.2)	(385.1,380.2)	(378.8,373.8)	(374.9,370)	(377.6,372.7)	(372.6,367.8)
150	(405.7,400.5)	(401.5,396.3)	(387.1,382.2)	(385.2,380.2)	(378.5,373.6)	(374.9,370)	(374.9,370)	(372.6,367.8)
160	(398,392.8)	(401.5,396.3)	(380.7,375.8)	(385.2,380.2)	(374.5,369.6)	(374.9,370)	(376.2,371.3)	(372.6,367.8)
170	(408.3,403.1)	(401.5,396.3)	(376.2,371.3)	(385.2,380.2)	(371.8,366.8)	(374.9,370)	(374.8,369.9)	(372.7,367.8)
180	(404,398.7)	(401.5,396.3)	(378.9,373.9)	(385.2,380.2)	(374.7,369.8)	(374.9,370)	(372.2,367.4)	(372.7,367.8)
190	(404.2,399)	(401.5,396.3)	(383.2,378.2)	(385.2,380.2)	(379.9,375)	(374.9,370)	(376,371.1)	(372.7,367.8)
200	(407.6,402.4)	(401.5,396.3)	(382.3,377.3)	(385.2,380.2)	(382,377.1)	(374.9,370)	(372.3,367.4)	(372.7,367.8)
sim	**(400.2,396.2)**		**(384.5 ,376.4)**		**(374.7,365.8)**		**(373.4,367.8)**	

3.3.2 Sensitivity analysis

Similarly with the "continuousified" two-sided SN EWMA control chart, an extensive numerical analysis has been performed, regarding the efficiency of the "continuousify" method, applied to the two- and upper-sided EWMA Sign chart, focussing on the effect of the chart's parameters (λ, K_1, h) the in-control ARL value, the in-control probability p_{+1} and the Kernel density estimation method. In particular for the proposed upper-sided Sign EWMA Sign chart based on the "continuousify" method we may draw the following:

- ***Effect of the design parameters*** λ, K_1 ***and fixed value of*** ARL_0

  For the C-SN EWMA (Table 3.13) chart we may conclude that using the "continuousify"method the ARL values become steady even when $m \approx 100$ regardless the sample size and the desired in-control $\text{ARL}_0 \in \{200, 370.4, 500\}$. Additionally, the value of h does not affect the results (see Table 3.12). In particular, when h is neither too small or too large the results the same. Consequently, similarly with the EWMA chart based on Signed Ranks, setting the value of $h \approx 0.2$ is a reasonable choice to be considered.

- ***Effect of the shift magnitude*** p_{+1}

Regarding the out-of-control cases, for small shifts in the process location parameter, $p_{+1} < 0.6$, the corresponding out-of-control values are affected by the number of subintervals. On the other hand, using the "continuousify"method the results become immediately stable (Table 3.15). On the contrary, for large shifts ($p_{+1} > 0.6$) minor differences exist (Table 3.14). Nevertheless, since we proved that for the in-control case the results are different, practitioner may not be sure about the true out-of-control performance of the chart in term of its RL properties.

- ***Effect of the Kernel density estimation***

  Similarly with the two-sided case, from Table 3.16 it can been observed that regardless the values of the predefined ARL_0 and sample size, corresponding in-control ARL values remain unaffected by the choice of the Kernel.

- ***Effect of the in-control value of*** p_{+1}

  For any value of the in-control quantile of interest p_{+1} the "continuousify" method yields to reliable results for the chart's RL properties regardless the number of the subintervals. (see, Figure 3.3)

Table 3.12: ARL values of the C-SN EWMA chart for $\lambda = 0.2$, $K_1 = 2.75$ and for fixed values of $h = \{0.1, 0.15, \ldots, 0.3\}$ and different values of n

	$(n, p_{+1}) = (5, 0.5)$					$(n, p_{+1}) = (8, 0.5)$					$(n, p_{+1}) = (11, 0.5)$				
	h					h					h				
m	0.1	0.15	0.2	0.25	0.3	0.1	0.15	0.2	0.25	0.3	0.1	0.15	0.2	0.25	0.3
50	401.0	400.8	400.8	400.9	400.9	384.9	385.0	385.0	385.1	385.2	383.9	382.7	381.9	381.1	380.4
60	401.2	401.1	401.1	401.1	401.1	385.3	385.2	385.3	385.4	385.4	383.8	382.8	382.0	381.2	380.5
70	401.4	401.2	401.2	401.2	401.3	385.5	385.4	385.4	385.5	385.6	383.8	382.9	382.1	381.3	380.6
80	401.5	401.3	401.3	401.3	401.4	385.6	385.5	385.5	385.6	385.6	383.8	382.9	382.1	381.4	380.7
90	401.5	401.3	401.3	401.4	401.4	385.7	385.6	385.6	385.6	385.7	383.8	383.0	382.2	381.4	380.7
100	401.6	401.4	401.4	401.4	401.4	385.8	385.6	385.6	385.7	385.8	383.8	383.0	382.2	381.4	380.7
110	401.6	401.4	401.4	401.4	401.5	385.8	385.6	385.6	385.7	385.8	383.8	383.0	382.2	381.5	380.8
120	401.6	401.4	401.4	401.5	401.5	385.8	385.7	385.7	385.7	385.8	383.8	383.0	382.2	381.5	380.8
130	401.6	401.4	401.4	401.5	401.5	385.9	385.7	385.7	385.8	385.8	383.8	383.0	382.2	381.5	380.8
140	401.7	401.5	401.4	401.5	401.5	385.9	385.7	385.7	385.8	385.8	383.9	383.0	382.3	381.5	380.8
150	401.7	401.5	401.5	401.5	401.5	385.9	385.7	385.7	385.8	385.9	383.9	383.1	382.3	381.5	380.8
160	401.7	401.5	401.5	401.5	401.6	385.9	385.7	385.7	385.8	385.9	383.9	383.1	382.3	381.5	380.8
170	401.7	401.5	401.5	401.5	401.6	385.9	385.8	385.7	385.8	385.9	383.9	383.1	382.3	381.5	380.8
180	401.7	401.5	401.5	401.5	401.6	385.9	385.8	385.7	385.8	385.9	383.9	383.1	382.3	381.5	380.8
190	401.7	401.5	401.5	401.5	401.6	385.9	385.8	385.8	385.8	385.9	383.9	383.1	382.3	381.5	380.8
200	401.7	401.5	401.5	401.5	401.6	385.9	385.8	385.8	385.8	385.9	383.9	383.1	382.3	381.5	380.8

	$(n, p_{+1}) = (13, 0.5)$					$(n, p_{+1}) = (15, 0.5)$					$(n, p_{+1}) = (20, 0.5)$				
	h					h					h				
m	0.1	0.15	0.2	0.25	0.3	0.1	0.15	0.2	0.25	0.3	0.1	0.15	0.2	0.25	0.3
50	375.0	375.4	375.4	375.3	375.1	371.0	369.9	370.1	370.3	370.5	370.7	370.8	370.4	370.0	369.6
60	375.3	375.6	375.6	375.4	375.2	369.9	370.0	370.2	370.5	370.7	371.6	371.0	370.6	370.2	369.8
70	375.7	375.8	375.7	375.5	375.3	369.9	370.1	370.3	370.6	370.8	371.5	371.1	370.7	370.3	369.9
80	375.8	375.8	375.8	375.6	375.4	369.9	370.2	370.4	370.6	370.9	371.5	371.1	370.7	370.3	369.9
90	375.8	375.9	375.8	375.6	375.4	370.0	370.2	370.4	370.7	370.9	371.5	371.2	370.8	370.4	370.0
100	375.8	375.9	375.8	375.7	375.5	370.0	370.2	370.5	370.7	370.9	371.6	371.2	370.8	370.4	370.0
110	375.8	375.9	375.9	375.7	375.5	370.0	370.3	370.5	370.7	371.0	371.6	371.2	370.8	370.4	370.0
120	375.9	375.9	375.9	375.7	375.5	370.1	370.3	370.5	370.8	371.0	371.6	371.3	370.9	370.4	370.1
130	375.9	376.0	375.9	375.7	375.5	370.1	370.3	370.5	370.8	371.0	371.6	371.3	370.9	370.5	370.1
140	375.9	376.0	375.9	375.7	375.5	370.1	370.3	370.5	370.8	371.0	371.7	371.3	370.9	370.5	370.1
150	375.9	376.0	375.9	375.8	375.5	370.1	370.3	370.5	370.8	371.0	371.7	371.3	370.9	370.5	370.1
160	375.9	376.0	375.9	375.8	375.5	370.1	370.3	370.6	370.8	371.0	371.7	371.3	370.9	370.5	370.1
170	375.9	376.0	375.9	375.8	375.5	370.1	370.3	370.6	370.8	371.0	371.7	371.3	370.9	370.5	370.1
180	375.9	376.0	375.9	375.8	375.5	370.1	370.3	370.6	370.8	371.0	371.7	371.3	370.9	370.5	370.1
190	375.9	376.0	375.9	375.8	375.6	370.1	370.3	370.6	370.8	371.0	371.7	371.3	370.9	370.5	370.1
200	375.9	376.0	375.9	375.8	375.6	370.1	370.3	370.6	370.8	371.0	371.7	371.3	370.9	370.5	370.1

Table 3.13: Comparison of in control ARL values for the upper-sided SN EWMA (without "continuousify") and C-SN EWMA (with "continuousify" and $h = 0.2$) for several desired ARL_0 values

(In-control ARL values for the SN EWMA and C-SN EWMA charts for desired $ARL_0 = 200$)

	$(n, \lambda, K_1) = (5, 0.2, 2.50)$		$(n, \lambda, K_1) = (8, 0.2, 2.507)$		$(n, \lambda, K_1) = (9, 0.2, 2.515)$		$(n, \lambda, K_1) = (11, 0.2, 2.514)$	
m	SN EWMA	C-SN EWMA	SN EWMA	C-SN EWMA	SN EWMA	C-SN EWMA	SN EWMA	C-SN EWMA
50	189.7	199.8	202.9	199.8	212.6	199.8	205.5	199.9
70	202.4	199.9	203.9	199.9	205.8	199.9	197.9	200.0
90	201.7	200.0	196.1	200.0	202.8	200.0	201.3	200.0
110	203.0	200.0	200.5	200.0	199.7	200.0	200.6	200.0
130	200.7	200.0	207.9	200.0	198.7	200.0	200.9	200.0
150	203.6	200.0	201.8	200.0	199.4	200.0	201.8	200.0
170	202.6	200.0	203.9	200.0	198.4	200.0	199.4	200.0
190	196.0	200.0	202.5	200.0	198.5	200.0	200.7	200.0
200	203.9	200.0	202.0	200.0	199.0	200.0	200.8	200.0

(In-control ARL values for the SN EWMA and C-SN EWMA charts for desired $ARL_0 = 370.4$)

	$(n, \lambda, K_1) = (5, 0.2, 2.722)$		$(n, \lambda, K_1) = (8, 0.2, 2.736)$		$(n, \lambda, K_1) = (9, 0.2, 2.736)$		$(n, \lambda, K_1) = (11, 0.2, 2.738)$	
m	SN EWMA	C-SN EWMA	SN EWMA	C-SN EWMA	SN EWMA	C-SN EWMA	SN EWMA	C-SN EWMA
50	390.3	369.9	368.0	369.9	380.5	370.0	381.7	370.1
70	370.3	370.2	369.9	370.2	378.6	370.3	373.3	370.3
90	361.7	370.4	383.9	370.4	370.4	370.4	368.9	370.4
110	376.6	370.4	374.2	370.4	369.8	370.4	375.1	370.4
130	348.5	370.5	373.6	370.5	366.9	370.5	377.3	370.4
150	370.2	370.5	369.6	370.5	370.3	370.5	377.6	370.5
170	375.6	370.5	379.6	370.5	370.1	370.5	367.9	370.5
190	367.8	370.5	372.2	370.5	369.4	370.5	377.2	370.5
200	368.6	370.5	368.4	370.5	370.3	370.5	368.1	370.5

(In-control ARL values for the SN EWMA and C-SN EWMA charts for desired $ARL_0 = 500$)

	$(n, \lambda, K_1) = (5, 0.2, 2.822)$		$(n, \lambda, K_1) = (7, 0.2, 2.837)$		$(n, \lambda, K_1) = (9, 0.2,)$		$(n, \lambda, K_1) = (11, 0.2, 2.84)$	
m	SN EWMA	C-SN EWMA	SN EWMA	C-SN EWMA	SN EWMA	C-SN EWMA	SN EWMA	C-SN EWMA
50	521.5	499.1	495.8	499.0	496.7	499.3	544.5	499.4
70	523.9	499.6	494.3	499.5	505.1	499.7	509.1	499.7
90	494.1	499.8	503.8	499.8	503.0	499.8	497.7	499.9
110	492.9	499.9	498.2	499.9	502.2	499.9	508.1	499.9
130	492.8	500.0	510.1	500.0	490.0	500.0	498.9	500.0
150	494.8	500.0	498.5	500.0	504.7	500.0	497.0	500.0
170	495.3	500.0	499.9	500.0	516.2	500.0	502.9	500.0
190	509.5	500.0	493.8	500.0	498.4	500.0	497.3	500.0
200	494.4	500.0	505.5	500.1	505.1	500.0	499.5	500.0

Table 3.14: ARL_1 values for the UPPER-sided C-SN EWMA (without "continuousify") for large shifts

	$n = 8$				$n = 11$				$n = 15$			
m	$p_{+1} = 0.55$	$p_{+1} = 0.6$	$p_{+1} = 0.64$	$p_{+1} = 0.7$	$p_{+1} = 0.55$	$p_{+1} = 0.6$	$p_{+1} = 0.64$	$p_{+1} = 0.7$	$p_{+1} = 0.55$	$p_{+1} = 0.6$	$p_{+1} = 0.64$	$p_{+1} = 0.7$
50	94.1	28.1	13.0	7.9	75.6	21.1	10.0	6.3	56.3	15.4	7.6	5.0
60	96.0	28.4	13.1	8.0	71.5	20.4	9.7	6.1	54.1	15.1	7.5	4.9
70	89.4	27.1	12.7	7.8	73.2	20.7	9.8	6.2	54.3	15.1	7.5	4.9
80	92.7	27.8	12.9	7.9	72.9	20.6	9.8	6.2	54.4	15.1	7.5	4.9
90	94.0	28.0	13.0	7.9	74.0	20.8	9.9	6.2	54.5	15.1	7.5	4.9
100	93.8	28.0	13.0	7.9	71.7	20.4	9.7	6.1	54.3	15.1	7.5	4.9
110	94.4	28.1	13.0	7.9	72.3	20.5	9.8	6.2	54.7	15.2	7.6	4.9
120	92.6	27.8	12.9	7.9	71.2	20.3	9.7	6.1	54.6	15.1	7.5	4.9
130	92.7	27.8	12.9	7.9	72.5	20.6	9.8	6.2	54.6	15.1	7.5	4.9
140	93.6	28.0	13.0	7.9	71.6	20.4	9.7	6.1	53.7	15.0	7.5	4.9
150	93.4	27.9	12.9	7.9	71.8	20.4	9.8	6.1	54.8	15.2	7.5	4.9
160	92.2	27.7	12.9	7.9	72.8	20.6	9.8	6.2	54.7	15.1	7.5	4.9
170	92.7	27.8	12.9	7.9	72.6	20.6	9.8	6.2	54.9	15.2	7.6	4.9
180	93.8	28.0	13.0	7.9	72.7	20.6	9.8	6.2	54.6	15.1	7.5	4.9
190	92.8	27.8	12.9	7.9	72.3	20.5	9.8	6.2	54.6	15.1	7.5	4.9
200	93.1	27.9	12.9	7.9	72.5	20.6	9.8	6.2	54.8	15.2	7.5	4.9

	$n = 20$				$n = 12$				$n = 16$			
$2m + 1$	$p_{+1} = 0.55$	$p_{+1} = 0.6$	$p_{+1} = 0.64$	$p_{+1} = 0.7$	$p_{+1} = 0.55$	$p_{+1} = 0.6$	$p_{+1} = 0.64$	$p_{+1} = 0.7$	$p_{+1} = 0.55$	$p_{+1} = 0.6$	$p_{+1} = 0.64$	$p_{+1} = 0.7$
50	42.4	11.7	6.1	4.1	66.6	18.7	9.0	5.8	52.4	14.4	7.2	4.7
60	43.4	11.8	6.1	4.1	69.0	19.1	9.2	5.8	51.6	14.3	7.2	4.7
70	43.3	11.8	6.1	4.1	66.8	18.8	9.0	5.8	52.4	14.4	7.2	4.7
80	42.7	11.7	6.1	4.1	67.8	19.0	9.1	5.8	51.6	14.3	7.2	4.7
90	42.8	11.8	6.1	4.1	66.3	18.7	9.0	5.8	52.4	14.4	7.2	4.7
100	42.5	11.7	6.1	4.1	66.2	18.7	9.0	5.8	52.3	14.4	7.2	4.7
110	43.0	11.8	6.1	4.1	66.7	18.8	9.1	5.8	52.7	14.4	7.2	4.7
120	42.8	11.8	6.1	4.1	67.2	18.8	9.1	5.8	52.2	14.4	7.2	4.7
130	42.6	11.7	6.1	4.1	65.7	18.6	9.0	5.8	51.9	14.3	7.2	4.7
140	42.8	11.8	6.1	4.1	65.9	18.6	9.0	5.8	52.0	14.3	7.2	4.7
150	42.6	11.7	6.1	4.1	66.4	18.7	9.0	5.8	52.5	14.4	7.2	4.7
160	42.8	11.8	6.1	4.1	66.6	18.7	9.1	5.8	52.3	14.4	7.2	4.7
170	41.9	11.6	6.0	4.0	66.8	18.8	9.1	5.8	52.3	14.4	7.2	4.7
180	42.4	11.7	6.1	4.1	66.7	18.8	9.1	5.8	52.3	14.4	7.2	4.7
190	42.5	11.7	6.1	4.1	66.9	18.8	9.1	5.8	53.2	14.5	7.2	4.7
200	42.4	11.7	6.1	4.1	66.5	18.7	9.0	5.8	51.9	14.3	7.2	4.7

Table 3.15: Comparison of in control ARL values for the upper-sided SN EWMA (without "continuousify") and upper-sided C-SN EWMA (with "continuousify" and $\sigma = 0.2$) using $(\lambda, K_1) = (0.2, 2.75)$ for smalls shifts.

	$(n, p_{+1}) = (4, 0.52)$		$(n, p_{+1}) = (4, 0.53)$		$(n, p_{+1}) = (4, 0.54)$		$(n, p_{+1}) = (4, 0.55)$	
m	SN EWMA	C-SN EWMA	SN EWMA	C-SN EWMA	SN EWMA	C-SN EWMA	SN EWMA	C-SN EWMA
50	262.2	261.5	205.2	204.6	162.1	161.6	129.4	129.0
70	256.4	261.7	200.5	204.7	158.4	161.7	126.3	129.1
90	258.7	261.7	202.2	204.7	159.7	161.8	127.3	129.1
110	285.2	261.8	221.5	204.8	173.8	161.8	137.8	129.1
130	271.7	261.8	211.6	204.8	166.5	161.8	132.4	129.1
150	273.1	261.8	212.8	204.8	167.4	161.8	133.1	129.1
170	263.0	261.8	205.5	204.8	162.2	161.8	129.3	129.1
190	263.3	261.8	205.8	204.8	162.5	161.8	129.5	129.1
200	261.4	261.8	204.3	204.8	161.2	161.8	128.5	129.1
	$(n, p_{+1}) = (7, 0.52)$		$(n, p_{+1}) = (7, 0.53)$		$(n, p_{+1}) = (7, 0.54)$		$(n, p_{+1}) = (1570.55)$	
m	SN EWMA	C-SN EWMA	SN EWMA	C-SN EWMA	SN EWMA	C-SN EWMA	SN EWMA	C-SN EWMA
50	198.7	199.9	146.2	147.1	109.4	110.1	83.3	83.8
70	196.7	200.1	144.9	147.2	108.5	110.1	82.7	83.9
90	198.6	200.1	146.1	147.2	109.3	110.1	83.2	83.9
110	195.8	200.1	144.2	147.2	108.0	110.2	82.4	83.9
130	195.6	200.1	144.1	147.2	107.9	110.2	82.2	83.9
150	195.3	200.2	143.9	147.2	107.8	110.2	82.2	83.9
170	197.4	200.2	145.3	147.2	108.7	110.2	82.8	83.9
190	198.2	200.2	145.9	147.2	109.2	110.2	83.2	83.9
200	197.9	200.2	145.7	147.2	109.0	110.2	83.0	83.9
	$(n, p_1) = (12, 0.52)$		$(n, p_1) = (12, 0.53)$		$(n, p_1) = (12, 0.54)$		$(n, p_1) = (12, 0.55)$	
m	SN EWMA	C-SN EWMA	SN EWMA	C-SN EWMA	SN EWMA	C-SN EWMA	SN EWMA	C-SN EWMA
50	163.3	160.0	111.3	204.6	78.1	76.8	56.5	55.6
60	161.3	160.1	109.9	204.6	77.2	76.8	55.9	55.7
80	160.6	160.1	109.6	204.7	77.0	76.8	55.8	55.7
100	163.6	160.2	111.4	204.8	78.2	76.8	56.5	55.7
120	158.4	160.2	108.1	204.8	76.0	76.8	55.1	55.7
140	161.4	160.2	109.9	204.8	77.2	76.8	55.9	55.7
160	159.9	160.2	109.1	204.8	76.7	76.8	55.5	55.7
180	160.0	160.2	109.1	204.8	76.6	76.8	55.5	55.7
190	161.8	160.2	110.2	204.8	77.3	76.8	56.0	55.7
200	162.5	160.2	110.6	204.8	77.6	76.8	56.1	55.7

Table 3.16: ARL values of the C-SN EWMA chart for $\sigma = 0.2$, $n \in \{5, 8, 9\}$ for the standardised kernels listed in Table 3.7

(In-control ARL values the C-SN EWMA chart for desired $ARL_0 = 370.4$)

	$(n, \lambda, K_1) = (5, 0.2, 2.722)$					$(n, \lambda, K_1) = (8, 0.2, 2.736)$					$(n, \lambda, K_1) = (9, 0.2, 2.736)$				
m	Parabolic	Biweight	Cosine	Triweight	Normal	Parabolic	Biweight	Cosine	Triweight	Normal	Parabolic	Biweight	Cosine	Triweight	Normal
50	370.0	369.9	370.0	369.9	369.9	369.8	369.8	369.8	369.8	369.9	369.9	370.1	370.0	370.1	370.0
60	370.1	370.1	370.1	370.1	370.1	370.1	370.1	370.1	370.1	370.1	370.4	370.2	370.3	370.2	370.2
70	370.2	370.2	370.2	370.2	370.2	370.2	370.2	370.2	370.2	370.2	370.3	370.3	370.3	370.3	370.3
80	370.3	370.3	370.3	370.3	370.3	370.2	370.3	370.2	370.3	370.3	370.4	370.4	370.4	370.4	370.3
90	370.4	370.4	370.4	370.4	370.4	370.3	370.3	370.3	370.3	370.4	370.4	370.4	370.4	370.4	370.4
100	370.4	370.4	370.4	370.4	370.4	370.3	370.4	370.4	370.4	370.4	370.5	370.4	370.5	370.4	370.4
110	370.4	370.4	370.4	370.4	370.4	370.4	370.4	370.4	370.4	370.4	370.5	370.5	370.5	370.5	370.4
120	370.5	370.4	370.5	370.4	370.4	370.4	370.4	370.4	370.4	370.5	370.5	370.5	370.5	370.5	370.4
130	370.5	370.5	370.5	370.5	370.5	370.4	370.4	370.4	370.4	370.5	370.5	370.5	370.5	370.5	370.5
140	370.5	370.5	370.5	370.5	370.5	370.4	370.4	370.4	370.5	370.5	370.6	370.5	370.5	370.5	370.5
150	370.5	370.5	370.5	370.5	370.5	370.4	370.5	370.4	370.5	370.5	370.6	370.5	370.5	370.5	370.5
160	370.5	370.5	370.5	370.5	370.5	370.5	370.5	370.5	370.5	370.5	370.6	370.5	370.6	370.5	370.5
170	370.5	370.5	370.5	370.5	370.5	370.5	370.5	370.5	370.5	370.5	370.6	370.5	370.6	370.5	370.5
180	370.5	370.5	370.5	370.5	370.5	370.5	370.5	370.5	370.5	370.5	370.6	370.5	370.6	370.5	370.5
190	370.5	370.5	370.5	370.5	370.5	370.5	370.5	370.5	370.5	370.5	370.6	370.6	370.6	370.5	370.5
200	370.5	370.5	370.5	370.5	370.5	370.5	370.5	370.5	370.5	370.5	370.6	370.6	370.6	370.5	370.5

(In-control ARL values for the C-SN EWMA chart for desired $ARL_0 = 500$)

	$(n, \lambda, K_1) = (5, 0.2, 2.822)$					$(n, \lambda, K_1) = (8, 0.2, 2.837)$					$(n, \lambda, K_1) = (9, 0.2, 2.843)$				
m	Parabolic	Biweight	Cosine	Triweight	Normal	Parabolic	Biweight	Cosine	Triweight	Normal	Parabolic	Biweight	Cosine	Triweight	Normal
50	499.2	499.1	499.1	499.1	499.1	498.9	499.0	498.9	499.0	499.0	499.2	499.3	499.2	499.3	499.3
60	499.4	499.4	499.5	499.4	499.4	499.2	499.3	499.3	499.3	499.3	499.5	499.5	499.5	499.5	499.6
70	499.6	499.6	499.6	499.6	499.6	499.6	499.5	499.6	499.5	499.5	499.6	499.6	499.6	499.7	499.7
80	499.8	499.7	499.8	499.7	499.7	499.6	499.6	499.6	499.7	499.7	499.7	499.8	499.7	499.8	499.8
90	499.8	499.8	499.8	499.8	499.8	499.8	499.8	499.8	499.8	499.8	499.8	499.8	499.8	499.8	499.8
100	499.9	499.9	499.9	499.9	499.9	499.8	499.8	499.8	499.8	499.8	499.8	499.8	499.8	499.9	499.9
110	499.9	499.9	499.9	499.9	499.9	499.9	499.9	499.9	499.9	499.9	499.9	499.9	499.9	499.9	499.9
120	499.9	499.9	499.9	499.9	499.9	499.9	499.9	499.9	499.9	499.9	499.9	499.9	499.9	499.9	500.0
130	499.9	499.9	499.9	500.0	500.0	499.9	499.9	499.9	499.9	500.0	499.9	499.9	499.9	499.9	500.0
140	500.0	500.0	500.0	500.0	500.0	499.9	500.0	499.9	500.0	500.0	499.9	499.9	499.9	499.9	500.0
150	500.0	500.0	500.0	500.0	500.0	500.0	500.0	500.0	500.0	500.0	499.9	499.9	499.9	500.0	500.0
160	500.0	500.0	500.0	500.0	500.0	500.0	500.0	500.0	500.0	500.0	499.9	500.0	499.9	500.0	500.0
170	500.0	500.0	500.0	500.0	500.0	500.0	500.0	500.0	500.0	500.0	500.0	500.0	499.9	500.0	500.0
180	500.0	500.0	500.0	500.0	500.0	500.0	500.0	500.0	500.0	500.0	500.0	500.0	500.0	500.0	500.0
190	500.0	500.0	500.0	500.0	500.0	500.0	500.0	500.0	500.0	500.0	500.0	500.0	500.0	500.0	500.0
200	500.0	500.0	500.0	500.0	500.0	500.0	500.0	500.0	500.0	500.1	500.0	500.0	500.0	500.0	500.0

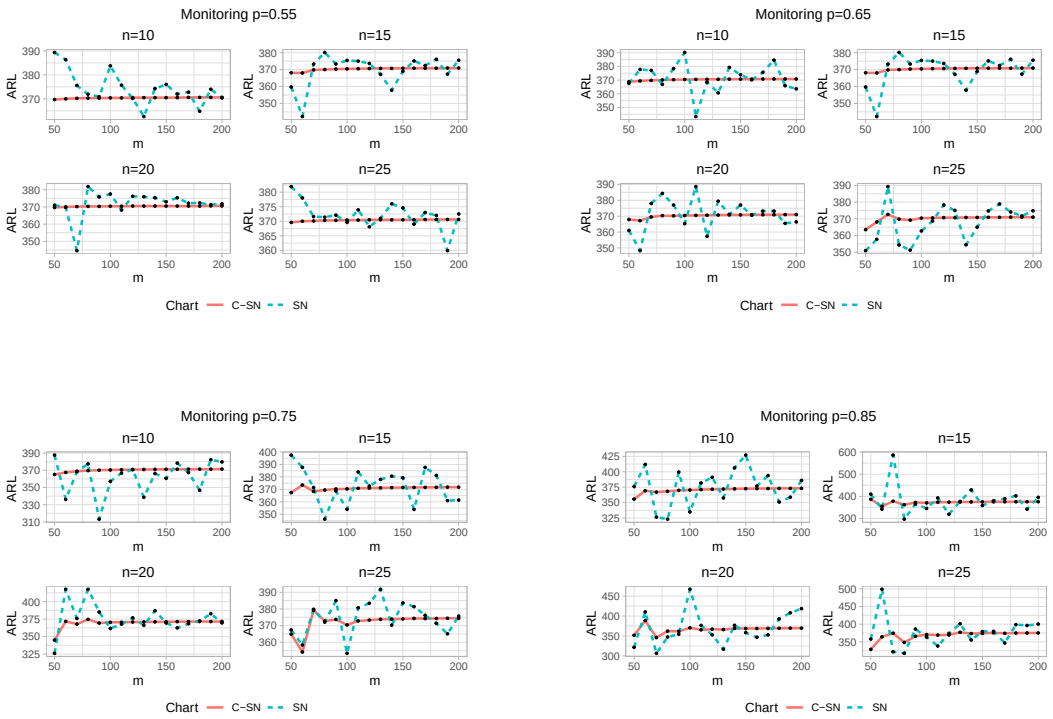

Figure 3.3: ARL_0 (plain lines) as a function of the number of sub-intervals $m \in \{50, 60, \ldots, 200\}$ for theSN EWMA and C-SN EWMA charts for different values of the in-control p_0

3.3.3 Optimal design of the C-SN EWMA chart

Following the same steps, with the two sided case, in Table 3.17 the optimal pairs of (λ, K_1) are given for different shifts in the process median along with the corresponding chart's out-of-control performance in terms of the ARL_1 values for each shift and sample size.

Table 3.17: optimal pairs of (λ, K_1) for the upper-sided C-SN EWMA chart, along with the corresponding chart's out-of-control performance in terms of the ARL_1 values for $p_{+1} \in \{0.55, 0.6, \ldots, 0.95\}$ and $n \in \{5, 6, \ldots, 20\}$

	p_{+1}								
n	0.55	0.6	0.65	0.7	0.75	0.8	0.85	0.9	0.95
5	(0.02,2.092),66.22	(0.05,2.422),28.34	(0.09,2.584),16.07	(0.14,2.679),10.49	(0.19,2.72),7.41	(0.245,2.733),5.56	(0.34,2.734),4.25	(0.425,2.704),3.27	(0.495,2.683),2.55
6	(0.025,2.181),59.85	(0.055,2.457),25.02	(0.105,2.623),14.08	(0.16,2.69),9.16	(0.235,2.74),6.42	(0.27,2.75),4.77	(0.375,2.744),3.71	(0.43,2.738),2.94	(0.47,2.724),2.39
7	(0.02,2.089),54.52	(0.065,2.502),22.5	(0.115,2.649),12.57	(0.185,2.727),8.13	(0.235,2.744),5.75	(0.345,2.758),4.25	(0.395,2.756),3.27	(0.435,2.754),2.63	(0.445,2.754),2.22
8	(0.025,2.173),50.65	(0.07,2.528),20.5	(0.125,2.657),11.4	(0.195,2.733),7.34	(0.25,2.76),5.16	(0.325,2.767),3.86	(0.445,2.751),3.01	(0.475,2.751),2.45	(0.925,2.8),1.94
9	(0.03,2.249),47.03	(0.075,2.547),18.86	(0.14,2.688),10.43	(0.2,2.737),6.73	(0.305,2.775),4.7	(0.355,2.779),3.51	(0.685,2.765),2.68	(0.72,2.743),1.93	(0.725,2.738),1.43
10	(0.03,2.251),44.1	(0.08,2.562),17.51	(0.15,2.698),9.64	(0.22,2.755),6.19	(0.295,2.773),4.37	(0.375,2.776),3.27	(0.575,2.777),2.46	(0.585,2.774),1.89	(0.61,2.765),1.44
11	(0.03,2.248),41.59	(0.085,2.582),16.35	(0.15,2.701),8.99	(0.26,2.773),5.75	(0.31,2.784),4.05	(0.48,2.782),3.01	(0.52,2.782),2.29	(0.53,2.78),1.82	(0.93,2.744),1.39
12	(0.035,2.307),39.37	(0.09,2.589),15.37	(0.165,2.719),8.41	(0.245,2.766),5.4	(0.345,2.786),3.79	(0.435,2.791),2.81	(0.7,2.771),2.17	(0.75,2.784),1.64	(0.945,2.835),1.22
13	(0.035,2.304),37.42	(0.1,2.621),14.49	(0.17,2.72),7.93	(0.255,2.776),5.07	(0.365,2.792),3.57	(0.4,2.792),2.69	(0.725,2.774),1.91	(0.73,2.771),1.44	(0.7,2.789),1.14
14	(0.04,2.354),35.69	(0.1,2.617),13.74	(0.185,2.738),7.48	(0.285,2.782),4.79	(0.355,2.798),3.37	(0.555,2.806),2.45	(0.58,2.802),1.85	(0.595,2.797),1.45	(0.95,2.712),1.13
15	(0.04,2.353),34.13	(0.11,2.643),13.06	(0.195,2.747),7.1	(0.285,2.787),4.55	(0.46,2.805),3.18	(0.49,2.806),2.35	(0.725,2.771),1.82	(0.93,2.824),1.37	(0.91,2.822),1.1
16	(0.04,2.351),32.72	(0.11,2.642),12.45	(0.195,2.745),6.77	(0.305,2.793),4.32	(0.42,2.802),3.03	(0.75,2.804),2.19	(0.75,2.804),1.58	(0.75,2.804),1.23	(0.76,2.797),1.04
17	(0.045,2.393),31.42	(0.12,2.66),11.91	(0.205,2.756),6.46	(0.36,2.802),4.13	(0.425,2.805),2.9	(0.6,2.817),2.07	(0.62,2.81),1.57	(0.92,2.72),1.24	(0.945,2.712),1.04
18	(0.045,2.392),30.27	(0.12,2.662),11.42	(0.215,2.758),6.19	(0.33,2.801),3.95	(0.51,2.821),2.73	(0.53,2.817),2.02	(0.77,2.78),1.55	(0.925,2.818),1.2	(0.93,2.819),1.03
19	(0.05,2.426),29.18	(0.13,2.676),10.97	(0.23,2.771),5.93	(0.345,2.804),3.79	(0.46,2.816),2.64	(0.765,2.817),1.87	(0.775,2.811),1.38	(0.775,2.811),1.12	(0.77,2.815),1.01
20	(0.05,2.426),28.23	(0.135,2.687),10.56	(0.24,2.776),5.7	(0.39,2.809),3.64	(0.95,2.622),2.46	(0.945,2.627),1.63	(0.945,2.627),1.23	(0.935,2.637),1.06	(0.94,2.632),1

3.4 Conclusions

In this Chapter a modified version of the conventional EWMA Sign chart was introduced. We we proposed the use of the "continuousify method, introdused by Wu et al. (2020), proving that this method leads to reliable results regardless the number of subintervals. Finally, an extensive sensitivity analysis was conducted stating the superiority of this method and the optimal design parameters for the proposed two- and upper-sided charts were provided.

Chapter 4

Performance of the Sign EWMA chart when ties are present

Introduction

In the previous Chapters, where extensions of nonparametric EWMA charts based on the Sign statistic were presented, an essential assumption was made, regarding the presence of ties between the sample's observations and the location parameter to be monitored. In particular, the assumption that the sample's distribution is a continuous one, prevents the occurrence of ties. However in practice, during the process monitoring, especially in the manufacturing industries the characteristic to be monitored is usually a continuous measurement (for instance length, weight, height etc). However, there might be cases where even though the characteristic to be monitored is a continuous measurement, possible ties might occur in the computation of the Sign statistic, due to the so called "*measurement errors*". As a consequence, there are some valid questions that need to be answered. " Is the performance of a nonparametric scheme affected by the presence of ties?", "Is there any efficient and simple way to tackle this issue?"

Over the past decades, the investigation of conventional control charts (i.e. charts assuming normality) under measurement errors has drawn the researchers' interest, in particular with reference to the bias and precision errors which introduce a rounding-off error resulting in a discretization of the observed measures. For a detailed literature review of control charts under measurement errors the reader is refered to Maleki et al. (2017). It is worth stretching that, rounding-off errors often result in "ties", even if their true distribution is continuous. Generally, in nonparametric statistical inference, the treatment of ties is of high importance due to the fact that the distribution of the nonparametric statistics such as the

Sign or the Wilcoxon signed rank statistics is seriously affected (Gibson and Melsa (1976); Putter (1955)). In this Chapter, the distribution-free property under measurement errors of the "continuousified" Sign EWMA chart is investigated and procedures to handle the occurrence of ties are discussed. Parts of this Chapter have been published in Perdikis et al. (2021c).

4.1 Distribution of the Sign statistic when ties are present

As presented in Section 2.1.1 considering θ_0 as the median of the distribution, the test statistic is defined as:

$$\mathrm{SN}_t = \sum_{j=1}^{n} S_{t,j},$$

with $\boldsymbol{p} = (p_{-1}, p_0, p_{+1})$ being the vector of probabilities:

$$\begin{aligned} p_{-1} &= \mathrm{P}(S_{t,j} = -1) = \mathrm{P}(X_{t,j} < \theta_0) = F_X(\theta_0|\theta), \\ p_0 &= \mathrm{P}(S_{t,j} = 0) = \mathrm{P}(X_{t,j} = \theta_0), \\ p_{+1} &= \mathrm{P}(S_{t,j} = +1) = \mathrm{P}(X_{t,j} > \theta_0) = 1 - F_X(\theta_0|\theta). \end{aligned}$$

Additionally, it was stated that when the characteristic to be monitored, X, is a continuous random variable, regardless the value of θ_0, we always have $p_0 = \mathrm{P}(X_{t,j} = \theta_0) = 0$. Then, the c.d.f. of SN_t can be easily derived through the Binomial distribution as presented in equation (2.3). However, in practice, due to the measurement system resolution, the real values $X_{t,j}$ are not directly observed. Instead, a measured value $X'_{t,j} \neq X_{t,j}$ is obtained introducing a rounding-off error which results in a discretization of the observed measures. Note that, even if the sample's true distribution is continuous, the presence of rounding-off errors might result in "ties" between the real values $X_{t,j}$ and the in-control value θ_0 of the median.

A well known linear measurement error model to account for three well-known sources of error is (see Linna and Woodall (2001)):

$$X'_{t,j} = \left\lfloor \frac{A + BX_{t,j} + \varepsilon_{t,j}}{\rho} + \frac{1}{2} \right\rfloor \rho, \tag{4.1}$$

where the constants (A, B) are related with the bias- linearity error, the noise $\varepsilon_{t,j}$ is the random variable which accounts for the precision error and ρ is a parameter quantifying the device resolution, which introduces a rounding-off error. More specifically, if ρ is the resolution of the measurement system then $X_{t,j}^{'} = x$ if $X_{t,j} \in (x-\frac{\rho}{2}, x+\frac{\rho}{2})$. For instance, if $\rho = 0.2$ and $\theta_0 = 100$ then possible measured values $X_{t,j}^{'}$ are $\{\ldots 99.6, 99.8, 100, 100.2, 100.4, \ldots\}$ and, if the real value is $X_{t,j} = 100.038$, then the measured observation is $X_{t,j}^{'} = 100$. As a consequence, a tie is generated. In general, the rounding-off error introduced by the device resolution in the measurement of the true value of a quality characteristic, results in a discretization of the observed quality characteristic and, in case of continuous measurements, the probability of having ties is therefore increased. It should be clarified the fact that, the primary goal of this work is to investigate the performance of a nonparametric scheme under the presence of ties. As a result, in order to make the interpretation of the results easier, we will investigate the effect of the tool resolution by maintaining the assumption of a perfect tool calibration, $(A, B) = (0, 1)$ and we will overlook the precision error. As a consequence, the error model given in (4.1) will simply be defined as:

$$X_{t,j}^{'} = \left\lfloor \frac{X_{t,j}}{\rho} + \frac{1}{2} \right\rfloor \rho, \tag{4.2}$$

In order to present a practical implementation regarding the effect of the rounding-off errors in the sample during the process monitoring, in Table 4.1 several samples of size $n = 10$ are considered, from the Normal distribution. At each column, the corresponding "observed" sample is presented computed through the measurement error model presented in equation (4.2) for different values of ρ along with the corresponding differences from the "true" sample (Table 4.2). It is clear, that as ρ starts to increases the "observed" sample differs from the "true" one. In particular, it can be seen that for $\rho > 0.2$ the observed values differ significantly from the true ones, or in many cases, tend to be the same. However, it is important to remind that the primary use of the measurement error model in this work, is to investigate the behaviour of the Sign EWMA chart under the occurrence of ties. As a consequence, aberrations of this magnitude, are not even practical for implementation and so it is relatively meaningless to perform any further investigation for large values of ρ. Nevertheless, in the rest of this Chapter, an extensive sensitivity analysis will be performed for different scenarios and general guidelines will be given for dealing with tied observations in the design of a nonparametric control chart.

Table 4.1: Effect of the rounding-off errors in the sample

	$N(0.5,1), \theta_0 = 0.5$								$N(0.5,5), \theta_0 = 0.5$							
	ρ								ρ							
$X_{i,j}$	0	0.01	0.05	0.10	0.20	0.30	0.40	0.70	0	0.01	0.05	0.10	0.20	0.30	0.40	0.70
1	1.7473	1.75	1.75	1.70	1.80	1.80	1.60	1.40	7.6155	7.62	7.60	7.60	7.60	7.50	7.60	7.70
2	2.8989	2.90	2.90	2.90	2.80	3.00	2.80	2.80	1.3327	1.33	1.35	1.3	1.4	1.2	1.2	1.4
3	-1.9247	-1.92	-1.90	-1.90	-2.00	-1.80	-2.00	-2.10	3.0070	3.01	3.00	3.00	3.00	3.00	3.20	2.80
4	0.0131	0.01	0.00	0.00	0.00	0.00	0.00	0.00	-0.0468	-0.05	-0.05	0.00	0.00	0.00	0.00	0.00
5	1.2718	1.27	1.25	1.30	1.20	1.20	1.20	1.40	3.9081	3.91	3.90	3.90	4.00	3.90	4.00	4.20
6	-1.1106	-1.11	-1.10	-1.10	-1.20	-1.20	-1.20	-1.40	4.8317	4.83	4.85	4.80	4.80	4.80	4.80	4.90
7	0.2560	0.26	0.25	0.30	0.20	0.30	0.40	0.00	-0.3215	-0.32	-0.30	-0.30	-0.40	-0.30	-0.40	0.00
8	1.2655	1.27	1.25	1.30	1.20	1.20	1.20	1.40	-1.3748	-1.37	-1.35	-1.40	-1.40	-1.50	-1.20	-1.40
9	-1.0723	-1.07	-1.05	-1.10	-1.00	-1.20	-1.20	-1.40	-6.6831	-6.680	-6.70	-6.70	-6.60	-6.60	-6.80	-7.00
10	0.5223	0.52	0.50	0.50	0.60	0.60	0.40	0.70	-5.2006	-5.20	-5.20	-5.20	-5.20	-5.10	-5.20	-4.90

	$N(10,1), \theta_0 = 10$								$N(10,5), \theta_0 = 10$							
	ρ								ρ							
$X_{i,j}$	0	0.01	0.05	0.10	0.20	0.30	0.40	0.70	0	0.01	0.05	0.10	0.20	0.30	0.40	0.70
1	10.5406	10.54	10.55	10.50	10.60	10.50	10.40	10.50	8.4316	8.43	8.45	8.40	8.40	8.40	8.40	8.40
2	10.4953	10.50	10.50	10.50	10.40	10.50	10.40	10.50	4.3207	4.32	4.30	4.30	4.40	4.20	4.40	4.20
3	8.3949	8.39	8.40	8.40	8.40	8.40	8.40	8.40	1.4402	1.44	1.45	1.40	1.40	1.50	1.60	1.40
4	8.4831	8.48	8.50	8.50	8.40	8.40	8.40	8.40	16.1216	16.12	16.10	16.10	16.20	16.20	16.00	16.10
5	9.5129	9.51	9.50	9.50	9.60	9.60	9.60	9.80	10.6650	10.66	10.65	10.70	10.60	10.80	10.80	10.50
6	8.7961	8.80	8.80	8.80	8.80	8.70	8.80	9.10	13.0649	13.06	13.05	13.10	13.00	13.20	13.20	13.30
7	10.7427	10.74	10.75	10.70	10.80	10.80	10.80	10.50	8.9060	8.91	8.90	8.90	9.00	9.00	8.80	9.10
8	8.4570	8.46	8.45	8.50	8.40	8.40	8.40	8.40	4.1332	4.13	4.15	4.10	4.20	4.20	4.00	4.20
9	11.8820	11.88	11.90	11.90	11.80	12.00	12.00	11.90	10.4116	10.41	10.40	10.40	10.40	10.50	10.40	10.50
10	9.3638	9.36	9.35	9.40	9.40	9.30	9.20	9.10	6.4064	6.41	6.40	6.40	6.40	6.30	6.40	6.30

Table 4.2: Differences between the "true" and "observed" samples

	$N(0.5,1), \theta_0 = 0.5$							$N(0.5,5), \theta_0 = 0.5$						
	ρ							ρ						
$X_{i,j}$	0.01	0.05	0.10	0.20	0.30	0.40	0.70	0.01	0.05	0.10	0.20	0.30	0.40	0.70
1	-0.00	-0.00	0.05	-0.05	-0.05	0.15	0.35	-0.00	0.02	0.02	0.02	0.12	0.02	-0.08
2	-0.00	-0.00	-0.00	0.10	-0.10	0.10	0.10	0.00	-0.02	0.03	-0.07	0.13	0.13	-0.07
3	-0.00	-0.02	-0.02	0.08	-0.12	0.08	0.18	-0.00	0.01	0.01	0.01	0.01	-0.19	0.21
4	0.00	0.01	0.01	0.01	0.01	0.01	0.01	0.00	0.00	-0.05	-0.05	-0.05	-0.05	-0.05
5	0.00	0.02	-0.03	0.07	0.07	0.07	-0.13	-0.00	0.01	0.01	-0.09	0.01	-0.09	-0.29
6	-0.00	-0.01	-0.01	0.09	0.09	0.09	0.29	0.00	-0.02	0.03	0.03	0.03	0.03	-0.07
7	-0.00	0.01	-0.04	0.06	-0.04	-0.14	0.26	-0.00	-0.02	-0.02	0.08	-0.02	0.08	-0.32
8	-0.00	0.02	-0.03	0.07	0.07	0.07	-0.13	-0.00	-0.02	0.03	0.03	0.13	-0.17	0.03
9	-0.00	-0.02	0.03	-0.07	0.13	0.13	0.33	-0.00	0.02	0.02	-0.08	-0.08	0.12	0.32
10	0.00	0.02	0.02	-0.08	-0.08	0.12	-0.18	-0.00	-0.00	-0.00	-0.00	-0.10	-0.00	-0.30

	$N(10,1), \theta_0 = 10$							$N(10,5), \theta_0 = 10$						
	ρ							ρ						
$X_{i,j}$	0.01	0.05	0.10	0.20	0.30	0.40	0.70	0.01	0.05	0.10	0.20	0.30	0.40	0.70
1	0.00	-0.01	0.04	-0.06	0.04	0.14	0.04	0.00	-0.02	0.03	0.03	0.03	0.03	0.03
2	-0.00	-0.00	-0.00	0.10	-0.00	0.10	-0.00	0.00	0.02	0.02	-0.08	0.12	-0.08	0.12
3	0.00	-0.01	-0.01	-0.01	-0.01	-0.01	-0.01	0.00	-0.01	0.04	0.04	-0.06	-0.16	0.04
4	0.00	-0.02	-0.02	0.08	0.08	0.08	0.08	0.00	0.02	0.02	-0.08	-0.08	0.12	0.02
5	0.00	0.01	0.01	-0.09	-0.09	-0.09	-0.29	0.00	0.01	-0.04	0.06	-0.14	-0.14	0.16
6	-0.00	-0.00	-0.00	-0.00	0.10	-0.00	-0.30	0.00	0.01	-0.04	0.06	-0.14	-0.14	-0.24
7	0.00	-0.01	0.04	-0.06	-0.06	-0.06	0.24	-0.00	0.01	0.01	-0.09	-0.09	0.11	-0.19
8	-0.00	0.01	-0.04	0.06	0.06	0.06	0.06	0.00	-0.02	0.03	-0.07	-0.07	0.13	-0.07
9	0.00	-0.02	-0.02	0.08	-0.12	-0.12	-0.02	0.00	0.01	0.01	0.01	-0.09	0.01	-0.09
10	0.00	0.01	-0.04	-0.04	0.06	0.16	0.26	-0.00	0.01	0.01	0.01	0.11	0.01	0.11

In order to fully understand the association between the magnitude of ρ and the number of tied observations, in Figure 4.1 some histograms are presented regarding the occurrence of ties for different values of ρ. In particular, for each case, a simulation of 50000 generated samples from $N(0,1)$ has been performed, and for each generated sample, the corresponding number of ties is reported. Then, for each case the corresponding histogram is presented regarding the distribution of the number of ties. It can be seen that for small values of ρ the number of ties is relative small. However, it is crucial to investigate if the chart's RL properties are affected by this small occurrence of ties.

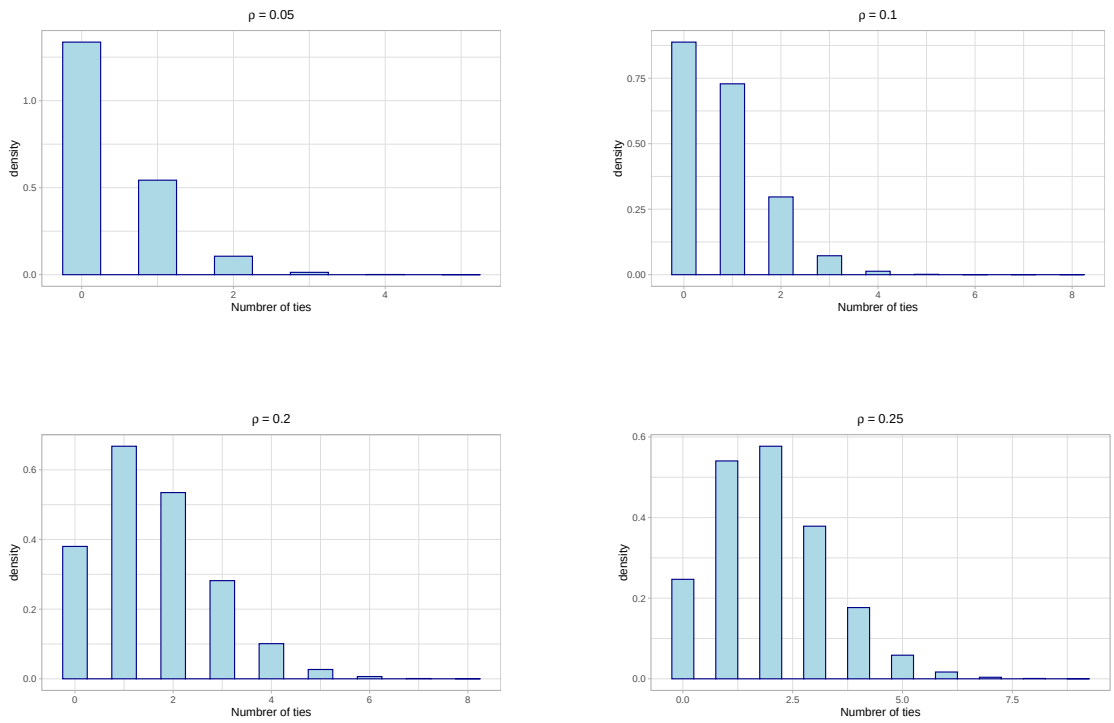

Figure 4.1: Distribution of the total number of ties for the random generated samples for $\mathrm{N}(0,1)$ for different values of $\rho = \{0, 005, 0.1, 0.2, 0.25\}$

Before we proceed to any further computations, the distribution of the SN_t statistic needs to be re-defined under the presence of ties. It is clear that, due to the occurrence of tied observations caused by the rounding-off errors of the measurement system, the statistic $S_{t,j}$ presented in Section 2.1.1 is no longer defined on $\{-1, 1\}$ but rather on $\{-1, 0, 1\}$. As a consequence, the quantity $S_{t,j} = \mathrm{sign}(X_{t,j} - \theta_0)$ has to be replaced by $S_{t,j} = \mathrm{sign}(X'_{t,j} - \theta_0)$ and the vector of probabilities $\boldsymbol{p} = (p_{-1}, p_0, p_{+1})$ must be re-defined as:

$$p_{-1} = \mathrm{P}(X'_{t,j} < \theta_0) = \mathrm{P}\left(X_{t,j} \leq \theta_0 - \frac{\rho}{2}\right) = F_X\left(\theta_0 - \frac{\rho}{2}|\theta\right),$$

$$\begin{aligned} p_0 &= \mathrm{P}(X'_{t,j} = \theta_0) = \mathrm{P}\left(\theta_0 - \frac{\rho}{2} < X_{t,j} \leq \theta_0 + \frac{\rho}{2}\right) \\ &= F_X\left(\theta_0 + \frac{\rho}{2}|\theta\right) - F_X\left(\theta_0 - \frac{\rho}{2}|\theta\right), \end{aligned}$$

$$p_{+1} = \mathrm{P}(X'_{t,j} > \theta_0) = \mathrm{P}\left(X_{t,j} > \theta_0 + \frac{\rho}{2}\right) = 1 - F_X\left(\theta_0 + \frac{\rho}{2}|\theta\right).$$

4.1.1 Cumulative distribution and probability mass functions of SN_t when ties are present

Based on the above statements, it can be clearly concluded that, the variable SN_t is no longer defined on $\{-n, -n+2, \ldots, n-2, n\}$ but it is rather defined on $\{-n, -n+1, \ldots, n-1, n\}$. Additionally, the p.m.f. of SN_t cannot longer be computed through to the Binomial distribution as for the "without ties" case. Castagliola et al. (2020) provided three different ways for evaluating, the p.m.f. of SN_t when ties are present. More specifically, the results obtained through these approaches are equivalent and consistent with the "no ties" case (i.e. when $\rho = 0$). Additionally, for illustration purposes, in Figures 4.2 and 4.3 the p.m.f. of SN_t with ($\rho = \{0.05, 0.1, 0.2, 0.5\}$) and without ties ($\rho = 0$) is presented for $n = 25$ and $n = 40$ respectively.

1^{st} approach

Firstly, a simple way to consider for the computation of the p.m.f., $f_{\mathrm{SN}_t}(s|n, p_{+1})$, of SN_t is a recursive one. In particular, since $\mathrm{SN}_t = S_{t,1} + S_{t,2}, \ldots, S_{t,n} = s$ equals to:

- $(S_{t,1} + S_{t,2}, \ldots, S_{t,n-1} = s+1) \cup (S_{t,n} = -1)$, or
- $(S_{t,1} + S_{t,2}, \ldots, S_{t,n-1} = s) \cup (S_{t,n} = 0)$, or
- $(S_{t,1} + S_{t,2}, \ldots, S_{t,n-1} = s-1) \cup (S_{t,n} = +1)$.

Then, for $s \in \{-n, -n+1, \ldots, n\}$ we have

$$f_{\mathrm{SN}_t}(s|n, p_{+1}) = p_{-1} f_{\mathrm{SN}_t}(s+1|n-1, p_{+1}) + p_0 f_{\mathrm{SN}_t}(s|n-1, p_{+1}) + p_{+1} f_{\mathrm{SN}_t}(s-1|n-1, p_{+1}),$$

with $f_{\mathrm{SN}_t}(s|n=1,p_{+1}) = p_s$ for $s \in \{-1,0,1\}$.

2^{nd} approach

The second method for the computation of the p.m.f. of SN_t is by considering the possible values of $\mathrm{SN}_t = \{-n, -n+1, \ldots, n-1, n\}$ as the states of a discrete time Markov chain with transition probability matrix $\mathbf{P}$:

		state i							
		$-n$	$-n+1$	$-n+2$	$\ldots$	$n-2$	$n-1$	n	$*$
	$-n$	p_0	p_{+1}	$\ldots$	$\ldots$	$\ldots$	$\ldots$	0	p_{-1}
	$-n+1$	p_{-1}	p_0	p_{+1}					0
	$-n+2$	0	p_{-1}	p_0	p_{+1}				$\vdots$
state j	$\vdots$	$\vdots$			-1				$\vdots$
	$n-2$	$\vdots$			p_{-1}	p_0	p_{+1}		$\vdots$
	$n-1$	$\vdots$				p_{-1}	p_0	p_{+1}	0
	n	$\vdots$			-1	.	p_{-1}	p_0	p_{+1}
	$*$	$\vdots$	$\vdots$			$\vdots$	0	0	1

where the state "$*$" corresponds to the absorbing state. Additionally, if we consider $\mathbf{p} = (0, \ldots, 0, 1, 0, \ldots, 0)^\intercal$ the vector of initial probabilities the corresponding p.m.f. vector

$$\mathbf{f} = (f_{\mathrm{SN}_t}(-n|n,p_{+1}), f_{\mathrm{SN}_t}(-n+1|n,p_{+1}), \ldots, f_{\mathrm{SN}_t}(n|n,p_{+1}))^\intercal,$$

can be computed through $\mathbf{f} = \mathbf{p}\mathbf{P}^n$.

3^{th} approach

Finally, an alternative way is to evaluate the p.m.f. of SN_t by summing all the possible combinations, like the Binomial distribution. More specifically, if we denote n_{-1} to be the number of occurrences of $S_{t,j} = -1$ in $\{S_{t,1}, S_{t,2}, \ldots, S_{t,n}\}$, then the possible values of SN_t falls between n_{-1} and $n_{-1} + n + n_{-1} = n - 2n_{-1}$. As a consequence, if $\mathrm{SN}_t = s$ we have that $-s \leq n_{-1} \leq \frac{n-s}{2}$ and as n_{-1} is a positive integer $\max(0,-s) \leq n_{-1} \leq \lfloor \frac{n-s}{2} \rfloor$. Therefore, for

each integer value in $i \in \{\max(0,-s),\ldots,\lfloor\frac{n-s}{2}\rfloor\}$ by counting all the possible combinations of

- i occurrences of $S_{t,j}=-1$
- $n-s-2i$ occurrences of $S_{t,j}=0$
- $s+i$ occurrences of $S_{t,j}=+1$

the following formula is obtained

$$f_{SN_t}(s|n,\boldsymbol{p}) = \sum_{i=max(0,-s)}^{\lfloor\frac{n-s}{2}\rfloor} \binom{n}{i}\binom{n-i}{s+i} p_{-1}^{i} p_0^{n-s-2i} p_{+1}^{s+i}$$

Mean and variance of SN_t when ties are present

Since $\mathrm{SN}_t = \sum_{k=1}^{n} S_i$, $S_{t,j} \in \{-1,0,1\}$, for the mean and variance of SN, we have:

$$\mathrm{E}_{tied}(\mathrm{SN}_t) = n \times m_1,$$

and

$$\mathrm{V}_{tied}(\mathrm{SN}_t) = n \times \mu_2$$

where m_1 and μ_2 are the corresponding mean and variance of $S_{t,j}$ defined as:

$$m_1 = \mathrm{E}(S_{t,j}) = \sum_{\forall S_{t,j}} p_i \times S_i = p_{-1}\times(-1) + p_0 \times 0 + p_{+1}\times(1) = p_{+1} - p_{-1},$$

and

$$\mu_2 = \mathrm{V}(S_{t,j}) = \sum_{\forall S_i t,j} p_i \times (S_{t,j}-m_1)^2 = p_{-1}\times(-1-m_1)^2 + p_0\times(0-m_1)^2 + p_{+1}\times(1-m_1)^2$$

It can be easily seen that when $p_{+1}=p_{-1}=0.5$ and $p_0=0$ (i.e. for $\rho=0$) we have that $\mathrm{E}(\mathrm{SN}_t)=0$ and $\mathrm{V}(\mathrm{SN}_t)=n$ which are the corresponding in-control mean and variance of SN_t where there is no tie.

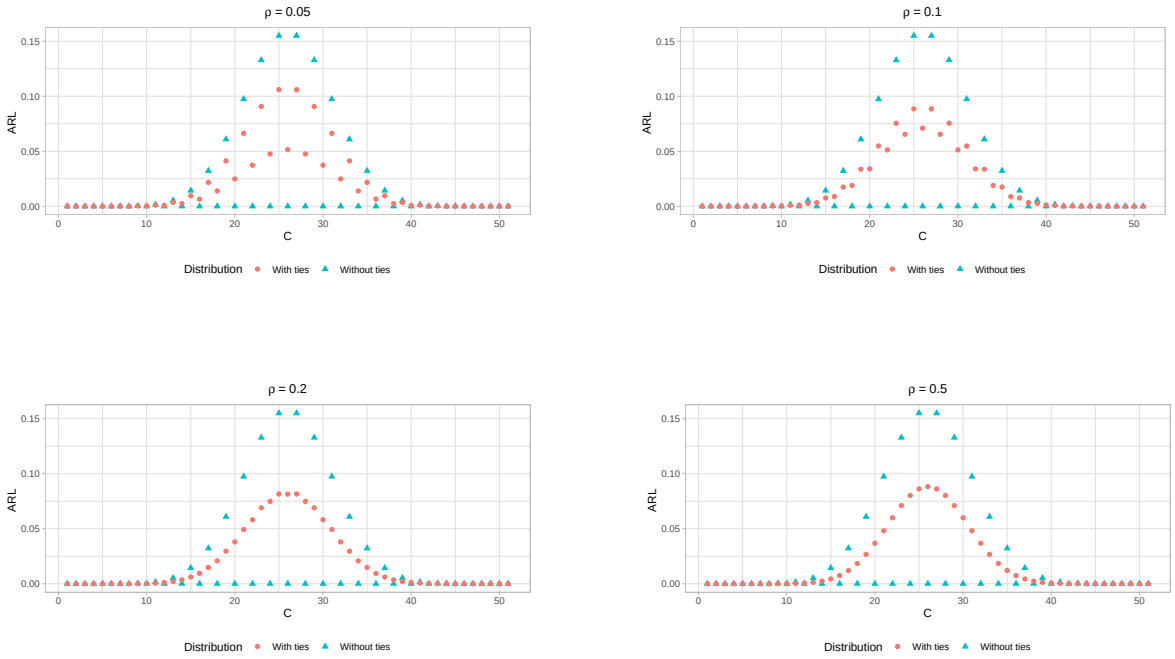

Figure 4.2: p.m.f. of SN_t with and without ties for $\rho = \{0.05, 0.1, 0.2, 0.5\}$ and $n = 25$

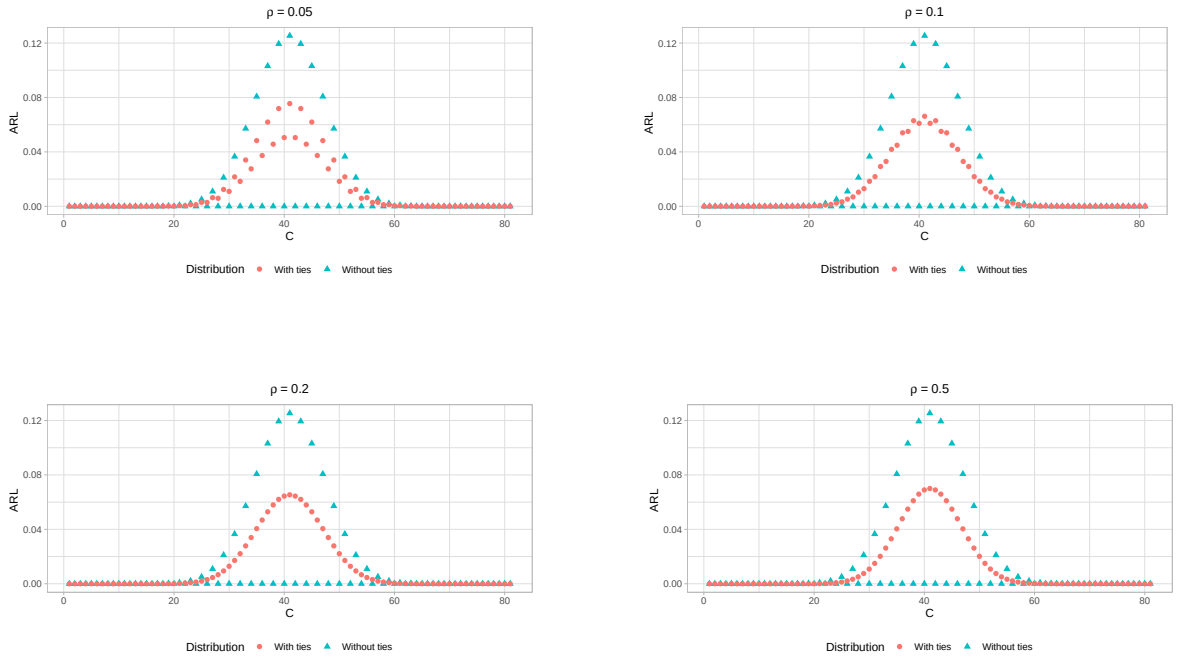

Figure 4.3: p.m.f. of SN_t with and without ties for $\rho = \{0.05, 0.1, 0.2, 0.5\}$ and $n = 40$

4.2 A short Review on the Shewhart SN chart when ties are present

Recently, Castagliola et al. (2020), investigated the distribution-free properties of the Shewhart Sign chart when ties are present. They showed that, when ties are present, the chart's RL properties are highly affected and its distribution-free properties are no longer valid. They investigated two approaches and came up with the solution of a Bernoulli-based approach called as the "flip a coin" strategy (see, Sections below). Additionally, they presented the chart's in- and out-of-control properties under the benchmark of several Johnson-type Distributions defined below and listed in Table 4.3.

Johnson Distributions

By definition, (see, Johnson (1949)) the random variable Z follows a Johnson distribution with parameters a, b, c, d where a, $b > 0$, $c \in \mathbb{R}$ and $d > 0$, if it can be reduced to a standard Normal variable $Y \sim \mathrm{N}(0, 1)$ through the following transformation:

$$Y = a + b f_J = \left(\frac{Z - c}{d} \right)$$

where f_J is a Johnson transformation that leads to two kind of distributions; the Johnson S_B defined on $[c, c+d]$ and the Johnson S_U defined on $(-\infty, +\infty)$. Generally, the c.d.f. $F_Z(\ldots)$ and inverse c.d.f. $F_Z^{-1}(\ldots)$ of a Johnson's-type distribution are defined as:

- bounded on $[c, c+d]$ (denoted as B in Table 4.3) with $F_Z(x)$ equal to:

$$F_Z(x) = F_{\mathrm{N}}\left(a + b\ln\left(\frac{x-c}{c+d-x}\right)\right), x \in [c, c+d]$$

$$F_Z^{-1}(u) = c + \frac{d}{1+\exp\left(\frac{a-F_{\mathrm{N}}^{-1}(u)}{b}\right)}, 0 < u < 1$$

- unbounded on $(-\infty, \infty)$ (denoted as U in Table 4.3) with $F_Z(x)$ equal to:

$$F_Z(x) = F_{\mathrm{N}}\left(a + b\sinh^{-1}\left(\frac{x-c}{d}\right)\right), x \in (-\infty, \infty)$$

$$F_Z^{-1}(u) = c + d\sinh\left(\frac{F_{\mathrm{N}}^{-1}(u) - a}{b}\right), 0 < u < 1.$$

where $F_{\mathrm{N}}^{-1}(\ldots)$ is the inverse c.d.f. of the standard normal distribution respectively.

Similarly, with the design of a conventional parametric control chart the process shift can be expressed in terms of the standardized distribution shift of magnitude δ, as $\theta_1 = \theta_0 + \delta\sigma$. Also, let $F_X(x|\theta)$ belongs to a location-scale family of distributions which can be rewritten as $F_X(x|\theta) = F_Z(\frac{x-\theta}{\sigma})$ where σ is the standard deviation of X. Finally, by defining the quantity $\kappa = \frac{\rho}{\sigma}$ as the *standardized resolution*, the vector of probabilities $\boldsymbol{p} = (p_{-1}, p_0, p_{+1})$, can be rewritten as a function of the system resolution:

$$\begin{aligned} p_{-1} &= F_Z\left(-\frac{\kappa}{2} - \delta\right), \\ p_0 &= F_Z\left(\frac{\kappa}{2} - \delta\right) - F_Z\left(-\frac{\kappa}{2} - \delta\right), \\ p_{+1} &= 1 - F_Z\left(\frac{\kappa}{2} - \delta\right). \end{aligned} \tag{4.3}$$

Table 4.3: Benchmark of 17 Johnson's type distributions.

case	γ_3	γ_4	type	a	b	c	d
1	0	-1.2	B	0	0.64646	-1.81530	3.63060
2	0	-0.6	B	0	1.39830	-3.10970	6.21950
3	0	0	U	0	100	0	100
4	0	1	U	0	2.3212	0	2.10940
5	0	3	U	0	1.6104	0	1.31180
6	0	6	U	0	1.3493	0	1
7	2	4.3	B	1.7464	0.69076	-0.48932	6.6213
8	2	6.1	B	3.3279	1.227	-1.0016	16.088
9	2	7.9	U	-4.85600	1.8044	-1.41900	0.19332
10	2	10.8	U	-1.0444	1.432	-0.65538	0.82361
11	2	16.7	U	-0.52977	1.2093	-0.33154	0.73314
12	2	25.5	U	-0.34371	1.0892	-0.2023	0.63054
13	5	52.6	B	5.2193	0.98134	-0.47316	97.043
14	5	65.3	U	-4.01870	1.0864	-0.56652	0.02806
15	5	86	U	-0.75701	0.98744	-0.32033	0.37954
16	5	128.7	U	-0.43187	0.90797	-0.18538	0.37543
17	5	192.1	U	-0.29868	0.85558	-0.12122	0.34029

When the process is in-control (i.e. $\delta = 0$) the above expressions can be simplified into

$$
\begin{aligned}
p_{-1} &= F_Z\left(-\frac{\kappa}{2}\right), \\
p_0 &= F_Z\left(\frac{\kappa}{2}\right) - F_Z\left(-\frac{\kappa}{2}\right), \\
p_{+1} &= 1 - F_Z\left(\frac{\kappa}{2}\right).
\end{aligned}
$$

In Table 4.3, 17 cases of the Johnson's family distributions are presented. Moreover, for each distribution, the corresponding values of the parameters a, b, c, d, have been selected in order to satisfy $\text{med}(Z) = 0$ (for the median) and $\sigma(Z) = 1$ (for the standard-deviation). These values have been obtained from Castagliola et al. (2020). The cases #1−#6 approximatively match some well known symmetric distributions. In particular, case #1 is close to the Uniform distribution, case #2 is close to the Triangular distribution while case #3 almost corresponds to the Standard Normal distribution. Additionally, cases #4−#6 are close to the Student t distribution with 10, 6 and 5 degrees of freedom, respectively. Finally, the remaining 12 cases, under different values for the skewness $\gamma_3 > 0$ and kurtosis $\gamma_4 > 0$ aim to cover a large variety of asymmetric and heavily-tailed distributions. For more details, a graphical representation of these distributions is provided in Figure 4.4 where, for each of them, the same scale has been used.

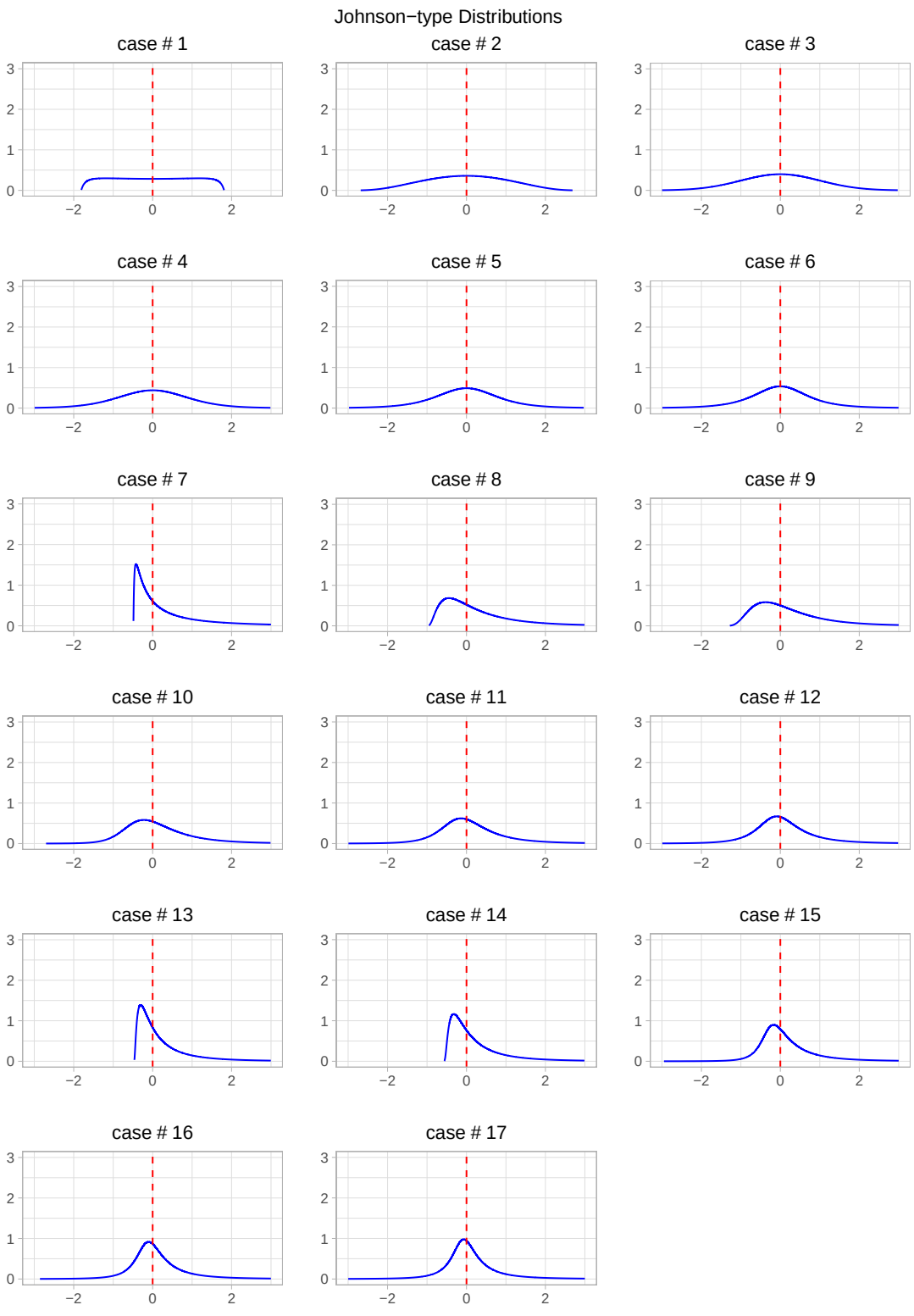

Figure 4.4: Johnson-type Distributions listed in Table 4.3

Performance of the S-SN chart when ties are present

An efficient strategy to handle ties in the design of a Sign chart, is the "flip a coin" strategy, originally proposed by Castagliola et al. (2020), in which the probability p_0 is equally allocated on both sides for values $S_{t,j} = +1$ and $S_{t,j} = -1$. More specifically, for each value $S_{t,j} = 0$ it is proposed the transformation $S_{t,j} = 2\Delta_{t,j} - 1$ where $\Delta_{t,j} \sim \text{Ber}(0.5)$ is a Bernoulli random variable of parameter 0.5. As a consequence, applying this strategy is equivalent to consider the two-sided Sign Shewhart control chart in the "without ties" case with the following new probabilities:

$$\begin{aligned} p'_{-1} &= p_{-1} + \frac{p_0}{2}, \\ p'_0 &= 0, \\ p'_{+1} &= p_{+1} + \frac{p_0}{2}. \end{aligned}$$

In Table 4.4, the in-control ($\delta = 0$) vectors of probabilities $\boldsymbol{p}' = (p'_{-1}, p'_0, p'_{+1})$ for the 17 distributions are reported for different values of κ. We can conclude that when $\kappa = 0$, as expected, we always have $p'_0 = 0, p'_{+1} = p'_{-1} = 0.5$ no matter the considered distribution. Moreover, for the *symmetric* cases $\#1 - \#6$, (when $\kappa > 0$) we always have $p'_{+1} = p'_{-1} = 0.5$ This is also an expected result. Finally, for the *asymmetric* cases, even though p'_{+1} differs from p'_{-1} all the p'_{+1} values remain really close to 0.5, since $|p'_{+1} - 0.5| < 0.01$ for the cases $\#7 - \#17$.

Table 4.4: Vector of in-control probabilities (p'_{-1}, p'_0, p'_{+1}) with the "flip a coin" strategy for the 17 distributions in Table 4.3.

case	$\kappa = 0$			$\kappa = 0.05$			$\kappa = 0.1$			$\kappa = 0.2$		
1	0.5000	0.0000	0.5000	0.5000	0.0000	0.5000	0.5000	0.0000	0.5000	0.5000	0.0000	0.5000
2	0.5000	0.0000	0.5000	0.5000	0.0000	0.5000	0.5000	0.0000	0.5000	0.5000	0.0000	0.5000
3	0.5000	0.0000	0.5000	0.5000	0.0000	0.5000	0.5000	0.0000	0.5000	0.5000	0.0000	0.5000
4	0.5000	0.0000	0.5000	0.5000	0.0000	0.5000	0.5000	0.0000	0.5000	0.5000	0.0000	0.5000
5	0.5000	0.0000	0.5000	0.5000	0.0000	0.5000	0.5000	0.0000	0.5000	0.5000	0.0000	0.5000
6	0.5000	0.0000	0.5000	0.5000	0.0000	0.5000	0.5000	0.0000	0.5000	0.5000	0.0000	0.5000
7	0.5000	0.0000	0.5000	0.4996	0.0000	0.5004	0.4986	0.0000	0.5014	0.4942	0.0000	0.5058
8	0.5000	0.0000	0.5000	0.4999	0.0000	0.5001	0.4994	0.0000	0.5006	0.4976	0.0000	0.5024
9	0.4999	0.0000	0.5001	0.4998	0.0000	0.5002	0.4995	0.0000	0.5005	0.4982	0.0000	0.5018
10	0.5000	0.0000	0.5000	0.4999	0.0000	0.5001	0.4996	0.0000	0.5004	0.4984	0.0000	0.5016
11	0.5000	0.0000	0.5000	0.4999	0.0000	0.5001	0.4996	0.0000	0.5004	0.4985	0.0000	0.5015
12	0.5000	0.0000	0.5000	0.4999	0.0000	0.5001	0.4996	0.0000	0.5004	0.4985	0.0000	0.5015
13	0.5000	0.0000	0.5000	0.4994	0.0000	0.5006	0.4978	0.0000	0.5022	0.4912	0.0000	0.5088
14	0.4999	0.0000	0.5001	0.4995	0.0000	0.5005	0.4983	0.0000	0.5017	0.4932	0.0000	0.5068
15	0.5000	0.0000	0.5000	0.4997	0.0000	0.5003	0.4987	0.0000	0.5013	0.4950	0.0000	0.5050
16	0.5000	0.0000	0.5000	0.4997	0.0000	0.5003	0.4989	0.0000	0.5011	0.4957	0.0000	0.5043
17	0.5000	0.0000	0.5000	0.4997	0.0000	0.5003	0.4989	0.0000	0.5011	0.4959	0.0000	0.5041

In table 4.5 the in-control ARL values of the S-SN chart are presented with and without the "flip a coin" strategy for $n = 20$ and $\kappa = \{0, 0.05, 0.1, 0.2\}$. It is clear that, when ties are present, the conventional S-SN chart is no longer distribution-free. In particular, even for small values of κ, the ARL_0 are highly affected and are far from 388.8 (i.e. the "no ties" case). On the other hand, the "flip a coin" strategy makes the results robust, and unaffected by the underlying distribution.

Table 4.5: Performance of the S-SN chart for $n = 20$ with and without the "flip a coin strategy"

	Without "flip a coin" strategy				With "flip a coin" strategy			
Cases	$\kappa = 0$	$\kappa = 0.05$	$\kappa = 0.1$	$\kappa = 0.2$	$\kappa = 0$	$\kappa = 0.05$	$\kappa = 0.1$	$\kappa = 0.2$
#1	388.07	468.83	551.73	722.16	388.07	388.07	388.07	388.07
#2	388.07	490.45	595.75	815.83	388.07	388.07	388.07	388.07
#3	388.07	502.13	619.58	868.52	388.07	388.07	388.07	388.07
#4	388.07	513.81	643.47	923.14	388.07	388.07	388.07	388.07
#5	388.07	528.64	673.93	995.93	388.07	388.07	388.07	388.07
#6	388.07	542.86	703.31	1070.04	388.07	388.07	388.07	388.07
#7	388.07	563.52	746.96	1183.49	388.07	388.05	387.77	383.29
#8	388.07	537.88	693.17	1044.11	388.07	388.07	388.02	387.24
#9	388.07	532.44	681.85	1015.69	388.07	388.07	388.04	387.61
#10	388.07	544.19	706.15	1077.52	388.07	388.07	388.05	387.71
#11	388.07	577.55	776.18	1273.13	388.07	388.07	388.05	387.76
#12	388.07	714.21	1095.10	2274.84	388.07	387.84	384.33	387.80
#13	388.07	629.74	891.35	1638.64	388.07	388.03	387.37	377.24
#14	388.07	609.63	846.21	1489.18	388.07	388.04	387.64	381.55
#15	388.07	618.18	864.95	1558.77	388.07	388.06	387.84	384.49
#16	388.07	639.55	913.25	1739.21	388.07	388.06	387.89	385.36
#17	388.07	663.39	969.14	1967.48	388.07	388.06	387.91	385.68

4.3 The "continuousified" two-sided 2C-SN EWMA chart when ties are present

Motivated by the fact that for nonparametric Shewhart charts the presence of ties affects their performance, we are going to investigate the effect of the measurement errors in the performance of the two-sided EWMA chart introduced in Sections 3.2. In particular, the exact same design will be used, with the only difference that, regarding computation of the p.m.f. of SN_t, the general expression of its distribution will be used as presented in Section 4.1.1. For the 17 Johnson's type distributions presented in Table 4.3, the ARL values of the two-sided EWMA control chart will be presented for shifts $\delta \in \{-0.5, -0.2, -0.1, 0, 0.1, 0.2, 0.5\}$ and for standardized resolution $\kappa = 0$ (without ties) and $\kappa \in \{0.05, 0.1, 0.2\}$ (with ties) using three different strategies. More specifically, in Section 4.3.1 the same control limits $(\mathrm{UCL}, \mathrm{LCL})$ will be used, for the 17 Johnson's type distributions. In Section 4.3.2 a semi-parametric approach will be used where, *new* control limits will be defined, adjusted to the underlying distribution. Lastly, in Section 4.3.3, the Bernoulli trial-based approach presented in Section 4.2 will be investigated where tied observations will be equally treated as negative or positive differences.

4.3.1 Run length properties of the 2C-SN EWMA chart using the traditional control limits

First, the RL properties of the two-sided 2C-SN EWMA chart will be examined, under tied scenarios using the charting statistic defined in equation (3.9) and the fixed control limits as defined in Section 3.2.2. Regarding the computation of the control limits, the in-control mean, $\mathrm{E}_0(\mathrm{SN}_t^*)$ and variance, $\mathrm{V}_0(\mathrm{SN}_t^*)$ of SN_t^* will be the same for all the cases regardless the underlying distribution as defined in (3.12). In Table 4.6 the performance of the 2C-SN EWMA chart is investigated under the benchmark of the 17 Johnson distributions for a fixed value of $n = 20$ and two optimal pairs (λ^*, K^*) listed in Table 3.10:

- The first optimal pair is $(\lambda^* = 0.12, K^* = 2.743)$. This one corresponds to the optimal pair (λ^*, K^*) for detecting a shift corresponding to a small value $p_{+1} = 0.6$ for $n = 20$. The value $p_{+1} = 0.6$ is considered as a small shift in the in-control process median.

- The second optimal pair is $(\lambda^* = 0.72, K^* = 2.928)$. This one corresponds to optimal pair (λ^*, K^*) for detecting a shift corresponding to a moderate to large value $p_{+1} = 0.85$ for $n = 20$. The value $p_{+1} = 0.85$ corresponds to a moderate shift in the in-control process median.

It should be noted that the pairs of (λ^*, K^*) have been randomly chosen only for presentation reasons, in order to examine how the Sign EWMA chart behaves when ties are present. In the following sections of the this Chapter, there will be an detailed examination regarding the effect of these parameters. From Table 4.6 we can conclude the following:

- For $\kappa = 0$ the in-control values of ARL are steady and *exactly* equal to 370.4 (as expected). Note that this is an advantage of our proposed scheme since, regardless the sample size, it can be designed giving a corresponding in-control ARL value, to be exactly equal to the predefined value of ARL_0. On the other hand, for $\kappa > 0$, even for small values of κ, the in-control ARL values are different. For example when $(p_{+1}, \lambda, K) = (0.6, 0.12, 2.743)$ and $\kappa = 0.05$ we have $\mathrm{ARL}_0 = 391.1$ for case 1 and $\mathrm{ARL}_0 = 432.2$ for case 15. In addition, for heavy tailed distributions (i.e. for large values of γ_4) the ARL_0 values become larger (see for example the last four cases).

- For the first 6 symmetric cases the corresponding out-of-control values are the same for shifts δ and $-\delta$ regardless the value of κ. On the other hand for asymmetric cases, negative shifts, $-\delta$ give larger ARL_1 values than positive ones. For example, for case #10, when $(p_{+1}, \lambda, K) = (0.6, 0.12, 2.743)$ and $\kappa = 0.2$ for $\delta = -0.1$ we have $\mathrm{ARL}_1 = 37.7$ and for $\delta = 0.1$ we have $\mathrm{ARL}_1 = 30.6$.

- Regardless the type of distribution, as κ increases the out-of-control ARL_1 values are becoming larger. For instance, for $\delta = 0.1$ and $(p_{+1}, \lambda, K) = (0.85, 0.72, 2.928)$ we have $\mathrm{ARL}_1 = 131.7$ for $\kappa = 0$, $\mathrm{ARL}_1 = 143.4$ for $\kappa = 0.05$, $\mathrm{ARL}_1 = 157.4$ for $\kappa = 0.1$ and $\mathrm{ARL}_1 = 193.9$ for $\kappa = 0.2$.

Table 4.6: ARL values when $n = 20$ for $(p_{+1}, \lambda, K) = (0.6, 0.12, 2.743)$ and $(p_{+1}, \lambda, K) = (0.85, 0.72, 2.928)$ using traditional control limits.

$(p_{+1}, \lambda, K) = (0.6, 0.12, 2.743)$

	$\kappa = 0$					$\kappa = 0.05$					$\kappa = 0.1$					$\kappa = 0.2$				
	δ					δ					δ					δ				
case	-0.2	-0.1	0	0.1	0.2	-0.2	-0.1	0	0.1	0.2	-0.2	-0.1	0	0.1	0.2	-0.2	-0.1	0	0.1	0.2
1	28.6	93.5	370.4	93.5	28.6	28.8	95.6	391.1	95.6	28.8	29.0	97.8	413.4	97.8	29.0	29.5	102.3	464.0	102.3	29.5
2	19.3	64.3	370.4	64.2	19.3	19.4	65.7	396.8	65.5	19.4	19.5	67.1	425.9	67.0	19.5	19.8	70.5	494.0	70.3	19.8
3	16.3	53.6	370.4	53.6	16.3	16.3	54.7	399.9	54.7	16.3	16.4	55.9	432.8	55.9	16.4	16.7	58.8	511.4	58.8	16.7
4	14.0	45.4	370.4	45.4	14.0	14.1	46.3	403.1	46.3	14.1	14.1	47.3	439.9	47.3	14.1	14.4	49.7	529.6	49.7	14.4
5	11.9	37.5	370.4	37.5	11.9	11.9	38.2	407.1	38.2	11.9	12.0	39.0	449.0	39.0	12.0	12.2	41.1	553.9	41.1	12.2
6	10.4	31.8	370.4	31.8	10.4	10.4	32.3	411.0	32.3	10.4	10.5	33.0	458.1	33.0	10.5	10.7	34.8	578.7	34.8	10.7
7	10.9	29.8	370.4	21.5	6.4	11.0	30.5	416.5	21.5	6.4	11.1	31.8	468.1	20.9	6.3	11.6	36.9	536.1	18.5	5.9
8	12.3	36.3	370.4	30.8	9.3	12.3	37.1	409.6	31.2	9.3	12.4	38.3	454.3	31.2	9.3	12.9	42.5	556.3	30.4	9.1
9	12.6	38.0	370.4	33.5	10.2	12.6	38.8	408.1	34.0	10.2	12.7	40.0	451.0	34.2	10.2	13.1	43.9	553.1	34.0	10.1
10	11.1	32.9	370.4	29.7	9.4	11.1	33.6	411.3	30.1	9.4	11.2	34.5	458.7	30.4	9.4	11.6	37.7	575.0	30.6	9.4
11	9.6	27.5	370.4	25.2	8.3	9.6	28.0	416.0	25.5	8.4	9.7	28.8	469.6	25.8	8.4	10.0	31.4	606.2	26.3	8.5
12	8.5	23.5	370.4	21.7	7.5	8.5	23.9	420.7	22.0	7.5	8.6	24.5	480.9	22.3	7.6	8.8	26.7	639.4	22.9	7.7
13	7.3	17.8	370.4	12.7	4.4	7.3	18.1	435.3	12.7	4.3	7.4	18.9	508.9	12.3	4.3	7.7	22.0	547.2	11.0	4.1
14	7.9	20.0	370.4	15.0	5.1	7.9	20.4	429.5	14.9	5.0	8.0	21.2	498.0	14.7	5.0	8.3	24.4	584.1	13.4	4.8
15	7.2	18.2	370.4	14.8	5.3	7.3	18.6	432.2	14.9	5.4	7.3	19.2	506.9	14.9	5.4	7.6	21.8	655.2	14.5	5.4
16	6.4	15.7	370.4	13.3	5.1	6.4	15.9	438.6	13.4	5.1	6.5	16.4	523.5	13.5	5.2	6.8	18.5	720.9	13.6	5.3
17	5.8	13.6	370.4	11.8	4.8	5.8	13.8	445.7	11.9	4.8	5.8	14.2	542.3	12.1	4.8	6.1	16.0	787.3	12.5	5.0

$(p_{+1}, \lambda, K) = (0.85, 0.72, 2.928)$

	$\kappa = 0$					$\kappa = 0.05$					$\kappa = 0.1$					$\kappa = 0.2$				
	δ					δ					δ					δ				
case	-0.2	-0.1	0	0.1	0.2	-0.2	-0.1	0	0.1	0.2	-0.2	-0.1	0	0.1	0.2	-0.2	-0.1	0	0.1	0.2
1	103.7	236.9	370.4	236.9	103.7	108.5	251.7	398.2	251.7	108.5	113.6	268.0	429.2	268.0	113.6	125.4	305.7	502.3	305.7	125.4
2	68.2	192.9	370.4	192.7	68.1	71.5	207.1	406.0	206.9	71.4	75.3	223.3	446.8	223.0	75.2	84.5	262.1	547.4	261.8	84.4
3	54.9	171.8	370.4	171.8	54.9	57.7	185.3	410.3	185.3	57.7	60.9	200.9	456.7	200.9	60.9	68.8	239.4	573.9	239.4	68.8
4	44.7	152.8	370.4	152.8	44.7	47.0	165.6	414.7	165.6	47.0	49.7	180.6	466.9	180.6	49.7	56.5	218.3	602.1	218.3	56.5
5	35.0	131.7	370.4	131.7	35.0	36.7	143.4	420.3	143.4	36.7	38.9	157.4	480.3	157.4	38.9	44.5	193.9	640.5	193.9	44.5
6	28.0	114.3	370.4	114.3	28.0	29.4	125.0	425.7	125.0	29.4	31.2	138.1	493.6	138.1	31.2	35.9	173.0	680.1	173.0	35.9
7	30.3	107.7	370.4	77.0	11.1	31.7	117.9	433.8	84.6	11.5	33.7	132.3	513.4	91.2	11.7	39.9	180.3	730.9	98.9	11.3
8	36.6	128.1	370.4	111.1	23.2	38.4	139.6	423.8	121.5	24.3	40.8	154.5	488.9	132.6	25.5	47.5	198.3	664.5	156.0	27.9
9	38.1	133.2	370.4	119.8	27.2	39.9	145.0	421.7	130.7	28.6	42.4	159.9	483.8	142.8	30.1	49.1	202.4	650.1	170.1	33.4
10	31.3	117.9	370.4	107.3	23.4	32.8	128.8	426.2	117.5	24.6	34.8	142.8	494.8	129.2	25.9	40.5	183.1	683.4	156.9	29.2
11	24.3	99.9	370.4	91.5	18.9	25.4	109.6	432.8	100.5	19.8	27.0	122.4	511.0	111.3	20.9	31.6	160.1	734.1	138.5	23.8
12	19.3	85.0	370.4	78.2	15.4	20.2	93.7	439.4	86.2	16.1	21.5	105.2	527.9	96.1	17.0	25.3	140.5	789.4	122.5	19.6
13	14.5	61.7	370.4	38.8	4.7	15.1	68.4	461.0	42.7	4.8	16.0	78.6	584.4	46.2	4.9	19.2	117.8	954.2	50.0	4.7
14	16.9	71.1	370.4	49.0	6.6	17.6	78.6	452.5	54.1	6.8	18.7	89.7	561.9	59.1	6.9	22.3	129.6	889.0	66.7	7.0
15	14.3	63.6	370.4	48.5	7.5	14.8	70.5	456.1	53.7	7.7	15.8	80.6	571.7	59.8	8.1	2.6	18.9	116.7	934.3	74.0
16	11.1	52.2	370.4	41.5	6.8	11.5	58.0	465.2	46.1	7.0	12.2	66.7	596.7	52.0	7.3	14.7	98.8	1032.8	68.3	8.5
17	8.8	42.7	370.4	34.7	5.9	9.1	47.5	475.6	38.6	6.0	9.7	55.1	626.0	44.0	6.4	11.6	83.9	1154.1	60.6	7.5

4.3.2 Run length properties of the 2C-SN EWMA chart using *new* control limits

As it was previously presented, when ties are present, the ARL_0 values of the Sign EWMA chart are seriously affected. In particular, as κ increases, the chart's distribution-free properties are no longer valid, even for small values of $\kappa = 0.05$. In this Section, an alternative approach is investigated in order to tackle this issue and ideally maintain the chart's distribution-free properties regardless the number of ties. Amin et al. (1995), for the design of the Sign Shewhart chart, suggested to maintain the values $S_{t,j} = 0$ in the computation of the SN_t statistic and the control limits $(\text{LCL}, \text{UCL}) = (-C', -C')$ should be defined through the Binomial distribution similarly with the "no ties" case. However, in this approach, the effect of the rounding-off error, is totally overlooked since this changes the distributional properties of the SN_t statistic. An alternative solution has been suggested by Chakraborti et al. (2001) who suggested to remove ties from the sample and to update the sample size n, if their probability of occurrence is small. This approach makes harder to define a priori the statistical performance of the SN control chart because varying n requires to redefine the control limit coefficient C'. In the work of Castagliola et al. (2020), the distribution-free properties of the Shewhart Sign chart were investigated by adjusting the control limit coefficient C' based on the underlying distribution. However, they showed that, this method is not efficient in the design of Sign Shewhart-type charts.

Motivated by the above statements, we will focus on adjusting the control limits (i.e. the in-control values of $\text{E}_0(\text{SN}_t^*)$ and $\text{V}_0(\text{SN}_t^*)$ along with the pair of (λ, K) based on the underlying distribution and the values of κ, using the expressions presented in Section 4.1.1. In Table 4.7, for the 17 distributions listed in Table 4.3 and $\kappa = \{0, 0.05, 0.1, 0.2\}$, the corresponding vector of probabilities $\boldsymbol{p} = (p_{-1}, p_0, p_{+1})$ along with the mean and variance of SN_t are illustrated when $n = 20$. From Table 4.7 we may conclude the following:

- When $\kappa = 0$ (i.e. the "no-ties" case) for every case the corresponding mean and variance of SN_t^* equal to $\text{E}_0(\text{SN}_t) = 0$ and $\text{V}_0(\text{SN}_t) = 20$. Note that, this is an expected result and consistent with the computations of the previous Chapter in the "no ties" case.

- As κ increases the result significantly change. In particular, regardless the values of κ (small or large) the corresponding values of the variance are no longer equal to n, but they tend to decrease instead. Moreover, the in-control value of the mean of SN_t is equal to zero only for cases #1-#6, (i.e. for symmetric distributions).

Table 4.7: Vector of probabilities (first line) along with the mean and variance (second row) when $\kappa = \{0, 0.05, 0.1, 0.2\}$ for the 17 distributions in Table 4.3.

case	$\kappa = 0$	$\kappa = 0.05$	$\kappa = 0.1$	$\kappa = 0.2$
#1	(0.5,0,0.5) (0,20)	(0.4929,0.0142,0.4929) (0,19.716)	(0.4858,0.0284,0.4858) (0,19.432)	(0.4716,0.0568,0.4716) (0,18.864)
#2	(0.5,0,0.5) (0,20)	(0.491,0.0179,0.491) (0,19.64)	(0.482,0.0359,0.4821) (0.002,19.282)	(0.4641,0.0717,0.4642) (0.002,18.566)
#3	(0.5,0,0.5) (0,20)	(0.49,0.0199,0.49) (0,19.6)	(0.4801,0.0399,0.4801) (0,19.204)	(0.4602,0.0797,0.4602) (0,18.408)
#4	(0.5,0,0.5) (0,20)	(0.489,0.0219,0.489) (0,19.56)	(0.4781,0.0439,0.4781) (0,19.124)	(0.4562,0.0876,0.4562) (0,18.248)
#5	(0.5,0,0.5) (0,20)	(0.4878,0.0245,0.4878) (0,19.512)	(0.4755,0.0489,0.4755) (0,19.02)	(0.4512,0.0976,0.4512) (0,18.048)
#6	(0.5,0,0.5) (0,20)	(0.4865,0.0269,0.4865) (0,19.46)	(0.4731,0.0538,0.4731) (0,18.924)	(0.4464,0.1072,0.4464) (0,17.856)
#7	(0.5,0,0.5) (0,20)	(0.4844,0.0304,0.4852) (0.016,19.397)	(0.4681,0.0609,0.471) (0.058,18.843)	(0.4329,0.1227,0.4444) (0.23,18.498)
#8	(0.5,0,0.5) (0,20)	(0.4868,0.0261,0.4871) (0.006,19.479)	(0.4733,0.0521,0.4745) (0.024,18.966)	(0.4455,0.1043,0.4503) (0.096,18.082)
#9	(0.4999,0,0.5001) (0.004,20)	(0.4873,0.0251,0.4876) (0.006,19.499)	(0.4744,0.0503,0.4754) (0.02,19.003)	(0.448,0.1004,0.4516) (0.072,18.085)
#10	(0.5,0,0.5) (0,20)	(0.4863,0.0271,0.4865) (0.004,19.456)	(0.4725,0.0542,0.4733) (0.016,18.921)	(0.4443,0.1082,0.4475) (0.064,17.91)
#11	(0.5,0,0.5) (0,20)	(0.4849,0.03,0.4851) (0.004,19.4)	(0.4697,0.0599,0.4704) (0.014,18.806)	(0.4388,0.1193,0.4419) (0.062,17.683)
#12	(0.5,0,0.5) (0,20)	(0.4835,0.0328,0.4837) (0.004,19.344)	(0.4669,0.0655,0.4676) (0.014,18.694)	(0.4334,0.1303,0.4363) (0.058,17.455)
#13	(0.5,0,0.5) (0,20)	(0.4709,0.0556,0.4735) (0.052,18.937)	(0.4389,0.1119,0.4491) (0.204,18.509)	(0.3645,0.2293,0.4062) (0.834,27.934)
#14	(0.5,0,0.5) (0,20)	(0.4786,0.0416,0.4798) (0.024,19.178)	(0.4561,0.0833,0.4606) (0.09,18.48)	(0.4075,0.1675,0.425) (0.35,18.855)
#15	(0.4999,0,0.5001) (0.004,20)	(0.4804,0.0382,0.4814) (0.02,19.243)	(0.46,0.0765,0.4635) (0.07,18.558)	(0.4165,0.1534,0.43) (0.27,18.242)
#16	(0.5,0,0.5) (0,20)	(0.4799,0.0396,0.4805) (0.012,19.211)	(0.4591,0.0792,0.4617) (0.052,18.465)	(0.4161,0.1578,0.4261) (0.2,17.564)
#17	(0.5,0,0.5) (0,20)	(0.4781,0.0432,0.4787) (0.012,19.139)	(0.4557,0.0863,0.458) (0.046,18.312)	(0.4102,0.171,0.4189) (0.174,17.127)

In order to apply the strategy where *new* control limits are defined based on the sample's underlying distribution, the following procedure will be followed. In particular, for a given value of n and κ for each distribution listed in Table 4.3:

- *step 1*: Compute the vector of probabilities $\boldsymbol{p} = (p_{-1}, p_0, p_{+1})$ for $\delta = 0$ and a given value of κ.
- *step 2*: Compute the in-control mean and variance of SN_t as defined in Section 4.1.1.
- *step 3*: For a given value of λ, compute the corresponding value of K' as presented in Section 3.2.5.
- *step 4*: Compute the new control limits using the formulas:

$$\mathrm{UCL}^{new} = \mathrm{E}_{tied}(\mathrm{SN}_t^*) + K'\sqrt{\frac{\lambda}{2-\lambda}\mathrm{V}_{tied}(\mathrm{SN}_t^*)}$$

$$\mathrm{LCL}^{new} = \mathrm{E}_{tied}(\mathrm{SN}_t^*) - K'\sqrt{\frac{\lambda}{2-\lambda}\mathrm{V}_{tied}(\mathrm{SN}_t^*)}$$

- *step 5*: Compute the chart's Run Length properties as presented in 3.2.

In Tables 4.8 ($n = 10$) and 4.9 ($n = 20$) the corresponding values of $(\lambda, K', \mathrm{ARL}_0)$ are presented (first line) along with the vector of probabilities (second line), for each distribution, for $\kappa = \{0, 0.05, 0.1, 0.15, 0.2\}$, using $\lambda = 0.2$ as a fixed constant. Based on these Tables we may conclude that:

- For a given value of κ and a priori information of the underlying distribution practitioners are capable of designing the chart in order to satisfy the condition $\mathrm{ARL}_0 = 370.4$ (or for any pre-defined value of the in-control ARL). In particular, based on the underlying distribution, adjusting not only the in-control values for the mean and variance, but also the coefficient K', is an efficient semi-parametric technique for dealing with tied observations without affecting the chart's RL properties.
- It is worth stretching that, as it has been already noted in Chapter 3, for small ($n = 10$) or even moderate ($n = 20$) values of n, the Shewhart Sign chart is impossible to be designed in order to give a corresponding ARL_0 value to be exactly equal to 370.4 (or even relatively close to that value). On the other hand, using the proposed EWMA Sign chart, regardless the value of the sample size, practitioners are able to design the chart for any pre-defined ARL_0 of their choice.

Table 4.8: Vector of probabilities (first line) along with the vector of of $(\lambda, K', \text{ARL}_0)$ (second line), for each distribution, for $\kappa = \{0, 0.05, 0.1, 0.15, 0.2\}$ and $n = 10$ using $\lambda = 0.2$ as a fixed constant

Case	$\kappa = 0$	$\kappa = 0.05$	$\kappa = 0.1$	$\kappa = 0.15$	$\kappa = 0.2$
1	(0.5,0,0.5) (0.2,2.8342,370.4)	(0.4929,0.0142,0.4929) (0.2,2.8337,370.4)	(0.4858,0.0284,0.4858) (0.2,2.8338,370.4)	(0.4787,0.0426,0.4787) (0.2,2.8335,370.4)	(0.4716,0.0568,0.4716) (0.2,2.8334,370.4)
2	(0.5,0,0.5) (0.2,2.8342,370.4)	(0.491,0.0179,0.491) (0.2,2.8337,370.4)	(0.482,0.0359,0.4821) (0.2,2.8337,370.4)	(0.4731,0.0538,0.4731) (0.2,2.8335,370.4)	(0.4641,0.0717,0.4642) (0.2,2.8334,370.4)
3	(0.5,0,0.5) (0.2,2.8342,370.4)	(0.49,0.0199,0.49) (0.2,2.8336,370.4)	(0.4801,0.0399,0.4801) (0.2,2.8335,370.4)	(0.4701,0.0598,0.4701) (0.2,2.8334,370.4)	(0.4602,0.0797,0.4602) (0.2,2.8333,370.4)
4	(0.5,0,0.5) (0.2,2.8342,370.4)	(0.489,0.0219,0.489) (0.2,2.8336,370.4)	(0.4781,0.0439,0.4781) (0.2,2.8334,370.4)	(0.4671,0.0658,0.4671) (0.2,2.8335,370.4)	(0.4562,0.0876,0.4562) (0.2,2.8335,370.4)
5	(0.5,0,0.5) (0.2,2.8342,370.4)	(0.4878,0.0245,0.4878) (0.2,2.8333,370.4)	(0.4755,0.0489,0.4755) (0.2,2.8336,370.4)	(0.4633,0.0733,0.4633) (0.2,2.8335,370.4)	(0.4512,0.0976,0.4512) (0.2,2.8336,370.4)
6	(0.5,0,0.5) (0.2,2.8342,370.4)	(0.4865,0.0269,0.4865) (0.2,2.8335,370.4)	(0.4731,0.0538,0.4731) (0.2,2.8335,370.4)	(0.4597,0.0805,0.4597) (0.2,2.8335,370.4)	(0.4464,0.1072,0.4464) (0.2,2.8338,370.4)
7	(0.5,0,0.5) (0.2,2.8342,370.4)	(0.4844,0.0304,0.4852) (0.2,2.8332,370.4)	(0.4681,0.0609,0.471) (0.2,2.8323,370.4)	(0.4509,0.0917,0.4574) (0.2,2.8283,370.4)	(0.4329,0.1227,0.4444) (0.2,2.8169,370.4)
8	(0.5,0,0.5) (0.2,2.8342,370.4)	(0.4868,0.0261,0.4871) (0.2,2.8335,370.4)	(0.4733,0.0521,0.4745) (0.2,2.8334,370.4)	(0.4596,0.0782,0.4623) (0.2,2.8324,370.4)	(0.4455,0.1043,0.4503) (0.2,2.8307,370.4)
9	(0.4999,0,0.5001) (0.2,2.8342,370.4)	(0.4873,0.0251,0.4876) (0.2,2.8334,370.4)	(0.4744,0.0503,0.4754) (0.2,2.8333,370.4)	(0.4613,0.0754,0.4634) (0.2,2.8328,370.4)	(0.448,0.1004,0.4516) (0.2,2.832,370.4)
10	(0.5,0,0.5) (0.2,2.8342,370.4)	(0.4863,0.0271,0.4865) (0.2,2.8335,370.4)	(0.4725,0.0542,0.4733) (0.2,2.8333,370.4)	(0.4585,0.0813,0.4602) (0.2,2.8331,370.4)	(0.4443,0.1082,0.4475) (0.2,2.8324,370.4)
11	(0.5,0,0.5) (0.2,2.8342,370.4)	(0.4849,0.03,0.4851) (0.2,2.8334,370.4)	(0.4697,0.0599,0.4704) (0.2,2.8334,370.4)	(0.4543,0.0897,0.456) (0.2,2.8332,370.4)	(0.4388,0.1193,0.4419) (0.2,2.8326,370.4)
12	(0.5,0,0.5) (0.2,2.8342,370.4)	(0.4835,0.0328,0.4837) (0.2,2.8333,370.4)	(0.4669,0.0655,0.4676) (0.2,2.8333,370.4)	(0.4502,0.098,0.4518) (0.2,2.8332,370.4)	(0.4334,0.1303,0.4363) (0.2,2.833,370.4)
13	(0.5,0,0.5) (0.2,2.8342,370.4)	(0.4786,0.0416,0.4798) (0.2,2.833,370.4)	(0.4561,0.0833,0.4606) (0.2,2.8309,370.4)	(0.4324,0.1252,0.4423) (0.2,2.8214,370.4)	(0.4075,0.1675,0.425) (0.2,2.7937,370.4)
14	(0.4999,0,0.5001) (0.2,2.8342,370.4)	(0.4804,0.0382,0.4814) (0.2,2.833,370.4)	(0.46,0.0765,0.4635) (0.2,2.8319,370.4)	(0.4387,0.1149,0.4464) (0.2,2.8263,370.4)	(0.4165,0.1534,0.43) (0.2,2.8104,370.4)
15	(0.5,0,0.5) (0.2,2.8342,370.4)	(0.4799,0.0396,0.4805) (0.2,2.8331,370.4)	(0.4591,0.0792,0.4617) (0.2,2.8326,370.4)	(0.4378,0.1186,0.4435) (0.2,2.8298,370.4)	(0.4161,0.1578,0.4261) (0.2,2.8212,370.4)
16	(0.5,0,0.5) (0.2,2.8342,370.4)	(0.4781,0.0432,0.4787) (0.2,2.833,370.4)	(0.4557,0.0863,0.458) (0.2,2.8329,370.4)	(0.433,0.1289,0.438) (0.2,2.831,370.4)	(0.4102,0.171,0.4189) (0.2,2.8245,370.4)
17	(0.5,0,0.5) (0.2,2.8342,370.4)	(0.4761,0.0472,0.4767) (0.2,2.833,370.4)	(0.4519,0.0941,0.454) (0.2,2.833,370.4)	(0.4275,0.1403,0.4322) (0.2,2.8313,370.4)	(0.4031,0.1857,0.4112) (0.2,2.8263,370.4)

Table 4.9: Vector of probabilities (first line) along with the vector of of $(\lambda, K', \text{ARL}_0)$ (second line), for each distribution, for $\kappa = \{0, 0.05, 0.1, 0.15, 0.2\}$ and $n = 20$ using $\lambda = 0.2$ as a fixed constant

Case	$\kappa = 0$	$\kappa = 0.05$	$\kappa = 0.1$	$\kappa = 0.15$	$\kappa = 0.2$
1	(0.5,0,0.5) (0.2,2.8442,370.4)	(0.4929,0.0142,0.4929) (0.2,2.8448,370.4)	(0.4858,0.0284,0.4858) (0.2,2.8456,370.4)	(0.4787,0.0426,0.4787) (0.2,2.8458,370.4)	(0.4716,0.0568,0.4716) (0.2,2.846,370.4)
2	(0.5,0,0.5) (0.2,2.8442,370.4)	(0.491,0.0179,0.491) (0.2,2.845,370.4)	(0.482,0.0359,0.4821) (0.2,2.8458,370.4)	(0.4731,0.0538,0.4731) (0.2,2.846,370.4)	(0.4641,0.0717,0.4642) (0.2,2.8462,370.4)
3	(0.5,0,0.5) (0.2,2.8442,370.4)	(0.49,0.0199,0.49) (0.2,2.8451,370.4)	(0.4801,0.0399,0.4801) (0.2,2.8457,370.4)	(0.4701,0.0598,0.4701) (0.2,2.8461,370.4)	(0.4602,0.0797,0.4602) (0.2,2.8462,370.4)
4	(0.5,0,0.5) (0.2,2.8442,370.4)	(0.489,0.0219,0.489) (0.2,2.8451,370.4)	(0.4781,0.0439,0.4781) (0.2,2.8458,370.4)	(0.4671,0.0658,0.4671) (0.2,2.8462,370.4)	(0.4562,0.0876,0.4562) (0.2,2.8463,370.4)
5	(0.5,0,0.5) (0.2,2.8442,370.4)	(0.4878,0.0245,0.4878) (0.2,2.845,370.4)	(0.4755,0.0489,0.4755) (0.2,2.846,370.4)	(0.4633,0.0733,0.4633) (0.2,2.8463,370.4)	(0.4512,0.0976,0.4512) (0.2,2.8464,370.4)
6	(0.5,0,0.5) (0.2,2.8442,370.4)	(0.4865,0.0269,0.4865) (0.2,2.8453,370.4)	(0.4731,0.0538,0.4731) (0.2,2.8461,370.4)	(0.4597,0.0805,0.4597) (0.2,2.8464,370.4)	(0.4464,0.1072,0.4464) (0.2,2.8466,370.4)
7	(0.5,0,0.5) (0.2,2.8442,370.4)	(0.4844,0.0304,0.4852) (0.2,2.8449,370.4)	(0.4681,0.0609,0.471) (0.2,2.8414,370.4)	(0.4509,0.0917,0.4574) (0.2,2.8229,370.4)	(0.4329,0.1227,0.4444) (0.2,2.7726,370.4)
8	(0.5,0,0.5) (0.2,2.8442,370.4)	(0.4868,0.0261,0.4871) (0.2,2.8452,370.4)	(0.4733,0.0521,0.4745) (0.2,2.8453,370.4)	(0.4596,0.0782,0.4623) (0.2,2.8421,370.4)	(0.4455,0.1043,0.4503) (0.2,2.8333,370.4)
9	(0.4999,0,0.5001) (0.2,2.8442,370.4)	(0.4873,0.0251,0.4876) (0.2,2.845,370.4)	(0.4744,0.0503,0.4754) (0.2,2.8453,370.4)	(0.4613,0.0754,0.4634) (0.2,2.8437,370.4)	(0.448,0.1004,0.4516) (0.2,2.8391,370.4)
10	(0.5,0,0.5) (0.2,2.8442,370.4)	(0.4863,0.0271,0.4865) (0.2,2.8453,370.4)	(0.4725,0.0542,0.4733) (0.2,2.8456,370.4)	(0.4585,0.0813,0.4602) (0.2,2.8447,370.4)	(0.4443,0.1082,0.4475) (0.2,2.8406,370.4)
11	(0.5,0,0.5) (0.2,2.8442,370.4)	(0.4849,0.03,0.4851) (0.2,2.8453,370.4)	(0.4697,0.0599,0.4704) (0.2,2.8458,370.4)	(0.4543,0.0897,0.456) (0.2,2.8447,370.4)	(0.4388,0.1193,0.4419) (0.2,2.841,370.4)
12	(0.5,0,0.5) (0.2,2.8442,370.4)	(0.4835,0.0328,0.4837) (0.2,2.8453,370.4)	(0.4669,0.0655,0.4676) (0.2,2.8459,370.4)	(0.4502,0.098,0.4518) (0.2,2.8449,370.4)	(0.4334,0.1303,0.4363) (0.2,2.8418,370.4)
13	(0.5,0,0.5) (0.2,2.8442,370.4)	(0.4786,0.0416,0.4798) (0.2,2.8447,370.4)	(0.4561,0.0833,0.4606) (0.2,2.8351,370.4)	(0.4324,0.1252,0.4423) (0.2,2.7912,370.4)	(0.4075,0.1675,0.425) (0.2,2.6757,370.4)
14	(0.4999,0,0.5001) (0.2,2.8442,370.4)	(0.4804,0.0382,0.4814) (0.2,2.8448,370.4)	(0.46,0.0765,0.4635) (0.2,2.8395,370.4)	(0.4387,0.1149,0.4464) (0.2,2.813,370.4)	(0.4165,0.1534,0.43) (0.2,2.743,370.4)
15	(0.5,0,0.5) (0.2,2.8442,370.4)	(0.4799,0.0396,0.4805) (0.2,2.8452,370.4)	(0.4591,0.0792,0.4617) (0.2,2.8425,370.4)	(0.4378,0.1186,0.4435) (0.2,2.8281,370.4)	(0.4161,0.1578,0.4261) (0.2,2.7882,370.4)
16	(0.5,0,0.5) (0.2,2.8442,370.4)	(0.4781,0.0432,0.4787) (0.2,2.8452,370.4)	(0.4557,0.0863,0.458) (0.2,2.8434,370.4)	(0.433,0.1289,0.438) (0.2,2.8323,370.4)	(0.4102,0.171,0.4189) (0.2,2.8015,370.4)
17	(0.5,0,0.5) (0.2,2.8442,370.4)	(0.4761,0.0472,0.4767) (0.2,2.8454,370.4)	(0.4519,0.0941,0.454) (0.2,2.8439,370.4)	(0.4275,0.1403,0.4322) (0.2,2.8338,370.4)	(0.4031,0.1857,0.4112) (0.2,2.8071,370.4)

Effect of the value of K': For each distribution listed in Table 4.3, the corresponding values of K' are plotted in Figures 4.5 and 4.6. For both cases, we may observe that:

- $n = 10$ *(small sample size)*: When $\kappa = 0$ the value of K' is the same for all the cases. This is an expected result, since we are referring to the "no ties" case. For $\kappa \leq 0.1$, the

values of K' are almost the same with some differences in the fourth decimal place. As κ increases, for the first six cases (i.e. for symmetric distributions) the corresponding values of K' are the same (strictly speaking, are almost the same). For asymmetry and heavily tailed distribution (cases $\#13 - \#17$) the values of K' are a little bit different.

- $n = 20$ *(moderate sample size)*: For $n = 20$ the exact same pattern occurs as in the previous case. The only difference is that for heavily tailed distributions (cases $\#13 - \#17$), as κ increases, the differences between the corresponding values of K' tend to be larger.

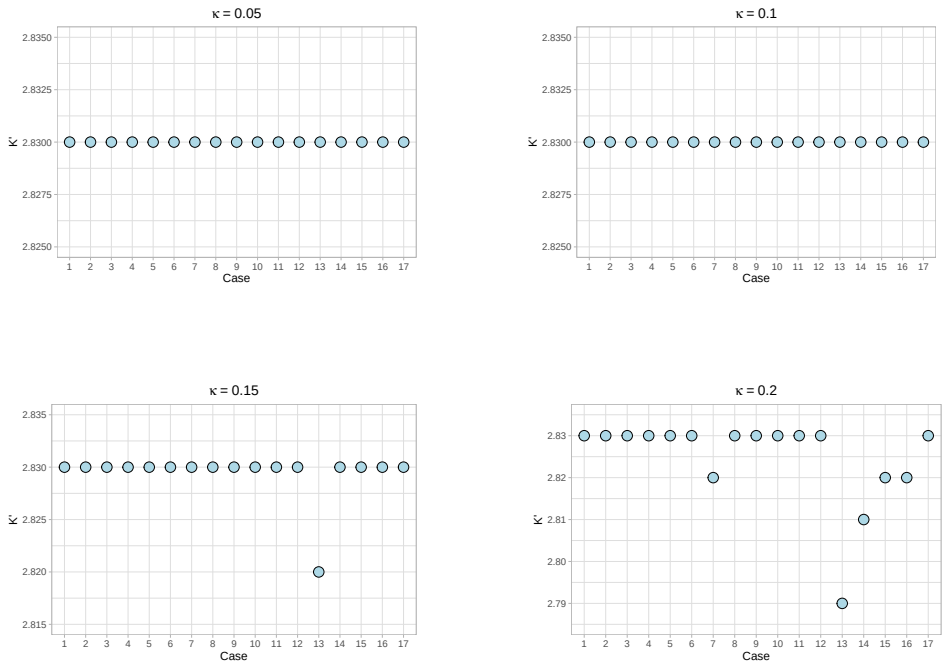

Figure 4.5: Corresponding values of K' for $\rho = \{0.05, 0.1, 0.15, 0.2\}$ and $n = 10$

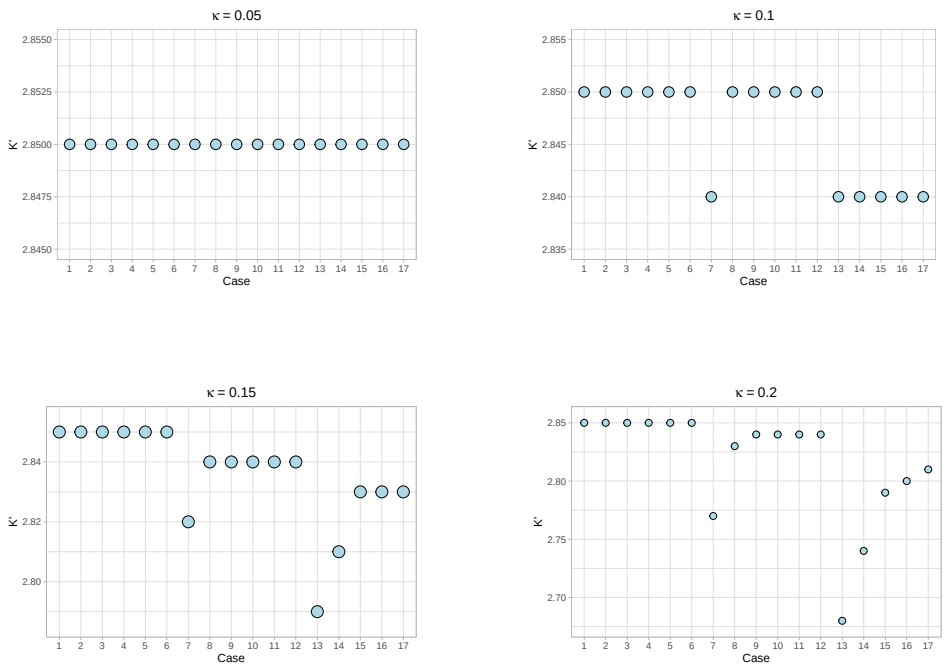

Figure 4.6: Corresponding values of K' for $\rho = \{0.05, 0.1, 0.15, 0.2\}$ and $n = 20$

It can be seen that the values of K' are quite close (almost the same) even for large values of κ. As a result, a logical question arises regarding the effect of the value of K'. In particular, since these values are quite close (differences in the third or even in the fourth decimal place), by setting the value of K' as a fixed constant, it is questionable if the corresponding ARL values will be affected by this choice. In Figures 4.7 and 4.8 the corresponding ARL values are presented for $\kappa = \{0.05, 0.1, 0.15, 0.2\}$ using for all the distributions the same value for the design parameter (λ, K') as the ones in the "no-ties" case. In particular, in Figures 4.7 and 4.8 the corresponding ARL values are reported for each distribution, for a fixed value of $\lambda = 0.2$. Additionally, the value $K' = 0.8342$ for $n = 10$ and $K' = 0.8442$ for $n = 20$ respectively. At each plot, the dashed red lines correspond to a fixed "interval" where 370.4 ± 2.

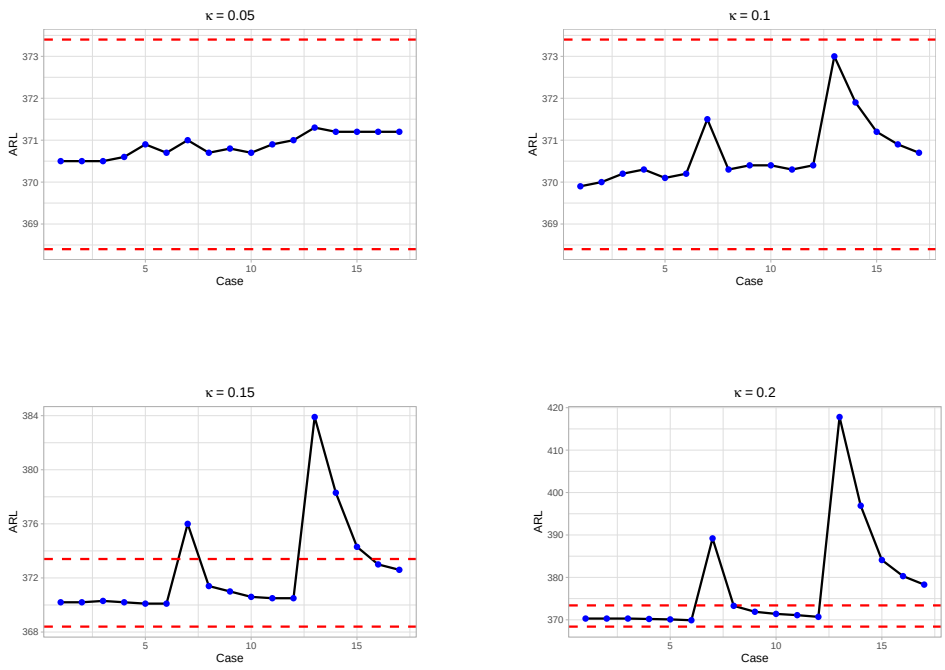

Figure 4.7: Corresponding values of ARL_0 for $\lambda = 0.2, K' = 2.8342$, when $\rho = \{0.05, 0.1, 0.15, 0.2\}$ and $n = 10$

From Figures 4.7 and 4.8 we may conclude the following:

- $n = 10$ *(small sample size)*: When $\kappa \leq 0.1$ the ARL_0 values are relative close and they do not exceed the interval $(370.4 - 2, 370.4 + 2)$. When $0.1 \leq \kappa \leq 0.15$, for the first six cases (i.e. for symmetric distributions) the chart's distribution-free properties are maintained. On the other hand, as κ increases, it can be observed that in cases #7 and #14 − #17 (heavily tailed distributions) the ARL values differ significantly. As a consequence, for small sample sizes (and symmetric distributions) K' is not affected by the underlying distribution.

- $n = 20$ *(moderate sample size)*: As κ increases the results change significantly, especially for heavily tailed distributions. Clearly it can be concluded that even quite small changes in the value of K' may significantly change the results.

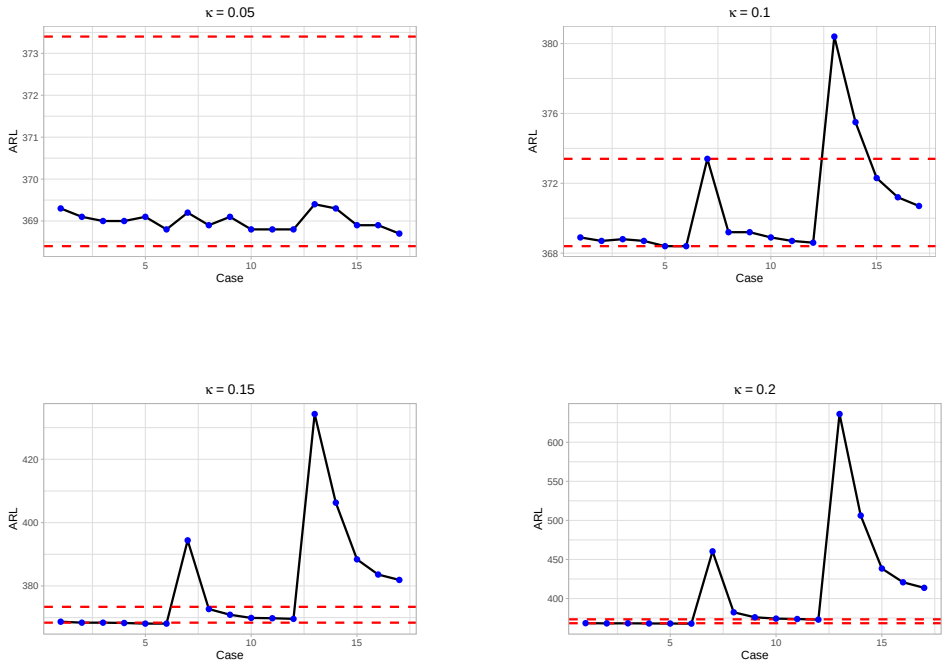

Figure 4.8: Corresponding values of ARL_0) for $\lambda = 0.2, K' = 2.8442$, when $\rho = \{0.05, 0.1, 0.15, 0.2\}$ and $n = 20$

Taking a closer look at Figures 4.7-4.8 (effect of K') and Figures 4.5-4.6 (ARL_0 values with fixed value of K'), and interesting relation between K' and the chart's distribution-free properties can be easily observed. In particular, in Figure 4.9 two plots are presented for $n = 20$ and $\kappa = 0.2$. The plot on the left corresponds to the "optimal" values of K' for each one of the 17 distributions while the plot on the right corresponds to the ARL_0 values when a fixed value of $K' = 2.8442$ is used. It can be seen that, there is a pattern that occurs between the values of K' and the type of distribution. In particular, for symmetric distributions, there is no impact in the chart's distribution-free properties. On the other hand, heavily tailed distributions correspond to smaller values for K' in order to achieve a distribution-free performance. As as general conclusion, adjusting the control limits and the coefficient K', with respect to the value of κ and the underlying distribution, is an efficient semi-parametric technique where practitioners are able to deal with tied observations and compute correctly the chart's Run Length properties.

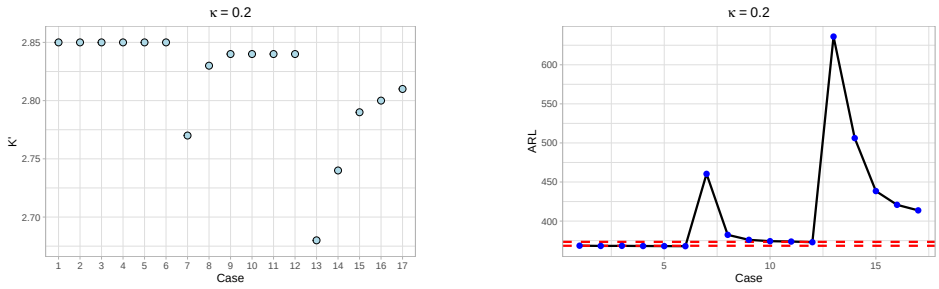

Figure 4.9: Relation between K' and ARL_0 when $\rho = 0.2$ and $n = 20$

4.3.3 Run length properties of the 2C-SN EWMA chart under the "flip a coin strategy"

In the previous Section it was proven that, when ties are present, using the semi-parametric approach of the "new limits" strategy is a quite efficient method for dealing with the problem of ties. Of course, someone might argue the fact that, this approach have a strict assumption regarding an a priori information about the parameters in the measurement error model (i.e. the value κ) and the knowledge of the underlying distribution. As a consequence, the "new control" limits might not be always applicable in practice. Motivated by the work of Castagliola et al. (2020) the "flip a coin" strategy will be tested in the design of the 2C-SN EWMA chart when ties are present. More specifically, using the same pairs of (λ, K) in Table 4.6, the corresponding in- and out-of control ARL values are presented in Table 4.10 for $\kappa = \{0, 0.05, 0.1, 0.2\}$ and $n = 20$ using the "flip a coin" strategy. From Table 4.10 we may conclude:

- For symmetric distributions, no matter the value of κ and the pair of (λ, K), the "flip a coin" strategy guarantees that our proposed nonparametric control chart maintains its distribution-free property. On the other hand, if we do not use the "flip a coin" strategy we proved that the chart is no longer distribution-free.

- Regarding the choice of the pair (λ, K) it seems that using larger values of λ, except from cases #14 and #15 improves significantly the distribution-free property of our chart for heavy-tailed distributions (cases $13 - 17$) and large values of κ. For example for $\kappa = 0.2$ using $(\lambda, K) = (0.12, 2.743)$ the in-control ARL value for case #16 is ARL $= 347.5$ and for case #17 it is ARL $= 350$. On the other hand, using the pair $(\lambda, K) = (0.72, 2.928)$,the in-control ARL value for case #16 is ARL $= 365.8$ and for case #17 it is ARL $= 366.3$.

- Similarly, for the out-of-control cases, we can conclude that no matter the value of κ the ARL_1 values are almost the same. For example, when $\delta = 0.1$ using using $(\lambda, K) = (0.72, 2.928)$ for $\kappa = \{0, 0.05, 0.1, 0.2\}$ the corresponding $\text{ARL}_1 = \{78.2, 78.2, 78.2, 78.5\}$.

Table 4.10: ARL values when $n = 20$ for $(p_{+1}, \lambda, K) = (0.6, 0.12, 2.743)$ and $(p_{+1}, \lambda, K) = (0.85, 0.72, 2.928)$ with the "flip a coin" strategy.

$(p_{+1}, \lambda, K) = (0.6, 0.12, 2.743)$

	$\kappa = 0$					$\kappa = 0.05$					$\kappa = 0.1$					$\kappa = 0.2$				
	δ					δ					δ					δ				
case	-0.2	-0.1	0	0.1	0.2	-0.2	-0.1	0	0.1	0.2	-0.2	-0.1	0	0.1	0.2	-0.2	-0.1	0	0.1	0.2
1	28.6	93.5	370.4	93.5	28.6	28.6	93.5	370.4	93.5	28.6	28.6	93.5	370.4	93.5	28.6	28.6	93.4	370.4	93.4	28.6
2	19.3	64.3	370.4	64.2	19.3	19.3	64.3	370.4	64.2	19.3	19.3	64.3	370.4	64.2	19.3	19.4	64.6	370.4	64.5	19.4
3	16.3	53.6	370.4	53.6	16.3	16.3	53.6	370.4	53.6	16.3	16.3	53.7	370.4	53.7	16.3	16.4	54.1	370.4	54.1	16.4
4	14.0	45.4	370.4	45.4	14.0	14.0	45.4	370.4	45.4	14.0	14.0	45.5	370.4	45.5	14.0	14.2	46.0	370.4	46.0	14.2
5	11.9	37.5	370.4	37.5	11.9	11.9	37.5	370.4	37.5	11.9	11.9	37.7	370.4	37.7	11.9	12.1	38.2	370.4	38.2	12.1
6	10.4	31.8	370.4	31.8	10.4	10.4	31.8	370.4	31.8	10.4	10.5	32.0	370.4	32.0	10.5	10.6	32.6	370.4	32.6	10.6
7	10.9	29.8	370.4	21.5	6.4	10.9	30.0	370.2	21.2	6.4	11.0	30.8	367.7	20.4	6.3	11.5	34.4	331.6	17.8	5.9
8	12.3	36.3	370.4	30.8	9.3	12.3	36.5	370.4	30.7	9.3	12.4	37.0	369.9	30.2	9.3	12.7	39.5	363.1	28.6	9.1
9	12.6	38.0	370.4	33.5	10.2	12.6	38.2	370.4	33.4	10.2	12.7	38.7	370.1	33.1	10.2	13.0	40.7	366.3	31.9	10.1
10	11.1	32.9	370.4	29.7	9.4	11.1	33.0	370.4	29.6	9.4	11.2	33.5	370.2	29.4	9.4	11.5	35.2	367.2	28.8	9.4
11	9.6	27.5	370.4	25.2	8.3	9.6	27.6	370.4	25.2	8.4	9.7	28.0	370.2	25.1	8.4	9.9	29.5	367.5	24.9	8.4
12	8.5	23.5	370.4	21.7	7.5	8.5	23.6	370.4	21.8	7.5	8.5	23.9	370.2	21.8	7.6	8.8	25.3	367.6	21.8	7.7
13	7.3	17.8	370.4	12.7	4.4	7.3	18.0	370.0	12.6	4.3	7.4	18.5	364.2	12.2	4.3	7.7	21.0	291.7	10.8	4.1
14	7.9	20.0	370.4	15.0	5.1	7.9	20.2	370.1	14.8	5.0	8.0	20.7	366.5	14.4	5.0	8.3	23.1	319.2	13.1	4.8
15	7.2	18.2	370.4	14.8	5.3	7.3	18.4	370.3	14.8	5.4	7.3	18.8	368.3	14.6	5.4	7.6	20.8	340.7	14.1	5.4
16	6.4	15.7	370.4	13.3	5.1	6.4	15.8	370.3	13.3	5.1	6.5	16.2	368.8	13.3	5.2	6.8	17.8	347.5	13.3	5.3
17	5.8	13.6	370.4	11.8	4.8	5.8	13.7	370.3	11.9	4.8	5.8	14.0	368.9	11.9	4.9	6.1	15.5	350.0	12.2	5.0

$(p_{+1}, \lambda, K) = (0.85, 0.72, 2.928)$

case	-0.2	-0.1	0	0.1	0.2	-0.2	-0.1	0	0.1	0.2	-0.2	-0.1	0	0.1	0.2	-0.2	-0.1	0	0.1	0.2
1	103.7	236.9	370.4	236.9	103.7	103.7	236.9	370.4	236.9	103.7	103.7	236.9	370.4	236.9	103.7	103.6	236.8	370.4	236.8	103.6
2	68.2	192.9	370.4	192.7	68.1	68.2	193.0	370.4	192.8	68.1	68.3	193.1	370.4	192.9	68.2	68.6	193.5	370.4	193.3	68.5
3		171.8	370.4	171.8	54.9	55.0	171.8	370.4	171.8	55.0	55.1	172.0	370.4	172.0	55.1	55.5	172.8	370.4	172.8	55.5
4	44.7	152.8	370.4	152.8	44.7	44.8	152.9	370.4	152.9	44.8	44.9	153.2	370.4	153.2	44.9	45.5	154.2	370.4	154.2	45.5
5	35.0	131.7	370.4	131.7	35.0	35.0	131.8	370.4	131.8	35.0	35.2	132.2	370.4	132.2	35.2	35.8	133.7	370.4	133.7	35.8
6	28.0	114.3	370.4	114.3	28.0	28.1	114.4	370.4	114.4	28.1	28.3	114.9	370.4	114.9	28.3	29.0	116.8	370.4	116.8	29.0
7	30.3	107.7	370.4	77.0	11.1	30.5	108.6	370.4	75.9	11.0	31.0	111.2	369.9	72.9	10.6	33.0	122.6	362.3	61.8	9.2
8	36.6	128.1	370.4	111.1	23.2	36.8	128.7	370.4	110.6	23.1	37.1	130.4	370.3	109.1	22.9	38.7	137.4	369.0	103.5	22.1
9	38.1	133.2	370.4	119.8	27.2	38.2	133.6	370.4	119.4	27.2	38.5	135.0	370.3	118.4	27.0	39.9	140.7	369.6	114.6	26.5
10	31.3	117.9	370.4	107.3	23.4	31.4	118.3	370.4	107.1	23.4	31.7	119.6	370.4	106.5	23.4	32.9	124.9	369.8	104.2	23.3
11	4.3	99.9	370.4	91.5	18.9	24.4	100.3	370.4	91.4	18.9	24.7	101.5	370.4	91.2	19.0	25.8	106.6	369.8	90.3	19.2
12	19.3	85.0	370.4	78.2	15.4	19.4	85.4	370.4	78.2	15.4	19.7	86.7	370.4	78.2	15.5	20.7	91.7	369.9	78.5	16.0
13	14.5	61.7	370.4	38.8	4.7	14.6	62.5	370.3	38.1	4.7	14.9	64.8	369.2	36.3	4.6	16.2	75.1	352.3	30.0	4.2
14	16.9	71.1	370.4	49.0	6.6	17.0	71.8	370.3	48.4	6.5	17.3	74.0	369.7	46.7	6.4	18.6	83.7	359.4	40.5	6.0
15	14.3	63.6	370.4	48.5	7.5	14.3	64.2	370.4	48.3	7.5	14.6	66.1	370.0	47.6	7.5	15.8	74.3	364.4	45.1	7.7
16	11.1	52.2	370.4	41.5	6.8	11.2	52.8	370.4	41.5	6.8	11.4	54.5	370.1	41.5	6.9	12.4	61.8	365.8	41.4	7.3
17	8.8	42.7	370.4	34.7	5.9	8.9	43.2	370.4	34.8	5.9	9.1	44.8	370.1	35.2	6.0	10.0	51.6	366.3	36.5	6.5

Sensitivity analysis

Ideally, during the design phase of a nonparametric EWMA control chart, for a given value of the sample size, practitioners should find the proper combination of (λ, K) which will guarantee its distribution-free (or at least approximately distribution-free) properties, regardless the type of the underlying distribution (symmetric/asymmetric) or the magnitude of κ. From the results presented above, it has been shown, that the "flip a coin strategy" is an efficient technique dealing with ties during the process monitoring. However, before we proceed to any conclusions or performance evaluations, the effect of the design parameters (λ, K), the sample size n and the magnitude of κ in the chart's distribution-free properties needs to be examined. In order to investigate the robustness of the "flip a coin" strategy, for each pair of (λ, K), listed in Table 4.11, and for different values of κ, the corresponding ARL_0 values will be presented and their stability will be examined under the Benchmark of the distributions listed in Table 4.3.

Table 4.11: Pairs of (λ, K) for different sample sizes when ties are not present for the 2C-SN EWMA chart

	$\lambda = 0.05$	$\lambda = 0.15$	$\lambda = 0.25$	$\lambda = 0.35$	$\lambda = 0.45$	$\lambda = 0.55$	$\lambda = 0.65$	$\lambda = 0.75$	$\lambda = 0.85$	$\lambda = 0.95$
$n = 5$	2.4813	2.7690	2.8230	2.8142	2.8003	2.7648	2.6972	2.6053	2.4983	2.3991
$n = 15$	2.4901	2.7860	2.8744	2.9034	2.9176	2.9140	2.9121	2.9042	2.9022	2.8771
$n = 20$	2.4891	2.7918	2.8808	2.9134	2.9310	2.9320	2.9327	2.9275	2.9153	2.8239
$n = 35$	2.4906	2.7946	2.8831	2.9204	2.9389	2.9427	2.9446	2.9422	2.9457	2.9834
$n = 25$	2.4893	2.7944	2.8843	2.9256	2.9439	2.9496	2.9528	2.9517	2.9506	2.9420
$n = 35$	2.4906	2.7953	2.8877	2.9288	2.9470	2.9548	2.9587	2.9584	2.9557	2.9190
$n = 40$	2.4909	2.7970	2.8895	2.9303	2.9491	2.9590	2.9629	2.9633	2.9612	2.9121

Effect of the charting parameter λ: In general, as it is presented in Table 3.10, large values of λ ($\lambda \to 1$) correspond to red shifts ($p_{+1} \to 1$) and small values of λ ($\lambda \to 0$) correspond to small shifts ($p_{+1} \to 0$). In Table 4.11, several pairs of (λ, K) are presented in the case where no ties exists which guarantee that $\text{ARL}_0 = 370.4$. In particular, for several values of n and $\lambda = 0.05, 0.15, \ldots, 0.95$ the corresponding values of K have been computed in order to satisfy the condition $\text{ARL}_0 = 370.4$. Additionally, for each pair of (λ, K) presented in Table 4.11 and for each distribution presented in Table 4.3, the corresponding ARL_0 have been computed (see, Tables, A1, A2 and A3 in appendix) and plotted in Figures 4.10, 4.11 and 4.12 for $n = 5$, $n = 20$ and $n = 30$, respectively. Moreover, at each plot, the red dashed lines represent the "reliability limits" ($\text{REL} = \text{ARL}_0 \pm 5$) as a decision rule that the chart approximately maintains its distribution-free properties. We can conclude the following:

- $n = 5$: For $\kappa \leq 0.1$ the value of λ does not significantly affects the ARL_0 values. For $0.1 \leq \kappa \leq 0.2$, beside cases #14, #15, when the value of the parameter $\lambda > 0.25$ the chart behaves approximately as a distribution-free scheme.

- $n = 20$ or $n = 30$: For the first 6 cases (symmetric distributions) λ does not affects the ARL_0 values. As κ increases the ARL_0 values are affected and larger aberrations occur for heavily-tailed distributions (#13-#17).

Based on the results presented above, for symmetric distributions, the value of λ has no impact in the chart's performance, regardless the sample size. On the other hand, for heavily tailed and skewed distributions larger values of λ are preferable. In conclusion, for moderate values of $\kappa \approx 0.2$, choosing the value of $\lambda \approx 0.8$ can be considered as a reasonable choice in order to have an approximately distribution-free behaviour.

Figure 4.10: Effect of λ for $n = 5$ when ties are present (Table A1)

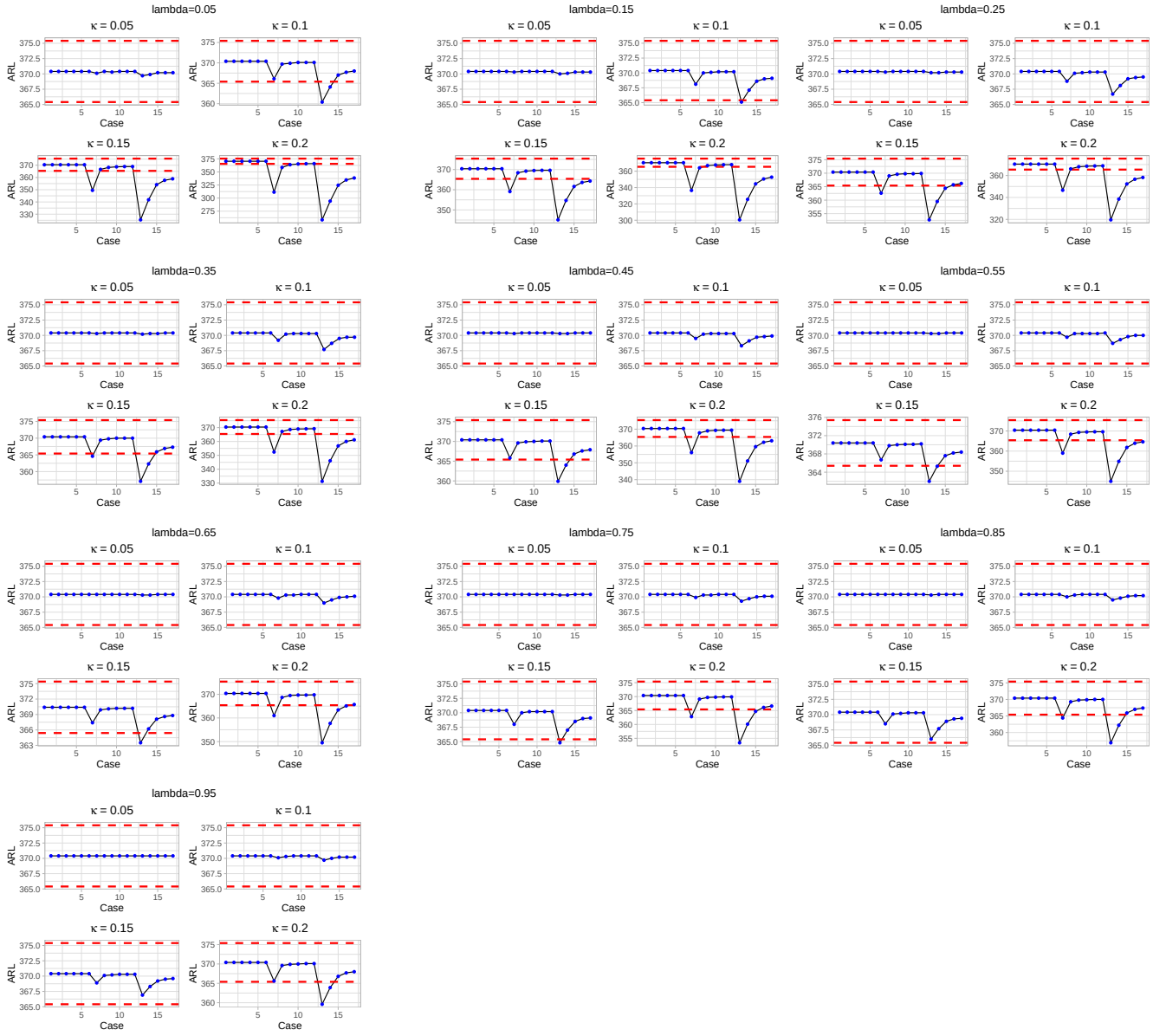

Figure 4.11: Effect of λ for $n = 20$ when ties are present(Table A3(top))

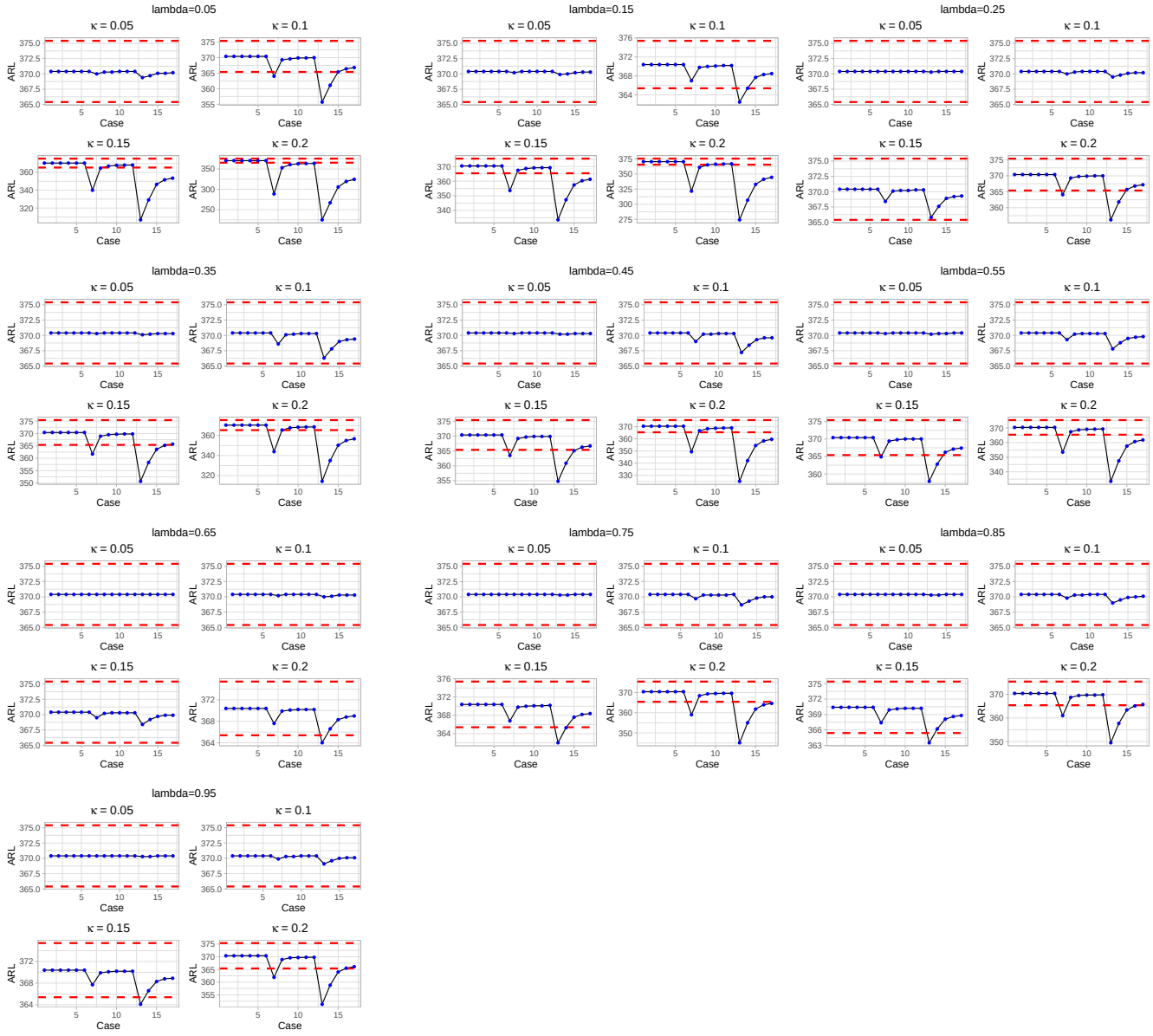

Figure 4.12: Effect of λ for $n = 30$ when ties are present(Table A3(botom))

Effect of the sample size (n) ***and magnitude of ties*** (κ): In Table 4.12, several in-control ARL. are presented for $\lambda = \{0.75, 0.8, \ldots, 0.95\}$, $n = \{5, 15\}$ and $\kappa = \{0.3, 0.35, 0.4, 0.45\}$. Similarly, in Table 4.13, for the same values of λ and κ, the corresponding ARL_0 values are presented for $n = \{30, 35, 40\}$. We may conclude the following:

- For the symmetric distributions, regardless the sample size or the value of κ, the "flip a coin" strategy guarantees the chart's distribution-free properties. As consequence,

for symmetric distributions and specified value of n, practitioners are able to design the proposed scheme in order to maintain its distribution free properties regardless the magnitude of κ.

- On the other hand, as κ and n increase, when the underlying distribution is heavily tailed or heavily skewed (see, cases $\#14 - \#17$) the ARL_0 values are affected and the chart tend to loose its distribution-free properties.

Table 4.12: ARL_0 for small/moderate sample sizes and large values of κ for the 2C-SN EWMA chart

n=5

	$\lambda = 0.75$				$\lambda = 0.85$				$\lambda = 0.95$			
	$\kappa = 0.3$	$\kappa = 0.35$	$\kappa = 0.4$	$\kappa = 0.45$	$\kappa = 0.3$	$\kappa = 0.35$	$\kappa = 0.4$	$\kappa = 0.45$	$\kappa = 0.3$	$\kappa = 0.35$	$\kappa = 0.4$	$\kappa = 0.45$
1	370.30	370.30	370.30	370.30	370.40	370.40	370.40	370.40	370.70	370.70	370.70	370.70
2	370.30	370.30	370.30	370.30	370.40	370.40	370.40	370.40	370.70	370.70	370.70	370.70
3	370.30	370.30	370.30	370.30	370.40	370.40	370.40	370.40	370.70	370.70	370.70	370.70
4	370.30	370.30	370.30	370.30	370.40	370.40	370.40	370.40	370.70	370.70	370.70	370.70
5	370.30	370.30	370.30	370.30	370.40	370.40	370.40	370.40	370.70	370.70	370.70	370.70
6	370.30	370.30	370.30	370.30	370.40	370.40	370.40	370.40	370.70	370.70	370.70	370.70
7	358.30	348.30	333.50	313.50	360.60	352.30	340.00	323.00	364.80	359.70	352.00	341.00
8	368.20	366.50	363.90	360.20	368.70	367.30	365.10	362.10	369.70	368.80	367.50	365.70
9	369.20	368.30	367.00	365.10	369.50	368.80	367.70	366.10	370.10	369.70	369.00	368.10
10	369.40	368.70	367.60	366.20	369.70	369.10	368.20	367.00	370.20	369.90	369.40	368.70
11	369.50	368.90	368.00	366.80	369.80	369.30	368.50	367.50	370.30	370.00	369.60	369.00
12	369.60	369.00	368.20	367.20	369.80	369.30	368.70	367.80	370.30	370.00	369.70	369.10
13	344.30	324.80	298.60	267.10	349.10	332.60	310.20	282.30	357.70	347.20	332.40	313.00
14	354.70	342.50	325.40	303.60	357.60	347.50	333.20	314.50	362.90	356.70	347.60	335.30
15	362.10	356.00	347.80	337.50	363.70	358.70	351.90	343.30	366.60	363.60	359.40	354.10
16	364.40	360.30	355.00	348.50	365.60	362.20	357.90	352.50	367.80	365.80	363.10	359.80
17	365.30	362.10	358.00	353.40	366.30	363.70	360.40	356.50	368.20	366.60	364.60	362.30

n=10

	$\lambda = 0.75$				$\lambda = 0.85$				$\lambda = 0.95$			
	$\kappa = 0.3$	$\kappa = 0.35$	$\kappa = 0.4$	$\kappa = 0.45$	$\kappa = 0.3$	$\kappa = 0.35$	$\kappa = 0.4$	$\kappa = 0.45$	$\kappa = 0.3$	$\kappa = 0.35$	$\kappa = 0.4$	$\kappa = 0.45$
1	370.40	370.40	370.40	370.40	370.40	370.40	370.40	370.40	370.50	370.50	370.50	370.50
2	370.40	370.40	370.40	370.40	370.40	370.40	370.40	370.40	370.50	370.50	370.50	370.50
3	370.40	370.40	370.40	370.40	370.40	370.40	370.40	370.40	370.50	370.50	370.50	370.50
4	370.40	370.40	370.40	370.40	370.40	370.40	370.40	370.40	370.50	370.50	370.50	370.50
5	370.40	370.40	370.40	370.40	370.40	370.40	370.40	370.40	370.50	370.50	370.50	370.50
6	370.40	370.40	370.40	370.40	370.40	370.40	370.40	370.40	370.50	370.50	370.50	370.50
7	342.70	321.20	292.00	256.20	345.70	326.30	299.50	266.10	349.10	332.10	308.10	277.40
8	365.40	361.30	355.20	346.80	366.00	362.40	356.90	349.40	366.70	363.60	358.90	352.40
9	367.80	365.60	362.50	358.00	368.10	366.20	363.40	359.40	368.50	366.90	364.50	361.10
10	368.30	366.60	364.00	360.60	368.50	367.00	364.80	361.70	368.90	367.60	365.70	363.00
11	368.50	367.00	364.90	362.00	368.70	367.40	365.50	363.00	369.10	368.00	366.30	364.10
12	368.60	367.30	365.40	362.90	368.80	367.60	366.00	363.70	369.20	368.20	366.70	364.80
13	313.10	275.80	232.40	187.80	319.00	284.50	243.40	200.00	325.50	294.40	256.20	214.50
14	334.70	309.30	277.00	240.20	338.50	315.50	285.60	250.80	342.80	322.40	295.40	263.20
15	351.20	337.70	320.20	299.50	353.30	341.20	325.40	306.50	355.70	345.20	331.20	314.30
16	356.40	347.10	335.40	321.70	358.00	349.70	339.10	326.80	359.80	352.60	343.40	332.50
17	358.60	351.20	342.10	331.90	359.90	353.30	345.20	336.00	361.50	355.80	348.70	340.60

Table 4.13: ARL_0 for large sample sizes and large values of κ for the 2C-SN EWMA chart

n=30

	$\lambda = 0.75$				$\lambda = 0.85$				$\lambda = 0.95$			
	$\kappa = 0.3$	$\kappa = 0.35$	$\kappa = 0.4$	$\kappa = 0.45$	$\kappa = 0.3$	$\kappa = 0.35$	$\kappa = 0.4$	$\kappa = 0.45$	$\kappa = 0.3$	$\kappa = 0.35$	$\kappa = 0.4$	$\kappa = 0.45$
1	370.4	370.4	370.4	370.4	370.4	370.4	370.4	370.4	370.4	370.4	370.4	370.4
2	370.4	370.4	370.4	370.4	370.4	370.4	370.4	370.4	370.4	370.4	370.4	370.4
3	370.4	370.4	370.4	370.4	370.4	370.4	370.4	370.4	370.4	370.4	370.4	370.4
4	370.4	370.4	370.4	370.4	370.4	370.4	370.4	370.4	370.4	370.4	370.4	370.4
5	370.4	370.4	370.4	370.4	370.4	370.4	370.4	370.4	370.4	370.4	370.4	370.4
6	370.4	370.4	370.4	370.4	370.4	370.4	370.4	370.4	370.4	370.4	370.4	370.4
7	317.6	281.3	237.2	190.4	326.1	294.4	254.4	210.0	329.7	300.0	262.0	218.8
8	360.4	352.3	340.7	325.1	362.2	355.5	345.7	332.5	362.9	356.8	347.8	335.7
9	365.1	360.8	354.5	346.0	366.0	362.5	357.3	350.2	366.4	363.2	358.5	351.9
10	366.1	362.7	357.7	350.8	366.9	364.0	359.9	354.2	367.2	364.6	360.8	355.6
11	366.6	363.6	359.4	353.7	367.3	364.8	361.3	356.6	367.6	365.3	362.1	357.8
12	366.8	364.1	360.3	355.3	367.5	365.3	362.1	358.0	367.7	365.7	362.9	359.1
13	268.5	215.3	162.8	117.8	283.0	233.8	182.8	136.6	289.2	242.1	191.9	145.4
14	303.7	262.8	216.8	171.5	314.1	277.8	235.2	191.4	318.5	284.3	243.5	200.5
15	333.0	308.8	279.7	248.1	339.3	318.5	293.0	264.4	341.9	322.7	298.7	271.6
16	342.9	325.7	304.9	282.1	347.6	333.0	315.1	295.1	349.6	336.1	319.5	300.7
17	347.0	333.1	316.6	298.9	351.1	339.3	325.3	309.9	352.7	341.9	328.9	314.6

n=35

	$\lambda = 0.75$				$\lambda = 0.85$				$\lambda = 0.95$			
	$\kappa = 0.3$	$\kappa = 0.35$	$\kappa = 0.4$	$\kappa = 0.45$	$\kappa = 0.3$	$\kappa = 0.35$	$\kappa = 0.4$	$\kappa = 0.45$	$\kappa = 0.3$	$\kappa = 0.35$	$\kappa = 0.4$	$\kappa = 0.45$
1	370.4	370.4	370.4	370.4	370.4	370.4	370.4	370.4	370.4	370.4	370.4	370.4
2	370.4	370.4	370.4	370.4	370.4	370.4	370.4	370.4	370.4	370.4	370.4	370.4
3	370.4	370.4	370.4	370.4	370.4	370.4	370.4	370.4	370.4	370.4	370.4	370.4
4	370.4	370.4	370.4	370.4	370.4	370.4	370.4	370.4	370.4	370.4	370.4	370.4
5	370.4	370.4	370.4	370.4	370.4	370.4	370.4	370.4	370.4	370.4	370.4	370.4
6	370.4	370.4	370.4	370.4	370.4	370.4	370.4	370.4	370.4	370.4	370.4	370.4
7	310.0	269.9	222.9	174.7	319.5	284.2	240.9	194.4	324.2	291.4	250.2	204.9
8	358.7	349.4	336.1	318.4	360.8	353.1	341.8	326.8	361.8	354.8	344.6	330.9
9	364.2	359.2	352.0	342.1	365.3	361.2	355.2	346.9	365.8	362.1	356.7	349.2
10	365.4	361.4	355.6	347.7	366.3	363.0	358.2	351.6	366.7	363.7	359.4	353.5
11	365.9	362.5	357.6	351.0	366.7	363.9	359.8	354.4	367.1	364.6	360.9	356.0
12	366.2	363.1	358.7	352.9	367.0	364.4	360.7	356.0	367.3	365.0	361.7	357.4
13	256.1	200.1	147.2	103.7	271.7	219.2	166.8	121.4	279.6	229.2	177.4	131.0
14	294.6	249.9	201.6	155.8	306.1	266.0	220.7	175.5	311.8	274.2	230.6	186.1
15	327.4	300.2	268.2	234.4	334.5	311.0	282.6	251.6	337.9	316.4	289.9	260.5
16	338.6	319.1	295.8	270.9	344.0	327.3	307.2	285.0	346.6	331.4	312.8	292.1
17	343.4	327.4	308.9	289.2	348.0	334.5	318.6	301.4	350.2	337.9	323.3	307.4

4.3.4 Guidelines for practitioners when dealing with rounding-off errors

In this Chapter has been shown that under the presence of ties the performance of a conventional chart based on a nonparametric statistic (such as the Sign statistic) is seriously affected. A new enhanced nonparametric Sign EWMA chart under the case of rounding-off errors was proposed, where two alternative approaches were considered for dealing with tied observations. After an extensive sensitivity analysis our results showed that:

- ***Symmetric distributions***: Both the "flip a coin" and the "new limits" strategies are equivalent regardless the sample size or the value of κ. In fact, an advantage of the "flip a coin strategy" is that, for symmetric distributions, if practitioners are unable

to estimate the underlying distribution or the value of κ, they can just use the same optimal pairs of (λ, K) with the ones in the "no ties" case for a specific value of n (see, Table 3.10). In particular for small, moderate and large shifts in the process median the corresponding pair of (λ, K) for $p_{+1} \approx 0.5$, $p_{+1} \approx 0.7$ and $p_{+1} \approx 1$ are recommended without any knowledge of the value of κ. Traditionally, the use of the proposed chart outperforms the Shewhart Sign chart for any shift magnitude.

- ***asymmetric distributions***: When the sample sample and the value of κ are not large the chart also maintain its approximately distribution-free properties as long as $\lambda \approx 0.8$. However, for large values of κ and n, for heavily skewed distributions (cases #7,#13), the use of the Shewhart or the 2C-SN EWMA charts might not be efficient under the "flip a coin strategy". As a result, choosing a relative small/moderate sample size is preferable for these cases.

4.3.5 Performance comparisons

Dealing with ties and rounding-off errors in nonparametric control charts, is a relative new research field. As far as we are concerned, the modified Shewhart Sign chart introduced by Castagliola et al. (2020) is the only existing scheme dealing with rounding-off errors. As a result, the performance of the 2C-SN EWMA chart under the "flip a coin strategy" will be compared with the Shewhart Sign chart (Castagliola et al. (2020)) under the benchmark of the distributions listed in Table 4.3. In Table 4.14 the corresponding differences between the 2C-SN EWMA and Shewhart Sign charts are presented for $n = 20$ and $\kappa = \{0, 0.050.1, 0.2\}$. It is clear that, negative values in this table, correspond to the superiority of our proposed scheme.

In order to perform fair comparisons, our chart has been optimized in order to have the same ARL_0 with the Shewhart chart ($\text{ARL}_0 = 388.1$). More specifically, for a fixed value of $\lambda > 0.7$, the corresponding value of K will be computed such that $\text{ARL}_0 = 388.1$ when $\kappa = 0$. Finally, the same optimal pair of (λ, K) will be used in order to compute the chart's performance for $\kappa = \{0.05, 0.1, 0.2\}$. Note that, as presented in the previous sections, under the "flip a coin strategy", when $n < 20$ and $\kappa < 0.2$, setting $\lambda > 0.7$ guarantees an approximately distribution-free behaviour for the 2C-SN EWMA chart. So it would be logical to optimize λ also. Nevertheless, it is not necessary to do this since, even by setting $\lambda = 0.7$, our chart outperforms the Shewhart chart. In particular, from Table 4.14 we may conclude that our chart performs better for any shift magnitude regardless the underlying distribution or the value of κ.

Table 4.14: Performance comparisons between the Sign Shewhart and 2-C SN EWMA charts when ties are present

	$\kappa = 0$									$\kappa = 0.05$								
case	-1	-0.5	-0.2	-0.1	0	0.1	0.2	0.5	1	-1	-0.5	-0.2	-0.1	0	0.1	0.2	0.5	1
#1	-0.70	-13.50	-60.80	-52.90	0.00	-52.90	-60.80	-13.50	-0.70	-0.70	-13.50	-60.80	-52.90	0.00	-52.90	-60.80	-13.50	-0.70
#2	-0.20	-7.20	-50.60	-61.80	0.00	-61.80	-50.50	-7.20	-0.20	-0.20	-7.20	-50.70	-61.80	0.00	-61.80	-50.60	-7.20	-0.20
#3	-0.20	-5.10	-44.70	-64.00	0.00	-64.00	-44.70	-5.10	-0.20	-0.20	-5.20	-44.80	-64.10	0.00	-64.10	-44.80	-5.20	-0.20
#4	-0.10	-3.70	-39.20	-64.90	0.00	-64.90	-39.20	-3.70	-0.10	-0.10	-3.70	-39.20	-65.00	0.00	-65.00	-39.20	-3.70	-0.10
#5	0.00	-2.60	-33.00	-64.40	0.00	-64.40	-33.00	-2.60	0.00	0.00	-2.60	-33.10	-64.60	0.00	-64.60	-33.10	-2.60	0.00
#6	0.00	-1.90	-27.70	-62.60	0.00	-62.60	-27.70	-1.90	0.00	0.00	-1.90	-27.90	-62.80	0.00	-62.80	-27.90	-1.90	0.00
#7	-0.30	-3.70	-29.60	-61.60	0.00	-53.80	-11.80	0.00	0.00	-0.30	-3.70	-29.90	-62.60	0.00	-52.40	-11.50	0.00	0.00
#8	-0.20	-3.90	-34.10	-64.10	0.00	-62.10	-23.70	-0.30	0.00	-0.20	-4.00	-34.30	-64.70	0.00	-61.50	-23.60	-0.30	0.00
#9	-0.20	-3.80	-35.10	-64.50	0.00	-63.30	-27.10	-0.70	0.00	-0.20	-3.80	-35.20	-65.00	0.00	-62.90	-27.00	-0.70	0.00
#10	-0.10	-2.80	-30.30	-63.00	0.00	-61.40	-24.00	-0.70	0.00	-0.10	-2.80	-30.50	-63.50	0.00	-61.20	-24.00	-0.70	0.00
#11	-0.10	-1.80	-24.70	-60.10	0.00	-58.10	-19.80	-0.60	0.10	-0.10	-1.80	-24.80	-60.60	0.00	-58.00	-19.90	-0.60	0.10
#12	0.00	-1.30	-20.20	-56.30	0.00	-54.20	-16.40	-0.40	0.10	0.00	-1.30	-20.40	-56.80	0.00	-54.20	-16.50	-0.40	0.10
#13	0.00	-1.20	-15.40	-47.80	0.00	-35.50	-3.80	0.00	0.00	0.00	-1.20	-15.60	-48.90	0.10	-34.40	-3.70	0.00	0.00
#14	0.00	-1.40	-17.90	-51.70	0.00	-41.60	-6.30	0.00	0.00	0.00	-1.40	-18.10	-52.70	0.10	-40.70	-6.20	0.00	0.00
#15	0.00	-0.90	-15.20	-48.70	0.00	-41.40	-7.40	0.00	0.00	0.00	-1.00	-15.40	-49.60	0.00	-41.00	-7.40	0.00	0.00
#16	0.00	-0.60	-11.70	-43.30	0.00	-37.20	-6.50	-0.10	0.00	0.00	-0.60	-11.90	-44.10	0.00	-37.20	-6.60	-0.10	0.00
#17	0.00	-0.40	-9.00	-37.90	0.00	-32.70	-5.40	-0.10	0.00	0.00	-0.40	-9.20	-38.70	0.00	-32.90	-5.50	-0.10	0.00
	$\kappa = 0.1$									$\kappa = 0.2$								
case	-1	-0.5	-0.2	-0.1	0	0.1	0.2	0.5	1	-1	-0.5	-0.2	-0.1	0	0.1	0.2	0.5	1
#1	-0.70	-13.50	-60.70	-52.90	0.00	-52.90	-60.70	-13.50	-0.70	-0.70	-13.40	-60.50	-52.70	0.00	-52.70	-60.50	-13.40	-0.70
#2	-0.20	-7.20	-50.80	-61.90	0.00	-61.90	-50.70	-7.20	-0.20	-0.30	-7.60	-52.40	-63.40	0.00	-63.40	-52.30	-7.60	-0.30
#3	-0.20	-5.20	-44.90	-64.30	0.00	-64.30	-44.90	-5.20	-0.20	-0.20	-5.60	-47.40	-67.00	0.00	-67.00	-47.40	-5.60	-0.20
#4	-0.10	-3.80	-39.40	-65.30	0.00	-65.30	-39.40	-3.80	-0.10	-0.10	-4.20	-42.70	-69.30	0.00	-69.30	-42.70	-4.20	-0.10
#5	0.00	-2.60	-33.30	-65.00	0.00	-65.00	-33.30	-2.60	0.00	-0.10	-3.10	-37.40	-71.00	0.00	-71.00	-37.40	-3.10	-0.10
#6	0.00	-1.90	-28.20	-63.30	0.00	-63.30	-28.20	-1.90	0.00	0.00	-2.40	-32.90	-71.50	0.00	-71.50	-32.90	-2.40	0.00
#7	-0.30	-3.80	-30.70	-65.80	0.30	-48.20	-10.60	0.00	0.00	-0.40	-4.50	-45.10	-120.30	42.50	1.60	-1.40	-0.20	0.00
#8	-0.20	-4.00	-34.90	-66.60	0.10	-59.80	-23.20	-0.30	0.00	-0.30	-4.70	-45.30	-96.20	7.70	-36.00	-17.80	-0.40	0.00
#9	-0.20	-3.90	-35.80	-66.50	0.10	-61.80	-26.80	-0.70	0.00	-0.30	-4.50	-44.80	-89.80	4.00	-45.70	-23.40	-0.90	0.00
#10	-0.10	-2.80	-31.00	-65.00	0.00	-60.50	-23.90	-0.70	0.00	-0.10	-3.40	-39.40	-87.90	3.30	-50.50	-23.40	-1.00	0.00
#11	-0.10	-1.90	-25.30	-62.10	0.00	-57.70	-20.00	-0.60	0.10	-0.10	-2.40	-33.50	-85.70	2.90	-54.00	-21.90	-1.00	0.00
#12	0.00	-1.30	-20.90	-58.50	0.00	-54.30	-16.70	-0.50	0.10	0.00	-1.80	-28.80	-83.20	2.60	-55.60	-20.10	-0.80	0.00
#13	-0.10	-1.20	-16.20	-52.20	0.70	-31.40	-3.50	0.00	0.00	-0.10	-1.60	-27.60	-116.50	83.60	-0.10	-1.20	0.00	0.00
#14	0.00	-1.50	-18.70	-55.70	0.50	-37.90	-5.90	0.00	0.00	0.00	-1.90	-29.90	-111.20	53.00	-7.30	-3.00	-0.10	0.00
#15	0.00	-1.00	-16.00	-52.30	0.30	-39.90	-7.50	0.00	0.00	0.00	-1.40	-25.90	-99.30	28.00	-28.10	-8.90	-0.20	0.00
#16	0.00	-0.60	-12.40	-46.70	0.20	-37.10	-6.80	-0.10	0.00	0.00	-1.00	-21.50	-90.80	19.80	-37.70	-10.40	-0.30	0.00
#17	0.00	-0.40	-9.70	-41.30	0.20	-33.50	-5.70	-0.10	0.00	0.00	-0.70	-18.10	-84.90	16.30	-42.20	-10.30	-0.20	0.00

4.4 An illustrative example

In this Section a modified version of the example originally discussed by Celano et al. (2016) is provided, to show a practical Phase II implementation of the design and operation of our proposed chart under the case of measurement error. In this example, the quality characteristic to be monitored is the radial error, defined as "a quality characteristic frequently monitored in hole drilling processes of mechanical parts and assembly processes of printed circuit boards". At each sampling point t, a subgroup of size $n = 20$ is collected in order to detect a shift in the median of the quality characteristic of interest such that $p_0 = 0.5$ shifts to $p_1 = 0.7$. Additionally, as shown in Celano et al. (2016) the in-control value of the median for the radial error is $\theta_0 = 0.338$. The original dataset is presented in Table 4.15 (top). For illustration purposes let us assume that the practitioner does not have at his disposal the true values due to a rounding-off error in the measurement system (the

resolution value is $\rho = 0.05$). A a results, through the model presented in equation (4.1), the practitioner obtains the values presented in Table 4.15 (bottom). Similarly the observed value of the median will be $\theta_0' = 0.3$ instead of the true one $\theta_0 = 0.338$.

Moreover, in Table 4.15 (top) the corresponding values of $S_{t,j} = \text{sign}(X_{t,j}^{'} - \theta_0')$ are presented. In can be clearly seen that due to the rounding-off error in the measurement system many ties occur (zero values for $S_{t,j}$). In order to overcome this problem we will use the "flip a coin" method presented in Section 4.3.2. More specifically, each $S_{t,j} = 0$ will be substituted by $S_{t,j}' = 2\Delta_{t,j} - 1$ where $\Delta_{t,j}$ will be a random number generated from Ber(0.5). These values are presented in Table 4.15 (bottom) along with the corresponding values of $\text{SN}_t, \text{SN}_t^*$ and Z_t^*. Additionally, for the design of the chart's parameters we used $\lambda^* = 0.305, K^* = 2.903$ (as the optimal pair for detecting a shift $p_{+1} = 0.7$ when $n = 20$), $\sigma = 0.2$ ("continuousify" parameter) and $Z_0^* = 0$ (no head-start feature). Then, by substituting these values in equations (3.10) and (3.11), we obtain the values of the control limits for the two-sided C-SN EWMA chart as $\text{LCL} = -5.5127, \text{UCL} = 5.5127$.
More specifically:

- For $t = 1$ we have $\text{SN}_1 = 8$. The corresponding value for SN_1^* is computed by generating a $\text{N}(8, 0.2)$ random variable. The value of the charting statistic is $Z_1^* = 0.305 \times (7.8729) + 0.695 \times 0) = 2.4012$.

- For $t = 2$ we have $\text{SN}_2 = 2$. The corresponding value for SN_2^* is computed by generating a $\text{N}(2, 0.2)$ random variable. The value of the charting statistic is $Z_2^* = 0.305 \times (1.6446) + 0.695 \times 2.4012) = 2.175$.
  $\vdots$

- For $t = 10$ we have $\text{SN}_{10} = 2$. The corresponding value for SN_{10}^* is computed by generating a $\text{N}(2, 0.2)$ random variable. The value of the charting statistic is $Z_{10}^* = 0.305 \times (1.8322) + 0.695 \times 0.6990) = 1.0447$

Finally, the values of the charting statistic Z_t^* are plotted in Figure 4.13. It can be seen that at the 4^{th} sampling point ($t = 4$) an out-of-control signal is given stating that the process median has changed.

4.5 Conclusions

In this Chapter, we aimed to present a general framework in order to tackle the occurrence of ties during the process monitoring. Through the measurement error model presented in Section 4.1, we saw that, when ties are present, the conventional Sign Shewhart and EWMA

Table 4.15: Radial error example: Phase II sample of $t = 1, \ldots 10$ subgroups of size $n = 20$ for the true values (top) and the observed values (bottom) along with the $S_{t,j}$ values with and without the "flip a coin strategy" when $\rho = 0.05$

Without the "flip a coin" strategy

$X_{t,j}$ true values

t	1	2	3	4	5	6	7	8	9	10	11	12	13	14	15	16	17	18	19	20
1	0.289	0.380	0.483	0.288	0.544	0.390	0.567	0.512	0.433	0.168	0.128	0.428	0.081	0.575	0.396	0.574	0.730	0.407	0.367	0.452
2	0.447	0.599	0.207	0.317	0.256	0.433	0.218	0.329	0.432	0.674	0.233	0.570	0.748	0.364	0.372	0.798	0.218	0.405	0.060	0.632
3	0.081	0.368	0.435	0.216	0.246	0.229	0.623	0.455	0.394	0.616	0.116	0.611	0.666	0.262	0.410	0.234	0.692	0.719	1.033	0.376
4	0.954	0.537	0.621	0.513	1.540	0.609	0.801	1.080	1.069	0.954	0.852	0.425	1.389	0.794	1.081	0.900	0.521	0.576	0.761	0.535
5	0.316	0.237	0.286	0.879	0.190	0.104	0.570	0.448	0.269	0.746	0.344	0.191	0.366	0.315	0.408	0.522	0.598	0.232	0.671	0.448
6	0.342	0.378	0.287	0.328	0.589	0.233	0.255	0.119	0.284	0.499	0.410	0.668	0.385	0.594	0.390	0.265	0.409	0.434	0.628	0.316
7	0.370	0.391	0.525	0.459	1.280	0.470	0.482	0.032	0.525	0.628	0.686	0.584	0.300	0.245	0.555	0.113	0.194	0.932	0.597	0.523
8	0.352	0.264	0.759	0.154	0.256	0.426	0.363	0.310	0.303	0.316	0.807	0.235	0.173	0.183	1.105	0.068	0.368	0.736	0.097	0.060
9	0.305	0.352	0.468	0.224	0.739	0.234	0.171	0.250	0.308	0.431	0.092	0.326	0.455	0.569	0.354	0.475	0.530	0.312	0.102	0.651
10	0.603	0.363	0.628	0.314	0.029	0.436	0.207	0.553	0.645	0.122	0.759	0.296	0.691	0.425	0.441	0.323	0.287	0.310	0.194	0.582

$S_{t,j}$ values when $\rho = 0.05$

t	$S_{t,j} = \text{sign}(X'_{t,j} - \theta'_0)$																			
1	-1	**0**	1	-1	1	**0**	1	1	1	-1	-1	1	-1	1	**0**	1	1	**0**	-1	1
2	1	1	-1	-1	-1	1	-1	-1	1	1	-1	1	1	-1	-1	1	-1	**0**	-1	1
3	-1	-1	1	-1	-1	-1	1	1	**0**	1	-1	1	1	-1	**0**	-1	1	1	1	**0**
4	1	1	1	1	1	1	1	1	1	1	1	1	1	1	1	1	1	1	1	1
5	-1	-1	-1	1	-1	-1	1	1	-1	1	-1	-1	-1	-1	**0**	1	1	-1	1	1
6	-1	**0**	-1	-1	1	-1	-1	-1	-1	1	**0**	1	**0**	1	**0**	-1	**0**	1	1	-1
7	-1	**0**	1	1	1	1	1	-1	1	1	1	1	-1	-1	1	-1	-1	1	1	1
8	-1	-1	1	-1	-1	1	-1	-1	-1	-1	1	-1	-1	-1	1	-1	-1	1	-1	-1
9	-1	-1	1	-1	1	-1	-1	-1	-1	1	-1	-1	1	1	-1	1	1	-1	-1	1
10	1	-1	1	-1	-1	1	-1	1	1	-1	1	-1	1	1	1	-1	-1	-1	-1	1

With the "flip a coin" strategy

$X'_{t,j}$ observed values when $\rho = 0.05$

t	1	2	3	4	5	6	7	8	9	10	11	12	13	14	15	16	17	18	19	20
1	0.30	0.40	0.50	0.30	0.55	0.40	0.55	0.50	0.45	0.15	0.15	0.45	0.10	0.55	0.40	0.55	0.75	0.40	0.35	0.45
2	0.45	0.60	0.20	0.30	0.25	0.45	0.20	0.35	0.45	0.65	0.25	0.55	0.75	0.35	0.35	0.80	0.20	0.40	0.05	0.65
3	0.10	0.35	0.45	0.20	0.25	0.25	0.60	0.45	0.40	0.60	0.10	0.60	0.65	0.25	0.40	0.25	0.70	0.70	1.05	0.40
4	0.95	0.55	0.60	0.50	1.55	0.60	0.80	1.10	1.05	0.95	0.85	0.45	1.40	0.80	1.10	0.90	0.50	0.60	0.75	0.55
5	0.30	0.25	0.30	0.90	0.20	0.10	0.55	0.45	0.25	0.75	0.35	0.20	0.35	0.30	0.40	0.50	0.60	0.25	0.65	0.45
6	0.35	0.40	0.30	0.35	0.60	0.25	0.25	0.10	0.30	0.50	0.40	0.65	0.40	0.60	0.40	0.25	0.40	0.45	0.65	0.30
7	0.35	0.40	0.55	0.45	1.30	0.45	0.50	0.05	0.55	0.65	0.70	0.60	0.30	0.25	0.55	0.10	0.20	0.95	0.60	0.50
8	0.35	0.25	0.75	0.15	0.25	0.45	0.35	0.30	0.30	0.30	0.80	0.25	0.15	0.20	1.10	0.05	0.35	0.75	0.10	0.05
9	0.30	0.35	0.45	0.20	0.75	0.25	0.15	0.25	0.30	0.45	0.10	0.35	0.45	0.55	0.35	0.45	0.55	0.30	0.10	0.65
10	0.60	0.35	0.65	0.30	0.05	0.45	0.20	0.55	0.65	0.10	0.75	0.30	0.70	0.45	0.45	0.30	0.30	0.30	0.20	0.60

$S'_{t,j}$ values using the "flip a coin strategy" along with the corresponding SN_t,SN^*_t,Z^*_t values

t	$S'_{t,j} = \text{sign}(X'_{t,j} - \theta'_0)$																				SN_t	SN^*_t	Z^*_t
1	-1	1	1	-1	1	-1	1	1	1	-1	-1	1	-1	1	1	1	1	1	-1	1	6	5.948	1.814
2	1	1	-1	-1	-1	1	-1	-1	1	1	-1	1	1	-1	-1	1	-1	1	-1	1	0	0.079	1.285
3	-1	-1	1	-1	-1	-1	1	1	1	1	-1	1	1	-1	-1	-1	1	1	1	-1	0	-0.170	0.841
4	1	1	1	1	1	1	1	1	1	1	1	1	1	1	1	1	1	1	1	1	20	20.530	6.846
5	-1	-1	-1	1	-1	-1	1	1	-1	1	-1	-1	-1	-1	1	1	1	-1	1	1	-2	-1.969	4.158
6	-1	1	-1	-1	1	-1	-1	-1	-1	1	-1	1	1	1	1	-1	-1	1	1	-1	-2	-1.774	2.348
7	-1	1	1	1	1	1	1	-1	1	1	1	1	-1	-1	1	-1	-1	1	1	1	8	7.542	3.933
8	-1	-1	1	-1	-1	1	-1	-1	-1	-1	1	-1	-1	-1	1	-1	-1	1	-1	-1	-10	-9.852	-0.272
9	-1	-1	1	-1	1	-1	-1	-1	-1	1	-1	-1	1	1	-1	1	1	-1	-1	1	-4	-4.263	-1.489
10	1	-1	1	-1	-1	1	-1	1	1	-1	1	-1	1	1	1	-1	-1	-1	-1	1	0	0.184	-0.979

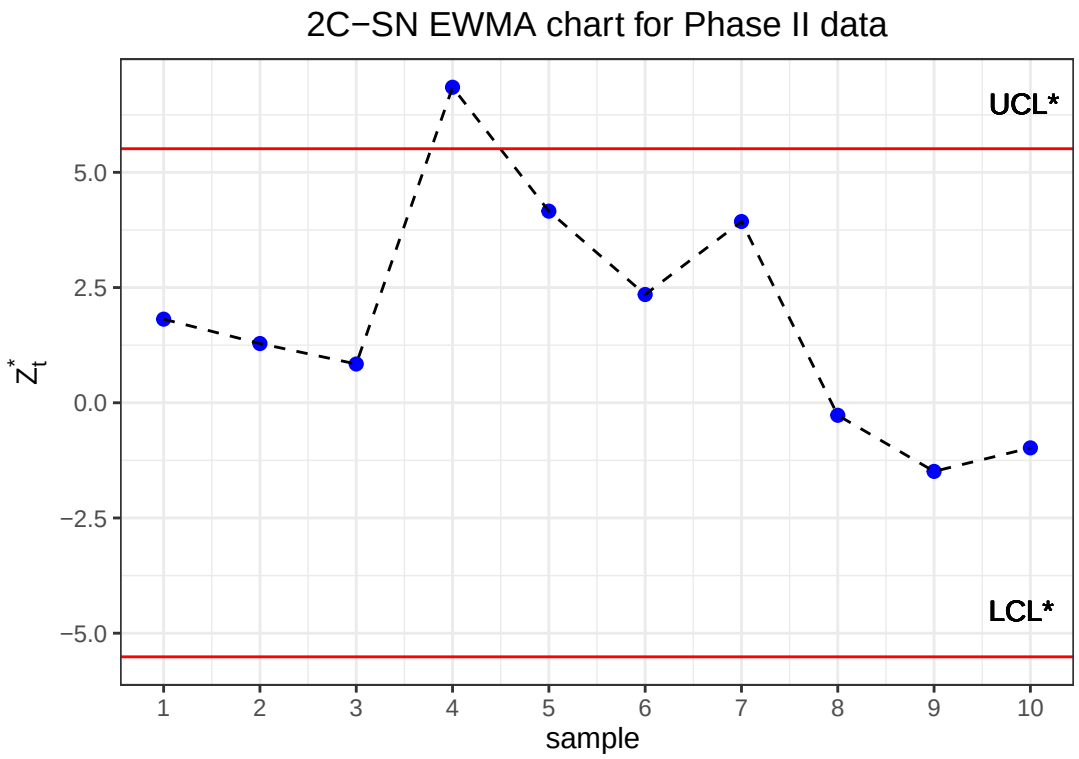

Figure 4.13: Radial error example: the C-SN EWMA chart for the Phase II data presented in Table 4.15 (bottom)

charts are unable to maintain their distribution-free properties. On the other hand, through the "flip coin strategy" these charts, under a reasonable number of ties and a sample size $n < 20$ are approximately distribution-free. Strictly speaking, for large values of κ and $n > 20$, when the underlying distribution is heavily skewed the RL properties are affected. An alternative solution was given via a semi parametric design with adjusted control limits, but still the values of the shift magnitude, the value of κ and the underlying distribution need to be known. Nevertheless, in the beginning of this Chapter, it was highlighted the fact that, large values of κ are practically not meant to exist in practice, and even if they are, due to the large differences between the true and observed samples, practitioners does not have a reliable sample measurements at the first place. Even so, for these extreme cases, if the underlying distribution is heavily-skewed, choosing a relative small/moderate sample size (i.e. $n \approx 10$) can be considered an efficient design.

Chapter 5

Improved Sign Shewhart and EWMA charts for monitoring shifts in the process dispersion

Introduction

In this Chapter, we will investigate a semi-parametric design of the two-sided Shewhart and EWMA charts, where a modified sign-type statistic is used, which can efficiently detect shifts in the process variability. In particular, for both charts, their exact in- and out-of-control performances will be provided and comparisons with other schemes will be performed. Additionally, specified and efficient method will be provided regarding the optimization procedure for both charts.

5.1 The Interquartile Range Sign statistic for dispersion

Suppose that, at each sampling point t, a random sample $\{X_{t,1}, X_{t,2}, \ldots, X_{t,n}\}$ of size n is collected, where $X_{t,j}$, $j = 1, 2, ..., n$, follows an unknown continuous distribution with corresponding cumulative distribution function (c.d.f.) $F_X(x|\sigma)$. The parameter σ corresponds to the scale parameter of interest (i.e. the standard deviation). It is assumed that $\sigma = \sigma_0$ when the process is in-control and $\sigma = \sigma_1 = \tau\sigma_0$ when the process is out-of-control. The parameter τ reflects the shift magnitude in the process variability, i.e. $\tau \in (0, 1)$ corresponds to a decrease in the variability (usually a process improvement) while $\tau \in (1, +\infty)$ corresponds to an increase in the variability (usually a process deterioration).

Let $X_{p_0/2}$ and $X_{1-p_0/2}$ be the $p_0/2$ and $1-p_0/2$ quantiles of $F_X(x|\sigma_0)$, i.e. when the process is *in-control*, where $p_0 \in (0,1)$ is a parameter considered to be known (or pre-specified). By definition, $X_{p_0/2}$ and $X_{1-p_0/2}$ are such that $F_X(X_{p_0/2}|\sigma_0) = p_0/2$, $F_X(X_{1-p_0/2}|\sigma_0) = 1 - p_0/2$ and we obviously have

$$p_0 = 1 - F_X(X_{1-p_0/2}|\sigma_0) + F_X(X_{p_0/2}|\sigma_0).$$

When the process shifts from σ_0 to σ_1, the corresponding probability is defined as

$$p_1 = 1 - F_X(X_{1-p_0/2}|\sigma_1) + F_X(X_{p_0/2}|\sigma_1).$$

If $\sigma_1 < \sigma_0$ (decrease in the variability) then we have $p_1 < p_0$ and if $\sigma_1 > \sigma_0$ (increase in the variability) then we have $p_1 > p_0$. Consequently, a shift from σ_0 to σ_1 in one direction is similar to a shift from p_0 to p_1 in the same direction. This suggests a simple distribution-free Shewhart-type Sign chart for monitoring shifts in the process variability based on the following statistic

$$\mathrm{SD}_t = \sum_{j=1}^{n} D_{t,j},$$

where

$$D_{t,j} = \begin{cases} 1, & \text{if } X_{t,j} < X_{p_0/2} \text{ or } X_{t,j} > X_{1-p_0/2} \\ 0, & \text{if } X_{t,j} = X_{p_0/2} \text{ or } X_{t,j} = X_{1-p_0/2} \\ -1, & \text{if } X_{p_0/2} < X_{t,j} < X_{1-p_0/2} \end{cases}.$$

Note that, due to the continuous nature of the variables to be monitored, the condition $D_{t,j} = 0$ is not supposed to hold in practice. Similarly with the theoretical properties of the traditional Sign statistic for testing changes in the median, the SD_t statistic belongs to $\{-n, -n+2, \ldots, n-2, n\}$. In addition, let us define the random variable $A_t = \frac{\mathrm{SD}_t + n}{2}$ as the number of observations less than $X_{p_0/2}$ or larger than $X_{1-p_0/2}$. By definition, this random variable A_t follows a binomial distribution $\mathrm{Bin}(n,p)$ with parameters n and $p \in \{p_0, p_1\}$ (depending on whether the process is in- or out-of-control). Therefore, we obtain the c.d.f. $F_{\mathrm{SD}_t}(s|n,p)$ of SD_t with the aid of the c.d.f. $F_{\mathrm{Bin}}(\cdot|n,p)$ of the $\mathrm{Bin}(n,p)$ distribution as

$$F_{\mathrm{SD}_t}(s|n,p) = F_{\mathrm{Bin}}\left(\frac{s+n}{2}|n,p\right),\ s \in \{-n, -n+2, \ldots, n-2, n\}.$$

In addition, the mean $\mathrm{E}(\mathrm{SD}_t)$ and the variance $\mathrm{V}(\mathrm{SD}_t)$ are given by

$$\mathrm{E}(\mathrm{SD}_t) = 2\mathrm{E}(A_t) - n = n(2p-1), \tag{5.1}$$

$$\mathrm{V}(\mathrm{SD}_t) = 4\mathrm{V}(A_t) = 4np(1-p). \tag{5.2}$$

5.2 The optimized Sign Shewhart chart for dispersion

Generally, the idea of varying the value of the parameter p_0 is not new. In fact, it has been originally introduced by Pawar et al. (2018). In their paper, they proposed a nonparametric upper-sided Shewhart chart for dispersion, based on the SD_t statistic where the value of p_0 is allowed to vary. However, during the design phase of their scheme, the value of p_0 is not optimized, and regarding its out-of-control performance, Pawar et al. (2018) only considered values of $\tau > 1$ (i.e., the case of increasing shifts in process variability) for a fixed value of p_0 . In this section, we aim to investigate the optimal design of the two-sided Sign chart for dispersion originally introduced by Pawar et al. (2018) (to be denoted as the S-SD chart) and examine its out-of-control performance for several distributions.

Charting statistic and RL properties

At each sampling point, a sample of size n is collected and the value of the plotting statistic SD_t is computed. Then if the value of this statistic falls beyond the interval $[L, U]$ an out of control signal is given, where $L, U \in \mathbb{N}$ are the upper and lower control limit coefficients to be fixed. In particular, during the design phase, for a given value of n and τ, a proper searching algorithm needs to be conducted in order to find the optimal values of L and U that minimise the corresponding value of ARL_1 where:

$$\mathrm{ARL}_1 = \frac{1}{1-\beta},$$

under the condition that

$$\mathrm{ARL}_0 = \frac{1}{\alpha} \approx \frac{1}{\alpha_0},$$

where a_0 denotes the maximum allowed false alarm rate. It is clear that, similarly with any conventional phase II Shewhart chart, the probabilities α and β accounts for the Type I and II error probabilities and equals to p_0 and p_1 respectively. In particular these probabilities depend on the control limits and the quantiles of the underlying distribution:

$$\begin{aligned}\alpha(L,U,p_0,\sigma_0|n) =& \mathrm{P}(\mathrm{SD}_t > U \cup \mathrm{SD}_t < U|\sigma_0) = 1 - \mathrm{P}(L \leq \mathrm{SD}_t \leq U|\sigma_0) \\ =& 1 - F_{\mathrm{Bin}}\left(\frac{U+n}{2}|n,p_0\right) + F_{\mathrm{Bin}}\left(\frac{(L-1)+n}{2}|n,p_0\right)\end{aligned}$$

$$\begin{aligned}\beta(L,U,p_0,\sigma_0,\tau|n) =& \mathrm{P}(L \leq \mathrm{SD}_t \leq U|\tau\sigma_0) \\ =& 1 - F_{\mathrm{Bin}}\left(\frac{U+n}{2}|n,p_1\right) + F_{\mathrm{Bin}}\left(\frac{(L-1)+n}{2}|n,p_1\right)\end{aligned}$$

where the probability p_1, associated with the corresponding chart's ARL_1 values will be derived as:

$$p_1 = 1 - F_Z(X_{1-p_0/2}|a,b,\tau c,\tau d) + F_Z(X_{p_0/2}|a,b,\tau c,\tau d).$$

where a, b, c, d are the parameters that define a distribution form the Johnson family. Note that the reason that we express p_1 in terms of the Johnson family distributions is that the chart's out-of-control performance will be examined under a benchmark of cases from this family of distributions, as we did in the Sign EWMA chart under the presence of ties.

It is clear that, the chart's parameters that need to optimised are p_0, L and U, and have to be optimally determined by solving the following mixed-integer non-linear problem:

$$\mathrm{Min} : \beta(L,U,p_0,\sigma_0,\tau|n)$$

subject to

$$\alpha(L,U,p_0,\sigma_0|n) \approx \alpha_0$$

$$0 < p_0 < 1, L \leq U$$

$$L, U \in \{-n, -n+2, \ldots, n-2, 2\}$$

where α_0 is a pre-defined constant. Note that the above model can be simplified by letting p_0 takes only a discrete set of values; say $p_0 = \{0.1, 0.15, \ldots, 0.95\}$. This discretization is justified by the fact that, in practice, only easy-to-manage values of p_0 are meant to be used (for instance, $p_0 = 0.5$ in the original definition of the sign statistic, as already remarked). As

a consequence, for the specification of the optimal values (p_0^*, L^*, U^*) the following procedure is utilised.

- ***step 1***: For a given value of n and $p_0 = \{0.1, 0.15, \ldots, 0.95\}$, find all the candidates (p_0, L, U) that satisfy the following condition:

$$D(p_0, L, U) = \frac{|\text{ARL}(p_0, L, U) - \text{ARL}_0|}{\text{ARL}_0} \leq \nu \tag{5.3}$$

  where ν is a fixed constant. Regarding the value of ν, it is up to practitioners to decide which will be the desired in-control ARL_0. In the following computations, in order to design the chart to be comparable with schemes with corresponding $\text{ARL}_0 \approx 370.4$ we set $\nu = 0.15$.

- ***step 2***: For a given shift, τ, among all the combinations of (p_0, L, U) , find the optimal one (p_0^*, L^*, U^*), that minimises the corresponding $ARL_1(\tau)$.

The above steps can be summarised as follows:

Algorithm 5.1 Computation of candidate combination of (p_0, L, U)

Define n and p_0.
$\text{ARL}_0 \leftarrow 370.4$.
$\text{ARL}^* \leftarrow \infty$.
for $L = -n, -n+2 \ldots, n-2, n$ **do**
  for $U = -n, -n+2 \ldots, n-2, n$ **do**
    compute and store $\text{ARL}(p_0, L, U)$
  end for
end for
exclude the ones where the condition in (5.3) does not hold

Algorithm 5.2 Computation of optimal combination of (p_0^*, L^*, U^*)

Define n, τ.
$\text{ARL}^* \leftarrow \infty$.
$p_0^* \leftarrow$Null.
$L^* \leftarrow$Null.
$U^* \leftarrow$Null.
for every candidate (p_0, L, U) **do**
  Compute the quantiles $X_{p_0/2}, X_{1-p_0/2}$ as:
  $X_{p_0/2} \leftarrow F_X(p_0/2|\sigma_0)$.
  $X_{1-p_0/2} \leftarrow F_X(1-p_0/2|\sigma_0)$.
  Compute $p_1 = 1 - F_X(X_{1-p_0/2}|\tau\sigma_0) + F_X(X_{p_0/2}|\tau\sigma_0)$.
  Compute $\text{ARL}(p_1, L, U)$.
  if $\text{ARL}(p_1, L, U) < \text{ARL}^*$ **then**
    $p_0^* \leftarrow p_0$.
    $L^* \leftarrow L$.
    $U^* \leftarrow U$.
  end if
end for

It should be clarified the fact that, for the optimization procedure presented in step 1, someone may argue that, regarding its potential computational cost, is not the optimal one. Nevertheless, even for a large value of n, following these steps, the computation of the ARL values is extremely fast, since at each iteration, only a simple probability needs to be computed. As a result, there is no need of investigating a more efficient procedure. Additionally, as it has been showed in Chapter 1, for nonparametric Shewhart charts, due to the discrete nature of the statistics to be monitored, is not always possible to be designed in order to satisfy that $\text{ARL}_0 \approx 370$ or even $\text{ARL}_0 \approx 500$. In particular, this is the main reason that the condition presented in (5.3) is being used; by setting $\nu = 0.15$ we are trying to be as consistent as possible in order to have $\text{ARL}_0 \approx 370$.

Effect of p_0

Before to proceed to any investigation of the chart's optimal performance a logical question arises: "Varying the value of p_0, does it really have a significant impact in the chart's

out-of-control performance?". In Table 5.2, for each Johnson-type distribution, three different cases are presented in which, for each case, the value of p_0 is different. In particular, for every distribution, and for $p_0 = \{0.15, 0.5, 0.7\}$ the corresponding in- and out-of-control RL properties are reported for $\tau = 0.25$ (large decrease), $\tau = 0.95$ (small decrease) and $\tau = 1.6$ (large increase) for $n = 45$. More specifically, in Table 5.2, for each type of distribution and shift magnitude τ, the corresponding pair of (L^*, U^*) is reported (first block) along with the pairs of $(\text{ARL}_1, \text{ARL}_0)$ (second block) and the pairs of (p_0, p_1) (third block). From the results presented in Table 5.2 we may conclude that the value of p_0 affects the chart's out-of-control performance. In particular, for $\tau = 0.25$ no significant differences exist. On the other hand, for $\tau = 0.95$, the choice of p_0 affects the results. For example in case #9, setting $p_0 = 0.15$, the optimal combination is $(L^*, U^*) = (-43, -17)$ giving a pair of $(\text{ARL}_1, \text{ARL}_0) = (408.37, 484.32)$. Similarly, for $p_0 = 0.5$ and $p_0 = 0.7$ we obtain $(L^*, U^*) = (-19, 19)$, $(\text{ARL}_1, \text{ARL}_0) = (268.97, 406.69)$ and $(L^*, U^*) = (1, 37)$, $(\text{ARL}_1, \text{ARL}_0) = (203.93, 389.75)$ respectively. As a consequence, for small decreases in the process variability ($\tau = 0.95$) setting $p_0 = 0.7$ gives better performance. Similarly, for $\tau = 1.6$, the smallest ARL_1 value is obtained by setting $p_0 = 0.15$. It should be noted that, taking as example case #9 when $\tau = 0.95$, the corresponding pairs of (p_0, ARL_0) are $(0.15, 484.32)$, $(0.5, 406.69)$ and $(0.4, 389.75)$. Strictly speaking, these ARL_0 values are relative close, but even so, not equal. So we may argue that, by comparing designs with different ARL_0 values, the theoretical comparisons in terms of the corresponding ARL_1's, might not be realistic. Nevertheless, in practice, varying the value of p_0, is an improvement in the design of the S-SD chart.

For the results presented in Table 5.1, a large value of the sample size was used $n = 45$ in order to maintain the in-control $\text{ARL}_0 \approx 370.4$. In general, as it has extensively mentioned in this work, the main disadvantage of Sign-type Shewhart schemes is that for small to moderate sample sizes it is not possible to find proper design parameters to satisfy $\text{ARL}_0 \approx 370$. For instance, in Table 5.1, the number of candidate vectors of (L, U, p_0), which satisfy the condition in (5.3) for $\nu = 0.2$, is presented for different values of n and p_0 when the desired $\text{ARL}_0 = 370$ or 512. As expected, for $n < 25$ it is not always possible to design the chart in order to satisfy $\text{ARL}_0 \approx 370$. Of course practitioners might search for a combination which will give $\text{ARL}_0 > 370.4$, but theoretically speaking, it will not be easy to optimally design it and compare it with other schemes.

Table 5.1: Number of vectors of (L, U, p_0), which satisfy the condition in (5.3) for 370.4,$\nu =$ 0.2 and different values of n and p_0

Desired $\text{ARL}_0 = 370$

n	$p_0 = 0.05$	$p_0 = 0.10$	$p_0 = 0.15$	$p_0 = 0.20$	$p_0 = 0.25$	$p_0 = 0.30$	$p_0 = 0.35$	$p_0 = 0.40$	$p_0 = 0.45$	$p_0 = 0.50$	$p_0 = 0.55$	$p_0 = 0.60$	$p_0 = 0.65$	$p_0 = 0.70$	$p_0 = 0.75$	$p_0 = 0.80$	$p_0 = 0.85$	$p_0 = 0.90$	$p_0 = 0.95$
10	0	0	0	0	0	0	0	0	2	0	2	0	0	0	0	0	0	0	0
12	0	0	0	0	1	0	0	2	0	2	0	2	0	0	1	0	0	0	0
14	0	0	0	1	0	0	4	0	4	0	4	0	4	0	0	1	0	0	0
15	0	0	0	0	0	0	1	1	1	0	1	1	1	0	0	0	0	0	0
18	0	0	1	0	0	1	0	1	4	0	4	1	0	1	0	0	1	0	0
20	1	1	0	1	9	0	1	0	1	1	1	0	1	0	9	1	0	1	1
23	0	0	0	1	1	10	2	0	1	1	1	0	2	10	1	1	0	0	0
25	0	1	0	0	1	1	5	8	7	2	7	8	5	1	1	0	0	1	0
28	1	0	0	1	13	3	0	13	8	2	8	13	0	3	13	1	0	0	1
30	1	0	1	1	3	3	2	6	1	16	1	6	2	3	3	1	1	0	1
35	0	0	0	0	17	21	3	1	2	18	2	1	3	21	17	0	0	0	0
40	0	0	1	3	1	24	7	7	13	20	13	7	7	24	1	3	1	0	0
45	0	0	1	26	1	28	19	1	12	23	12	1	19	28	1	26	1	0	0

Desired $\text{ARL}_0 = 512$

n	$p_0 = 0.05$	$p_0 = 0.10$	$p_0 = 0.15$	$p_0 = 0.20$	$p_0 = 0.25$	$p_0 = 0.30$	$p_0 = 0.35$	$p_0 = 0.40$	$p_0 = 0.45$	$p_0 = 0.50$	$p_0 = 0.55$	$p_0 = 0.60$	$p_0 = 0.65$	$p_0 = 0.70$	$p_0 = 0.75$	$p_0 = 0.80$	$p_0 = 0.85$	$p_0 = 0.90$	$p_0 = 0.95$
10	0	1	0	0	0	0	0	1	0	1	0	1	0	0	0	0	0	1	0
12	1	0	0	0	0	1	0	2	1	0	1	2	0	1	0	0	0	0	1
14	0	0	1	1	1	1	3	0	2	1	2	0	3	1	1	1	1	0	0
15	0	1	0	0	0	0	1	2	3	0	3	2	1	0	0	0	0	1	0
18	0	0	0	0	0	7	1	0	0	0	0	0	1	7	0	0	0	0	0
20	0	1	0	0	0	1	7	2	1	0	1	2	7	1	0	0	0	1	0
23	0	0	0	0	0	2	0	1	0	0	0	1	0	2	0	0	0	0	0
25	0	1	1	0	1	4	9	8	11	10	11	8	9	4	1	0	1	1	0
28	1	0	0	16	0	0	1	0	1	14	1	0	1	0	0	16	0	0	1
30	0	1	0	1	15	16	13	2	1	0	1	2	13	16	15	1	0	1	0
35	0	1	0	2	2	17	7	6	12	1	12	6	7	17	2	2	0	1	0
40	0	0	1	1	3	3	2	15	1	1	1	15	2	3	3	1	1	0	0
45	0	0	2	3	2	3	1	9	2	2	2	9	1	3	2	3	2	0	0

Table 5.2: ARL_1 values for different fixed values of p_0 and $n = 45$ under the benchmark of the Johnson distributions for $\tau = \{0.25, 0.95, 1.6\}$ using $\nu = 0.15$.

	$p_0 = 0.15$			$p_0 = 0.5$			$p_0 = 0.7$		
	$\tau = 0.25$	$\tau = 0.95$	$\tau = 1.6$	$\tau = 0.25$	$\tau = 0.95$	$\tau = 1.6$	$\tau = 0.25$	$\tau = 0.95$	$\tau = 1.6$
1	(-43,-17) (1,424.32) (0.15,0)	(-43,-17) (159.38,424.32) (0.15,0.107)	(-43,-17) (1.02,424.32) (0.15,0.474)	(-19,19) (1,406.69) (0.5,0)	(-19,19) (242.39,406.69) (0.5,0.473)	(-19,19) (3.08,406.69) (0.5,0.69)	(-43,33) (1,389.22) (0.7,0)	(1,37) (196.68,389.75) (0.7,0.684)	(-3,33) (7.72,346.83) (0.7,0.813)
2	(-43,-17) (1,424.32) (0.15,0)	(-43,-17) (382.36,424.32) (0.15,0.126)	(-43,-17) (1.2,424.32) (0.15,0.393)	(-19,19) (1,406.69) (0.5,0)	(-19,19) (271.76,406.69) (0.5,0.477)	(-19,19) (3.82,406.69) (0.5,0.677)	(1,37) (1,389.75) (0.7,0.085)	(1,37) (203.22,389.75) (0.7,0.685)	(-3,33) (8.28,346.83) (0.7,0.81)
3	(-43,-17) (1,424.32) (0.15,0)	(-43,-17) (436.63,424.32) (0.15,0.13)	(-43,-17) (1.36,424.32) (0.15,0.368)	(-19,19) (1,406.69) (0.5,0.007)	(-19,19) (279.4,406.69) (0.5,0.478)	(-19,19) (4.07,406.69) (0.5,0.673)	(1,37) (1,389.75) (0.7,0.123)	(1,37) (205,389.75) (0.7,0.685)	(-3,33) (8.44,346.83) (0.7,0.81)
4	(-43,-17) (1,424.32) (0.15,0)	(-43,-17) (464.85,424.32) (0.15,0.132)	(-43,-17) (1.54,424.32) (0.15,0.351)	(-19,19) (1,406.69) (0.5,0.02)	(-19,19) (284.69,406.69) (0.5,0.478)	(-19,19) (4.27,406.69) (0.5,0.671)	(1,37) (1,389.75) (0.7,0.147)	(1,37) (206.28,389.75) (0.7,0.685)	(-3,33) (8.57,346.83) (0.7,0.809)
5	(-43,-17) (1.03,424.32) (0.15,0.001)	(-43,-17) (484.06,424.32) (0.15,0.134)	(-43,-17) (1.78,424.32) (0.15,0.334)	(-19,19) (1,406.69) (0.5,0.034)	(-19,19) (289.99,406.69) (0.5,0.479)	(-19,19) (4.5,406.69) (0.5,0.668)	(1,37) (1,389.75) (0.7,0.167)	(1,37) (207.63,389.75) (0.7,0.685)	(-3,33) (8.7,346.83) (0.7,0.809)
6	(-43,-17) (1.08,424.32) (0.15,0.002)	(-43,-17) (494.22,424.32) (0.15,0.135)	(-43,-17) (2.02,424.32) (0.15,0.323)	(-19,19) (1,406.69) (0.5,0.046)	(-19,19) (294.06,406.69) (0.5,0.479)	(-19,19) (4.69,406.69) (0.5,0.666)	(1,37) (1,389.75) (0.7,0.182)	(1,37) (208.71,389.75) (0.7,0.685)	(-3,33) (8.81,346.83) (0.7,0.808)
7	(-43,-17) (1,424.32) (0.15,0)	(-43,-17) (188.06,424.32) (0.15,0.11)	(-43,-17) (1.08,424.32) (0.15,0.428)	(-19,19) (1,406.69) (0.5,0.046)	(-19,19) (245.47,406.69) (0.5,0.473)	(-19,19) (3.56,406.69) (0.5,0.681)	(1,37) (1,389.75) (0.7,0.147)	(1,37) (197.33,389.75) (0.7,0.684)	(-3,33) (8.11,346.83) (0.7,0.811)
8	(-43,-17) (1.01,424.32) (0.15,0)	(-43,-17) (364.57,424.32) (0.15,0.125)	(-43,-17) (1.22,424.32) (0.15,0.389)	(-19,19) (1,406.69) (0.5,0.035)	(-19,19) (268.97,406.69) (0.5,0.476)	(-19,19) (3.9,406.69) (0.5,0.676)	(1,37) (1,389.75) (0.7,0.122)	(1,37) (202.56,389.75) (0.7,0.685)	(-3,33) (8.34,346.83) (0.7,0.81)
9	(-43,-17) (1.03,424.32) (0.15,0.001)	(-43,-17) (408.37,424.32) (0.15,0.128)	(-43,-17) (1.3,424.32) (0.15,0.376)	(-19,19) (1,406.69) (0.5,0.031)	(-19,19) (274.86,406.69) (0.5,0.477)	(-19,19) (4.02,406.69) (0.5,0.674)	(1,37) (1,389.75) (0.7,0.119)	(1,37) (203.93,389.75) (0.7,0.685)	(-3,33) (8.42,346.83) (0.7,0.81)
10	(-43,-17) (1.06,424.32) (0.15,0.001)	(-43,-17) (474.69,424.32) (0.15,0.133)	(-43,-17) (1.63,424.32) (0.15,0.344)	(-19,19) (1,406.69) (0.5,0.038)	(-19,19) (285.59,406.69) (0.5,0.478)	(-19,19) (4.36,406.69) (0.5,0.67)	(1,37) (1,389.75) (0.7,0.158)	(1,37) (206.4,389.75) (0.7,0.685)	(-3,33) (8.62,346.83) (0.7,0.809)
11	(-43,-17) (1.12,424.32) (0.15,0.003)	(-43,-17) (495.58,424.32) (0.15,0.135)	(-43,-17) (2.04,424.32) (0.15,0.322)	(-19,19) (1,406.69) (0.5,0.052)	(-19,19) (293.53,406.69) (0.5,0.479)	(-19,19) (4.69,406.69) (0.5,0.666)	(1,37) (1,389.75) (0.7,0.184)	(1,37) (208.47,389.75) (0.7,0.685)	(-3,33) (8.81,346.83) (0.7,0.808)
12	(-43,-17) (1.19,424.32) (0.15,0.004)	(-43,-17) (503.18,424.32) (0.15,0.136)	(-43,-17) (2.4,424.32) (0.15,0.309)	(-19,19) (1,406.69) (0.5,0.062)	(-19,19) (298.52,406.69) (0.5,0.48)	(-19,19) (4.94,406.69) (0.5,0.663)	(1,37) (1,389.75) (0.7,0.2)	(1,37) (209.89,389.75) (0.7,0.686)	(-3,33) (8.94,346.83) (0.7,0.808)
13	(-43,-17) (1.19,424.32) (0.15,0.004)	(-43,-17) (318.14,424.32) (0.15,0.121)	(-43,-17) (1.19,424.32) (0.15,0.395)	(-19,19) (1,406.69) (0.5,0.057)	(-19,19) (262.74,406.69) (0.5,0.476)	(-19,19) (3.88,406.69) (0.5,0.676)	(1,37) (1,389.75) (0.7,0.145)	(1,37) (201.14,389.75) (0.7,0.685)	(-3,33) (8.33,346.83) (0.7,0.81)
14	(-43,-17) (1.17,424.32) (0.15,0.003)	(-43,-17) (344.48,424.32) (0.15,0.123)	(-43,-17) (1.21,424.32) (0.15,0.39)	(-19,19) (1,406.69) (0.5,0.053)	(-19,19) (266,406.69) (0.5,0.476)	(-19,19) (3.92,406.69) (0.5,0.675)	(1,37) (1,389.75) (0.7,0.14)	(1,37) (201.89,389.75) (0.7,0.685)	(-3,33) (8.36,346.83) (0.7,0.81)
15	(-43,-17) (1.25,424.32) (0.15,0.005)	(-43,-17) (498.84,424.32) (0.15,0.136)	(-43,-17) (2.08,424.32) (0.15,0.32)	(-19,19) (1,406.69) (0.5,0.064)	(-19,19) (291.85,406.69) (0.5,0.479)	(-19,19) (4.68,406.69) (0.5,0.666)	(1,37) (1,389.75) (0.7,0.188)	(1,37) (207.73,389.75) (0.7,0.685)	(-3,33) (8.8,346.83) (0.7,0.808)
16	(-43,-17) (1.38,424.32) (0.15,0.007)	(-43,-17) (508.78,424.32) (0.15,0.138)	(-43,-17) (2.9,424.32) (0.15,0.296)	(-19,19) (1,406.69) (0.5,0.079)	(-19,19) (302.41,406.69) (0.5,0.481)	(-19,19) (5.19,406.69) (0.5,0.661)	(1,37) (1,389.75) (0.7,0.216)	(1,37) (210.82,389.75) (0.7,0.686)	(-3,33) (9.07,346.83) (0.7,0.807)
17	(-43,-17) (1.5,424.32) (0.15,0.009)	(-43,-17) (511.12,424.32) (0.15,0.138)	(-43,-17) (3.48,424.32) (0.15,0.286)	(-19,19) (1,406.69) (0.5,0.089)	(-19,19) (307.77,406.69) (0.5,0.481)	(-19,19) (5.52,406.69) (0.5,0.658)	(1,37) (1,389.75) (0.7,0.23)	(1,37) (212.56,389.75) (0.7,0.686)	(-3,33) (9.24,346.83) (0.7,0.806)

Optimal parameters and out-of-control performance

With respect to the findings mentioned above, in Tables 5.3 and 5.4 the optimal design of the D-SN chart is presented under the benchmark of the 17 Johnson distributions for $n = 20$ and $n = 30$ respectively. In particular, for each distribution, the step presented in

Algorithms 5.1 and 5.2 will be followed. Regarding the decision rule presented in (5.3) we set $\nu = 0.05$. The criterion for choosing this value, yields to the fact that we are interested to optimise the chart in order to be comparable with other schemes with $\text{ARL}_0 \approx 370$. From the results presented in Tables 5.3 and 5.4 we may conclude that:

- For a large increase ($\tau \approx 2$) or a large decrease ($\tau \approx 0.25$) the corresponding ARL_1 values of the D-SN chart are really close to 1. Theoreticaly speaking, this was an expected result, since for large shifts and large sample sizes we expect that the ARL_1 values to be close to 1. As $\tau \to 0$ the ARL_1 values tend to increase. Note that, this is also an expected result, due to the fact Shewhart schemes (parametric or not) are not preferable for detecting small shifts.

- Regarding the optimal p_0^* it can be clearly seen that it varies depending on the shift magnitude τ. In particular, large values of p_0 are preferable for small values of τ; as $\tau \to 1$ the optimal p_0^* tends to decrease. For example for case #17 (Table 5.3), for $\tau < 1$ the optimal value $p_0^* = \{0.5, 0.8\}$ while for $\tau > 1$ the optimal $p_0^* = 0.2$.

Table 5.3: Out-of-control performance for the S-SD chart along with the corresponding optimal parameters for $n = 20$

case	$\tau = 0.25$	$\tau = 0.5$	$\tau = 0.75$	$\tau = 0.95$	$\tau = 1.25$	$\tau = 1.5$	$\tau = 1.75$	$\tau = 1.95$	$\tau = 2.0$
	(-12,12)	(-12,12)	(-12,12)	(2,20)	(-20,-2)	(-20,-2)	(-20,-2)	(-20,-2)	(-20,-2)
	(1,388.07)	(1,388.07)	(15.14,388.07)	(258.39,385.38)	(6.68,385.38)	(2.05,385.38)	(1.34,385.38)	(1.19,385.38)	(1.13,385.38)
1	(0.5,0.183)	(0.5,0.598)	(0.5,0.733)	(0.8,0.789)	(0.2,0.84)	(0.2,0.867)	(0.2,0.886)	(0.2,0.895)	(0.2,0.9)
	(-12,12)	(-12,12)	(-12,12)	(2,20)	(-20,-2)	(-20,-2)	(-20,-2)	(-20,-2)	(-20,-2)
	(1,388.07)	(1.55,388.07)	(27.87,388.07)	(260.53,385.38)	(14.58,385.38)	(3.6,385.38)	(1.88,385.38)	(1.52,385.38)	(1.37,385.38)
2	(0.5,0.29)	(0.5,0.609)	(0.5,0.735)	(0.8,0.79)	(0.2,0.84)	(0.2,0.866)	(0.2,0.885)	(0.2,0.894)	(0.2,0.899)
	(-12,12)	(-12,12)	(-12,12)	(2,20)	(-20,-2)	(-20,-2)	(-20,-2)	(-20,-2)	(-20,-2)
	(1,388.07)	(1.94,388.07)	(32.32,388.07)	(261.11,385.38)	(18.67,385.38)	(4.46,385.38)	(2.18,385.38)	(1.7,385.38)	(1.51,385.38)
3	(0.5,0.311)	(0.5,0.612)	(0.5,0.736)	(0.8,0.79)	(0.2,0.839)	(0.2,0.866)	(0.2,0.885)	(0.2,0.894)	(0.2,0.899)
	(-12,12)	(-12,12)	(-12,12)	(2,20)	(-20,-2)	(-20,-2)	(-20,-2)	(-20,-2)	(-20,-2)
	(1,388.07)	(2.28,388.07)	(35.72,388.07)	(261.53,385.38)	(22.2,385.38)	(5.25,385.38)	(2.46,385.38)	(1.87,385.38)	(1.64,385.38)
4	(0.5,0.324)	(0.5,0.614)	(0.5,0.736)	(0.8,0.79)	(0.2,0.839)	(0.2,0.866)	(0.2,0.885)	(0.2,0.894)	(0.2,0.899)
	(-12,12)	(-12,12)	(-12,12)	(2,20)	(-20,-2)	(-20,-2)	(-20,-2)	(-20,-2)	(-20,-2)
	(1,388.07)	(2.67,388.07)	(39.38,388.07)	(261.98,385.38)	(26.22,385.38)	(6.22,385.38)	(2.81,385.38)	(2.09,385.38)	(1.8,385.38)
5	(0.5,0.337)	(0.5,0.617)	(0.5,0.736)	(0.8,0.79)	(0.2,0.839)	(0.2,0.866)	(0.2,0.885)	(0.2,0.894)	(0.2,0.899)
	(-12,12)	(-12,12)	(-12,12)	(2,20)	(-20,-2)	(-20,-2)	(-20,-2)	(-20,-2)	(-20,-2)
	(1.01,388.07)	(3.01,388.07)	(42.37,388.07)	(262.34,385.38)	(29.6,385.38)	(7.09,385.38)	(3.14,385.38)	(2.29,385.38)	(1.95,385.38)
6	(0.5,0.347)	(0.5,0.618)	(0.5,0.737)	(0.8,0.79)	(0.2,0.839)	(0.2,0.865)	(0.2,0.884)	(0.2,0.893)	(0.2,0.899)
	(2,20)	(-12,12)	(-12,12)	(2,20)	(-20,-2)	(-20,-2)	(-20,-2)	(-20,-2)	(-20,-2)
	(1,385.38)	(1.44,388.07)	(13.99,388.07)	(258.6,385.38)	(8.66,385.38)	(2.69,385.38)	(1.65,385.38)	(1.41,385.38)	(1.31,385.38)
7	(0.8,0.226)	(0.5,0.59)	(0.5,0.733)	(0.8,0.789)	(0.2,0.84)	(0.2,0.866)	(0.2,0.885)	(0.2,0.894)	(0.2,0.899)
	(-12,12)	(-12,12)	(-12,12)	(2,20)	(-20,-2)	(-20,-2)	(-20,-2)	(-20,-2)	(-20,-2)
	(1,388.07)	(1.47,388.07)	(25.51,388.07)	(260.31,385.38)	(14.21,385.38)	(3.69,385.38)	(1.97,385.38)	(1.59,385.38)	(1.44,385.38)
8	(0.5,0.263)	(0.5,0.606)	(0.5,0.735)	(0.8,0.79)	(0.2,0.84)	(0.2,0.866)	(0.2,0.885)	(0.2,0.894)	(0.2,0.899)
	(-12,12)	(-12,12)	(-12,12)	(2,20)	(-20,-2)	(-20,-2)	(-20,-2)	(-20,-2)	(-20,-2)
	(1,388.07)	(1.7,388.07)	(29.09,388.07)	(260.77,385.38)	(16.64,385.38)	(4.14,385.38)	(2.11,385.38)	(1.67,385.38)	(1.49,385.38)
9	(0.5,0.289)	(0.5,0.609)	(0.5,0.735)	(0.8,0.79)	(0.2,0.839)	(0.2,0.866)	(0.2,0.885)	(0.2,0.894)	(0.2,0.899)
	(-12,12)	(-12,12)	(-12,12)	(2,20)	(-20,-2)	(-20,-2)	(-20,-2)	(-20,-2)	(-20,-2)
	(1.01,388.07)	(2.41,388.07)	(36.24,388.07)	(261.56,385.38)	(23.57,385.38)	(5.6,385.38)	(2.61,385.38)	(1.97,385.38)	(1.72,385.38)
10	(0.5,0.324)	(0.5,0.614)	(0.5,0.736)	(0.8,0.79)	(0.2,0.839)	(0.2,0.866)	(0.2,0.885)	(0.2,0.894)	(0.2,0.899)
	(-12,12)	(-12,12)	(-12,12)	(2,20)	(-20,-2)	(-20,-2)	(-20,-2)	(-20,-2)	(-20,-2)
	(1.02,388.07)	(3.02,388.07)	(42,388.07)	(262.25,385.38)	(29.75,385.38)	(7.13,385.38)	(3.16,385.38)	(2.31,385.38)	(1.97,385.38)
11	(0.5,0.344)	(0.5,0.618)	(0.5,0.737)	(0.8,0.79)	(0.2,0.839)	(0.2,0.865)	(0.2,0.884)	(0.2,0.893)	(0.2,0.899)
	(-12,12)	(-12,12)	(-12,12)	(2,20)	(-20,-2)	(-20,-2)	(-20,-2)	(-20,-2)	(-20,-2)
	(1.03,388.07)	(3.47,388.07)	(45.91,388.07)	(262.73,385.38)	(34.11,385.38)	(8.33,385.38)	(3.61,385.38)	(2.59,385.38)	(2.18,385.38)
12	(0.5,0.356)	(0.5,0.62)	(0.5,0.737)	(0.8,0.79)	(0.2,0.839)	(0.2,0.865)	(0.2,0.884)	(0.2,0.893)	(0.2,0.899)
	(2,20)	(-12,12)	(-12,12)	(2,20)	(-20,-2)	(-20,-2)	(-20,-2)	(-20,-2)	(-20,-2)
	(1,385.38)	(1.45,388.07)	(21.64,388.07)	(259.85,385.38)	(12.62,385.38)	(3.49,385.38)	(1.94,385.38)	(1.59,385.38)	(1.45,385.38)
13	(0.8,0.232)	(0.5,0.601)	(0.5,0.734)	(0.8,0.79)	(0.2,0.84)	(0.2,0.866)	(0.2,0.885)	(0.2,0.894)	(0.2,0.899)
	(2,20)	(-12,12)	(-12,12)	(2,20)	(-20,-2)	(-20,-2)	(-20,-2)	(-20,-2)	(-20,-2)
	(1,385.38)	(1.45,388.07)	(23.48,388.07)	(260.1,385.38)	(13.56,385.38)	(3.65,385.38)	(1.99,385.38)	(1.62,385.38)	(1.46,385.38)
14	(0.8,0.245)	(0.5,0.603)	(0.5,0.734)	(0.8,0.79)	(0.2,0.84)	(0.2,0.866)	(0.2,0.885)	(0.2,0.894)	(0.2,0.899)
	(-12,12)	(-12,12)	(-12,12)	(2,20)	(-20,-2)	(-20,-2)	(-20,-2)	(-20,-2)	(-20,-2)
	(1.04,388.07)	(3.05,388.07)	(40.91,388.07)	(261.97,385.38)	(30.06,385.38)	(7.18,385.38)	(3.18,385.38)	(2.33,385.38)	(1.99,385.38)
15	(0.5,0.339)	(0.5,0.615)	(0.5,0.736)	(0.8,0.79)	(0.2,0.839)	(0.2,0.865)	(0.2,0.884)	(0.2,0.893)	(0.2,0.899)
	(-12,12)	(-12,12)	(-12,12)	(2,20)	(-20,-2)	(-20,-2)	(-20,-2)	(-20,-2)	(-20,-2)
	(1.07,388.07)	(3.98,388.07)	(49.3,388.07)	(263.02,385.38)	(39.05,385.38)	(9.75,385.38)	(4.15,385.38)	(2.94,385.38)	(2.45,385.38)
16	(0.5,0.364)	(0.5,0.621)	(0.5,0.737)	(0.8,0.79)	(0.2,0.839)	(0.2,0.865)	(0.2,0.884)	(0.2,0.893)	(0.2,0.898)
	(2,20)	(-12,12)	(2,20)	(2,20)	(-20,-2)	(-20,-2)	(-20,-2)	(-20,-2)	(-20,-2)
	(1.09,385.38)	(4.57,388.07)	(51.46,385.38)	(263.63,385.38)	(44.16,385.38)	(11.41,385.38)	(4.82,385.38)	(3.36,385.38)	(2.77,385.38)
17	(0.8,0.376)	(0.5,0.624)	(0.8,0.738)	(0.8,0.79)	(0.2,0.839)	(0.2,0.865)	(0.2,0.884)	(0.2,0.893)	(0.2,0.898)

Table 5.4: Out-of-control performance for the S-SD chart along with the corresponding optimal parameters for $n = 30$

case	$\tau = 0.25$	$\tau = 0.5$	$\tau = 0.75$	$\tau = 0.95$	$\tau = 1.25$	$\tau = 1.5$	$\tau = 1.75$	$\tau = 1.95$	$\tau = 2.0$
	(-26,0)	(-26,0)	(-26,0)	(-26,0)	(-30,-2)	(-30,-2)	(-30,-2)	(-30,-2)	(-30,-2)
	(1,359.27)	(1,359.27)	(1.12,359.27)	(128.82,359.27)	(5.38,363.7)	(1.68,363.7)	(1.18,363.7)	(1.08,363.7)	(1.05,363.7)
1	(0.25,0.009)	(0.25,0.496)	(0.25,0.666)	(0.25,0.737)	(0.25,0.8)	(0.25,0.834)	(0.25,0.857)	(0.25,0.869)	(0.25,0.875)
	(-26,0)	(-26,0)	(-26,0)	(-14,18)	(-30,-2)	(-30,-2)	(-30,-2)	(-30,-2)	(-30,-2)
	(1,359.27)	(1.01,359.27)	(6.56,359.27)	(179.68,360.5)	(10.52,363.7)	(2.59,363.7)	(1.46,363.7)	(1.24,363.7)	(1.16,363.7)
2	(0.25,0.171)	(0.25,0.518)	(0.25,0.67)	(0.5,0.737)	(0.25,0.799)	(0.25,0.832)	(0.25,0.856)	(0.25,0.867)	(0.25,0.874)
	(-14,18)	(-24,4)	(-24,4)	(-14,18)	(-30,-2)	(-30,-2)	(-30,-2)	(-30,-2)	(-30,-2)
	(1,360.5)	(1.12,365.04)	(9.81,365.04)	(184.81,360.5)	(12.97,363.7)	(3.06,363.7)	(1.62,363.7)	(1.33,363.7)	(1.22,363.7)
3	(0.5,0.202)	(0.3,0.524)	(0.3,0.671)	(0.5,0.737)	(0.25,0.799)	(0.25,0.832)	(0.25,0.856)	(0.25,0.867)	(0.25,0.873)
	(-14,18)	(-14,18)	(-24,4)	(-14,18)	(-30,-2)	(-30,-2)	(-30,-2)	(-30,-2)	(-30,-2)
	(1,360.5)	(1.27,360.5)	(12.45,365.04)	(188.43,360.5)	(15.07,363.7)	(3.47,363.7)	(1.75,363.7)	(1.41,363.7)	(1.28,363.7)
4	(0.5,0.222)	(0.5,0.528)	(0.3,0.672)	(0.5,0.737)	(0.25,0.799)	(0.25,0.831)	(0.25,0.855)	(0.25,0.867)	(0.25,0.873)
	(-14,18)	(-14,18)	(-14,18)	(-14,18)	(-30,-2)	(-30,-2)	(-30,-2)	(-30,-2)	(-30,-2)
	(1,360.5)	(1.39,360.5)	(14.17,360.5)	(192.12,360.5)	(17.46,363.7)	(3.97,363.7)	(1.92,363.7)	(1.51,363.7)	(1.35,363.7)
5	(0.5,0.24)	(0.5,0.532)	(0.5,0.672)	(0.5,0.737)	(0.25,0.798)	(0.25,0.831)	(0.25,0.855)	(0.25,0.866)	(0.25,0.873)
	(-14,18)	(-14,18)	(-14,18)	(-14,18)	(-30,-2)	(-30,-2)	(-30,-2)	(-30,-2)	(-30,-2)
	(1,360.5)	(1.49,360.5)	(15.28,360.5)	(195,360.5)	(19.5,363.7)	(4.41,363.7)	(2.07,363.7)	(1.6,363.7)	(1.42,363.7)
6	(0.5,0.253)	(0.5,0.535)	(0.5,0.673)	(0.5,0.738)	(0.25,0.798)	(0.25,0.831)	(0.25,0.855)	(0.25,0.866)	(0.25,0.873)
	(-26,0)	(-14,18)	(-24,4)	(-26,0)	(-30,-2)	(-30,-2)	(-30,-2)	(-30,-2)	(-30,-2)
	(1,359.27)	(1.05,360.5)	(2.71,365.04)	(136.37,359.27)	(6.79,363.7)	(2.09,363.7)	(1.35,363.7)	(1.2,363.7)	(1.14,363.7)
7	(0.25,0.183)	(0.5,0.48)	(0.3,0.665)	(0.25,0.737)	(0.25,0.8)	(0.25,0.833)	(0.25,0.856)	(0.25,0.867)	(0.25,0.874)
	(2,30)	(-14,18)	(-24,4)	(-14,18)	(-30,-2)	(-30,-2)	(-30,-2)	(-30,-2)	(-30,-2)
	(1,363.7)	(1.06,360.5)	(5.97,365.04)	(177.84,360.5)	(10.35,363.7)	(2.66,363.7)	(1.51,363.7)	(1.28,363.7)	(1.19,363.7)
8	(0.75,0.164)	(0.5,0.512)	(0.3,0.669)	(0.5,0.737)	(0.25,0.799)	(0.25,0.832)	(0.25,0.856)	(0.25,0.867)	(0.25,0.874)
	(-14,18)	(-14,18)	(-24,4)	(-14,18)	(-30,-2)	(-30,-2)	(-30,-2)	(-30,-2)	(-30,-2)
	(1,360.5)	(1.11,360.5)	(7.96,365.04)	(181.75,360.5)	(11.81,363.7)	(2.9,363.7)	(1.58,363.7)	(1.32,363.7)	(1.22,363.7)
9	(0.5,0.182)	(0.5,0.518)	(0.3,0.67)	(0.5,0.737)	(0.25,0.799)	(0.25,0.832)	(0.25,0.856)	(0.25,0.867)	(0.25,0.873)
	(-14,18)	(-14,18)	(-14,18)	(-14,18)	(-30,-2)	(-30,-2)	(-30,-2)	(-30,-2)	(-30,-2)
	(1,360.5)	(1.31,360.5)	(13.01,360.5)	(189.05,360.5)	(15.83,363.7)	(3.65,363.7)	(1.82,363.7)	(1.46,363.7)	(1.32,363.7)
10	(0.5,0.226)	(0.5,0.527)	(0.5,0.672)	(0.5,0.737)	(0.25,0.799)	(0.25,0.831)	(0.25,0.855)	(0.25,0.866)	(0.25,0.873)
	(-14,18)	(-14,18)	(-14,18)	(-14,18)	(-30,-2)	(-30,-2)	(-30,-2)	(-30,-2)	(-30,-2)
	(1,360.5)	(1.49,360.5)	(15.14,360.5)	(194.63,360.5)	(19.52,363.7)	(4.42,363.7)	(2.08,363.7)	(1.61,363.7)	(1.43,363.7)
11	(0.5,0.252)	(0.5,0.533)	(0.5,0.673)	(0.5,0.738)	(0.25,0.798)	(0.25,0.831)	(0.25,0.855)	(0.25,0.866)	(0.25,0.873)
	(-14,18)	(-14,18)	(-14,18)	(-14,18)	(-30,-2)	(-30,-2)	(-30,-2)	(-30,-2)	(-30,-2)
	(1,360.5)	(1.63,360.5)	(16.61,360.5)	(198.22,360.5)	(22.2,363.7)	(5.04,363.7)	(2.29,363.7)	(1.74,363.7)	(1.52,363.7)
12	(0.5,0.267)	(0.5,0.537)	(0.5,0.674)	(0.5,0.738)	(0.25,0.798)	(0.25,0.831)	(0.25,0.854)	(0.25,0.866)	(0.25,0.872)
	(2,30)	(-14,18)	(-24,4)	(-24,4)	(-30,-2)	(-30,-2)	(-30,-2)	(-30,-2)	(-30,-2)
	(1,363.7)	(1.06,360.5)	(4.49,365.04)	(170.9,365.04)	(9.39,363.7)	(2.56,363.7)	(1.51,363.7)	(1.29,363.7)	(1.2,363.7)
13	(0.75,0.18)	(0.5,0.502)	(0.3,0.668)	(0.3,0.737)	(0.25,0.799)	(0.25,0.832)	(0.25,0.856)	(0.25,0.867)	(0.25,0.873)
	(2,30)	(-14,18)	(-24,4)	(-14,18)	(-30,-2)	(-30,-2)	(-30,-2)	(-30,-2)	(-30,-2)
	(1,363.7)	(1.06,360.5)	(5.26,365.04)	(175.89,360.5)	(9.97,363.7)	(2.64,363.7)	(1.53,363.7)	(1.3,363.7)	(1.21,363.7)
14	(0.75,0.175)	(0.5,0.507)	(0.3,0.669)	(0.5,0.737)	(0.25,0.799)	(0.25,0.832)	(0.25,0.856)	(0.25,0.867)	(0.25,0.873)
	(-14,18)	(-14,18)	(-14,18)	(-14,18)	(-30,-2)	(-30,-2)	(-30,-2)	(-30,-2)	(-30,-2)
	(1,360.5)	(1.5,360.5)	(14.73,360.5)	(193.43,360.5)	(19.49,363.7)	(4.42,363.7)	(2.09,363.7)	(1.62,363.7)	(1.44,363.7)
15	(0.5,0.251)	(0.5,0.53)	(0.5,0.672)	(0.5,0.737)	(0.25,0.798)	(0.25,0.831)	(0.25,0.855)	(0.25,0.866)	(0.25,0.872)
	(-14,18)	(-14,18)	(-14,18)	(-14,18)	(-30,-2)	(-30,-2)	(-30,-2)	(-30,-2)	(-30,-2)
	(1,360.5)	(1.8,360.5)	(17.89,360.5)	(201.06,360.5)	(25.1,363.7)	(5.73,363.7)	(2.54,363.7)	(1.89,363.7)	(1.63,363.7)
16	(0.5,0.279)	(0.5,0.54)	(0.5,0.674)	(0.5,0.738)	(0.25,0.798)	(0.25,0.83)	(0.25,0.854)	(0.25,0.865)	(0.25,0.872)
	(-14,18)	(-14,18)	(-14,18)	(-14,18)	(-30,-2)	(-30,-2)	(-30,-2)	(-30,-2)	(-30,-2)
	(1,360.5)	(1.99,360.5)	(19.7,360.5)	(205.06,360.5)	(28.42,363.7)	(6.6,363.7)	(2.86,363.7)	(2.08,363.7)	(1.78,363.7)
17	(0.5,0.293)	(0.5,0.544)	(0.5,0.675)	(0.5,0.738)	(0.25,0.797)	(0.25,0.83)	(0.25,0.854)	(0.25,0.865)	(0.25,0.872)

5.3 The two-sided D-SN-C EWMA chart for dispersion (The "continuousified" approach)

In the previous Chapters, the design of a modified EWMA chart based on the Sign statistic, with and without the presence of tied observations, was presented, using the "continuousify" method. Motivated by the efficiency and the robust design of this chart, in this Section a modified version of this scheme is presented (entitled as the D-SN-C EWMA chart) capable of monitoring shifts in the process variability.

Regarding the charting statistic of the proposed two-sided D-SN-C EWMA chart, it will be simply defined as:

$$Z_t^* = \lambda \mathrm{SD}_t^* + (1-\lambda) Z_{t-1}^*, Z_0^* = \mathrm{E}_0(\mathrm{SD}_t^*). \tag{5.4}$$

Practically speaking, the distribution of SD_t^* is exactly the same with the one of SN_t^* as presented in Chapter 3. The only difference is that the probability of "success ", p_{+1}, is now accounted for shifts in the process variability as defined in Section 5.1. The reason that the definition and notation for the testing statistics, SD_t^*, SN_t^* are different, is to avoid causing any confusions to the readers. Moreover, similarly with the median case, the p.d.f. $f_{\mathrm{SD}_t^*}(s|n,p)$ and c.d.f. $F_{\mathrm{SD}_t^*}(s|n,p)$ of SD_t^* will be defined for $s \in \mathbb{R}$ and they are equal to

$$f_{\mathrm{SD}_t^*}(s|n,p) = \sum_{\psi \in \Psi} f_{\mathrm{Bin}}\left(\frac{\psi+n}{2}|n,p\right) f_{\mathrm{N}}(s|\psi,h), \tag{5.5}$$

$$F_{\mathrm{SD}_t^*}(s|n,p) = \sum_{\psi \in \Psi} f_{\mathrm{Bin}}\left(\frac{\psi+n}{2}|n,p\right) F_{\mathrm{N}}(s|\psi,h). \tag{5.6}$$

As for the computation of the mean and the variance of SD_t^*, we also have:

$$\mathrm{E}(\mathrm{SD}_t^*) = \mathrm{E}(\mathrm{SD}_t), \tag{5.7}$$

$$\mathrm{V}(\mathrm{SD}_t^*) = \mathrm{V}(\mathrm{SD}_t) + h^2. \tag{5.8}$$

Lastly, the control limits, are defined as:

$$\begin{aligned} \mathrm{LCL} &= \mathrm{E}_0(\mathrm{SD}_t) - K\sqrt{\mathrm{V}_0(\mathrm{SD}_t)} \times \sqrt{\frac{\lambda}{2-\lambda}}, \\ \mathrm{UCL} &= \mathrm{E}_0(\mathrm{SD}_t) + K\sqrt{\mathrm{V}_0(\mathrm{SD}_t)} \times \sqrt{\frac{\lambda}{2-\lambda}}. \end{aligned} \tag{5.9}$$

When the process is in-control, the above expressions can be rewritten as:

$$\mathrm{LCL}^* = n(2p_0 - 1) - K\sqrt{\frac{\lambda(4np_0(1-p_0) + h^2)}{2-\lambda}}, \tag{5.10}$$

$$\mathrm{UCL}^* = n(2p_0 - 1) + K\sqrt{\frac{\lambda(4np_0(1-p_0) + h^2)}{2-\lambda}}. \tag{5.11}$$

5.3.1 Optimization of the D-SN-C EWMA chart

The out-of-control performance of our proposed chart will be examined under the benchmark of the 17 Johnson's type distributions listed in Table 4.3, for different sample sizes and shifts in the process variability. More specifically, regarding the optimization procedure, for each distribution, the following simple steps have been followed.

- *Step 1*: For $p_0 = \{0.05, 0.1, 0.15, \ldots, 0.9\}$ and $\lambda = \{0.05, 0.1, \ldots, 0.95\}$ the corresponding value for K is obtained for $2m + 1 = 151$ in order to satisfy a desired in-control ARL equal to $\mathrm{ARL}_0 = 370.4$. Note that, the number $2m + 1 = 151$ has been chosen in order to not be too large but large enough to guarantee the stability of the results. Of course, practitioners can also set any value for $2m + 1 > 151$. It should be noted that, the ARL and SDRL values are computed by using the exact same procedure as in the 2-C SN EWMA chart, with the only difference that the transient probabilities will be computed by using the distribution of SD_t as presented in 5.3.

- *Step 2*: Among all the combinations of (p_0, λ, K), for a given shift τ, the optimal set (p_0^*, λ^*, K^*) is chosen which gives the smallest out-of-control ARL at a specific shift τ.

In Tables 5.5 and 5.6 the optimal combinations of (λ^*, K^*) (first line of each block) are presented, along with the corresponding out-of-control ARL values (second line) and the corresponding pairs of (p_0^*, p_1) (third line) for $n = 10$ (Table 5.5) and $n = 20$ (Table 5.6). It should be clarified that p_0^* defines the suggested quantiles for the test for dispersion for a specific value of τ. Also, it is related to the in-control case (i.e. when $p = p_0^*$ we are referring to an in-control process while when, $p \neq p_0^*$ the process is out-of-control). For example, from the first six symmetric distributions we may see that:

- For large decreases in the process variability (e.g., $\tau = 0.25$), it can be seen that, for $p_0^* > 0.6$, the corresponding out-of-control ARL values are $\mathrm{ARL}_1 \approx 1$. On the other hand, for a large increase ($\tau = 2$), small values for p_0^* are preferable. For instance, from Table 5.5 it can be seen that, when $\tau = 0.25$, the optimal value of p_0 is $p_0^* \geq 0.7$. On the other hand, $p_0^* = 0.1$ for large increases (i.e. $\tau = 2$).

- For moderate decreases in the variability (such as $\tau = 0.5$ or 0.75), from Table 5.5 we may see that p_0^* takes values between 0.3 and 0.6. On the other hand, for moderate

increases in the variability ($\tau = 1.5$ or 1.75), the optimal value of p_0 is $p_0^* \leq 0.2$ for all the cases.

- Finally, for small decreases (such as $\tau = 0.95$) or increases ($\tau = 1.25$) the optimal value of p_0 ranges from 0.05 to 0.25.
- From Table 5.6 we may see that all the above statements are also valid for $n = 20$.

In addition, for the remaining cases (heavy-skewed distributions) similar conclusions are made. In particular,

- For large decrease in the process variance a value for the optimal $p_0^* = \{0.75, 0.55\}$, is suggested.
- For moderate decreases in the variability (such as $\tau = 0.5$ or 0.75), from Table 5.5 setting $p_0^* \approx 0.5$ or $p_0^* \approx 0.35$ respectively.
- For small decreases (such as $\tau = 0.95$) or increases ($\tau = 1.25$) the optimal p_0^* could take values from 0.15 to 0.2.

As a consequence, it can be concluded that as the value of τ increases then p_0^* decreases.

Table 5.5: Out-of-control performance for the proposed chart along with the corresponding optimal parameters for $n = 10$

case	$\tau = 0.25$	$\tau = 0.5$	$\tau = 0.75$	$\tau = 0.95$	$\tau = 1.25$	$\tau = 1.5$	$\tau = 1.75$	$\tau = 1.95$	$\tau = 2.0$
	(0.75,2.845)	(0.75,2.845)	(0.3,2.908)	(0.05,2.478)	(0.3,3.349)	(0.3,3.349)	(0.35,3.434)	(0.8,3.755)	(0.8,3.755)
	1	1.12	4.26	27.22	2.88	1.61	1.27	1.15	1.13
#1	(0.5,0)	(0.5,0.0130)	(0.25,0.018)	(0.05,0.014)	(0.05,0.233)	(0.05,0.364)	(0.05,0.457)	(0.05,0.514)	(0.05,0.526)
	(0.75,2.845)	(0.65,2.867)	(0.15,2.791)	(0.05,2.481)	(0.15,2.93)	(0.3,3.349)	(0.3,3.349)	(0.3,3.349)	(0.3,3.349)
	1	2.66	9.11	106.13	7.11	2.92	1.93	1.59	1.53
#2	(0.5,0)	(0.5,0.150)	(0.25,0.107)	(0.15,0.125)	(0.05,0.139)	(0.05,0.231)	(0.05,0.313)	(0.05,0.369)	(0.05,0.382)
	(0.65,2.88)	(0.4,2.89)	(0.1,2.691)	(0.05,2.483)	(0.1,2.722)	(0.25,3.244)	(0.3,3.349)	(0.3,3.349)	(0.3,3.349)
	1.05	3.07	10.99	131.57	10.33	3.97	2.43	1.92	1.83
#3	(0.6,0.0359)	(0.5,0.177)	(0.3,0.167)	(0.25,0.22)	(0.05,0.116)	(0.05,0.191)	(0.05,0.262)	(0.05,0.314)	(0.05,0.327)
	(0.7,2.876)	(0.4,2.89)	(0.1,2.695)	(0.05,2.49)	(0.15,2.829)	(0.2,2.929)	(0.3,3.349)	(0.3,3.349)	(0.3,3.349)
	1.11	3.34	12.22	145.23	12.77	5.01	2.97	2.27	2.15
#4	(0.6,0.057)	(0.5,0.193)	(0.35,0.221)	(0.3,0.27)	(0.1,0.176)	(0.1,0.252)	(0.05,0.228)	(0.05,0.276)	(0.05,0.287)
	(0.65,2.88)	(0.4,2.89)	(0.1,2.695)	(0.05,2.486)	(0.1,2.697)	(0.2,2.929)	(0.4,3.239)	(0.4,3.239)	(0.4,3.239)
	1.19	3.62	13.44	156.8	15.23	5.86	3.51	2.64	2.49
#5	(0.6,0.078)	(0.5,0.208)	(0.35,0.229)	(0.35,0.327)	(0.15,0.231)	(0.1,0.235)	(0.1,0.299)	(0.1,0.345)	(0.1,0.356)
	(0.7,2.876)	(0.35,2.889)	(0.1,2.689)	(0.05,2.486)	(0.1,2.697)	(0.2,2.88)	(0.4,3.096)	(0.4,3.239)	(0.4,3.239)
	1.25	3.81	14.3	164.51	16.93	6.47	3.92	2.93	2.75
#6	(0.6,0.092)	(0.55,0.268)	(0.4,0.281)	(0.35,0.328)	(0.15,0.225)	(0.15,0.296)	(0.15,0.359)	(0.1,0.327)	(0.1,0.337)
	(0.75,3.052)	(0.65,2.88)	(0.2,2.832)	(0.05,2.487)	(0.25,3.244)	(0.3,3.349)	(0.35,3.434)	(0.35,3.434)	(0.35,3.434)
	1.11	1.93	5.6	40.16	3.52	1.99	1.55	1.38	1.35
#7	(0.75,0.183)	(0.6,0.194)	(0.35,0.136)	(0.1,0.062)	(0.05,0.205)	(0.05,0.306)	(0.05,0.376)	(0.05,0.4195)	(0.05,0.429)
	(0.7,3.039)	(0.65,2.867)	(0.15,2.783)	(0.05,2.481)	(0.2,3.107)	(0.3,3.349)	(0.3,3.349)	(0.3,3.349)	(0.3,3.349)
	1.08	2.54	8.71	98.21	6.47	2.85	1.98	1.66	1.6
#8	(0.75,0.164)	(0.5,0.143)	(0.3,0.145)	(0.15,0.124)	(0.05,0.146)	(0.05,0.235)	(0.05,0.307)	(0.05,0.355)	(0.05,0.366)
	(0.95,2.848)	(0.4,2.89)	(0.1,2.691)	(0.05,2.489)	(0.15,2.93)	(0.3,3.349)	(0.3,3.349)	(0.3,3.349)	(0.3,3.349)
	1.1	2.86	10.01	117.81	8.27	3.39	2.22	1.81	1.74
#9	(0.7,0.118)	(0.5,0.162)	(0.3,0.158)	(0.2,0.175)	(0.05,0.129)	(0.05,0.210)	(0.05,0.280)	(0.05,0.329)	(0.05,0.340)
	(0.65,2.88)	(0.4,2.89)	(0.1,2.695)	(0.05,2.49)	(0.15,2.829)	(0.2,2.929)	(0.4,3.239)	(0.4,3.239)	(0.4,3.239)
	1.19	3.43	12.6	148.82	13.88	5.35	3.22	2.46	2.33
#10	(0.6,0.077)	(0.5,0.199)	(0.35,0.224)	(0.3,0.277)	(0.1,0.172)	(0.1,0.245)	(0.1,0.311)	(0.1,0.359)	(0.1,0.370)
	(0.65,2.88)	(0.35,2.889)	(0.1,2.689)	(0.05,2.49)	(0.1,2.697)	(0.2,2.88)	(0.4,3.096)	(0.4,3.239)	(0.4,3.239)
	1.28	3.8	14.28	164.24	17.08	6.51	3.95	2.96	2.78
#11	(0.6,0.097)	(0.55,0.267)	(0.4,0.280)	(0.4,0.378)	(0.15,0.224)	(0.15,0.295)	(0.15,0.358)	(0.1,0.325)	(0.1,0.335)
	(0.7,3.039)	(0.35,2.889)	(0.1,2.694)	(0.05,2.49)	(0.1,2.695)	(0.2,2.88)	(0.25,2.939)	(0.4,3.096)	(0.4,3.096)
	1.34	4.04	15.3	172.13	18.96	7.28	4.37	3.27	3.08
#12	(0.75,0.266)	(0.55,0.278)	(0.45,0.334)	(0.4,0.379)	(0.2,0.278)	(0.15,0.284)	(0.15,0.344)	(0.15,0.387)	(0.15,0.397)
	(0.75,3.052)	(0.5,2.886)	(0.15,2.783)	(0.05,2.487)	(0.25,3.244)	(0.3,3.349)	(0.3,3.349)	(0.3,3.349)	(0.3,3.349)
	1.1	2.35	7.65	78.08	5.31	2.58	1.89	1.63	1.58
#13	(0.75,0.179)	(0.55,0.175)	(0.3,0.132)	(0.1,0.07)	(0.05,0.162)	(0.05,0.252)	(0.05,0.318)	(0.05,0.361)	(0.05,0.370)
	(0.75,3.052)	(0.5,2.886)	(0.15,2.783)	(0.05,2.487)	(0.2,3.107)	(0.3,3.349)	(0.3,3.349)	(0.3,3.349)	(0.3,3.349)
	1.09	2.46	8.21	89.88	5.91	2.74	1.96	1.67	1.62
#14	(0.75,0.175)	(0.55,0.185)	(0.3,0.139)	(0.1,0.07)	(0.05,0.153)	(0.05,0.241)	(0.05,0.309)	(0.05,0.3528)	(0.05,0.362)
	(0.75,3.052)	(0.35,2.889)	(0.1,2.694)	(0.05,2.490)	(0.1,2.695)	(0.2,2.880)	(0.4,3.096)	(0.4,3.096)	(0.4,3.096)
	1.28	3.78	14.17	162.79	17.22	6.6	4	3.01	2.84
#15	(0.75,0.250)	(0.55,0.2664)	(0.45,0.328)	(0.4,0.378)	(0.2,0.283)	(0.15,0.294)	(0.15,0.357)	(0.15,0.401)	(0.15,0.411)
	(0.7,3.039)	(0.35,2.886)	(0.1,2.694)	(0.05,2.487)	(0.1,2.696)	(0.2,2.855)	(0.3,2.940)	(0.4,3.096)	(0.4,3.096)
	1.39	4.23	16.21	178.51	20.93	8.07	4.83	3.64	3.42
#16	(0.75,0.279)	(0.6,0.340)	(0.45,0.338)	(0.45,0.430)	(0.25,0.329)	(0.2,0.339)	(0.2,0.398)	(0.15,0.370)	(0.15,0.380)
	(0.7,3.039)	(0.35,2.886)	(0.1,2.689)	(0.05,2.487)	(0.05,2.49)	(0.2,2.855)	(0.25,2.905)	(0.35,2.971)	(0.35,2.971)
	1.45	4.49	17.31	185.84	22.91	8.92	5.27	3.96	3.74
#17	(0.75,0.293)	(0.6,0.3495)	(0.5,0.393)	(0.45,0.430)	(0.3,0.379)	(0.2,0.330)	(0.2,0.3867)	(0.2,0.426)	(0.2,0.436)

Table 5.6: Out-of-control performance for the proposed chart along with the corresponding optimal parameters for $n = 20$

case	$\tau = 0.25$	$\tau = 0.5$	$\tau = 0.75$	$\tau = 0.95$	$\tau = 1.25$	$\tau = 1.5$	$\tau = 1.75$	$\tau = 1.95$	$\tau = 2.0$
	(0.65,2.948)	(0.65,2.948)	(0.4,2.949)	(0.05,2.487)	(0.5,3.4)	(0.55,3.445)	(0.45,3.357)	(0.5,3.4)	(0.5,3.4)
	1	1	2.35	15.84	1.73	1.1	1.02	1	1
#1	(0.35,0)	(0.35,0)	(0.25,0.018)	(0.05,0.014)	(0.05,0.233)	(0.05,0.364)	(0.05,0.457)	(0.05,0.514)	(0.05,0.526)
	(0.65,2.948)	(0.7,2.937)	(0.25,2.888)	(0.05,2.489)	(0.25,3.075)	(0.5,3.4)	(0.6,3.49)	(0.55,3.445)	(0.55,3.445)
	1	1.38	5.3	58.21	4.31	1.75	1.22	1.09	1.07
#2	(0.35,0)	(0.4,0.0613368)	(0.25,0.107)	(0.1,0.0792381)	(0.05,0.139)	(0.05,0.231)	(0.05,0.313)	(0.05,0.369)	(0.05,0.382)
	(0.7,2.947)	(0.7,2.931)	(0.2,2.847)	(0.05,2.49)	(0.2,2.966)	(0.5,3.4)	(0.5,3.4)	(0.55,3.445)	(0.55,3.445)
	1	1.67	6.46	76.22	6.28	2.38	1.48	1.22	1.18
#3	(0.35,0)	(0.45,0.130)	(0.3,0.167)	(0.2,0.177)	(0.05,0.116)	(0.05,0.191)	(0.05,0.263)	(0.05,0.314)	(0.05,0.327)
	(0.7,2.931)	(0.7,2.93)	(0.15,2.793)	(0.05,2.49)	(0.2,2.888)	(0.5,3.181)	(0.5,3.4)	(0.55,3.445)	(0.55,3.445)
	1	1.86	7.22	87.22	7.76	3	1.78	1.39	1.33
#4	(0.45,0.01)	(0.5,0.193)	(0.35,0.221)	(0.25,0.227)	(0.1,0.176)	(0.1,0.252)	(0.05,0.228)	(0.05,0.276)	(0.05,0.287)
	(0.75,2.927)	(0.7,2.93)	(0.15,2.792)	(0.05,2.489)	(0.2,2.867)	(0.3,3.004)	(0.55,3.21)	(0.55,3.21)	(0.55,3.21)
	1	2.06	7.9	96.79	9.22	3.54	2.07	1.59	1.52
#5	(0.5,0.034)	(0.5,0.208)	(0.4,0.276)	(0.3,0.278)	(0.15,0.231)	(0.1,0.235)	(0.1,0.299)	(0.1,0.345)	(0.1,0.356)
	(0.75,2.927)	(0.7,2.931)	(0.15,2.792)	(0.05,2.489)	(0.15,2.802)	(0.3,2.946)	(0.55,3.21)	(0.55,3.21)	(0.55,3.21)
	1.01	2.19	8.4	103.28	10.28	3.92	2.32	1.75	1.66
#6	(0.5,0.045)	(0.55,0.268)	(0.4,0.281)	(0.35,0.328)	(0.15,0.225)	(0.15,0.296)	(0.1,0.282)	(0.1,0.327)	(0.1,0.337)
	(0.85,2.969)	(0.7,2.937)	(0.35,2.92)	(0.05,2.487)	(0.5,3.4)	(0.55,3.445)	(0.55,3.445)	(0.5,3.4)	(0.5,3.4)
	1	1.19	3.25	22.66	2.1	1.25	1.08	1.04	1.03
#7	(0.7,0.146)	(0.6,0.194)	(0.35,0.136)	(0.05,0.022)	(0.05,0.205)	(0.05,0.306)	(0.05,0.376)	(0.05,0.419)	(0.05,0.429)
	(0.75,2.927)	(0.75,2.927)	(0.25,2.888)	(0.05,2.489)	(0.25,3.075)	(0.5,3.4)	(0.55,3.445)	(0.5,3.4)	(0.5,3.4)
	1	1.38	5.09	53.13	3.94	1.71	1.25	1.12	1.1
#8	(0.5,0.034)	(0.5,0.143)	(0.25,0.103)	(0.1,0.078)	(0.05,0.146)	(0.05,0.235)	(0.05,0.307)	(0.05,0.355)	(0.05,0.366)
	(0.75,2.927)	(0.75,2.927)	(0.2,2.847)	(0.05,2.49)	(0.2,2.966)	(0.5,3.4)	(0.5,3.4)	(0.6,3.49)	(0.5,3.4)
	1	1.53	5.84	66.68	5.02	2.03	1.37	1.17	1.15
#9	(0.5,0.030)	(0.5,0.162)	(0.3,0.158)	(0.15,0.127)	(0.05,0.129)	(0.05,0.210)	(0.05,0.280)	(0.05,0.329)	(0.05,0.340)
	(0.7,2.931)	(0.7,2.93)	(0.15,2.793)	(0.05,2.489)	(0.2,2.867)	(0.3,3.004)	(0.55,3.21)	(0.55,3.445)	(0.55,3.445)
	1	1.93	7.44	90.67	8.4	3.23	1.91	1.49	1.42
#10	(0.55,0.054)	(0.5,0.1991)	(0.35,0.224)	(0.3,0.277)	(0.15,0.236)	(0.1,0.245)	(0.1,0.311)	(0.05,0.260)	(0.05,0.270)
	(0.7,2.931)	(0.7,2.931)	(0.15,2.792)	(0.05,2.489)	(0.15,2.799)	(0.3,2.946)	(0.45,3.038)	(0.55,3.21)	(0.55,3.21)
	1.01	2.19	8.38	103.09	10.32	3.94	2.34	1.77	1.67
#11	(0.55,0.071)	(0.55,0.267)	(0.4,0.280)	(0.35,0.328)	(0.2,0.284)	(0.15,0.295)	(0.15,0.358)	(0.1,0.325)	(0.1,0.335)
	(0.75,2.929)	(0.65,2.939)	(0.15,2.792)	(0.05,2.489)	(0.15,2.799)	(0.35,2.953)	(0.45,3.038)	(0.65,3.038)	(0.65,3.038)
	1.02	2.34	9.02	110.36	11.48	4.39	2.58	1.97	1.86
#12	(0.55,0.083)	(0.6,0.332)	(0.4,0.286)	(0.4,0.379)	(0.2,0.278)	(0.2,0.350)	(0.15,0.344)	(0.2,0.453)	(0.2,0.463)
	(0.6,2.959)	(0.75,2.929)	(0.3,2.911)	(0.05,2.489)	(0.45,3.357)	(0.5,3.4)	(0.55,3.445)	(0.6,3.49)	(0.5,3.4)
	1	1.3	4.46	42.1	3.24	1.56	1.21	1.1	1.09
#13	(0.7,0.1459)	(0.55,0.175)	(0.3,0.132)	(0.1,0.074)	(0.05,0.162)	(0.05,0.252)	(0.05,0.318)	(0.05,0.361)	(0.05,0.370)
	(0.65,2.948)	(0.75,2.929)	(0.25,2.885)	(0.05,2.489)	(0.25,3.075)	(0.5,3.4)	(0.55,3.445)	(0.55,3.445)	(0.55,3.445)
	1	1.36	4.81	48.16	3.62	1.65	1.24	1.12	1.1
#14	(0.65,0.111)	(0.55,0.185)	(0.3,0.139)	(0.1,0.076)	(0.05,0.153)	(0.05,0.241)	(0.05,0.309)	(0.05,0.3529)	(0.05,0.362)
	(0.75,2.929)	(0.65,2.939)	(0.15,2.792)	(0.05,2.489)	(0.15,2.799)	(0.3,2.946)	(0.45,3.038)	(0.55,3.21)	(0.55,3.21)
	1.02	2.16	8.34	102.38	10.4	4	2.37	1.8	1.71
#15	(0.55,0.083)	(0.6,0.32)	(0.4,0.280)	(0.35,0.328)	(0.2,0.283)	(0.15,0.294)	(0.15,0.357)	(0.1,0.321)	(0.1,0.331)
	(0.7,2.937)	(0.65,2.939)	(0.15,2.792)	(0.05,2.489)	(0.1,2.697)	(0.3,2.927)	(0.45,3.038)	(0.6,3.028)	(0.6,3.028)
	1.04	2.47	9.57	116.03	12.65	4.86	2.89	2.14	2.02
#16	(0.6,0.130)	(0.6,0.340)	(0.45,0.338)	(0.4,0.380)	(0.25,0.329)	(0.2,0.339)	(0.15,0.329)	(0.2,0.440)	(0.2,0.450)
	(0.95,2.876)	(0.45,2.935)	(0.15,2.792)	(0.05,2.489)	(0.1,2.698)	(0.3,2.918)	(0.4,2.971)	(0.6,3.028)	(0.6,3.028)
	1.05	2.65	10.25	123.14	13.75	5.33	3.16	2.34	2.2
#17	(0.65,0.181)	(0.6,0.349)	(0.45,0.343)	(0.4,0.381)	(0.3,0.379)	(0.25,0.391)	(0.2,0.386)	(0.2,0.426)	(0.2,0.436)

5.3.2 Performance comparisons

5.3.2.1 Comparisons under Normality

It is clear that, similarly with the Shewhart chart presented in Section 5.2, the proposed EWMA chart, follows a semi-parametric design regarding the determinations of its optimal design parameters. As a consequence, it is logical to examine first its performance by assuming that the sample's underlying distribution is the Normal one.

In Table 5.7, the out-of-control performance of the D-SN-C EWMA chart is compared with three parametric Shewhart-type control charts for monitoring the process variability for $n = \{5, 20, 30\}$ and different values of τ along with the corresponding ARL_1 values. In particular, the D-SN-C EWMA chart is compared with the modified R and S charts proposed by Zhang (2014) and an enhanced R chart proposed by Khoo and Lim (2005). Of course, there is an enormous amount of parametric Shewhart schemes for monitoring the variability; the choice for these charts has been made motivated by the fact that their design yields to robust determinations of their RL properties. For each case, the proposed chart is optimized as explained in Section 5.3.1 assuming a normal distribution. It can be clearly seen that, regardless the sample size or the shift magnitude τ, the D-SN-C EWMA chart has the best performance among its competitors. It should be noted that, for small to moderate decreases ($0.5 < \tau < 0.9$) or increases ($1.1 < \tau < 1.5$), the proposed chart's corresponding ARL_1 are significantly smaller compared with their parametric counterparts. For instance, for $n = 20$, and $\tau = 0.9$ the ARL_1 values for the Zhang's R chart, S chart and Khoo and Lim's R chart are 188.04, 174.67 and 232.12, respectively, while for the proposed chart it is $\text{ARL}_1 = 26.21$. Similarly, when $\tau = 1.1$ the ARL_1 values of Zhang's R chart, S chart and Khoo and Lim's R chart are 127.59, 78.82 and 139.9, respectively, while for the proposed chart it is $\text{ARL}_1 = 24.47$. It should be noted that these comparisons are not entirely fair since the competitors are Shewhart-type charts and is performance are weak when they are compared with a memory-based control chart such as the proposed EWMA scheme. As a result, in the rest of this Section we consider history-based control charts (EWMA and CUSUM schemes) in order to examines our chart's performance.

A well known EWMA scheme, capable of monitoring shifts in the process variability is the S^2 EWMA chart, proposed by Castagliola (2005). In Table 5.8 (top) its optimal design is presented for $n = \{3, 5, 9, 11\}$. Additionally it Table 5.8 (bottom) the optimal design and performance of the D-SN-C EWMA chart is presented for the same combinations of n and τ. Finally, in Table 5.9, the corresponding percentage of the differentness between these

schemes is presented via the quantity:

$$\frac{ARL_1^{\mathrm{SD}} - ARL_1^{S2}}{ARL_1^{\mathrm{SD}}} \times 100\% \tag{5.12}$$

where the upper-script $S2$ is referring to the S^2 EWMA chart, while the upper-script SD refers to the D-SN-C EWMA chart. It is clear that negative values, correspond to the superiority of the proposed chart. From Table 5.9 we may conclude that for small sample sizes ($n = \{3, 5\}$) when $\tau < 1$ (i.e. for decreases in the process variability) the D-SN-C EWMA chart has better performance. On the other hand, for $n = \{3, 5\}$ and $\tau > 1$ (i.e. for increases in the process variability) the S^2 chart performs better. As the sample size increases (see for $n = 10$), for large increases in the process variability, the D-SN-C EWMA chart performs slightly better. It should be noted that as n increases, in most cases, the fact that the parametric S^2 EWMA chart performs better than the proposed nonparametric scheme is an expected result. However, the results, show that for small samples sizes and $\tau < 1$ (i.e. decreases in the process variability) the D-SN-C EWMA chart performs better. Additionally, as n increase, when $\tau > 1.5$ (i.e. moderate to large increases in the process variability) the D-SN-C EWMA chart tends to perform slightly better. As a result, under the assumption of normality the proposed scheme can be considered as an efficient alternative.

Table 5.7: Out-of-control performance of the D-SN-C EWMA chart versus several parametric control charts when the underling distribution is the Normal for $n = \{5, 20, 30\}$

	Zhang's R Chart			Zhang's S Chart			Khoo and Lim's R Chart			D-SN-C EWMA Chart		
τ	$n=5$	$n=10$	$n=20$	$n=5$	$n=10$	$n=20$	$n=5$	$n=10$	$n=20$	$n=5$	$n=10$	$n=20$
0.1	1.04	1.00	1.00	1.03	1.00	1.00	1.14	1.00	1.00	(0.7,2.951) 1 (0.7,0)	(0.75,2.846) 1 (0.5,0)	(0.65,2.948) 1 (0.35,0)
0.2	2.66	1.00	1.00	2.62	1.00	1.00	4.22	1.01	1.00	(0.65,2.958) 1.27 (0.7,0.05)	(0.65,2.881) 1 (0.6,0.008)	(0.65,2.948) 1 (0.35,0)
0.3	8.58	1.23	1.00	8.45	1.14	1.00	15.13	1.46	1.00	(0.6,2.958) 2.14 (0.7,0.199)	(0.65,2.881) 1.2 (0.6,0.080)	(0.75,2.935) 1 (0.4,0.005)
0.4	23.08	2.53	1.08	22.62	2.27	1.01	41.19	3.57	1.15	(0.5,2.787) 3.31 (0.5,0.091)	(0.7,2.861) 1.85 (0.5,0.091)	(0.75,2.929) 1.11 (0.45,0.058)
0.5	51.96	6.75	1.71	51.79	6.14	1.34	90.55	10.45	2.04	(0.3,2.827) 5.24 (0.55,0.231)	(0.4,2.886) 3.06 (0.5,0.177)	(0.7,2.932) 1.67 (0.45,0.130)
0.6	101.99	19.12	4.20	103.07	17.71	3.10	173.87	30.56	5.55	(0.15,2.764) 8.28 (0.45,0.208)	(0.3,2.892) 4.88 (0.45,0.2080)	(0.45,2.935) 2.82 (0.4,0.160)
0.7	181.22	52.19	13.60	185.49	49.66	10.58	288.14	79.70	18.89	(0.1,2.684) 13.89 (0.35,0.181)	(0.05,2.123) 7.83 (0.35,0.181)	(0.25,2.884) 4.73 (0.35,0.181)
0.8	301.02	134.53	50.44	307.97	129.11	42.94	433.69	189.02	68.61	(0.05,2.482) 26.12 (0.3,0.195)	(0.05,2.123) 13.34 (0.35,0.242)	(0.15,2.797) 9.27 (0.25,0.150)
0.9	423.90	308.45	188.04	444.64	300.21	174.67	520.23	373.87	232.12	(0.05,2.482) 80.41 (0.3,0.249)	(0.05,2.123) 34.88 (0.35,0.299)	(0.05,2.491) 26.21 (0.2,0.154)
1.05	266.38	258.73	248.50	263.01	225.27	187.23	268.00	260.36	250.36	(0.05,2.467) 124.63 (0.05,0.061)	(0.05,2.207) 81.34 (0.25,0.273)	(0.05,2.49) 64.72 (0.1,0.117)
1.1	172.68	148.12	127.59	157.38	120.29	78.82	182.01	160.40	139.97	(0.05,2.467) 57.26 (0.05,0.074)	(0.05,2.207) 36.6 (0.25,0.295)	(0.1,2.701) 24.47 (0.1,0.134)
1.15	110.96	87.26	66.21	99.95	63.97	35.54	123.02	98.38	76.27	(0.05,2.467) 33.61 (0.05,0.088)	(0.1,2.738) 21.65 (0.05,0.088)	(0.15,2.85) 13.36 (0.05,0.088)
1.2	73.80	52.27	37.91	64.13	12.57	18.32	84.63	62.24	44.01	(0.05,2.467) 22.88 (0.05,0.1023985)	(0.1,2.738) 14.22 (0.05,0.102)	(0.15,2.85) 8.66 (0.05,0.102)
1.3	35.50	22.35	14.32	30.48	14.99	6.72	44.69	28.29	17.77	(0.1,2.84) 12.99 (0.05,0.1316303)	(0.15,2.935) 8.03 (0.05,0.131)	(0.2,2.966) 4.86 (0.05,0.131)
1.4	19.61	11.53	7.11	16.85	7.76	3.43	25.91	15.27	8.86	(0.1,2.84) 8.87 (0.05,0.16150788)	(0.25,3.255) 5.39 (0.05,0.161)	(0.45,3.358) 3.27 (0.05,0.161)
1.5	12.23	6.89	4.17	10.49	4.74	2.20	16.70	9.27	5.20	(0.15,3.105) 6.65 (0.05,0.19131831)	(0.25,3.255) 3.99 (0.05,0.191)	(0.5,3.4) 2.38 (0.05,0.191)
1.6	8.30	4.63	2.78	7.20	3.26	1.64	11.89	6.26	3.49	(0.2,3.288) 5.28 (0.05,0.2205657)	(0.3,3.356) 3.16 (0.05,0.220)	(0.5,3.4) 1.88 (0.05,0.220)
1.8	4.70	2.62	1.68	1.80	2.01	1.20	7.00	3.60	2.07	(0.25,3.424) 3.75 (0.05,0.27619046)	(0.3,3.356) 2.28 (0.05,0.276)	(0.55,3.445) 1.39 (0.05,0.276)
2	3.17	1.84	1.28	2.87	1.51	1.07	4.85	2.49	1.53	(0.25,3.424) 2.95 (0.05,0.32707178)	(0.3,3.356) 1.83 (0.05,0.327)	(0.55,3.445) 1.18 (0.05,0.327)
3	1.41	1.07	1.00	1.35	1.03	1.00	2.03	1.25	1.04	(0.3,3.536) 1.64 (0.05,0.51352518)	(0.8,3.756) 1.15 (0.05,0.513)	(0.5,3.4) 1 (0.05,0.513)

Table 5.8: Optimal combinations and smallest possible out-of-control values for $\tau \in (0.5, 2)$, $n = \{3, 5, 7, 9\}$ and $\text{ARL}_0 = 370$, for the S^2 EWMA chart, (top) and for the D-SN-C EWMA chart(bottom)

S^2 EWMA chart

	$n=3$			$n=5$			$n=7$			$n=9$		
τ	λ	K	ARL_1	λ	K	ARL_0	λ	K	ARL_1	λ	K	ARL_1
0.5	0.14	2.755	12.3	0.24	2.819	6.2	0.34	2.850	4.2	0.44	2.866	3.2
0.6	0.10	2.689	17.7	0.18	2.790	9.0	0.25	2.836	6.1	0.31	2.863	4.7
0.7	0.08	2.642	28.4	0.12	2.724	14.6	0.17	2.791	10.0	0.20	2.822	7.7
0.8	0.05	2.546	54.2	0.08	2.634	28.1	0.10	2.689	19.5	0.12	2.732	15.1
0.9	0.05	2.546	155.2	0.05	2.514	80.8	0.05	2.505	56.7	0.06	2.555	44.5
0.95	0.05	2.546	323.5	0.05	2.514	202.1	0.05	2.505	150.1	0.05	2.501	120.5
1.05	0.05	2.546	153.5	0.05	2.514	121.2	0.05	2.505	99.3	0.05	2.501	84.1
1.1	0.05	2.546	65.1	0.05	2.514	44.9	0.05	2.505	35.0	0.05	2.501	29.1
1.2	0.05	2.546	21.8	0.05	2.514	15.3	0.05	2.505	12.5	0.05	2.501	10.8
1.3	0.05	2.546	11.7	0.05	2.514	8.8	0.05	2.505	7.4	0.05	2.501	6.6
1.4	0.05	2.546	7.9	0.05	2.514	6.2	0.05	2.505	5.4	0.05	2.501	4.8
1.5	0.05	2.546	5.9	0.05	2.514	4.8	0.05	2.505	4.3	0.05	2.501	3.9
1.6	0.05	2.546	4.8	0.05	2.514	4.0	0.05	2.505	3.6	0.05	2.501	3.2
1.7	0.05	2.546	4.1	0.05	2.514	3.5	0.05	2.505	3.1	0.05	2.501	2.9
1.8	0.05	2.546	3.6	0.05	2.514	3.1	0.05	2.505	2.8	0.05	2.501	2.6
1.9	0.05	2.546	3.2	0.05	2.514	2.8	0.05	2.505	2.5	0.05	2.501	2.4
2	0.05	2.546	2.9	0.05	2.514	2.5	0.05	2.505	2.3	0.05	2.501	2.2

D-SN-C EWMA chart

	$n=3$			$n=5$			$n=7$			$n=9$		
τ	λ	K	ARL_1	λ	K	ARL_1	λ	K	ARL_1	λ	K	ARL_1
			(0.25,2.775)			(0.3,2.827)			(0.35,2.86)			(0.4,2.882)
			7.76			5.24			4			3.31
0.5	-	-	(0.55,0.231)	-	-	(0.55,0.231)	-	-	(0.45,0.130)	-	-	(0.5,0.177)
			(0.1,2.667)			(0.15,2.764)			(0.2,2.821)			(0.25,2.856)
			12.25			8.28			6.34			5.26
0.6	-	-	(0.45,0.208)	-	-	(0.45,0.208)	-	-	(0.4,0.160)	-	-	(0.4,0.160)
			(0.05,2.488)			(0.1,2.684)			(0.1,2.692)			(0.15,2.786)
			20.3			13.89			10.7			8.84
0.7	-	-	(0.35,0.181)	-	-	(0.35,0.181)	-	-	(0.35,0.181)	-	-	(0.3,0.138)
			(0.05,2.486)			(0.05,2.482)			(0.05,2.491)			(0.1,2.691)
			38.77			26.12			20.45			17.3
0.8	-	-	(0.3,0.195)	-	-	(0.3,0.195)	-	-	(0.3,0.195)	-	-	(0.25,0.150)
			(0.05,2.486)			(0.05,2.482)			(0.05,2.489)			(0.05,2.49)
			121.16			80.41			60.82			49.14
0.9	-	-	(0.3,0.249)	-	-	(0.3,0.249)	-	-	(0.25,0.201)	-	-	(0.2,0.154)
			(0.25,2.825)			(0.05,2.482)			(0.05,2.491)			(0.05,2.49)
			251.62			204.69			167.75			142.08
0.95	-	-	(0.7,0.685)	-	-	(0.3,0.275)	-	-	(0.3,0.275)	-	-	(0.25,0.225)
			(0.05,2.473)			(0.05,2.467)			(0.05,2.474)			(0.1,2.737)
			147.11			124.63			110.63			99.81
1.05	-	-	(0.05,0.061)	-	-	(0.05,0.061)	-	-	(0.05,0.061)	-	-	(0.05,0.061)
			(0.05,2.473)			(0.05,2.467)			(0.05,2.474)			(0.1,2.737)
			74.65			57.26			47.68			41.58
1.1	-	-	(0.05,0.074)	-	-	(0.05,0.074)	-	-	(0.05,0.074)	-	-	(0.05,0.074)
			(0.05,2.473)			(0.05,2.467)			(0.1,2.78)			(0.1,2.737)
			31.26			22.88			18.08			15.14
1.2	-	-	(0.05,0.102)	-	-	(0.05,0.102)	-	-	(0.05,0.102)	-	-	(0.05,0.102)
			(0.05,2.473)			(0.1,2.84)			(0.1,2.78)			(0.15,2.95)
			18.45			12.99			10.26			8.64
1.3	-	-	(0.05,0.131)	-	-	(0.05,0.131)	-	-	(0.05,0.131)	-	-	(0.05,0.131)
			(0.1,2.942)			(0.1,2.84)			(0.15,3.016)			(0.2,3.121)
			12.7			8.87			7			5.79
1.4	-	-	(0.05,0.161)	-	-	(0.05,0.161)	-	-	(0.05,0.161)	-	-	(0.05,0.161)
			(0.1,2.942)			(0.15,3.105)			(0.2,3.178)			(0.25,3.266)
			9.54			6.65			5.26			4.3
1.5	-	-	(0.05,0.191)	-	-	(0.05,0.191)	-	-	(0.05,0.191)	-	-	(0.05,0.191)
			(0.15,3.24)			(0.2,3.288)			(0.25,3.314)			(0.25,3.266)
			7.61			5.28			4.2			3.42
1.6	-	-	(0.05,0.220)	-	-	(0.05,0.220)	-	-	(0.05,0.220)	-	-	(0.05,0.220)
			(0.15,3.24)			(0.25,3.424)			(0.45,3.707)			(0.25,3.266)
			6.32			4.39			3.45			2.87
1.7	-	-	(0.05,0.248)	-	-	(0.05,0.248)	-	-	(0.05,0.248)	-	-	(0.05,0.248)
			(0.2,3.454)			(0.25,3.424)			(0.45,3.707)			(0.3,3.38)
			5.43			3.75			2.91			2.48
1.8	-	-	(0.05,0.276)	-	-	(0.05,0.276)	-	-	(0.05,0.276)	-	-	(0.05,0.276)
			(0.2,3.454)			(0.25,3.424)			(0.5,3.768)			(0.25,3.266)
			4.77			3.29			2.53			2.21
1.9	-	-	(0.05,0.302)	-	-	(0.05,0.302)	-	-	(0.05,0.302)	-	-	(0.05,0.302)
			(0.2,3.454)			(0.25,3.424)			(0.5,3.768)			(0.3,3.38)
			4.28			2.95			2.24			2
2	-	-	(0.05,0.327)	-	-	(0.05,0.327)	-	-	(0.05,0.327)	-	-	(0.05,0.327)

Table 5.9: Performance comparisons between the S^2 EWMA chart, and for the D-SN-C EWMA charts based on the metric defined in equation (5.12)

τ	$n=3$	$n=5$	$n=7$	$n=9$
0.5	**-58.51**	**-18.32**	**-5.00**	3.32
0.6	**-44.49**	**-8.70**	3.79	10.65
0.7	**-39.90**	**-5.11**	6.54	12.90
0.8	**-39.80**	**-7.58**	4.65	12.72
0.9	**-28.10**	**-0.49**	6.77	9.44
0.95	**-28.57**	1.27	10.52	15.19
1.05	**-4.34**	2.75	10.24	15.74
1.1	12.79	21.59	26.59	30.01
1.2	30.26	33.13	30.86	28.67
1.3	36.59	32.26	27.88	23.61
1.4	37.80	30.10	22.86	17.10
1.5	38.16	27.82	18.25	9.30
1.6	36.93	24.24	14.29	6.43
1.7	35.13	20.27	10.14	**-1.05**
1.8	33.70	17.33	3.78	**-4.84**
1.9	32.91	14.89	1.19	**-8.60**
2	32.24	15.25	**-2.68**	**-10.00**

5.3.2.2 Comparisons versus other Nonparametric schemes

Since the motivation of designing the D-SN-C chart is to provide to practitioners a new semi-parametric scheme capable of detecting shifts in the process variability, necessary comparisons with existing non- or semi- parametric schemes need to be made. So far, it has been proven that the D-SN-C EWMA chart has, in most cases, a better performance among several schemes in monitoring shifts in the process variability when the underlying distribution is the Normal one. As an extension of investigating the out-of-control performance of the D-SN-C EWMA chart, it would be interesting to examine its efficiency under the benchmark of the distributions listed in Table 4.3 against the Sign Shewhart presented in 5.2. In order to perform fair comparisons between the Shewhart S-SD and the EWMA D-SN-C charts, for each distribution, the optimal parameters of the D-SN-C EWMA chart will be derived in order to have the same in-control ARL as the ones listed in Table 5.3 ($n=20$) and Table 5.4 ($n=30$). In particular, since in Table 5.3 for most of the cases the corresponding $\text{ARL}_0 \approx 385$, the same value will be set at a desired in-control value for the

EWMA chart. Similarly, for $n = 30$ the desired in-control ARL will be $\text{ARL}_0 \approx 365$. Finally the performance of the two charts is compared through the same quantity a before, i.e.

$$\frac{\text{ARL}_1^{\text{SD}} - \text{ARL}_1^{Sh}}{\text{ARL}_1^{\text{SD}}} \times 100\% \tag{5.13}$$

where ARL_1^{Sh} denotes the out-of-control performance of the Shewhart chart. These differences are presented in Table 5.10 ($n = 20$) and Table 5.11 ($n = 30$). It can be clearly concluded that the EWMA chart outperforms the Shewhart chart regardless the sample size, shift magnitude or the underlying distribution. Practically speaking, for large increases ($\tau > 2$) or decreases ($\tau \to 0$) in the process variability these two schemes have similar performance, but for small shifts clearly the D-SN-C chart is superior. Moreover, another advantage of the proposed Sign EWMA chart is that it can be designed to have an in-control ARL to be exactly equal to the desired value (for example 370.4).

Table 5.10: Performance comparisons Between the Shewhart and EWMA Sign charts for dispersion when $n = 20$

case	$\tau = 0.25$	$\tau = 0.5$	$\tau = 0.75$	$\tau = 0.95$	$\tau = 1.25$	$\tau = 1.5$	$\tau = 1.75$	$\tau = 1.95$	$\tau = 2.0$
1	0.00	0.00	-541.53	-1514.94	-286.13	-86.36	-31.37	-19.00	-13.00
2	0.00	-12.32	-421.91	-339.34	-235.17	-105.71	-52.85	-39.45	-28.04
3	0.00	-15.48	-398.00	-235.66	-194.48	-85.83	-47.30	-39.34	-27.97
4	0.00	-20.63	-389.99	-193.39	-183.52	-72.13	-37.43	-34.53	-23.31
5	0.00	-28.37	-392.25	-164.65	-181.94	-74.72	-34.45	-30.62	-18.42
6	0.00	-35.59	-397.30	-148.12	-185.44	-79.49	-34.19	-30.11	-16.77
7	0.00	-21.01	-327.83	-1027.29	-310.43	-115.20	-52.78	-35.58	-27.18
8	0.00	-6.52	-398.24	-381.25	-257.93	-114.53	-57.60	-41.96	-30.91
9	0.00	-10.39	-395.57	-283.54	-228.85	-102.94	-54.01	-41.53	-29.57
10	-1.00	-23.59	-382.56	-182.22	-177.95	-72.31	-35.23	-31.33	-20.28
11	-0.99	-36.65	-393.54	-148.51	-185.78	-79.60	-34.47	-29.78	-17.26
12	-0.98	-47.03	-402.30	-132.67	-194.56	-88.04	-38.85	-30.15	-12.30
13	0.00	-18.85	-504.47	-844.91	-428.03	-158.52	-71.68	-48.60	-36.79
14	0.00	-10.69	-421.78	-508.14	-313.41	-133.97	-64.46	-47.27	-33.94
15	-4.00	-124.26	-747.00	-434.85	-725.82	-335.15	-156.45	-108.04	-80.91
16	-4.90	-82.57	-482.05	-150.97	-272.26	-141.94	-74.37	-61.54	-42.44
17	-4.81	-83.53	-431.61	-121.93	-245.81	-133.33	-65.64	-54.84	-35.78

Table 5.11: Performance comparisons Between the Shewhart and EWMA Sign charts for dispersion when $n = 30$

case	$\tau = 0.25$	$\tau = 0.5$	$\tau = 0.75$	$\tau = 0.95$	$\tau = 1.25$	$\tau = 1.5$	$\tau = 1.75$	$\tau = 1.95$	$\tau = 2.0$
1	0.00	0.00	25.33	-1015.32	-304.51	-64.71	-18.00	-8.00	-5.00
2	0.00	4.72	-70.83	-335.59	-228.75	-93.28	-37.74	-22.77	-14.85
3	0.00	7.44	-109.17	-238.67	-178.92	-73.86	-37.29	-25.47	-17.31
4	0.00	4.51	-137.14	-197.30	-161.18	-58.45	-28.68	-23.68	-15.32
5	0.00	4.79	-144.31	-171.82	-156.01	-53.88	-23.08	-19.84	-11.57
6	0.00	3.87	-147.65	-156.68	-156.92	-53.66	-21.76	-20.30	-10.94
7	0.00	-0.96	-15.32	-709.32	-332.48	-95.33	-33.66	-20.00	-14.00
8	0.00	3.64	-61.79	-370.60	-253.24	-101.52	-41.12	-25.49	-16.67
9	0.00	3.48	-88.18	-283.12	-217.47	-90.79	-39.82	-26.92	-18.45
10	0.00	5.76	-140.04	-186.22	-154.09	-55.98	-24.66	-22.69	-13.79
11	0.00	3.87	-145.78	-156.06	-156.17	-52.94	-21.64	-20.15	-11.72
12	0.00	1.21	-150.53	-141.70	-161.48	-56.04	-20.53	-20.00	-10.14
13	0.00	-0.95	-72.69	-751.94	-436.57	-128.57	-46.60	-27.72	-18.81
14	0.00	0.93	-64.37	-480.69	-317.15	-114.63	-45.71	-27.45	-19.80
15	0.00	-37.61	-323.28	-462.13	-624.54	-245.31	-95.33	-58.82	-41.18
16	0.00	-16.88	-191.84	-165.50	-226.82	-95.56	-46.82	-40.00	-25.38
17	0.00	-13.07	-180.23	-134.52	-205.26	-84.36	-34.27	-31.65	-19.46

Generally, the design of control schemes (distribution-free or semi-parametric) for detecting shifts in the process variability is a growing research area, so it is practically impossible to compare all of them with our scheme. In this work, our proposed chart is compared with schemes which are relatively new additions into the literature, and the most important, the distribution of the statistic to be monitored is derived without any approximation. In particular, based on the results presented in this work, it is our belief that, for discrete statistics (such as the Sign or the Wilcoxon signed rank), any approximation of the statistic's actual distribution though a continuous distribution (such as the Normal) should be avoided or, at least, be used with caution. For instance, In Chapter 2, we saw that, even though the Normal distribution is a reliable approximation of the distribution of SR_t^+, the approximated and the true values of $\mathrm{ARL}_0 \approx 370.4$ are significantly different. As a consequence, schemes where the Normal approximation is applied, should be treated cautiously when are being used in practice.

Recently, a non-parametric upper-sided CUSUM (denoted as D-CUSUM) chart was proposed into the literature by Shirke and Barale (2018) for monitoring upwards shifts in the process variability. In particular, it is an extension of the approach of Amin et al. (1995)

and (Pawar et al., 2018) in which the in-control probability is fixed and equals to $p_0 = 0.2$. In the work of Shirke and Barale (2018), it has been stated that the D-CUSUM chart is an efficient scheme for detecting small to moderate increases in the process variability. In Table 5.12 the out-of-control performance of the D-CUSUM chart (as presented in Shirke and Barale (2018)) is compared with the proposed chart for different sample sizes, shifts and underlying distributions. Note that, in order to perform fair comparisons, our chart was optimised in order to have the same in-control ARL with the D-CUSUM chart. Moreover, since in the work of Shirke and Barale (2018) the same design parameters were used fro all the shifts, in order to performed unbiased comparisons, the optimal value of p_0 was set to be fixed to $p_0^* = 0.05$ (for Normal and Laplce distributions) and $p_0^* = 0.2$ (for the Exponential distribution) for all the shifts. Note that, this value has not be chosen at rand. In particular, based on our findings presented in the previous Sections, when it is desired to monitor small increases in the process variability for symmetric distributions, setting $p_0^* = 0.05$ is a reasonable choice. In Table 5.12 the results presented by Shirke and Barale (2018) (top) are compared with the proposed chart. It can be clearly seen, that our chart, for any shifts and sample size, outperforms the D-CUSUM chart. As a consequence, the D-SN-C EWMA chart can be considered as an efficient scheme capable of monitoring small to moderate increases in the process variability.

Table 5.12: Performance comparisons between the D-CUSUM and the D-SN-C EWMA charts for different sample sizes and underling distributions

D-SN-C chart

	Normal			Laplace			Exponential		
τ	$n = 10$	$n = 15$	$n = 20$	$n = 10$	$n = 15$	$n = 20$	$n = 10$	$n = 15$	$n = 20$
	(0.1,2.589)	(0.15,2.746)	(0.15,2.726)	(0.1,2.589)	(0.1,2.596)	(0.15,2.726)	(0.05,2.374)	(0.05,2.375)	(0.05,2.375)
	13.07	9.88	8.13	24.41	18.82	15.64	40.43	31	25.37
1.2	(0.05,0.102)	(0.05,0.102)	(0.05,0.102)	(0.05,0.082)	(0.05,0.082)	(0.05,0.082)	(0.2,0.242)	(0.2,0.242)	(0.2,0.242)
	(0.2,2.954)	(0.25,3.002)	(0.4,3.171)	(0.15,2.779)	(0.2,2.888)	(0.2,2.832)	(0.1,2.59)	(0.15,2.695)	(0.15,2.7)
	5.01	3.81	3.06	9.45	7.11	5.81	15.93	11.95	9.71
1.4	(0.05,0.161)	(0.05,0.161)	(0.05,0.161)	(0.05,0.117)	(0.05,0.117)	(0.05,0.117)	(0.2,0.284)	(0.2,0.284)	(0.2,0.284)
	(0.25,3.094)	(0.55,3.4)	(0.45,3.222)	(0.2,2.954)	(0.25,3.002)	(0.4,3.171)	(0.2,2.752)	(0.25,2.802)	(0.25,2.8)
	3.01	2.27	1.83	5.48	4.15	3.36	9.2	6.86	5.57
1.6	(0.05,0.220)	(0.05,0.220)	(0.05,0.220)	(0.05,0.153)	(0.05,0.153)	(0.05,0.153)	(0.2,0.322)	(0.2,0.322)	(0.2,0.322)
	(0.25,3.094)	(0.65,3.486)	(0.45,3.222)	(0.25,3.094)	(0.25,3.002)	(0.4,3.171)	(0.25,2.803)	(0.35,2.853)	(0.35,2.858)
	2.21	1.62	1.38	3.81	2.95	2.32	6.3	4.7	3.8
1.8	(0.05,0.276)	(0.05,0.276)	(0.05,0.276)	(0.05,0.189)	(0.05,0.189)	(0.05,0.189)	(0.2,0.358)	(0.2,0.358)	(0.2,0.358)

D-CUSUM chart
(Shirke and Barale (2018))

	Normal			Laplace			Exponential		
τ	$n = 10$	$n = 15$	$n = 20$	$n = 10$	$n = 15$	$n = 20$	$n = 10$	$n = 15$	$n = 20$
1	284.00	284.40	283.10	284.00	284.40	283.10	284.00	284.40	283.10
1.2	20.20	15.30	12.40	28.20	21.90	17.90	75.3	64.40	56.00
1.4	9.20	6.80	5.50	12.10	9.00	7.30	29.4	22.90	18.80
1.6	6.30	4.70	3.80	8.00	5.90	4.80	16.4	12.30	10.00
1.8	5.10	3.80	3.10	6.20	4.60	3.80	11.3	8.40	6.80

5.3.3 An illustrative example

In this section, two examples are presented, in order to show a practical Phase II implementation of the operation of the proposed D-SN-C EWMA chart. The datasets of each example, which have been originally introduced in Castagliola et al. (2006), are presented in Table A4 in appendix and plotted in Figures 5.1 and 5.2, respectively. Both datasets consists of 30 subgroups of size $n = 5$ where the first 20 subgroups are the same for both examples. In particular, for the first example, we are interested to detect a shift of magnitude $\tau = 2$ (i.e. an increase in the process variability) and for the second one we are interested to detect a shift of magnitude $\tau = 0.5$ (i.e. detect a decrease in the process variability). Regarding the values of the optimal parameters, they have been chosen following the same steps of the optimization procedure presented in Section 5.3.1. Additionally, the control limits for each case are computed using the expressions (5.10) and (5.11) presented in Section 5.3 where the value of the "continuousify" parameter is set to $h = 0.2$. More specifically, the optimal vector of parameters (p_0^*, λ^*, K^*) for detecting shifts of magnitude $\tau = 2$ is $(p_0^* = 0.05, \lambda^* = 0.25, K^* = 3.424)$ with corresponding control limits $\text{LCL}^* = -5.789$,

$\text{UCL}^* = -3.212$. Similarly, for detecting shifts of magnitude $\tau = 0.5$ the optimal vector of parameters is $(p_0^* = 0.5, \lambda^* = 0.25, K^* = 2.823)$ and the control limits are equal to $\text{LCL}^* = -2.395$, $\text{UCL}^* = 2.395$. Finally, the corresponding values of SD_t, SD_t^* and Z_t^* are presented in Table 5.13.

From Figure 5.3, it can be seen that the proposed chart can efficiently detect the increase in the process variability at the 22th sampling point. Similarly, for the second example, which corresponds to a decrease in the process variability (Figure 5.4), we may see that the D-SN-C EWMA chart also detects this shift at the 29th sampling point.

Table 5.13: Values of SD_t, SD_t^*, Z_t^* of each subgroups for the two examples

	Example plotted in Figure 5.3			Example plotted in Figure 5.4		
Subgroup	SD_t	SD_t^*	Z_t^*	SD_t	SD_t^*	Z_t^*
1	-5	-4.905	-4.601	-1	-1.033	-0.258
2	-5	-5.142	-4.736	-1	-1.051	-0.456
3	-5	-4.878	-4.772	-1	-0.861	-0.557
4	-3	-3.187	-4.376	1	1.111	-0.140
5	-5	-5.251	-4.594	-1	-1.138	-0.390
6	-5	-4.942	-4.681	3	2.859	0.422
7	-3	-3.089	-4.283	5	5.073	1.585
8	-5	-5.000	-4.462	-5	-4.846	-0.023
9	-5	-4.985	-4.593	1	0.978	0.227
10	-5	-5.118	-4.724	3	3.176	0.965
11	-5	-5.114	-4.822	1	1.080	0.993
12	-5	-5.027	-4.873	-3	-3.122	-0.036
13	-3	-2.764	-4.346	3	3.068	0.740
14	-5	-5.305	-4.586	1	0.774	0.749
15	-3	-2.881	-4.159	3	3.287	1.383
16	-5	-4.933	-4.353	3	3.396	1.886
17	-5	-4.787	-4.462	3	2.927	2.146
18	-5	-5.061	-4.611	3	2.791	2.308
19	-5	-4.926	-4.690	1	1.114	2.009
20	-3	-2.947	-4.254	1	0.973	1.750
21	-3	-3.109	-3.968	-3	-2.520	0.683
22	-1	-0.758	-3.165	-5	-5.008	-0.740
23	-3	-2.768	-3.066	-1	-0.862	-0.770
24	-3	-2.860	-3.015	-3	-2.994	-1.326
25	-1	-0.683	-2.432	1	0.851	-0.782
26	1	1.112	-1.546	-5	-4.962	-1.827
27	-3	-3.255	-1.973	-3	-3.361	-2.211
28	-1	-1.115	-1.759	-3	-2.707	-2.335
29	-5	-5.245	-2.630	-3	-2.969	-2.493
30	-1	-1.095	-2.246	-5	-4.565	-3.011

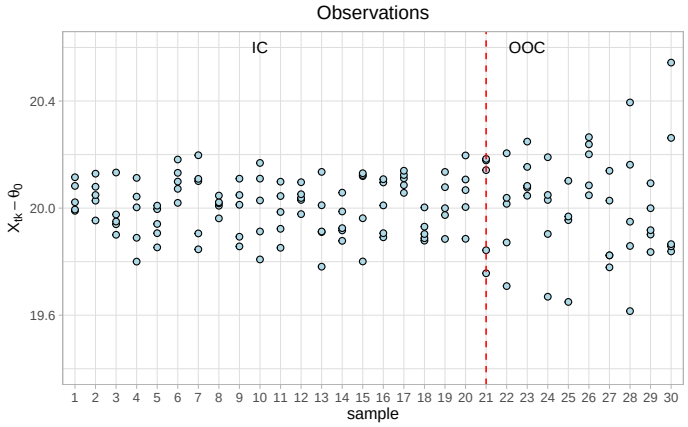

Figure 5.1: Dataset for the first example

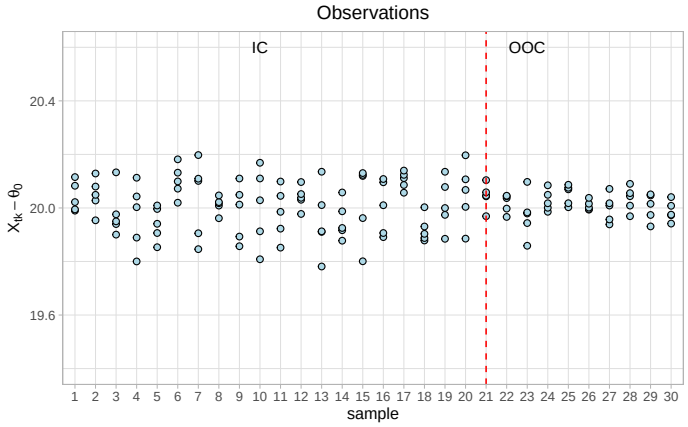

Figure 5.2: Dataset for the second example

5.4 Conclusions

In this Chapter two new Shewhart and EWMA Sign-type control schemes have been presented for monitoring shifts in the process variability. In their design, the in-control value of the probability, p_0, instead of being fixed was allowed to vary. It was proven that, by varying the value of p_0, the chart's performance is improved significantly for detecting

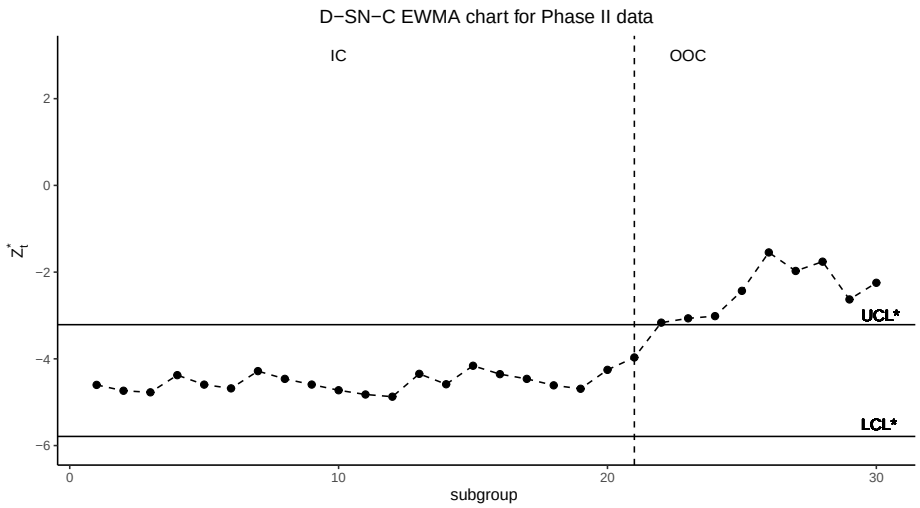

Figure 5.3: The D-SN-C EWMA chart for the Phase II data presented in Figure 5.1

increases or decreases in the process dispersion. After performing several comparisons it was proven that the proposed Sign-type EWMA chart is an efficient scheme and it can be considered as a good alternative since its superiority was proven against nonparametric or even parametric existing control charts.

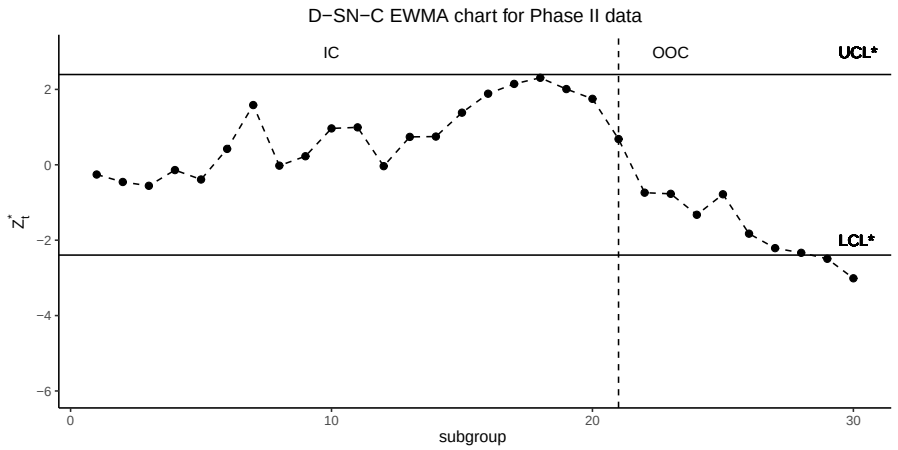

Figure 5.4: The D-SN-C EWMA chart for the Phase II data presented in Figure 5.2

Chapter 6

EWMA Signed Ranks Control Charts with Reliable Run Length Performances

6.1 The EWMA-type chart based on Signed ranks for monitoring discrete statistics

Introduction

In this Section, using the approach of Rakitzis et al. (2015) and the Shewhart sign control chart proposed by Amin et al. (1995), we will propose a modified distribution EWMA-type control chart using the Wilcoxon Signed Rank statistic. Parts of this Chapter have been published in Perdikis et al. (2021a) and Perdikis et al. (2021b).

6.1.1 A short review on the CEWMA SN chart

Castagliola et al. (2019), following the approach of Rakitzis et al. (2015), introduced a new nonparametric EWMA-type chart based on the Sign statistic (denoted as CEWMA SN chart) for monitoring shifts in the location parameter providing exact results for its Run Length distribution. In particular, Castagliola et al. (2019) proposed a modified recursive formula, equivalent with the original one presented in Chapter 2, with the only difference that now the plotting statistic is discrete. More specifically, the following recursive formula is considered

$$Y_t = \gamma_x \mathrm{SN}_t + \gamma_y Y_{t-1}, , t \leq 1, \tag{6.1}$$

where $(\gamma_x, \gamma_y) \in \mathbb{N}^2$ are two fixed positive *integer-valued* parameters. It should be noted that, even though using the formula in (6.1) we obtain integer values for Y_t, the sequence $Y_1, Y_2, \ldots$ goes (rather) rapidly to infinity. This fact has been originally mentioned by Rakitzis et al. (2015). In order to tackle this problem, a simple "standardization" is applied by dividing the term in the right hand side (RHS) of (6.1) with $\gamma_x + \gamma_y$:

$$Y_t = \frac{\gamma_x + \mathrm{SN}_t + \gamma_y Y_{t-1}}{\gamma_x + \gamma_y}. \tag{6.2}$$

It is clear that the above expression is the same with the conventional EWMA formula presented in Chapter 2 with $\lambda = \frac{\gamma_x}{\gamma_x+\gamma_y}$. However, let us keep in mind that the primary goal is to obtain integer values for Y_t but in (6.2), Y_t is no longer an integer. As a solution, Rakitzis et al. (2015), in order to ensure only integer values for Y_t's, the Euclidean division is used with a remainder R_t as:

$$(\gamma_x + \gamma_y)Y_t + R_t = \gamma_x \mathrm{SN}_t + \gamma_y Y_{t-1} \tag{6.3}$$

Note that, at the $t-1$-th sampling point, in equation (6.2), apart from Y_{t-1}, the remainder R_{t-1} is also available and must contribute to the value of Y_t at time t and so:

$$(\gamma_x + \gamma_y)Y_t + R_t = \gamma_x \mathrm{SN}_t + \gamma_y Y_{t-1} + R_{t-1}. \tag{6.4}$$

It is worth stretching that solving (6.4) with respect to Y_t we obtain the classical formula of a two-sided Sign EWMA chart as:

$$Y_t = \frac{\gamma_x}{\gamma_x + \gamma_y}\mathrm{SN}_t + \frac{\gamma_y}{\gamma_x + \gamma_y}Y_{t-1} + \frac{R_{t-1} - R_t}{\gamma_x + \gamma_y}. \tag{6.5}$$

where $\lambda = \frac{\gamma_x}{\gamma_x+\gamma_y}$ is the smoothing parameter as shown before and $\frac{R_{t-1}-R_t}{\gamma_x+\gamma_y}$ the is rounding factor, defined in:

$$\{-1 + \frac{1}{\gamma_x + \gamma_y}, -1 + \frac{2}{\gamma_x + \gamma_y}, \ldots, 1 - \frac{1}{\gamma_x + \gamma_y}\}$$

Finally, the plotting statistic, Y_t, for the CEWMA SN control chart is obtained as the quotient of the Euclidean division:

$$\left\lfloor \frac{\gamma_x \mathrm{SN}_t + B_{t-1}}{\gamma_x + \gamma_y} \right\rceil,$$

where $\lfloor \ldots \rceil$ denotes the rounded towards zero integer, $B_{t-1} \stackrel{\text{def}}{=} \gamma_y Y_{t-1} + R_{t-1}$, and R_t is the remainder of this Euclidean division defined as:

$$R_t = \gamma_x \mathrm{SN}_t + B_{t-1} - (\gamma_x + \gamma_y)Y_t.$$

When the initial values $Y_0 = y_0$, $R_0 = r_0$ and the current values SN_t, Y_{t-1}, R_{t-1} are fixed, both Y_t and R_t are uniquely defined. The initial values y_0 and r_0, are set equal to $y_0 = r_0 = 0$. However, if a head-start feature is desired, any choice of $y_0 \neq 0$ or $r_0 \neq 0$ can be considered.

As explained by Castagliola et al. (2019), the former design allows practitioners to adjust *any* nonparametric statistic besides the Sign statistic in order to design an EWMA-type scheme in which the charting statistic will be an integer value. As a consequence, a proper Discrete Markov Chain method similar to the Brook and Evans (1972) method can be established in order to guarantee exact Run Length properties for the control chart.

6.1.2 Design of the CEWMA WSR control chart

Similarly with the design of the CEWMA SN control chart, at each sampling point, the plotting statistic Y_t for the CEWMA WSR control chart is obtained through the following formula:

$$(\gamma_x + \gamma_y)Y_t + R_t = \gamma_x \text{SR}_t + \underbrace{\gamma_y Y_{t-1} + R_{t-1}}_{B_{t-1}}. \tag{6.6}$$

Concerning the initial values y_0 and r_0 for Y_0 and R_0 they are both set to $y_0 = r_0 = 0$. The process is declared to be in-control if $-K < Y_t < K$ and out-of-control otherwise where $K \in \{2, \ldots, \frac{n(n+1)}{2}\}$. Let us consider an example presented in Table 6.1 in order to clarify the design and operations of the charting statistic Y_t of our proposed scheme. A simulated dataset containing $m = 15$ subgroups of size $n = 10$ have been simulated where the first 10 subgroups are considered as in-control samples ($p_0 = 0.5$) and the other 5 subgroups as out-of-control samples ($p_1 = 0.8$). For illustrative purposes the design parameters are $\gamma_x = 1$ and $\gamma_y = 5$, respectively and no head-start feature is used (i.e. $Y_0 = 0$ and $R_0 = 0$). The values of Y_t are computed as follows:

- For $t = 1$ we have $Y_0 = 0$, $R_0 = 0$, $\text{SR}_1 = -17$ and the equation to be solved is $6 \times Y_1 + R_1 = 1 \times (-17) + 5 \times 0 + 0 = -17$. The unique solution of this equation (as an Euclidean division) is $Y_1 = -2$ and $R_1 = -5$.

- For $t = 2$ we have $Y_1 = -2$, $R_1 = -5$, $\text{SR}_2 = 15$ and the equation to be solved is $6 \times Y_2 + R_2 = 1 \times (15) + 5 \times (-2) - 5 = 0$. The unique solution of this equation is $Y_2 = 0$ and $R_2 = 0$.
  $\vdots$

- For $t = 15$ we have $Y_{14} = 15$, $R_{14} = 0$, $\text{SR}_{15} = 47$ and the equation to be solved is

Table 6.1: An example of calculation of Y_t and R_t given SR_t

t	SR_t	Y_t	R_t
0	-	0	0
1	-17	-2	-5
2	15	0	0
3	21	3	3
4	-7	1	5
5	-15	0	-5
6	-13	-3	0
7	-31	-7	-4
8	-9	-8	0
9	37	0	-3
10	47	7	2
11	25	10	2
12	13	10	5
13	27	13	4
14	21	15	0
15	47	20	2

$6 \times Y_{15} + R_{15} = 1 \times (47) + 5 \times (15) + 0 = 122$. The unique solution of this equation is $Y_{15} = 20$ and $R_{15} = 2$.

It is interesting to note that the values of the charting statistic, Y_t reacts similarly as for a classical EWMA chart, i.e. they are randomly distributed around zero when the process is in-control (samples $1 - 10$) and they start to increase when a shift occurs (samples $11 - 15$). This fact has also been mentioned in Castagliola et al. (2019). Also note that, our proposed scheme can both be extended to monitor any particular quantiles (provided that the sample size n is large enough) by changing the value $p_0 = 0.5$ to any other value of interest.

It is well acknowledged into the literature that in a conventional EWMA chart varying the value of the smoothing parameter, λ, allows more weight to be assigned to the past ($\lambda \to 0$), or to the current observations ($\lambda \to 1$). As pointed out in Rakitzis et al. (2015), if $\gamma_x < \gamma_y$ then the CEWMA scheme assigns more weight to the past observations while, if $\gamma_x > \gamma_y$, this scheme assigns more weight to the most recent ones. For instance, setting $\gamma_x = 2, \gamma_y = 98$ the corresponding value for the "conventional" smoothing parameter equals to $\lambda = \frac{\gamma_x}{\gamma_x + \gamma_y} = \frac{2}{100} = 0.02$ which is close to zero. On the other hand, if we set $\gamma_x = 9, \gamma_y = 1$ then $\lambda = \frac{9}{10} = 0.9$ which is close to 1.

Additionally, the corresponding limiting conditions for the CEWMA WSR chart in the case where $\lambda = 1$ or $\lambda = 0$ can be expressed respectively as:

- for $\gamma_x > 0$ and $\gamma_y = 0$ we have $Y_t = \mathrm{SR}_t$ and $R_t = r_0$, $t = 1, 2, \ldots$. Consequently, in this situation, the CEWMA WSR chart coincides with the nonparametric Shewhart-type control chart based on signed ranks proposed by Bakir (2004).
- for $\gamma_x = 0$ and $\gamma_y > 0$ we have $Y_t = y_0$ and $R_t = r_0$, $t = 1, 2, \ldots$

6.1.3 Run length properties of the CEWMA WSR chart

Using the design proposed by Castagliola et al. (2019), we are able to obtain an integer value for the charting statistic, even though that the value to be monitored (such as the Sign or the Wilcoxon) is discrete.

In order to obtain the exact RL properties of our proposed scheme, the discrete-time Markov chain approach presented for the CEWMA SN control chart is used. Specifically, the transition probability matrix $\mathbf{P}$ is defined as:

$$\mathbf{P} = \begin{pmatrix} \mathbf{Q} & \mathbf{r} \\ \mathbf{0}^\intercal & 1 \end{pmatrix} = \begin{pmatrix} q_{-b,-b} & q_{-b,-b+1} & \cdots & q_{-b,b-1} & q_{-b,b} & r_{-b} \\ q_{-b+1,-b} & q_{-b+1,-b+1} & \cdots & q_{-b+1,b-1} & q_{-b+1,b} & r_{-b+1} \\ \vdots & \vdots & \ddots & \vdots & \vdots & \vdots \\ q_{-b+1,-b} & q_{b-1,-b+1} & \cdots & q_{b-1,b-1} & q_{b-1,b} & r_{b-1} \\ 0 & 0 & \ldots & 0 & 0 & 1 \end{pmatrix}$$

where $\mathbf{Q}$ is the $(2b+1, 2b+1)$ matrix of transient probabilities $q_{i,j}$, $\mathbf{0}^\intercal = (0, 0, \ldots, 0)$ and $\mathbf{r} = \mathbf{1} - \mathbf{Q}\mathbf{1}$. Similar to the approach used for the CEWMA (Rakitzis et al. (2015)) and CEWMA SN (Castagliola et al. (2019)) charts, at time $t-1$ the transient states of the discrete-time Markov chain will be defined as the integers $b_{t-1} \in \{-b, -b+1, \ldots, +b\}$ where $b = \gamma_x + K\gamma_y - 1$. More specifically, assuming that at time $t-1$, as long as $y_{t-1} \in \{-K+1, \ldots, K-1\}$ the process is declared to be in-control, the transient states of the discrete-time Markov chain are defined as the integers $b_{t-1} \in \{\gamma_y \times y_{t-1} + r_{t-1}\}$ where $r_{t-1} \in \{-\gamma_x - \gamma_y + 1, \ldots, \gamma_x + \gamma_y - 1\}$. As a consequence, the minimum, $b_{\min}$, and the maximum, $b_{\max}$, numbers of states are respectively defined as

$$\begin{aligned} b_{\min} &= \gamma_y(-K+1) - \gamma_x - \gamma_y + 1 = -\gamma_x - K\gamma_y + 1, \\ b_{\max} &= \gamma_y(K-1) + \gamma_x + \gamma_y - 1 = \gamma_x + K\gamma_y - 1, \end{aligned}$$

where $b = b_{\max} = -b_{\min}$. As a result, the total number of transient states is $2b + 1 =$

$2(\gamma_x + K\gamma_y - 1) + 1$. Finally, each transient probability $q_{i,j}$ is computed using the p.m.f. of SR_t as introduced in Chapter 2. In summary, the transient probabilities $q_{i,j}$ will be computed as detailed in Algorithm 6.1. So far, regarding the design of our proposed two important advantages may be highlighted:

- The *exact* number of transient states b has been defined and so the chart's Run Length properties will be no longer depend on the number of subintervals nor on any approximation.
- Since the general distribution of SR_t has been defined we are able to compute exactly any probabilities, not only for the in-control case but also for the out-of-control one.

For a better understanding of the structure of the matrix of the transient probabilities $\mathbf{q}$ an example is presented for $K = 2, \gamma_x = 3, \gamma_y = 2$ and $n = 5$ in Table 6.2. In particular, the integer values inside the matrix are the values of SR_t that must be replaced by the probability $f_{\mathrm{SR}_t}(s|n, p_1)$ in matrix $\mathbf{Q}$ and the "." are the positions where the probabilities are equal to 0. More specifically, since $K = 2, \gamma_x = 3, \gamma_y = 2$ the total number of transient states is $2b+1 = 2 \times (\gamma_x + K\gamma_y - 1) + 1 = 2 \times (3 + 2 \times 2 - 1) + 1 = 13$, i.e. $i, j \in \{-6, \ldots 0, \ldots, 6\}$. If we take as an example state $i = -6$, since $\mathrm{SR}_t \in \{-15, -13, \ldots, 15\}$ we have the following:

- For $\mathrm{SR}_t = -1$ then $Y_t = \left\lfloor \frac{3\times 1-6}{5} \right\rceil = -2$, and since $-2 < Y_t < 2$, we have $r = 3 \times (-1) - 5 \times (-2) = 1$ and the process moves to the transient state $j = -6$ with a probability $f_{SR_t}(-1|5, p_1)$.
- For $\mathrm{SR}_t = 1$ then $Y_t = \left\lfloor \frac{3\times(-1)-6}{5} \right\rceil = -1$, and since $-2 < Y_t < 2$, we have $r = 3 \times 1 - 5 \times (-1) = 2$ and the process moves to the transient state $j = -3$ with a probability $f_{SR_t}(1|5, p_1)$.
- For $\mathrm{SR}_t = 3$ then $Y_t = \left\lfloor \frac{3\times 3-6}{5} \right\rceil = 0$, and since $-2 < Y_t < 2$, we have $r = 3\times 3-5\times 0 = 2$ and the process moves to the transient state $j = 3$ with a probability $f_{SR_t}(3|5, p_1)$.
- For $\mathrm{SR}_t = 5$ then $Y_t = \left\lfloor \frac{3\times 5-6}{5} \right\rceil = 1$, and since $-2 < Y_t < 2$, we have $r = 3\times 5-5\times 1 = 4$ and the process moves to the transient state $j = 6$ with a probability $f_{SR_t}(5|5, p_1)$.
- For the remaining values of $\mathrm{SR}_t \notin \{-1, 1, 5\}$ the process moves to the absorbing state.

Algorithm 6.1 Computation of transient probabilities $q_{i,j}$

Define n, K, γ_x, γ_y and p_1.
$b \leftarrow \gamma_x + K\gamma_y - 1$.
for $i = -b, -b+1, \ldots, b-1, b$ **do**
  for $\mathrm{SR} = -\frac{n(n+1)}{2}, -\frac{n(n+1)}{2}+2, \ldots, \frac{n(n+1)}{2}-2, \frac{n(n+1)}{2}$ **do**
    $y \leftarrow \left\lfloor \frac{\gamma_x \times \mathrm{SR}+i}{\gamma_x+\gamma_y} \right\rceil$.
    if $-K < y < K$ **then**
      $r \leftarrow \gamma_x \times \mathrm{SR} + i - (\gamma_x + \gamma_y) \times y$.
      $j \leftarrow \gamma_y \times y + r$.
      $q_{i,j} \leftarrow q_{i,j} + f_{\mathrm{SR}^+}\left(\frac{\mathrm{SR}+\frac{n(n+1)}{2}}{2} | n, p_1\right)$.
    end if
  end for
end for

Table 6.2: Structure of matrix when $K = 2, \gamma_x = 3, \gamma_y = 2$ and $n = 5$

		j												
		-6	-5	-4	-3	-2	-1	0	1	2	3	4	5	6
	-6	-1	.	.	1	.	.	.	.	.	3	.	.	5
	-5	.	-1	.	.	1	.	.	.	.	.	3	.	.
	-4	.	.	-1	.	.	1	.	.	3	.	.	.	.
	-3	.	.	.	-1	.	.	1	.	.	3	.	.	.
	-2	.	.	.	.	-1	.	.	1	.	.	3	.	.
i	-1	.	.	-1	.	.	.	.	.	1	.	.	3	.
	0	-3	.	.	-1	.	.	.	.	.	1	.	.	3
	1	.	-3	.	.	-1	.	.	.	.	.	1	.	.
	2	.	.	-3	.	.	-1	.	.	1	.	.	.	.
	3	.	.	.	-3	.	.	-1	.	.	1	.	.	.
	4	.	.	.	.	-3	.	.	-1	.	.	1	.	.
	5	.	.	-3	.	.	.	.	.	-1	.	.	1	.
	6	-5	.	.	-3	.	.	.	.	.	-1	.	.	1

Finally, since we defined the exact number of transient probabilities and the structure of matrix $\mathbf{Q}$, the RL properties of the CEWMA WSR chart will be obtained using the same equations presented in (1.7) and (1.8).

6.1.4 Performance Comparisons

In this work, the parameter θ_0 will be considered as the median of the process distribution, so we assume $p_0 = 0.5$. For fixed values of the sample size n and $p_1 = \mathrm{P}(X_{t,j} > \theta_0 | \theta = \theta_1)$, in order to obtain the optimal combination of the design parameters $(K^*, \gamma_x^*, \gamma_y^*)$ which will provide the minimum corresponding out-of-control ARL, a specific search algorithm is used aiming to select the optimal values of (K, γ_x, γ_y) which guarantee the following conditions:

$$(K^*, \gamma_x^*, \gamma_y^*) = \underset{(K,\gamma_x,\gamma_y)}{\operatorname{argmin}} \mathrm{ARL}(K, \gamma_x, \gamma_y, n, p_1)$$

$$\mathrm{ARL}(K^*, \gamma_x^*, \gamma_y^*, n, p_0) = \mathrm{ARL}_0$$

where $\mathrm{ARL}_0 = 370.4$ is the target in-control ARL value. Due to the fact that the charting statistic, Y_t, is a discrete random variable, it is not possible to find an optimal combination $(K^*, \gamma_x^*, \gamma_y^*)$ that *exactly* meets the constraint $\mathrm{ARL}(K^*, \gamma_x^*, \gamma_y^*, n, p_0) = \mathrm{ARL}_0$. Similarly to the design of the CEWMA SN chart, we suggest to accept, as tentative design parameters, all those combinations of parameters $(K^*, \gamma_x^*, \gamma_y^*)$ satisfying the following condition:

$$D(K^*, \gamma_x^*, \gamma_y^*, n) = \frac{\left|\mathrm{ARL}(K^*, \gamma_x^*, \gamma_y^*, n, p_0) - \mathrm{ARL}_0\right|}{\mathrm{ARL}_0} \leq \delta \tag{6.7}$$

where δ is a predefined constant. For the determination of the optimal parameters for $n = \{10, \ldots, 25\}$ in the CEWMA SN chart, Castagliola et al. set $\delta = 0.05$ (see Castagliola et al. (2019)), to ensure that the corresponding optimal combination of $(K^*, \gamma_x^*, \gamma_y^*)$ will be obtained successfully. Based on our findings, we saw that, in general, the CEWMA WSR chart guarantees a smaller error than the CEWMA SN chart with respect to the constraint on the nominal in-control performance. As a consequence, for the determination of the design parameters of the CEWMA WSR control chart we suggest to set $\delta = 0.01$. Additionally, since $\mathrm{ARL}(K, \gamma_x, \gamma_y, n, p_1) = \mathrm{ARL}(K, \gamma_x, \gamma_y, n, 1-p_1)$ we will only focus on shifts $p_1 \in (0, 0.5)$ as the same results would have been obtained for $p_1 \in (0.5, 1)$. As a consequence, for given values of n and p_1, the optimal combination of the design parameters $(K^*, \gamma_x^*, \gamma_y^*)$ will be obtained through the searching Algorithm 6.2.

In the following tables some results regarding the performance of our proposed chart are provided, including comparisons with the CEWMA SN chart. In Table 6.3, the optimal combinations $(K^*, \gamma_x^*, \gamma_y^*)$ for our proposed chart are given, along with the corresponding in-control and out-of-control ARLs for $n = \{10, \ldots, 25\}$. Based on the results presented in Table 6.3 it can be concluded that when $p_1 < 0.5$, for large values of the sample size or large shifts ($p_1 \simeq 0$) the corresponding optimal ARL_1 values tend to decrease. In addition, for

Algorithm 6.2 Computation of optimal combination $(K^*, \gamma_x^*, \gamma_y^*)$

Define n and $p_1 \in (0, 0.5)$.
$\text{ARL}_0 \leftarrow 370.4$.
$\text{ARL}^* \leftarrow \infty$.
for $K = 1, \ldots, \frac{n(n+1)}{2}$ **do**
  for $\gamma_x = 1, 2, \ldots$ **do**
    $\gamma_y \leftarrow 0$.
    repeat
      $\gamma_y \leftarrow \gamma_y + 1$
    until $D(K, \gamma_x, \gamma_y, n) \leq 0.01$
    if $\text{ARL}(K, \gamma_x, \gamma_y, n, p_1) < \text{ARL}^*$ **then**
      $\text{ARL}^* \leftarrow \text{ARL}(K, \gamma_x, \gamma_y, n, p_1)$,
      $K^* \leftarrow K$, $\gamma_x^* \leftarrow \gamma_x$ and $\gamma_y^* \leftarrow \gamma_y$.
    end if
  end for
end for

fixed values in the sample size, as the value of $p_1 < 0.5$ becomes closer to 0.5 the "smoothing ratio" $\frac{\gamma_x}{\gamma_x+\gamma_y}$ and the value of the control limit K of our proposed chart also tend to decrease. For example for $n = 20$ and $p_1 \in \{0.05, \ldots, 0.2\}$, we have $\frac{\gamma_x}{\gamma_x+\gamma_y} = \frac{10}{10+3} = 0.77$ and the control limit equals to $K = 117$. On the other hand for $p_1 = 0.4$ the corresponding smoothing ratio equals to $\frac{\gamma_x}{\gamma_x+\gamma_y} = \frac{4}{4+27} = 0.13$ and $K = 39$. It is worth mentioning that these findings are consistent with the ones of the CEWMA (see Rakitzis et al. (2015)) and CEWMA SN (see Castagliola et al. (2019)) charts.

In Table 6.4 the performance of our proposed chart is compared to the CEWMA SN chart for $n \in \{5, \ldots, 25\}$ and $p_1 \in \{0.05, 0.1, \ldots, 0.45\}$. In order to make fair comparisons, we obtained the optimal design parameters of the CEWMA SN with corresponding $D(K^*, \gamma_x^*, \gamma_y^*, n) \leq 0.01$ (except from some values of n where the bound 0.01 in (6.7) has been replaced by 0.02), for $n \in \{5, 6, \ldots, 25\}$ and $p_1 \in \{0.05, 0.1, \ldots, 0.45\}$. The Δ values are defined as:

$$\Delta = 100 \times \frac{\text{ARL}_{\text{SR}} - \text{ARL}_{\text{SN}}}{\text{ARL}_{\text{SN}}},$$

where ARL_{SN} and ARL_{SR} are the ARL values of the CEWMA SN and CEWMA WSR charts respectively. A negative value for Δ corresponds to an outperformance of the CEWMA WSR scheme versus the CEWMA SN chart. According to our findings, it can be concluded that when $5 \leq n \leq 15$, for large shifts ($p_1 \leq 0.2$) in 55% of the cases the CEWMA WSR scheme has a better performance. In addition for small to moderate shifts ($p_1 > 0.2$) in 60% of the cases the CEWMA WSR chart also outperforms the CEWMA SN chart. On the other

Table 6.3: Optimal combinations $(K^*, \gamma_x^*, \gamma_y^*)$ (first line of each block) for the CEWMA WSR chart along with the corresponding in-control ARL's (second line) and the out-of-control (ARL, SDRL) (first line) for $n \in \{10, \ldots, 25\}$ and $p_1 \in \{0.05, 0.1, \ldots, 0.45\}$

	p_1								
n	0.05	0.1	0.15	0.2	0.25	0.3	0.35	0.4	0.45
	(26,8,15)	(26,8,15)	(26,8,15)	(26,8,15)	(22,10,28)	(19,7,27)	(15,9,57)	(9,1,16)	(5,6,249)
	369	369	369	369	369.4	368.4	369.3	367.7	367.8
10	(2.2,0.4)	(2.6,0.7)	(3.2,1.1)	(4.1,1.8)	(5.5,2.5)	(7.8,4)	(12.3,6.7)	(22.4,12.1)	(57.6,35.4)
	(47,5,2)	(47,5,2)	(36,10,11)	(27,5,12)	(25,7,20)	(20,8,37)	(16,8,58)	(12,9,110)	(6,3,115)
	373.9	373.9	369.3	367.4	374	368.9	371.6	370.3	366.9
11	(1.5,0.7)	(2.1,1.1)	(2.9,1.1)	(3.8,1.5)	(5.1,2.3)	(7.3,3.4)	(11.5,5.9)	(21,12)	(54.2,33.4)
	(55,9,3)	(53,5,2)	(34,6,11)	(34,6,11)	(29,10,27)	(25,10,38)	(21,7,38)	(13,7,92)	(7,7,255)
	367.3	368.1	370.4	370.4	370.5	371.2	369.9	366.7	370.3
12	(1.5,0.7)	(2,1)	(2.8,0.9)	(3.6,1.5)	(4.8,2.1)	(6.9,3.3)	(10.8,5.9)	(19.7,10.8)	(51.5,31.6)
	(43,3,4)	(43,3,4)	(43,9,12)	(43,9,12)	(32,6,17)	(30,8,26)	(22,6,37)	(15,7,87)	(7,1,43)
	368.4	368.4	368.4	368.4	373.2	368.2	368.7	368.1	368.2
13	(2,0.2)	(2.2,0.5)	(2.7,0.9)	(3.4,1.5)	(4.6,1.9)	(6.5,3.2)	(10.1,5.2)	(18.6,10.2)	(49.1,28.5)
	(73,8,2)	(73,8,2)	(57,9,7)	(49,4,5)	(36,9,25)	(34,7,22)	(24,5,32)	(16,3,40)	(9,3,103)
	369.1	369.1	367.6	368	369.9	367.3	371.1	369.1	369.1
14	(1.4,0.6)	(1.9,0.9)	(2.4,1)	(3.2,1.4)	(4.3,1.8)	(6.1,3)	(9.6,4.7)	(17.8,9.3)	(46.7,28.2)
	(81,4,1)	(81,4,1)	(71,4,2)	(57,10,11)	(49,9,15)	(34,7,27)	(29,8,43)	(21,6,59)	(11,4,117)
	366.8	366.8	371.5	373.6	368.8	367.2	366.8	368.9	372.6
15	(1.3,0.5)	(1.7,0.9)	(2.3,1.1)	(3,1.3)	(4.1,1.9)	(5.8,2.6)	(9.1,4.6)	(16.9,9.5)	(44.8,27.7)
	(91,9,2)	(91,9,2)	(67,9,8)	(55,7,11)	(45,5,13)	(47,9,21)	(31,3,17)	(23,6,59)	(12,3,88)
	367	367	370.7	366.8	371.3	368.6	372.8	368.3	366.7
16	(1.3,0.5)	(1.7,0.8)	(2.2,0.8)	(2.9,1.1)	(3.9,1.6)	(5.6,2.9)	(8.7,4.3)	(16.1,8.9)	(42.8,26.1)
	(96,7,2)	(96,7,2)	(83,7,4)	(74,7,6)	(60,5,8)	(45,7,22)	(37,4,19)	(23,2,23)	(14,3,79)
	369.2	369.2	372.4	367.4	371.3	369.8	371.2	368.3	367.8
17	(1.2,0.4)	(1.6,0.7)	(2.1,0.9)	(2.8,1.3)	(3.7,1.7)	(5.3,2.4)	(8.3,4.2)	(15.4,8)	(41.2,25.4)
	(117,8,1)	(117,8,1)	(98,5,2)	(77,10,10)	(69,8,11)	(51,8,23)	(40,5,24)	(30,7,58)	(14,1,30)
	367.1	367.1	372.5	371.7	368.6	370.6	368.3	367.3	369.6
18	(1.1,0.4)	(1.5,0.8)	(2,1)	(2.7,1.1)	(3.6,1.7)	(5.1,2.3)	(8,4)	(14.8,8.3)	(39.7,23.4)
	(108,8,3)	(108,8,3)	(96,8,5)	(96,8,5)	(71,7,11)	(60,8,19)	(48,7,27)	(29,6,61)	(16,2,55)
	370.5	370.5	367.5	367.5	370.5	370	367.8	368.4	370.3
19	(1.1,0.4)	(1.4,0.6)	(1.9,0.8)	(2.5,1.3)	(3.4,1.5)	(4.9,2.4)	(7.7,4)	(14.2,7.4)	(38.3,22.8)
	(117,8,3)	(117,8,3)	(117,8,3)	(102,9,6)	(75,3,5)	(57,7,22)	(51,8,32)	(39,4,27)	(17,2,56)
	372.7	372.7	372.7	373.6	370.5	369.5	371.8	368.2	368
20	(1.1,0.3)	(1.4,0.6)	(1.8,0.9)	(2.5,1.2)	(3.3,1.4)	(4.7,2)	(7.4,3.8)	(13.8,8)	(37,21.7)
	(131,10,3)	(131,10,3)	(131,10,3)	(118,10,5)	(85,9,13)	(70,3,7)	(52,7,31)	(37,2,17)	(23,3,58)
	373.1	373.1	373.1	370.8	367.3	371.3	368.8	368.9	370.6
21	(1.1,0.3)	(1.3,0.5)	(1.8,0.9)	(2.4,1.2)	(3.2,1.4)	(4.5,2.1)	(7.1,3.4)	(13.2,7)	(36.1,23)
	(156,7,1)	(156,7,1)	(148,9,2)	(107,10,9)	(91,9,13)	(80,7,14)	(63,9,31)	(44,4,28)	(23,2,43)
	367.8	367.8	368.6	367.5	370.4	367.3	367.9	366.9	367.1
22	(1.1,0.2)	(1.3,0.5)	(1.7,0.9)	(2.3,0.9)	(3.1,1.3)	(4.4,2.1)	(6.9,3.6)	(12.8,7.1)	(34.7,21.3)
	(164,6,1)	(164,6,1)	(139,9,4)	(123,7,5)	(107,9,10)	(92,9,15)	(69,4,13)	(41,1,9)	(28,3,52)
	368.8	368.8	373.2	370.2	369.2	373.1	371.8	370.8	368.8
23	(1.1,0.2)	(1.2,0.5)	(1.6,0.7)	(2.2,1)	(3,1.4)	(4.3,2.2)	(6.7,3.5)	(12.4,6.3)	(34,21.9)
	(157,6,2)	(148,9,4)	(157,9,3)	(131,7,5)	(109,8,10)	(88,6,13)	(71,4,14)	(49,4,29)	(17,1,42)
	371.3	367.6	371.3	373.4	368	366.8	372.5	368.5	372
24	(1,0.2)	(1.2,0.5)	(1.6,0.7)	(2.1,0.9)	(2.9,1.2)	(4.1,1.9)	(6.5,3.2)	(12,6.4)	(33.7,17.1)
	(163,8,3)	(148,7,4)	(163,8,3)	(148,7,4)	(104,3,5)	(102,8,14)	(78,4,13)	(56,3,19)	(29,1,20)
	373	372.1	373	372.1	369.6	366.9	368.7	370.6	369.2
25	(1,0.2)	(1.2,0.5)	(1.5,0.7)	(2,0.9)	(2.8,1.1)	(4,1.9)	(6.2,3.2)	(11.7,6.5)	(31.9,19.3)

Table 6.4: Comparison between the CEWMA SN and CEWMA WSR chart for $n \in \{5, \ldots, 25\}$ and $p_1 \in \{0.05, 0.1, \ldots, 0.45\}$

	p_1								
n	0.05	0.1	0.15	0.2	0.25	0.3	0.35	0.4	0.45
5	**-37.21**	**-22.45**	**-10.53**	**-2.90**	3.45	11.21	18.75	6.91	**-11.55**
6	37.50	26.67	12.20	0.00	**-14.89**	**-31.93**	**-32.31**	**-18.97**	1.42
7	**-22.58**	**-8.82**	0.00	8.16	12.70	15.91	9.72	**-6.23**	**-2.05**
8	9.09	11.54	15.62	16.67	8.33	12.20	12.50	1.16	**-3.06**
9	57.14	35.00	21.43	**-2.22**	**-24.36**	**-44.44**	**-38.32**	**-25.00**	**-3.61**
10	**-69.01**	**-67.09**	**-64.44**	**-60.58**	**-55.65**	**-49.68**	**-40.00**	**-27.04**	**-5.73**
11	**-28.57**	**-12.50**	3.57	8.57	15.91	17.74	16.16	**-1.41**	**-6.39**
12	0.00	11.11	21.74	16.13	6.67	**-8.00**	**-28.95**	**-50.50**	**-63.14**
13	81.82	57.14	42.11	21.43	2.22	**-24.42**	**-44.20**	**-31.11**	**-8.74**
14	16.67	26.67	20.00	10.34	**-6.52**	**-25.61**	**-44.19**	**-30.74**	**-8.61**
15	**-35.00**	**-26.09**	**-14.81**	**-6.25**	5.13	11.54	18.18	19.01	5.66
16	30.00	41.67	37.50	31.82	11.43	16.67	19.18	20.15	9.18
17	**-77.78**	**-74.19**	**-70.00**	**-65.43**	**-61.46**	**-55.46**	**-47.47**	**-34.47**	**-11.59**
18	**-63.33**	**-57.14**	**-50.00**	**-42.55**	**-35.71**	**-27.14**	**-14.89**	0.68	16.08
19	0.00	7.69	11.76	13.64	6.25	**-10.91**	**-35.29**	**-36.61**	**-13.93**
20	0.00	7.69	5.88	19.05	17.86	14.63	15.62	21.05	15.62
21	**-78.00**	**-76.79**	**-71.43**	**-67.12**	**-63.22**	**-58.33**	**-50.35**	**-38.03**	**-14.45**
22	**-35.29**	**-31.58**	**-15.00**	0.00	10.71	18.92	21.05	17.43	**-11.93**
23	10.00	0.00	6.67	15.79	20.00	19.44	3.08	**-6.06**	14.48
24	0.00	9.09	23.08	23.53	20.83	13.89	12.07	20.00	11.22
25	0.00	9.09	15.38	17.65	21.74	14.29	19.23	20.62	19.03

hand, for $n > 15$, when $p_1 \leq 0.2$ or $p_1 > 0.2$ the CEWMA WSR chart performs better only in 38% of the cases. As a consequence, in most cases, our proposed scheme has an overall better performance when $n < 15$ and, as the sample size increases, the CEWMA SN chart performs better.

In Tables 6.5 (for $n = 10$) and 6.6 (for $n = 20$) the CEWMA WSR chart is compared with other nonparametric schemes presented in the literature. More specifically, we examined the performance of the CEWMA WSR chart against the CEWMA SN chart, the two EWMA sign charts proposed by Yang et al. in Yang et al. (2011), denoted as standard sign EWMA (EWMA) and arcsine sign EWMA (A-EWMA), the distribution free cumulative sum mean chart (CUSUM) of Yang et al. in Yang and Cheng (2011) and the modified sign EWMA chart proposed by Lu in Lu (2015) (S-GWMA). For the computation of the in- and out-of-control ARL values of the competitors of the CEWMA WSR chart, a Monte Carlo simulation was performed, except for the CEWMA SN chart where the exact Markov chain approach was used. Regarding the design parameters of each chart, for the CEWMA WSR and CEWMA SN charts (K, γ_x, γ_y) have been selected to get the optimal performance for each chart; for the EWMA charts proposed in Yang et al. (2011), the pair (λ, W) corresponds to the optimal values of the smoothing parameter λ and the distance W. Moreover, the pair (k, h) corresponds to the values of the reference value k and the decision interval h of the CUSUM chart. Finally, (q, α, W) correspond to the values of the design parameters for the S-GWMA chart. For more information regarding the design and operations of the above schemes the reader is advised to see Yang et al. (2011); Yang and Cheng (2011); Lu (2015).

Based on the results presented in Tables 6.5 and 6.6 it can be concluded that the CEWMA WSR chart outperforms its competitors for moderate to large shifts ($p_1 < 0.3$). On the other hand, for small shifts, i.e. when p_1 tends to be close to 0.5 the standard or the arcsine transformed EWMA chart have better performance. Finally, in cases where $0.25 < p_1 < 0.3$ the use of the S-GWMA chart or the SN EWMA can be considered.

6.2 The "continuousified" WSR EWMA chart with exact RL properties

6.2.1 Charting statistic, control limits and RL properties

As proposed by Wu et al. (2020), any discrete random variable, can be well-presented by a new *continuous* one as a mixture of Normal distributions. As a result, for the proposed scheme based on the Wilcoxon Signed Rank statistic, since the domain in which SR_t is defined

Table 6.5: ARL values of the CEWMA WSR chart, the CEWMA SN chart, the standard and the arcsine transformed EWMA chart, the CUSUM chart and the S-GWMA chart ($n = 10$, $p_0 = 0.50$, $\text{ARL}_0 \approx 370$)

p	CEWMA WSR	CEWMA SN	EWMA	A-EWMA	CUSUM	S-GWMA
0.50	369.0	371.4	366.3	367.6	370.0	370.6
0.45	131.4	61.1	**51.4**	51.4	63.2	58.0
0.40	38.0	30.9	**19.0**	19.0	20.2	19.0
0.30	8.6	15.5	8.1	7.9	7.9	**7.2**
0.25	5.6	12.4	6.3	6.1	6.0	**5.4**
0.20	**4.0**	10.4	5.2	4.9	4.9	4.3
0.15	**3.2**	9	4.4	4.1	4.2	3.6
0.10	**2.6**	7.0	3.9	3.4	3.6	3.1
0.05	**2.2**	7.0	3.4	2.9	3.2	2.7
γ_X	8	1	-	-	-	-
γ_Y	15	1	-	-	-	-
K	26	58	-	-	-	-
λ	-	-	0.05	0.05	-	-
W	-	-	2.487	2.487	-	2.698
k	-	-	-	-	0.5	-
h	-	-	-	-	10.65	-
q	-	-	-	-	-	0.9
α	-	-	-	-	-	0.9

Table 6.6: ARL values of the CEWMA WSR chart, the CEWMA SN chart, the standard and the arcsine transformed EWMA chart, the CUSUM chart and the S-GWMA chart ($n = 20$, $p_0 = 0.50$, $\text{ARL}_0 \approx 370$)

p	CEWMA WSR	CEWMA SN	EWMA	A-EWMA	CUSUM	S-GWMA
0.50	370.6	370.2	370.0	367.6	373.7	370.9
0.45	84.7	37.3	31.0	**30.9**	40.3	33.0
0.40	20.2	**11.4**	12.3	12.2	11.7	11.5
0.30	4.9	**4.5**	5.6	5.4	4.5	4.7
0.25	**3.3**	3.5	4.4	4.2	3.5	3.7
0.20	**2.6**	2.9	3.7	3.5	2.9	3.0
0.15	**2.1**	2.4	3.2	2.9	2.4	2.5
0.10	**1.8**	2.1	2.9	2.5	2.1	2.2
0.05	**1.5**	2.0	2.6	2.1	2.0	2.0
γ_X	3	3	-	-	-	-
γ_Y	5	16	-	-	-	-
K	75	4	-	-	-	-
λ	-	-	0.05	0.05	-	-
W	-	-	2.487	2.487	-	2.709
k	-	-	-	-	1.0	-
h	-	-	-	-	11.62	-
q	-	-	-	-	-	0.9
α	-	-	-	-	-	0.9

is $\Psi = \{-\frac{n(n+1)}{2}, -\frac{n(n+1)}{2}+2, \ldots, \frac{n(n+1)}{2}-2, \frac{n(n+1)}{2}\}$, the statistic SR_t can be transformed into a new *continuous* one denoted as SR_t^*:

$$f_{\mathrm{SR}_t^*}(s|n,p_1) = \sum_{\psi\in\Psi} f_{\mathrm{SR}_t^+}\left(\frac{\psi+\frac{n(n+1)}{2}}{2}|n,p_1\right) f_{\mathrm{N}}(s|\psi,h), \tag{6.8}$$

$$F_{\mathrm{SR}_t^*}(s|n,p_1) = \sum_{\psi\in\Psi} f_{\mathrm{SR}_t^+}\left(\frac{\psi+\frac{n(n+1)}{2}}{2}|n,p_1\right) F_{N}(s|\psi,h), \tag{6.9}$$

The two-sided case: Following the same design with the conventional two-sided EWMA chart, the charting statistic of the "continuousified" two-sided WSR EWMA (denoted as 2C-WSR EWMA chart) will be defined as:

$$Z_t^* = \lambda \mathrm{SR}_t^* + (1-\lambda)Z_{t-1}^*, Z_0^* = \mathrm{E}_0(\mathrm{SR}_t^*), \tag{6.10}$$

with fixed asymptotic control limits:

$$\mathrm{LCL}^* = \mathrm{E}_0(\mathrm{SR}_t^*) - K\sqrt{\mathrm{E}_0(\mathrm{SR}_t^*)} \times \sqrt{\frac{\lambda}{2-\lambda}}.$$

$$\mathrm{UCL}^* = \mathrm{E}_0(\mathrm{SR}_t^*) + K\sqrt{\mathrm{V}_0(\mathrm{SR}_t^*)} \times \sqrt{\frac{\lambda}{2-\lambda}}.$$

Finally, for the in-control case (i.e. for $p_0 = 0.5$, assuming θ as the process median) the in-control mean and variance of SR_t^* will be:

$$\begin{aligned} &\mathrm{E}(\mathrm{SR}_t^*) = 0, \\ &\mathrm{V}(\mathrm{SR}_t^*) = \frac{n(n+1)(2n+1)}{6} + h^2, \end{aligned} \tag{6.11}$$

and the upper and lower control limits of the 2-C WSR EWMA chart can be rewritten as:

$$\mathrm{LCL}^* = -K\sqrt{\frac{\lambda}{2-\lambda}\frac{n(n+1)(2n+1)}{6} + h^2}.$$

$$\mathrm{UCL}^* = +K\sqrt{\frac{\lambda}{2-\lambda}\frac{n(n+1)(2n+1)}{6} + h^2}.$$

The upper-sided case: The charting statistic of the "continuousified" upper-sided

WSR EWMA (denoted as C-WSR EWMA chart) will be defined as:

$$Z_t^* = \max(0, \lambda \mathrm{SR}_t^* + (1-\lambda) Z_{t-1}^*), Z_0^* = \mathrm{E}_0(\mathrm{SR}_t^*),$$

with fixed upper asymptotic control limit:

$$\mathrm{UCL}^* = \mathrm{E}_0(\mathrm{SR}_t^*) + K_1 \sqrt{\mathrm{V}_0(\mathrm{SR}_t^*)} \times \sqrt{\frac{\lambda}{2-\lambda}}.$$

Similarly with the two-sided case, for $p_0 = 0.5$ we have

$$\mathrm{UCL}^* = + K_1 \sqrt{\frac{\lambda}{2-\lambda}\left(\frac{n(n+1)(2n+1)}{6} + h^2\right)}.$$

$$\mathrm{CL} = 0.$$

Finally The RL properties for both 2C-WSR EWMA and C-WSR EWMA charts, are obtained based on the standard discrete-time Markov chain approach of Brook and Evans (1972) presented in Section 2.5 with the only difference that the p.m.f. of SR_t will be replaced by the p.d.f. of SR_t^* in the computation of the transient probabilities.

6.2.2 Comparisons with and without the "continuousify" method

As is has been illustrated in Figures 2.5 and 2.7 (see, Section 2.5) it can been clearly concluded that, the RL properties of the EWMA chart based on Signed Ranks are highly affected by the number of subintervals. In order to clarify this statement, and justify the advantages of our proposed chart in Tables 6.7 and 6.8 several comparisons of ARL values for the 2-WSR EWMA (without "continuousify") and 2C-WSR EWMA (with "continuousify" and $h = 0.2$) charts are reported as a function of the number of subintervals.

The two-sided case

Based on the results in Table 6.7 we draw the following conclusions:

- As this has been already shown in Figure 2.5, the ARL_0 values obtained without "continuousify" (i.e. the 2-WSR EWMA chart) strongly fluctuate depending on the value of $2m+1$. Clearly, they do not exhibit any monotonic convergence when the number of subintervals $2m+1$ increases. For instance, when $n = 5$, the in control ARL values obtained without "continuousify" fluctuate from 463.9 to 503.8.

- On the contrary, for $2m+1 \geq 100$, the ARL values obtained with the "continuousify" method (i.e. the 2C-WSR EWMA chart) exhibit a *strong* stability and they seem to converge rapidly to a reliable value. Even for $2m+1 = 101$ the results obtained with the "continuousify" approach are very reliable. For instance, using the same case when $n = 5$, the ARL_0 values obtained with "continuousify" converge rapidly to 496.1.

The upper-sided case

As expected, the advantages of the "continuousify"method are also present for the upper-sided C-WSR EWMA control chart. From Table 6.8 it can be seen that no matter the value of n the in-control pair of $(\text{ARL}, \text{SDRL})$ values are steady and converge quickly even for a relative small number of subintervals ≈ 50. It should be noted that, these results are also consistent for the out-of-control case (more informations are provided in the next Section where an extensive sensitivity analysis will be performed). In particular:

- As this has been already shown in Figure 2.7, the ARL values obtained without "continuousify" (i.e. the WSR EWMA chart) when $n = 15$, vary from 293.4 to 535.5 and the corresponding simulated value is 494.8. Similarly, when $n = 20$, the in-control ARL values vary from 342.4 to 437.3 and the corresponding simulated value is 450.7. It is worth stretching that, comparing with the two-sided case the differences are larger.

- On the contrary, for $m \geq 100$, using the "continuousify" method (i.e. the C-WSR EWMA chart) the corresponding ARL and SDRL values converge rapidly to a reliable value. For instance, using the same cases $n = 15$, and $n = 20$ the ARL values obtained with "continuousify" converge rapidly to 385.2 and 377.7 and respectively.

- As expected, the exact pattern occurs for the corresponding SDRL values which converge rapidly giving steady results. Additionally, these finding are consistent with the corresponding two-sided design of the EWMA chart based on the Sign statistic presented in the previous chapter.

Table 6.7: Comparison of in- and out-of-control pairs of (ARL, SDRL) values for the two-sided 2-WSR EWMA (without "continuousify") and two-sided 2C-WSR EWMA (with "continuousify" and $h = 0.2$) charts when $\lambda = 0.2$ and $K = 2.85$

(ARL values for the 2-WSR EWMA and 2C-WSR EWMA charts)

	$(n = 5, p_1 = 0.5)$		$(n = 7, p_1 = 0.5)$		$(n = 11, p_1 = 0.5)$		$(n = 14, p_1 = 0.5)$	
$2m+1$	2-WSR EWMA	2C-WSR EWMA	2-WSR EWMA	2C-WSR EWMA	2-WSR EWMA	2C-WSR EWMA	2-WSR EWMA	2C-WSR EWMA
51	503.8	499.9	435.2	446.4	405.5	409.7	397.5	397.6
61	491.2	494.1	444.7	449.7	405.2	410.9	406.6	402.0
71	492.8	495.3	454.8	448.3	408.8	411.2	400.1	399.4
81	493.8	493.6	458.0	449.2	409.5	410.4	396.1	397.3
91	495.9	494.4	436.9	441.8	411.6	411.2	384.3	397.9
101	485.2	496.0	440.0	447.4	412.4	412.3	405.9	400.1
111	468.9	494.2	452.6	448.2	415.0	412.2	394.7	400.3
121	506.8	495.8	448.0	448.0	409.7	412.4	416.1	413.1
131	507.8	495.8	439.7	447.7	412.5	412.4	401.5	399.9
141	490.3	495.8	451.0	448.9	411.7	412.5	399.0	400.1
151	501.7	495.9	450.9	448.8	412.0	412.6	407.2	400.2
161	491.7	496.0	447.4	448.9	413.8	412.9	403.8	400.4
171	500.2	496.0	454.1	448.8	404.2	408.7	400.1	400.3
181	487.2	496.0	438.1	448.5	413.0	412.6	401.7	400.6
191	497.6	496.1	445.9	448.8	411.5	412.6	399.9	400.4
201	509.0	496.1	447.9	448.9	414.0	412.7	399.7	400.4
sim	493.9		446.0		409.7		397.4	

(SDRL values for the 2-WSR EWMA and 2C-WSR EWMA charts)

	$(n = 5, p_1 = 0.5)$		$(n = 7, p_1 = 0.5)$		$(n = 11, p_1 = 0.5)$		$(n = 14, p_1 = 0.5)$	
$2m+1$	2-WSR EWMA	2C-WSR EWMA	2-WSR EWMA	2C-WSR EWMA	2-WSR EWMA	2C-WSR EWMA	2-WSR EWMA	2C-WSR EWMA
51	498.7	494.7	430.4	441.6	400.9	405.1	393.0	393.1
61	486.1	489.0	439.9	444.8	400.6	406.3	402.1	397.5
71	487.7	490.2	449.9	443.5	404.2	406.6	395.6	394.9
81	488.6	488.5	453.1	444.4	404.9	405.8	391.6	392.8
91	490.9	489.3	432.1	437.0	407.0	406.6	379.8	393.4
101	480.1	490.9	435.2	442.6	407.8	407.7	401.4	395.6
111	463.9	489.1	447.8	443.4	410.4	407.6	390.2	395.8
121	501.7	490.7	443.2	443.2	405.1	407.8	411.5	408.6
131	502.7	490.7	434.8	442.8	407.9	407.8	397.0	395.4
141	485.2	490.7	446.1	444.1	407.1	407.9	394.4	395.6
151	496.6	490.8	446.1	444.0	407.4	408.0	402.6	395.7
161	486.6	490.9	442.5	444.0	409.2	408.3	399.2	395.8
171	495.1	490.9	449.2	444.0	399.6	404.1	395.6	395.8
181	482.2	490.9	433.3	443.6	408.4	408.0	397.1	396.0
191	492.5	491.0	441.1	444.0	406.9	408.0	395.4	395.9
201	503.8	491.0	443.1	444.1	409.3	408.1	395.2	395.9
sim	490.8		441.6		405.8742		394.7	

Table 6.8: Comparison of in- and out-of-control pairs of (ARL, SDRL) values for the upper-sided WSR EWMA (without "continuousify") and upper-sided C-WSR EWMA (with "continuousify" and $h = 0.2$) charts when $\lambda = 0.2$ and $K_1 = 2.75$

(ARL values for the WSR EWMA and C-WSR EWMA charts)

	$(n = 5, p_1 = 0.5)$		$(n = 10, p_1 = 0.5)$		$(n = 15, p_1 = 0.5)$		$(n = 20, p_1 = 0.5)$	
m	WSR EWMA	C-WSR EWMA	WSR EWMA	C-WSR EWMA	WSR EWMA	C-WSR EWMA	WSR EWMA	2-WSR EWMA
50	462.9	455.7	400.5	400.2	384.4	384.5	347.0	378.2
60	456.0	456.4	390.7	400.6	303.4	384.6	395.1	377.6
70	454.8	456.5	400.9	400.4	417.7	385.3	383.1	377.6
80	468.3	456.6	402.5	401.3	530.0	387.1	348.7	377.7
90	453.5	456.7	392.4	400.9	360.1	385.0	360.7	377.8
100	459.3	456.7	400.9	401.0	385.2	385.1	378.5	376.4
110	464.2	456.7	400.4	401.0	393.6	385.1	382.9	377.6
120	462.1	456.8	400.2	401.0	535.5	385.2	402.7	377.8
130	455.0	456.8	400.5	401.1	432.5	384.6	386.6	377.6
140	459.0	456.8	400.9	401.1	509.6	385.2	432.8	377.7
150	464.8	456.8	401.3	401.2	347.2	385.2	383.1	377.7
160	462.9	456.8	401.5	401.2	458.5	385.4	433.3	377.7
170	449.8	456.8	401.5	401.2	293.4	385.2	342.4	377.7
180	455.6	456.8	390.7	401.1	313.8	385.2	432.5	377.7
190	460.3	456.9	401.4	401.2	301.0	385.2	436.0	377.7
200	460.2	456.9	401.5	401.2	418.1	385.2	437.3	377.8
sim	453.8		400.		382.6		374.8	

(SDRL values for the WSR EWMA and C-WSR EWMA charts)

	$(n = 5, p_1 = 0.5)$		$(n = 10, p_1 = 0.5)$		$(n = 15, p_1 = 0.5)$		$(n = 20, p_1 = 0.5)$	
m	WSR EWMA	C-WSR EWMA	WSR EWMA	C-WSR EWMA	WSR EWMA	C-WSR EWMA	WSR EWMA	2-WSR EWMA
50	462.9	450.1	400.5	395.0	384.4	379.6	347.0	373.3
60	456.0	450.9	390.7	395.4	303.4	379.6	395.1	372.7
70	454.8	451.0	400.9	395.3	417.7	380.3	383.1	372.6
80	468.3	451.1	402.5	396.1	530.0	382.1	348.7	372.7
90	453.5	451.1	392.4	395.7	360.1	380.0	360.7	372.8
100	459.3	451.2	400.9	395.9	385.2	380.1	378.5	371.5
110	464.2	451.2	400.4	395.9	393.6	380.2	382.9	372.7
120	462.1	451.3	400.2	395.9	535.5	380.2	402.7	372.9
130	455.0	451.3	400.5	396.0	432.5	379.6	386.6	372.7
140	459.0	451.3	400.9	396.0	509.6	380.2	432.8	372.7
150	464.8	451.3	401.3	396.0	347.2	380.2	383.1	372.8
160	462.9	451.3	401.5	396.0	458.5	380.4	433.3	372.8
170	449.8	451.3	401.5	396.0	293.4	380.2	342.4	372.8
180	455.6	451.3	390.7	396.0	313.8	380.2	432.5	372.8
190	460.3	451.3	401.4	396.1	301.0	380.3	436.0	372.8
200	460.2	451.3	401.5	396.1	418.1	380.2	437.3	372.9
sim	490.8		393.8		380.0		370.8	

6.2.3 Sensitivity analysis

Similarly with the "continuousified" EWMA control chart based on the Sign statistic presented in Chapter 3, an extensive numerical analysis will be performed, regarding the efficiency of the "continuousify" method, applied to the "continuousified" two- and upper-sided WSR EWMA chart , focussing on the effect of the chart's parameters (λ, K_1, h) and the Kernel density estimation method. The results that have been found are consistent with the "continuousified" EWMA chart based on the Sign statistic. In particular for the proposed modified WSR EWMA charts based on the "continuousify" method we may drawn the following conclusions:

Effect of the design parameters λ, K, h ***and fixed value of*** ARL_0

For both 2C-WSR EWMA (Table A6 in appendix) and C-WSR EWMA (Table A10 in appendix) charts using the "continuousify"method, the ARL values become steady and remain unaffected by the number of subintervals, regardless the sample size and the desired in-control $\mathrm{ARL}_0 \in \{200, 370.4, 500\}$. Additionally, the value of h does not have any impact to the results (see Table A5 for the two-sided and Table A9 for the one-sided case in appendix). In particular, when h is neither too small or too large the results are the same. Consequently, similarly with the Sign EWMA chart, setting the value of $h \approx 0.2$ is a reasonable choice to be considered.

Effect of the shift magnitude p_1

Regarding the out-of-control cases, for small shifts in the process location parameter $(p_1 < 0.6)$ the corresponding out-of-control values are affected by the number of subintervals. On the other hand, using the "continuousify"method the results become immediately stable (Tables and A7 and A11). On the contrary, for large shifts $(p_1 < 0.6)$ minor differences exist (Figure 6.1 for the two-sided, and Table A12, presented in appendix, for the upper-sided case). Nevertheless, since we proved that for the in-control case the results are different, practitioner may not be sure about the true out-of-control performance of the chart in term of its RL properties.

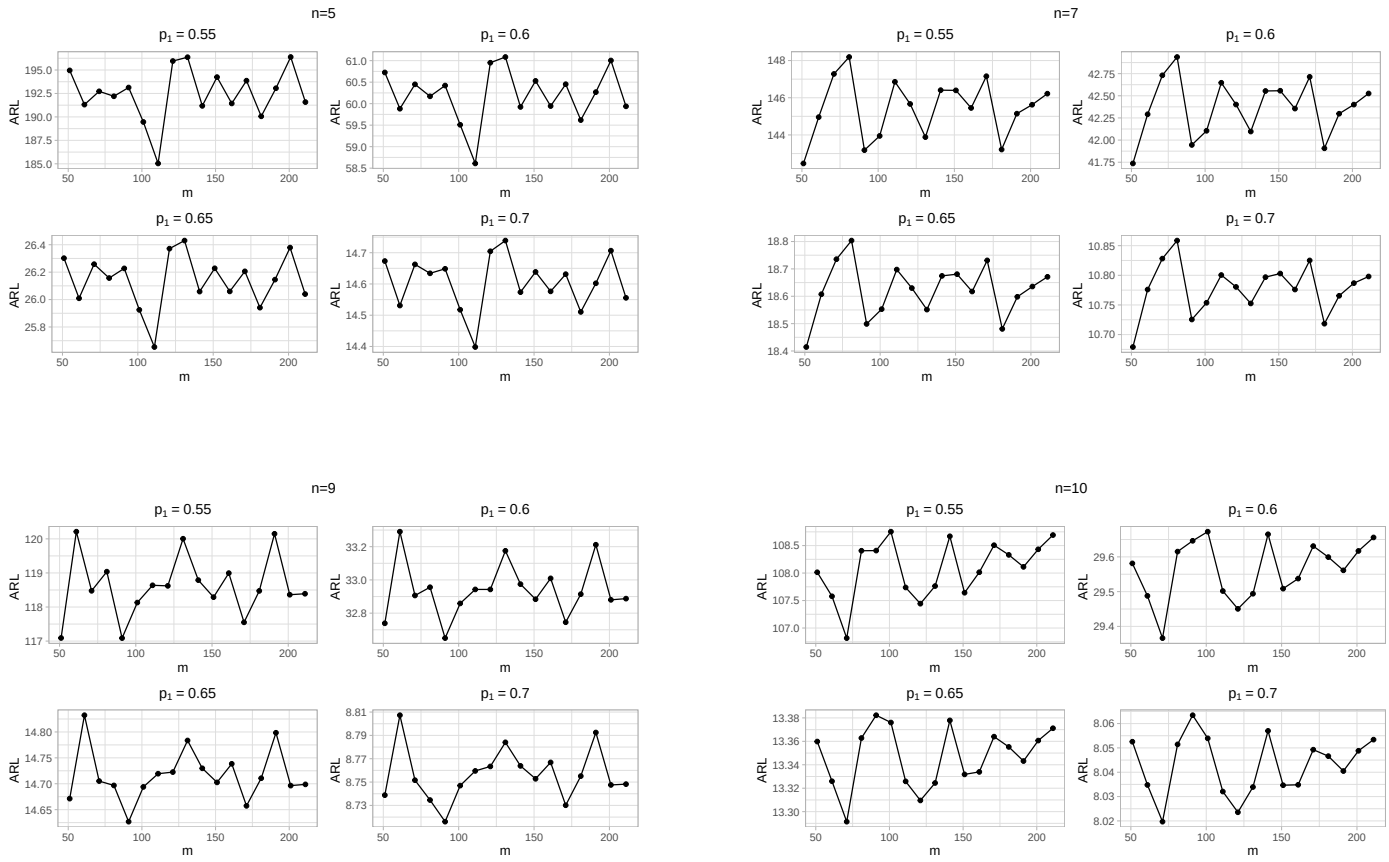

Figure 6.1: ARL_1 values in function of the subintervals $2m + 1$ for the two-sided WSR EWMA chart under different combinations of n and p_1

Effect of the Kernel density estimation

For both 2C-WSR EWMA (Table A8 in appendix) and C-WSR EWMA (Table A13 in appendix) charts it can been observed that, regardless the values of the predefined ARL_0 and sample size, corresponding in-control ARL values remain unaffected by the choice of the Kernels defined in Section 3.2.4.3.

Effect of the in-control value of p_0

As it has been stated in previous Sections, both 2C-WSR EWMA and C-WSR EWMA charts, can be designed in order to monitor any percentile of interest. For instance, considering as an example that we interested in monitoring shifts in the 3^{rd} quantile, the in-control value of p_0 will be equal to $p_0 = 0.75$. By setting $p_0 = 0.75$ in equations(2.24) (2.25) the in-control mean and variance of SR_t^+ are equal to $E_0(SR_t) = \frac{n(n+1)}{4}$ and $V_0(SR_t) = \frac{n(n+1)(2n+1)}{8}$.

As a result, the charting statistic and control limits of the 2C-WSR EWMA chart will be adjusted as:

$$Z_t^* = \lambda \mathrm{SR}_t^* + (1-\lambda) Z_{t-1}^*, Z_0^* = \frac{n(n+1)}{4},$$

with fixed asymptotic control limits:

$$\mathrm{UCL}^* = \frac{n(n+1)}{4} + K\sqrt{\frac{\lambda}{2-\lambda}\left(\frac{n(n+1)(2n+1)}{8} + h^2\right)}.$$

$$\mathrm{LCL}^* = \frac{n(n+1)}{4} - K\sqrt{\frac{\lambda}{2-\lambda}\left(\frac{n(n+1)(2n+1)}{8} + h^2\right)}.$$

Following the same procedure with the Sign EWMA chart, in order to examine the stability of the in-control ARL with and without the "continuousify" method, 3 cases regarding the in-control value of p_0 are considered (Tables A6 and A10 for the two-sided and upper-sided cases respectively presented in appendix). In Figures 6.3 and 6.2 the corresponding in-control ARL values for the two- and upper-sided case are plotted, for monitoring the different percentiles of interest, $p_0 = \{0.65, 0.75, 0.85\}$. From these figures we may conclude that regardless the value of p_0 the "continuousify" method is a great improvement for the stability of the ARL_0 values.

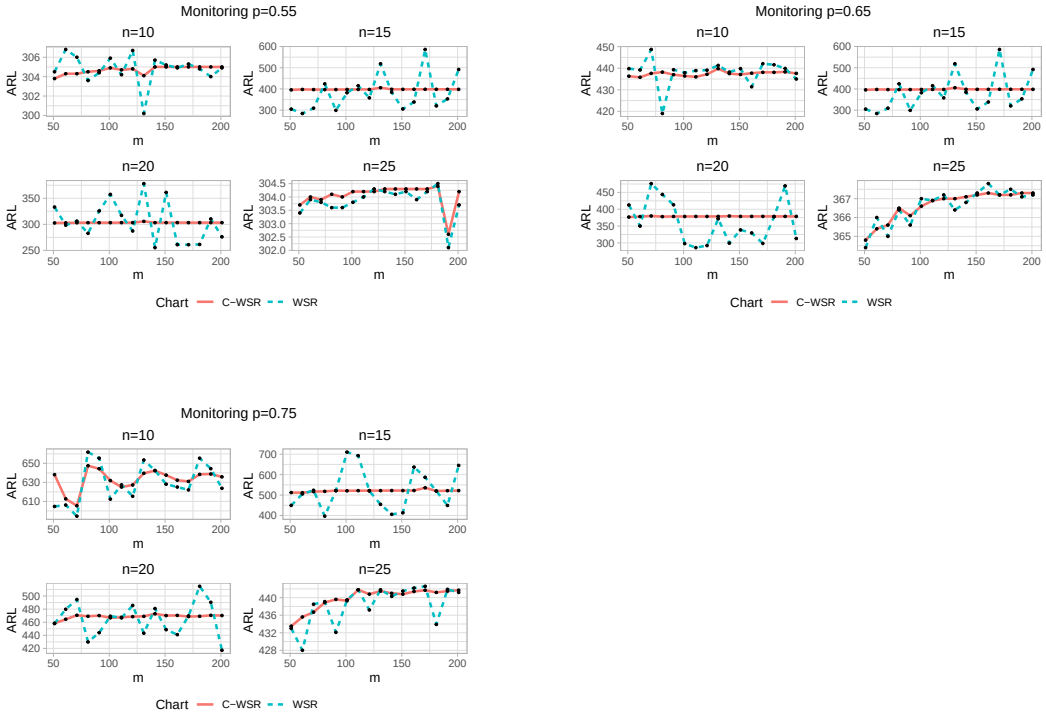

Figure 6.2: ARL_0 values in function of the subintervals for the WSR EWMA chart with (blue plain lines) and without (red plain lines) the "continuousify" method for different percentiles of interest using $\lambda = 0.2, K_1 = 2.5$

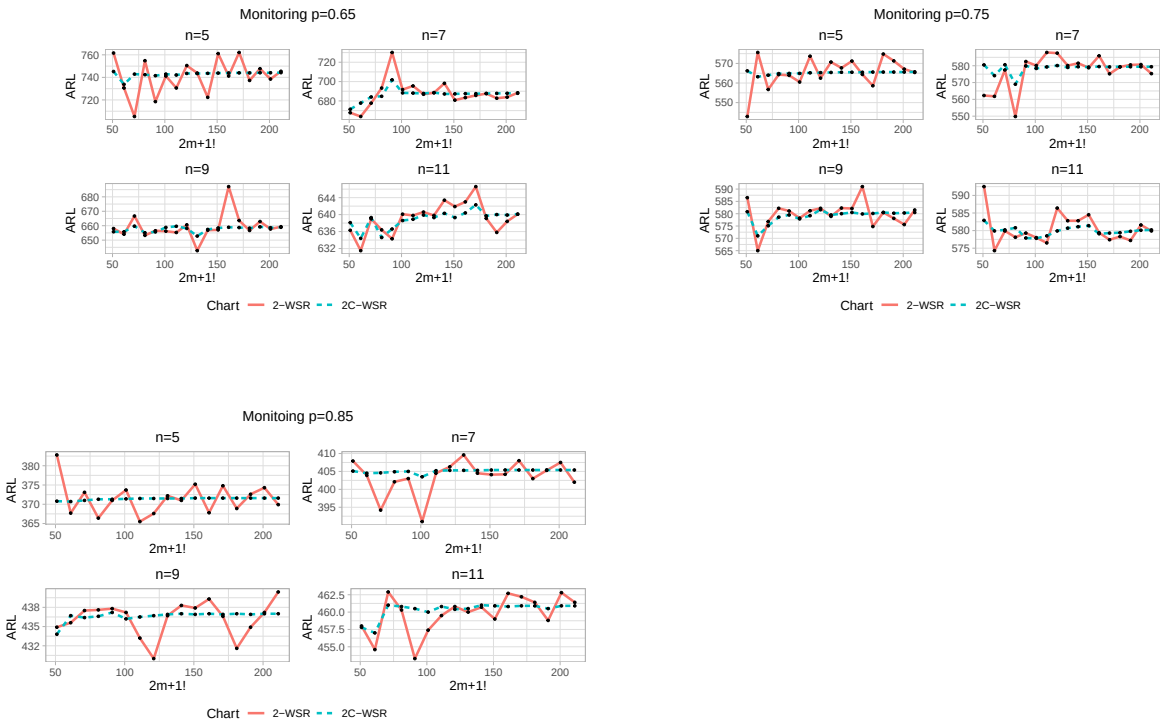

Figure 6.3: ARL_0 values in function of the subintervals $2m+1$ for the two-sided WSR EWMA chart with (blue plain lines) and without (red plain lines) the "continuousify" method for monitoring different percentiles of interest $\lambda = 0.2, K = 3$

6.2.4 Optimal design of the upper- and two-sided "continuousified" WSR EWMA chart

Since the superiority and efficiency of the "continuousify" method in the nonparametric EWMA chart based on the Wilcoxon Signed Rank statistic was verified, the chart's optimal design parameters are given for different shift magnitudes and sample sizes. The optimization method that has been utilised is the same as the one used for the Sign EWMA chart. In Table 6.9 the optimal pairs of (λ^*, K^*) for the 2C-WSR EWMA and (λ^*, K_1^*) for the C-WSR EWMA charts are presented along with the corresponding ARL_1 values for $n \in \{5, 6, \ldots, 20\}$.

Table 6.9: Optimal combinations of (λ^*, K^*) for the 2C-WSR EWMA and (λ^*, K_1^*) for the C-WSR EWMA charts along with the corresponding ARL_1 values

	C-WSR EWMA chart								
	p_1								
n	0.55	0.60	0.65	0.70	0.75	0.80	0.85	0.90	0.95
5	(0.015,1.965,73.23)	(0.045,2.389,32.01)	(0.08,2.55,18.31)	(0.135,2.648,11.96)	(0.18,2.679,8.43)	(0.26,2.685,6.23)	(0.5,2.57,4.6)	(0.5,2.57,3.43)	(0.525,2.549,2.61)
6	(0.015,1.964,66.97)	(0.05,2.423,28.62)	(0.09,2.58,16.23)	(0.14,2.66,10.55)	(0.2,2.696,7.43)	(0.325,2.693,5.44)	(0.45,2.646,4.09)	(0.525,2.598,3.14)	(0.705,2.463,2.44)
7	(0.02,2.087,61.69)	(0.055,2.452,25.98)	(0.1,2.606,14.62)	(0.155,2.68,9.47)	(0.25,2.716,6.64)	(0.29,2.716,4.91)	(0.4,2.69,3.74)	(0.53,2.634,2.91)	(0.605,2.589,2.34)
8	(0.02,2.086,57.41)	(0.055,2.453,23.87)	(0.11,2.627,13.35)	(0.17,2.697,8.62)	(0.26,2.727,6.03)	(0.35,2.721,4.45)	(0.415,2.704,3.42)	(0.465,2.688,2.72)	(0.945,2.518,2.04)
9	(0.025,2.176,53.81)	(0.065,2.502,22.09)	(0.12,2.646,12.3)	(0.19,2.713,7.92)	(0.275,2.737,5.54)	(0.365,2.731,4.09)	(0.405,2.722,3.16)	(0.855,2.612,2.3)	(0.86,2.61,1.53)
10	(0.025,2.176,50.75)	(0.07,2.523,20.6)	(0.13,2.663,11.42)	(0.195,2.72,7.35)	(0.275,2.743,5.14)	(0.36,2.741,3.8)	(0.5,2.708,2.96)	(0.715,2.66,2.11)	(0.825,2.646,1.5)
11	(0.03,2.247,48.01)	(0.075,2.542,19.32)	(0.135,2.671,10.68)	(0.215,2.734,6.85)	(0.31,2.752,4.79)	(0.37,2.748,3.56)	(0.62,2.695,2.65)	(0.62,2.695,1.99)	(0.76,2.668,1.46)
12	(0.03,2.246,45.68)	(0.075,2.542,18.22)	(0.14,2.679,10.04)	(0.225,2.741,6.43)	(0.305,2.757,4.5)	(0.395,2.752,3.35)	(0.555,2.721,2.49)	(0.645,2.704,1.89)	(0.78,2.676,1.41)
13	(0.03,2.246,43.56)	(0.085,2.575,17.25)	(0.15,2.693,9.48)	(0.23,2.746,6.07)	(0.31,2.762,4.25)	(0.5,2.741,3.13)	(0.565,2.73,2.37)	(0.705,2.702,1.8)	(0.785,2.689,1.35)
14	(0.03,2.246,41.68)	(0.075,2.543,16.39)	(0.16,2.704,8.98)	(0.25,2.755,5.74)	(0.355,2.767,4.02)	(0.46,2.756,2.97)	(0.61,2.731,2.25)	(0.765,2.703,1.7)	(0.92,2.659,1.28)
15	(0.035,2.303,40)	(0.1,2.615,15.63)	(0.165,2.71,8.55)	(0.26,2.761,5.46)	(0.35,2.771,3.83)	(0.48,2.76,2.83)	(0.67,2.73,2.14)	(0.855,2.692,1.6)	(0.93,2.664,1.21)
16	(0.035,2.303,38.42)	(0.11,2.637,14.92)	(0.18,2.724,8.15)	(0.26,2.763,5.21)	(0.39,2.773,3.65)	(0.495,2.763,2.7)	(0.68,2.736,2.03)	(0.93,2.68,1.49)	(0.94,2.679,1.13)
17	(0.035,2.303,37.02)	(0.1,2.616,14.32)	(0.18,2.725,7.79)	(0.275,2.769,4.98)	(0.385,2.777,3.49)	(0.525,2.765,2.58)	(0.755,2.729,1.91)	(0.885,2.701,1.42)	(0.945,2.675,1.11)
18	(0.04,2.35,35.74)	(0.105,2.627,13.75)	(0.19,2.734,7.48)	(0.275,2.771,4.78)	(0.385,2.781,3.35)	(0.57,2.764,2.46)	(0.73,2.741,1.82)	(0.835,2.722,1.37)	(0.835,2.722,1.1)
19	(0.035,2.302,34.58)	(0.105,2.628,13.24)	(0.195,2.739,7.19)	(0.29,2.776,4.59)	(0.405,2.783,3.22)	(0.605,2.764,2.35)	(0.73,2.747,1.75)	(0.875,2.714,1.32)	(0.875,2.714,1.08)
20	(0.04,2.35,33.45)	(0.115,2.648,12.76)	(0.2,2.743,6.92)	(0.34,2.785,4.41)	(0.47,2.782,3.09)	(0.605,2.769,2.26)	(0.805,2.738,1.67)	(0.9,2.712,1.27)	(0.9,2.712,1.06)

	2C-WSR EWMA chart								
	p_1								
n	0.55	0.60	0.65	0.70	0.75	0.80	0.85	0.90	0.95
5	(0.01,2.032,89.87)	(0.06,2.541,36.49)	(0.06,2.541,19.99)	(0.11,2.694,12.84)	(0.16,2.747,9.04)	(0.26,2.77,6.66)	(0.31,2.752,5.09)	(0.56,2.586,3.69)	(0.61,2.538,2.72
6	(0.01,1.838,79.3)	(0.06,2.548,32.01)	(0.11,2.694,17.75)	(0.11,2.694,11.35)	(0.16,2.757,7.95)	(0.26,2.788,5.88)	(0.41,2.745,4.38)	(0.51,2.689,3.32)	(0.61,2.617,2.54
7	(0.01,1.851,73.79)	(0.06,2.545,28.73)	(0.11,2.702,15.87)	(0.16,2.745,10.14)	(0.21,2.799,7.1)	(0.31,2.801,5.24)	(0.41,2.781,3.97)	(0.56,2.705,3.06)	(0.61,2.675,2.42
8	(0.01,1.846,67.61)	(0.06,2.546,26.18)	(0.11,2.707,14.39)	(0.16,2.773,9.22)	(0.26,2.82,6.46)	(0.31,2.819,4.75)	(0.36,2.813,3.64)	(0.51,2.766,2.85)	(0.56,2.743,2.31
9	(0.01,1.839,63.56)	(0.06,2.55,24.16)	(0.11,2.711,13.24)	(0.16,2.778,8.48)	(0.26,2.817,5.93)	(0.36,2.828,4.37)	(0.41,2.818,3.35)	(0.91,2.641,2.54)	(0.91,2.641,1.67
10	(0.01,1.839,60.29)	(0.06,2.551,22.46)	(0.11,2.707,12.27)	(0.21,2.818,7.87)	(0.26,2.835,5.49)	(0.36,2.842,4.05)	(0.46,2.823,3.12)	(0.81,2.715,2.31)	(0.81,2.715,1.55
11	(0.01,1.838,56.8)	(0.06,2.553,21.05)	(0.11,2.713,11.48)	(0.21,2.823,7.34)	(0.26,2.841,5.12)	(0.36,2.852,3.78)	(0.41,2.844,2.94)	(0.71,2.771,2.15)	(0.71,2.771,1.53
12	(0.01,1.838,54.13)	(0.06,2.551,19.85)	(0.11,2.714,10.82)	(0.21,2.826,6.87)	(0.31,2.856,4.79)	(0.36,2.858,3.56)	(0.66,2.805,2.74)	(0.66,2.805,2.02)	(0.76,2.78,1.49
13	(0.01,1.837,51.79)	(0.06,2.558,18.81)	(0.16,2.79,10.18)	(0.21,2.835,6.48)	(0.31,2.862,4.52)	(0.36,2.864,3.37)	(0.56,2.841,2.54)	(0.71,2.808,1.93)	(0.76,2.799,1.43
14	(0.01,1.835,49.68)	(0.06,2.553,17.9)	(0.16,2.792,9.63)	(0.21,2.832,6.14)	(0.31,2.867,4.29)	(0.41,2.871,3.2)	(0.61,2.842,2.42)	(0.76,2.814,1.83)	(0.76,2.814,1.38
15	(0.06,2.553,47.61)	(0.11,2.717,17.1)	(0.16,2.797,9.15)	(0.26,2.859,5.83)	(0.31,2.871,4.08)	(0.51,2.868,3.04)	(0.61,2.852,2.31)	(0.81,2.819,1.75)	(0.91,2.808,1.31
16	(0.06,2.555,45.36)	(0.11,2.724,16.28)	(0.16,2.795,8.72)	(0.26,2.862,5.55)	(0.36,2.881,3.89)	(0.51,2.875,2.89)	(0.66,2.853,2.2)	(0.81,2.831,1.65)	(0.91,2.821,1.24
17	(0.06,2.554,43.36)	(0.11,2.719,15.53)	(0.16,2.797,8.34)	(0.26,2.864,5.31)	(0.36,2.886,3.73)	(0.46,2.885,2.77)	(0.66,2.862,2.1)	(0.81,2.841,1.57)	(0.91,2.833,1.18
18	(0.06,2.554,41.55)	(0.11,2.72,14.88)	(0.16,2.797,8.01)	(0.26,2.866,5.09)	(0.41,2.891,3.57)	(0.51,2.887,2.66)	(0.66,2.87,2)	(0.81,2.848,1.48)	(0.86,2.846,1.14
19	(0.06,2.553,39.91)	(0.11,2.72,14.29)	(0.16,2.799,7.69)	(0.26,2.868,4.9)	(0.41,2.895,3.43)	(0.56,2.888,2.55)	(0.71,2.87,1.9)	(0.86,2.855,1.42)	(0.86,2.855,1.12
20	(0.06,2.554,38.4)	(0.11,2.72,13.75)	(0.21,2.844,7.41)	(0.31,2.886,4.71)	(0.41,2.898,3.31)	(0.61,2.888,2.45)	(0.71,2.877,1.83)	(0.86,2.862,1.37)	(0.91,2.859,1.09

6.3 Conclusions

In this Chapter we investigated the design of two EWMA control charts based on the Wilcoxon Signed rank statistic. For both schemes, our interest was mainly focused on providing methodologies for the exact determination of their RL properties. In particular, we introduced the CEWMA WSR chart which is a modified EWMA-type scheme with a discrete plotting statistic. Using a specific discrete Markov chain approach we were able to determine its exact in- and out-of control performance. Additionally, we presented an application of the "continuousify" method in the design of two- and upper sided EWMA charts (denoted as 2C-WSR EWMA and C-WSR EWMA charts respectively) proving that "continuousified" method lead to steady and reliable results for the chart's performance.

Chapter 7

Conclusions and Perspectives

7.1 Conclusions

The proper determination of the chart's design parameters plays a vital role for its optimal and robust performance. In "classical" (i.e. parametric) control charts, the assumptions of Normality is a strong one even if it is commonly violated in practice. On the other hand, the operation and design of non-parametric schemes does not requires the knowledge of the samples' underlying distribution. In this current thesis, we mainly focused on providing robust methods which guarantee the optimal design of a univariate distribution-free EWMA control chart. In particular, in Chapter 2, we proved that, there are might be cases that for the determination of the RL properties of a nonparametric EWMA chart based on the Sign or the Wilcoxon Signed Rank statistics, the conventional method of Brook and Evans (1972) does not yield to robust results. Moreover, due to the discrete nature of the nonparametric statistics being considered, practitioners may not be able to find a proper combination of (λ, K) that corresponds to an in-control ARL value which will not be exactly equal to the desired one. In order to tackle these problems, in Chapter 3, we use a simple method called as the "the continuousify method" in which the discrete statistic to be monitored (i.e. the Sign statistic) is transformed into a continuous one through Normal Kernels. After an extensive sensitivity analysis we proved that the use of this approach yields to robust results for both upper- and two-sided EWMA charts based on the sign statistic. Additionally, for different combinations of n, p_{+1}, we provided the corresponding optimal pairs of (λ, K) which give the minimum ARL_1. It should be noted that, even though the use of Normal Kernels was used for the determination of the chart's optimal design parameters, we proved that the choice of Kernel type does not have any impact in the chart's performance.

In general, sign-type statistics should be treated with caution when ties are present. For instance, under the presence of ties, the distribution of the Sign statistic cannot longer be

derived through the Binomial distribution. As a consequence, this may have a huge impact in the smooth operation of a control chart when ties are present. It should be noted that, theoretically, assuming that the sample follows a continuous distribution prevents the presence of ties. However, during the data collection, the presence of rounding-off errors might lead to a tie between the observation and the in-control value of the location parameter to be monitored (such as the median). In Chapter 4, we proved that under the presence of ties the operation of a Sign EWMA chart is significantly affected. As a solution to this drawback we proved that, when ties are present, using a Bernoulli-based approach called as the "flip a coin" strategy will provide an approximately distribution-free performance for the Sign EWMA chart. In particular, using this strategy we proved that the in-control performance of the chart is no longer affected by the presence of ties with only some differences for heavily-skewed attributions. However, even for these cases, we proved that choosing a relative small sample size and a value for $\lambda > 0.75$ allows the chart to approximately maintains its distribution-free properties.

Additionally, in Chapter 5 a Sign-type EWMA chart (called as the D-SN-C EWMA chart) for monitoring the process variability was introduced. More specifically, using a similar design with the "continuousified" Sign EWMA chart for the process location presented in Chapter 3, in Chapter 5 a nonparametric "continuousified" EWMA chart was proposed based on the inner-quantiles Sign-type statistic. Additionally, the chart's in-and out-control performance was investigated under different symmetric and asymmetric distributions and its optimal performance was examined under several existing parametric and nonparametric schemes. Based on our findings, our proposed chart has the best performance among its nonparametric competitors and it can be also considered as an efficient alternative for monitoring Normal data.

Moreover, in Chapter 6 two different distribution-free EWMA charts based on the Wilcoxon Signed Rank statistic were proposed. In particular, An EWMA-Type control chart based on Signed Ranks was firstly introduced (called as the CEWMA WSR chart) and its exact in-and out-control properties were investigated. More specifically, for this particular scheme, the plotting statistic being considered, in contrast with a conventional non-parametric EWMA chart, is discrete. As a result, a proper Discrete-type Markov Chain method was proposed in which the exact number of states was determined. Finally, its out-of-control performance was compared with other schemes and our results shown that it can be considered as an efficient alternative for moderate to large shift magnitudes. Finally, the "continuousify" method, presented in Chapter 3, was used for the design of a EWMA chart based on the Wilcoxon Signed Ranks statistic (called as the C-WSR EWMA chart). Our work was mainly

focused on commenting the advantages of the "continuousify" approach in the design of an EWMA chart based on Signed Ranks, rather than examining its out-of-control performance comparing it with other schemes, since it is something that has been already investigated into the literature. It is worth stretching that in both schemes, the *general* distribution of the Wilcoxon Signed Rank statistic was properly defined not only for the in-control case but also for the out-of-control one. As we proved in Chapter 2, even-though the Normal approximation can be considered as an efficient alternative, is not reliable for the computation of the chart's RL properties. On the other hand, using the p.g.f of the SR_t^+ the general distribution of the Wilcoxon Signed Ranks statistic can be properly computed without any approximation.

7.2 Perspectives

As a further work, there are several interesting research fields that could be considered in combination with our contributions. For instance, for the schemes presented in this thesis, the adaptive feature in their design parameters (such as the sample size, smoothing parameter or sampling interval) can be considered and their out-of-control performance could be investigated. In general, using adaptive sample sizes or sampling intervals significantly improves the chart's out-of-control performance. For instance it would be interesting design schemes such as the CEWMA WSR or the D-SN-C EWMA charts using variable sample sizes. In this current work, we focused on the design of distribution-free control schemes under the univariate setting. As an extension of our work, the stability of the chart's RL properties could be investigated under the bivariate or the multivariate frameworks. For instance, it would be interesting to consider the use of multivariate Kernels and test their efficiency. Moreover, it would be challenging to investigate the performance of the Wilcoxon Signed rank statistic under the presence of ties. Finally, an interesting extension of our work would be to investigate the design of nonparametric Univariate or Multivariate schemes for monitoring correlated samples. As a conclusion, it is our belief that, nonparametric control chart is a powerful tool of SPC and practitioners are encouraged to work on this field of research.

Appendix

Table A1: ARL_0 for small sample sizes when ties are present for the 2C-SN EWMA chart

n=5

	$\lambda = 0.05$					$\lambda = 0.15$					$\lambda = 0.25$					$\lambda = 0.35$					$\lambda = 0.45$				
	$\kappa = 0.05$	$\kappa = 0.1$	$\kappa = 0.15$	$\kappa = 0.2$		$\kappa = 0.05$	$\kappa = 0.1$	$\kappa = 0.15$	$\kappa = 0.2$		$\kappa = 0.05$	$\kappa = 0.1$	$\kappa = 0.15$	$\kappa = 0.2$		$\kappa = 0.05$	$\kappa = 0.1$	$\kappa = 0.15$	$\kappa = 0.2$		$\kappa = 0.05$	$\kappa = 0.1$	$\kappa = 0.15$	$\kappa = 0.2$	
#1	370.4	370.4	370.4	370.4		370.4	370.4	370.4	370.4		370.4	370.4	370.4	370.4		370.4	370.4	370.4	370.4		370.4	370.4	370.4	370.4	
#2	370.4	370.4	370.4	370.4		370.4	370.4	370.4	370.4		370.4	370.4	370.4	370.4		370.4	370.4	370.4	370.4		370.4	370.4	370.4	370.4	
#3	370.4	370.4	370.4	370.4		370.4	370.4	370.4	370.4		370.4	370.4	370.4	370.4		370.4	370.4	370.4	370.4		370.4	370.4	370.4	370.4	
#4	370.4	370.4	370.4	370.4		370.4	370.4	370.4	370.4		370.4	370.4	370.4	370.4		370.4	370.4	370.4	370.4		370.4	370.4	370.4	370.4	
#5	370.4	370.4	370.4	370.4		370.4	370.4	370.4	370.4		370.4	370.4	370.4	370.4		370.4	370.4	370.4	370.4		370.4	370.4	370.4	370.4	
#6	370.4	370.4	370.4	370.4		370.4	370.4	370.4	370.4		370.4	370.4	370.4	370.4		370.4	370.4	370.4	370.4		370.4	370.4	370.4	370.4	
#7	370.3	369.3	365.0	353.7		370.4	370.0	368.4	364.1		370.4	370.1	368.9	365.7		370.4	370.1	368.9	365.7		370.4	370.2	369.2	366.6	
#8	370.4	370.2	369.4	367.4		370.4	370.3	370.1	369.3		370.4	370.3	370.1	369.3		370.4	370.4	370.2	369.6		370.4	370.4	370.2	369.7	
#9	370.4	370.3	369.8	368.7		370.4	370.3	370.1	369.5		370.4	370.4	370.2	369.8		370.4	370.4	370.2	369.9		370.4	370.4	370.3	370.0	
#10	370.4	370.3	370.0	369.1		370.4	370.4	370.2	369.7		370.4	370.4	370.2	369.9		370.4	370.4	370.3	370.0		370.4	370.4	370.3	370.1	
#11	370.4	370.3	370.0	369.2		370.4	370.4	370.2	369.8		370.4	370.4	370.3	370.0		370.4	370.4	370.3	370.1		370.4	370.4	370.3	370.1	
#12	370.4	370.3	370.0	369.3		370.4	370.4	370.2	369.8		370.4	370.4	370.3	370.0		370.4	370.4	370.3	370.1		370.4	370.4	370.3	370.2	
#13	370.2	367.9	358.1	334.2		370.3	369.1	363.7	350.1		370.3	369.5	365.8	356.2		370.4	369.7	367.0	359.8		370.4	369.8	367.6	361.8	
#14	370.3	368.8	362.9	347.9		370.4	369.6	366.3	358.1		370.4	369.8	367.6	361.8		370.4	370.0	368.3	364.0		370.4	370.1	368.7	365.2	
#15	370.3	369.6	366.2	357.8		370.4	369.9	368.2	363.6		370.4	370.1	368.9	365.7		370.4	370.2	369.3	366.9		370.4	370.2	369.5	367.6	
#16	370.4	369.7	367.2	360.8		370.4	370.0	368.7	365.2		370.4	370.2	369.2	366.8		370.4	370.2	369.5	367.7		370.4	370.3	369.7	368.3	
#17	370.4	369.8	367.5	361.9		370.4	370.1	368.8	365.8		370.4	370.2	369.3	367.2		370.4	370.2	369.6	368.1		370.4	370.3	369.8	368.5	
	$\lambda = 0.55$					$\lambda = 0.65$					$\lambda = 0.75$					$\lambda = 0.85$					$\lambda = 0.95$				
	$\kappa = 0.05$	$\kappa = 0.1$	$\kappa = 0.15$	$\kappa = 0.2$		$\kappa = 0.05$	$\kappa = 0.1$	$\kappa = 0.15$	$\kappa = 0.2$		$\kappa = 0.05$	$\kappa = 0.1$	$\kappa = 0.15$	$\kappa = 0.2$		$\kappa = 0.05$	$\kappa = 0.1$	$\kappa = 0.15$	$\kappa = 0.2$		$\kappa = 0.05$	$\kappa = 0.1$	$\kappa = 0.15$	$\kappa = 0.2$	
#1	370.4	370.4	370.4	370.4		370.4	370.4	370.4	370.4		370.4	370.4	370.4	370.4		370.4	370.4	370.4	370.4		370.4	370.4	370.4	370.4	
#2	370.4	370.4	370.4	370.4		370.4	370.4	370.4	370.4		370.4	370.4	370.4	370.4		370.4	370.4	370.4	370.4		370.4	370.4	370.4	370.4	
#3	370.4	370.4	370.4	370.4		370.4	370.4	370.4	370.4		370.4	370.4	370.4	370.4		370.4	370.4	370.4	370.4		370.4	370.4	370.4	370.4	
#4	370.4	370.4	370.4	370.4		370.4	370.4	370.4	370.4		370.4	370.4	370.4	370.4		370.4	370.4	370.4	370.4		370.4	370.4	370.4	370.4	
#5	370.4	370.4	370.4	370.4		370.4	370.4	370.4	370.4		370.4	370.4	370.4	370.4		370.4	370.4	370.4	370.4		370.4	370.4	370.4	370.4	
#6	370.4	370.4	370.4	370.4		370.4	370.4	370.4	370.4		370.4	370.4	370.4	370.4		370.4	370.4	370.4	370.4		370.4	370.4	370.4	370.4	
#7	370.4	370.2	369.4	367.2		370.4	370.2	369.5	367.6		370.4	370.3	369.6	368.0		370.4	370.3	369.8	368.5		370.4	370.3	370.0	369.2	
#8	370.4	370.4	370.2	369.8		370.4	370.4	370.2	369.9		370.4	370.4	370.3	370.0		370.4	370.4	370.3	370.1		370.4	370.4	370.3	370.2	
#9	370.4	370.4	370.3	370.1		370.4	370.4	370.3	370.2		370.4	370.4	370.3	370.2		370.4	370.4	370.3	370.2		370.4	370.4	370.4	370.3	
#10	370.4	370.4	370.3	370.2		370.4	370.4	370.3	370.2		370.4	370.4	370.3	370.2		370.4	370.4	370.4	370.3		370.4	370.4	370.4	370.3	
#11	370.4	370.4	370.3	370.2		370.4	370.4	370.3	370.2		370.4	370.4	370.3	370.2		370.4	370.4	370.4	370.3		370.4	370.4	370.4	370.3	
#12	370.4	370.4	370.3	370.2		370.4	370.4	370.3	370.2		370.4	370.4	370.4	370.2		370.4	370.4	370.4	370.3		370.4	370.4	370.4	370.3	
#13	370.4	369.9	368.0	363.0		370.4	370.0	368.4	364.0		370.4	370.1	368.7	365.0		370.4	370.1	369.0	366.0		370.4	370.2	369.6	367.8	
#14	370.4	370.1	369.0	366.0		370.4	370.1	369.2	366.6		370.4	370.2	369.3	367.1		370.4	370.2	369.5	367.8		370.4	370.3	369.9	368.8	
#15	370.4	370.2	369.6	368.0		370.4	370.3	369.7	368.3		370.4	370.3	369.8	368.6		370.4	370.3	369.9	368.6		370.4	370.3	370.1	369.5	
#16	370.4	370.3	369.8	368.6		370.4	370.3	369.9	368.8		370.4	370.3	370.0	369.1		370.4	370.3	370.0	369.3		370.4	370.4	370.2	369.7	
#17	370.4	370.3	369.9	368.8		370.4	370.3	369.9	369.0		370.4	370.3	370.0	369.2		370.4	370.3	370.1	369.4		370.4	370.4	370.2	369.8	

Table A2: ARL_0 for moderate sample sizes when ties are present for the 2C-SN EWMA chart

n=15

	$\lambda = 0.05$				$\lambda = 0.15$				$\lambda = 0.25$				$\lambda = 0.35$				$\lambda = 0.45$			
	$\kappa = 0.05$	$\kappa = 0.1$	$\kappa = 0.15$	$\kappa = 0.2$	$\kappa = 0.05$	$\kappa = 0.1$	$\kappa = 0.15$	$\kappa = 0.2$	$\kappa = 0.05$	$\kappa = 0.1$	$\kappa = 0.15$	$\kappa = 0.2$	$\kappa = 0.05$	$\kappa = 0.1$	$\kappa = 0.15$	$\kappa = 0.2$	$\kappa = 0.05$	$\kappa = 0.1$	$\kappa = 0.15$	$\kappa = 0.2$
#1	370.4	370.4	370.4	370.4	370.4	370.4	370.4	370.4	370.4	370.4	370.4	370.4	370.4	370.4	370.4	370.4	370.4	370.4	370.4	370.4
#2	370.4	370.4	370.4	370.4	370.4	370.4	370.4	370.4	370.4	370.4	370.4	370.4	370.4	370.4	370.4	370.4	370.4	370.4	370.4	370.4
#3	370.4	370.4	370.4	370.4	370.4	370.4	370.4	370.4	370.4	370.4	370.4	370.4	370.4	370.4	370.4	370.4	370.4	370.4	370.4	370.4
#4	370.4	370.4	370.4	370.4	370.4	370.4	370.4	370.4	370.4	370.4	370.4	370.4	370.4	370.4	370.4	370.4	370.4	370.4	370.4	370.4
#5	370.4	370.4	370.4	370.4	370.4	370.4	370.4	370.4	370.4	370.4	370.4	370.4	370.4	370.4	370.4	370.4	370.4	370.4	370.4	370.4
#6	370.4	370.4	370.4	370.4	370.4	370.4	370.4	370.4	370.4	370.4	370.4	370.4	370.4	370.4	370.4	370.4	370.4	370.4	370.4	370.4
#7	370.2	367.2	354.5	324.3	370.3	368.7	361.8	344.5	370.3	369.2	364.5	352.2	370.3	369.5	366.0	356.7	370.4	369.7	366.9	359.6
#8	370.4	369.8	367.5	361.5	370.4	370.1	368.9	365.6	370.4	370.2	369.4	367.1	370.4	370.3	369.6	368.0	370.4	370.3	369.8	368.5
#9	370.4	370.0	368.7	365.4	370.4	370.2	369.5	367.8	370.4	370.3	369.8	368.6	370.4	370.3	369.9	369.0	370.4	370.3	370.0	369.3
#10	370.4	370.2	369.1	366.5	370.4	370.3	369.7	368.3	370.4	370.3	369.9	369.0	370.4	370.3	370.1	369.3	370.4	370.3	370.1	369.6
#11	370.4	370.2	369.2	366.8	370.4	370.3	369.8	368.5	370.4	370.3	370.0	369.1	370.4	370.3	370.1	369.4	370.4	370.4	370.2	369.6
#12	370.4	370.2	369.3	367.0	370.4	370.3	369.8	368.6	370.4	370.3	370.0	369.2	370.4	370.3	370.1	369.5	370.4	370.4	370.2	369.7
#13	369.9	362.9	335.6	279.5	370.1	366.4	351.1	315.6	370.2	367.7	357.0	331.0	370.3	368.4	360.3	340.3	370.3	368.8	362.4	346.3
#14	370.0	365.7	348.5	310.1	370.2	367.9	358.5	335.7	370.3	368.7	362.2	346.0	370.3	369.1	364.3	351.9	370.3	369.4	365.6	355.7
#15	370.2	367.9	358.1	334.8	370.3	369.1	363.8	350.7	370.3	369.5	365.8	356.7	370.4	369.7	367.0	360.1	370.4	369.9	367.7	362.3
#16	370.3	368.4	360.8	342.9	370.3	369.3	365.3	355.3	370.4	369.7	366.9	359.9	370.4	369.9	367.8	362.6	370.4	370.0	368.3	364.2
#17	370.3	368.6	361.7	345.9	370.3	369.4	365.8	357.0	370.4	369.7	367.2	361.1	370.4	369.9	368.0	363.5	370.4	370.0	368.5	364.9
	$\lambda = 0.55$				$\lambda = 0.65$				$\lambda = 0.75$				$\lambda = 0.85$				$\lambda = 0.95$			
	$\kappa = 0.05$	$\kappa = 0.1$	$\kappa = 0.15$	$\kappa = 0.2$	$\kappa = 0.05$	$\kappa = 0.1$	$\kappa = 0.15$	$\kappa = 0.2$	$\kappa = 0.05$	$\kappa = 0.1$	$\kappa = 0.15$	$\kappa = 0.2$	$\kappa = 0.05$	$\kappa = 0.1$	$\kappa = 0.15$	$\kappa = 0.2$	$\kappa = 0.05$	$\kappa = 0.1$	$\kappa = 0.15$	$\kappa = 0.2$
#1	370.4	370.4	370.4	370.4	370.4	370.4	370.4	370.4	370.4	370.4	370.4	370.4	370.4	370.4	370.4	370.4	370.4	370.4	370.4	370.4
#2	370.4	370.4	370.4	370.4	370.4	370.4	370.4	370.4	370.4	370.4	370.4	370.4	370.4	370.4	370.4	370.4	370.4	370.4	370.4	370.4
#3	370.4	370.4	370.4	370.4	370.4	370.4	370.4	370.4	370.4	370.4	370.4	370.4	370.4	370.4	370.4	370.4	370.4	370.4	370.4	370.4
#4	370.4	370.4	370.4	370.4	370.4	370.4	370.4	370.4	370.4	370.4	370.4	370.4	370.4	370.4	370.4	370.4	370.4	370.4	370.4	370.4
#5	370.4	370.4	370.4	370.4	370.4	370.4	370.4	370.4	370.4	370.4	370.4	370.4	370.4	370.4	370.4	370.4	370.4	370.4	370.4	370.4
#6	370.4	370.4	370.4	370.4	370.4	370.4	370.4	370.4	370.4	370.4	370.4	370.4	370.4	370.4	370.4	370.4	370.4	370.4	370.4	370.4
#7	370.4	369.9	367.6	361.8	370.4	370.0	368.1	363.3	370.4	370.0	368.6	364.7	370.4	370.1	368.8	365.4	370.4	370.1	369.0	366.1
#8	370.4	370.3	369.9	368.9	370.4	370.3	370.0	369.2	370.4	370.3	370.1	369.4	370.4	370.3	370.1	369.5	370.4	370.4	370.2	369.6
#9	370.4	370.3	370.1	369.6	370.4	370.3	370.2	369.7	370.4	370.4	370.2	369.9	370.4	370.4	370.2	369.9	370.4	370.4	370.3	370.0
#10	370.4	370.4	370.2	369.7	370.4	370.4	370.2	369.9	370.4	370.4	370.3	370.0	370.4	370.4	370.3	370.0	370.4	370.4	370.3	370.1
#11	370.4	370.4	370.2	369.8	370.4	370.4	370.2	369.9	370.4	370.4	370.3	370.0	370.4	370.4	370.3	370.1	370.4	370.4	370.3	370.1
#12	370.4	370.4	370.2	369.8	370.4	370.4	370.3	369.9	370.4	370.4	370.3	370.0	370.4	370.4	370.3	370.1	370.4	370.4	370.3	370.1
#13	370.3	370.3	369.1	351.1	370.3	369.4	365.2	354.5	370.3	369.6	366.2	357.6	370.4	369.7	366.7	359.1	370.4	369.8	367.2	360.6
#14	370.3	369.6	366.6	358.7	370.4	369.7	367.3	360.8	370.4	369.9	367.9	362.7	370.4	369.9	368.2	363.6	370.4	370.0	368.5	364.5
#15	370.4	370.0	368.3	363.9	370.4	370.1	368.7	365.1	370.4	370.1	369.0	366.2	370.4	370.2	369.2	366.6	370.4	370.2	369.3	367.2
#16	370.4	370.1	368.8	365.5	370.4	370.1	369.1	366.4	370.4	370.2	369.3	367.2	370.4	370.2	369.5	367.6	370.4	370.2	369.6	368.0
#17	370.4	370.1	368.9	366.1	370.4	370.1	369.2	366.8	370.4	370.2	369.4	367.6	370.4	370.2	369.5	367.9	370.4	370.2	369.7	368.2

Table A3: ARL_0 for large sample sizes when ties are present for the 2C-SN EWMA chart

n=20

	$\lambda=0.05$				$\lambda=0.15$				$\lambda=0.25$				$\lambda=0.35$				$\lambda=0.45$			
	$\kappa=0.05$	$\kappa=0.1$	$\kappa=0.15$	$\kappa=0.2$	$\kappa=0.05$	$\kappa=0.1$	$\kappa=0.15$	$\kappa=0.2$	$\kappa=0.05$	$\kappa=0.1$	$\kappa=0.15$	$\kappa=0.2$	$\kappa=0.05$	$\kappa=0.1$	$\kappa=0.15$	$\kappa=0.2$	$\kappa=0.05$	$\kappa=0.1$	$\kappa=0.15$	$\kappa=0.2$
#1	370.4	370.4	370.4	370.4	370.4	370.4	370.4	370.4	370.4	370.4	370.4	370.4	370.4	370.4	370.4	370.4	370.4	370.4	370.4	370.4
#2	370.4	370.4	370.4	370.4	370.4	370.4	370.4	370.4	370.4	370.4	370.4	370.4	370.4	370.4	370.4	370.4	370.4	370.4	370.4	370.4
#3	370.4	370.4	370.4	370.4	370.4	370.4	370.4	370.4	370.4	370.4	370.4	370.4	370.4	370.4	370.4	370.4	370.4	370.4	370.4	370.4
#4	370.4	370.4	370.4	370.4	370.4	370.4	370.4	370.4	370.4	370.4	370.4	370.4	370.4	370.4	370.4	370.4	370.4	370.4	370.4	370.4
#5	370.4	370.4	370.4	370.4	370.4	370.4	370.4	370.4	370.4	370.4	370.4	370.4	370.4	370.4	370.4	370.4	370.4	370.4	370.4	370.4
#6	370.4	370.4	370.4	370.4	370.4	370.4	370.4	370.4	370.4	370.4	370.4	370.4	370.4	370.4	370.4	370.4	370.4	370.4	370.4	370.4
#7	370.1	366.1	349.5	311.4	370.3	368.1	359.1	336.5	370.3	368.8	362.6	346.6	370.3	369.2	364.6	352.4	370.3	369.5	365.8	356.1
#8	370.4	369.7	366.6	358.6	370.4	370.0	368.4	364.1	370.4	370.1	369.0	366.1	370.4	370.2	369.4	367.2	370.4	370.2	369.6	367.8
#9	370.3	369.9	368.2	363.8	370.4	370.1	369.2	366.9	370.4	370.2	369.6	368.0	370.4	370.3	369.8	368.6	370.4	370.3	369.9	369.0
#10	370.4	370.1	368.7	365.2	370.4	370.2	369.5	367.6	370.4	370.3	369.8	368.5	370.4	370.3	370.0	369.0	370.4	370.3	370.0	369.3
#11	370.4	370.1	368.9	365.7	370.4	370.2	369.6	367.9	370.4	370.3	369.8	368.7	370.4	370.3	370.0	369.1	370.4	370.3	370.1	369.4
#12	370.4	370.1	368.9	365.9	370.4	370.2	369.6	368.0	370.4	370.3	369.9	368.8	370.4	370.3	370.0	369.2	370.4	370.3	370.1	369.4
#13	369.7	360.4	325.4	258.5	370.0	365.1	345.1	300.5	370.2	366.7	352.7	319.6	370.2	367.7	357.1	331.3	370.3	368.3	359.9	339.0
#14	369.9	364.1	341.8	294.2	370.1	367.1	354.7	325.5	370.2	368.1	359.5	338.5	370.3	368.7	362.3	346.1	370.3	369.1	364.0	351.1
#15	370.2	367.0	354.1	324.5	370.3	368.6	361.6	344.5	370.3	369.2	364.4	352.3	370.3	369.5	365.9	356.8	370.4	369.7	366.8	359.6
#16	370.2	367.7	357.7	334.6	370.3	369.0	363.6	350.5	370.3	369.4	365.7	356.6	370.4	369.7	366.9	360.0	370.4	369.8	367.6	362.2
#17	370.2	368.0	358.9	338.4	370.3	369.1	364.3	352.7	370.3	369.5	366.2	358.2	370.4	369.7	367.3	361.2	370.4	369.9	367.9	363.1
	$\lambda=0.55$				$\lambda=0.65$				$\lambda=0.75$				$\lambda=0.85$				$\lambda=0.95$			
	$\kappa=0.05$	$\kappa=0.1$	$\kappa=0.15$	$\kappa=0.2$	$\kappa=0.05$	$\kappa=0.1$	$\kappa=0.15$	$\kappa=0.2$	$\kappa=0.05$	$\kappa=0.1$	$\kappa=0.15$	$\kappa=0.2$	$\kappa=0.05$	$\kappa=0.1$	$\kappa=0.15$	$\kappa=0.2$	$\kappa=0.05$	$\kappa=0.1$	$\kappa=0.15$	$\kappa=0.2$
#1	370.4	370.4	370.4	370.4	370.4	370.4	370.4	370.4	370.4	370.4	370.4	370.4	370.4	370.4	370.4	370.4	370.4	370.4	370.4	370.4
#2	370.4	370.4	370.4	370.4	370.4	370.4	370.4	370.4	370.4	370.4	370.4	370.4	370.4	370.4	370.4	370.4	370.4	370.4	370.4	370.4
#3	370.4	370.4	370.4	370.4	370.4	370.4	370.4	370.4	370.4	370.4	370.4	370.4	370.4	370.4	370.4	370.4	370.4	370.4	370.4	370.4
#4	370.4	370.4	370.4	370.4	370.4	370.4	370.4	370.4	370.4	370.4	370.4	370.4	370.4	370.4	370.4	370.4	370.4	370.4	370.4	370.4
#5	370.4	370.4	370.4	370.4	370.4	370.4	370.4	370.4	370.4	370.4	370.4	370.4	370.4	370.4	370.4	370.4	370.4	370.4	370.4	370.4
#6	370.4	370.4	370.4	370.4	370.4	370.4	370.4	370.4	370.4	370.4	370.4	370.4	370.4	370.4	370.4	370.4	370.4	370.4	370.4	370.4
#7	370.4	369.7	366.7	359.0	370.4	369.8	367.4	361.0	370.4	369.9	368.0	362.8	370.4	370.0	368.5	364.4	370.4	370.1	368.9	365.6
#8	370.4	370.3	369.8	368.4	370.4	370.3	369.9	368.7	370.4	370.3	370.0	369.1	370.4	370.3	370.1	369.3	370.4	370.3	370.1	369.6
#9	370.4	370.3	370.0	369.3	370.4	370.3	370.1	369.5	370.4	370.3	370.2	369.7	370.4	370.4	370.2	369.8	370.4	370.4	370.2	369.9
#10	370.4	370.3	370.1	369.5	370.4	370.4	370.2	369.7	370.4	370.4	370.2	369.8	370.4	370.4	370.3	369.9	370.4	370.4	370.3	370.0
#11	370.4	370.3	370.1	369.6	370.4	370.4	370.2	369.7	370.4	370.4	370.2	369.9	370.4	370.4	370.3	370.0	370.4	370.4	370.3	370.1
#12	370.4	370.4	370.2	369.6	370.4	370.4	370.2	369.8	370.4	370.4	370.2	369.9	370.4	370.4	370.3	370.0	370.4	370.4	370.3	370.1
#13	370.3	368.7	362.0	345.0	370.3	369.0	363.5	349.5	370.3	369.3	364.8	353.4	370.3	369.5	366.0	356.9	370.4	369.7	366.9	359.6
#14	370.3	369.3	365.3	354.9	370.3	369.5	366.2	357.7	370.3	369.7	367.0	360.1	370.4	369.8	367.7	362.2	370.4	370.0	368.3	363.9
#15	370.4	369.8	367.6	361.8	370.4	369.9	368.1	363.4	370.4	370.0	368.5	364.7	370.4	370.1	368.9	365.9	370.4	370.2	369.2	366.8
#16	370.4	370.0	368.2	363.9	370.4	370.0	368.6	365.1	370.4	370.1	369.0	366.1	370.4	370.2	369.3	367.0	370.4	370.2	369.5	367.7
#17	370.4	370.0	368.4	364.6	370.4	370.1	368.8	365.7	370.4	370.1	369.1	366.6	370.4	370.2	369.4	367.4	370.4	370.2	369.6	368.0

n=30

	$\lambda=0.05$				$\lambda=0.15$				$\lambda=0.25$				$\lambda=0.35$				$\lambda=0.45$			
	$\kappa=0.05$	$\kappa=0.1$	$\kappa=0.15$	$\kappa=0.2$	$\kappa=0.05$	$\kappa=0.1$	$\kappa=0.15$	$\kappa=0.2$	$\kappa=0.05$	$\kappa=0.1$	$\kappa=0.15$	$\kappa=0.2$	$\kappa=0.05$	$\kappa=0.1$	$\kappa=0.15$	$\kappa=0.2$	$\kappa=0.05$	$\kappa=0.1$	$\kappa=0.15$	$\kappa=0.2$
#1	370.4	370.4	370.4	370.4	370.4	370.4	370.4	370.4	370.4	370.4	370.4	370.4	370.4	370.4	370.4	370.4	370.4	370.4	370.4	370.4
#2	370.4	370.4	370.4	370.4	370.4	370.4	370.4	370.4	370.4	370.4	370.4	370.4	370.4	370.4	370.4	370.4	370.4	370.4	370.4	370.4
#3	370.4	370.4	370.4	370.4	370.4	370.4	370.4	370.4	370.4	370.4	370.4	370.4	370.4	370.4	370.4	370.4	370.4	370.4	370.4	370.4
#4	370.4	370.4	370.4	370.4	370.4	370.4	370.4	370.4	370.4	370.4	370.4	370.4	370.4	370.4	370.4	370.4	370.4	370.4	370.4	370.4
#5	370.4	370.4	370.4	370.4	370.4	370.4	370.4	370.4	370.4	370.4	370.4	370.4	370.4	370.4	370.4	370.4	370.4	370.4	370.4	370.4
#6	370.4	370.4	370.4	370.4	370.4	370.4	370.4	370.4	370.4	370.4	370.4	370.4	370.4	370.4	370.4	370.4	370.4	370.4	370.4	370.4
#7	370.0	364.0	340.0	288.6	370.2	367.0	353.6	321.7	370.2	368.1	358.8	335.8	370.3	368.6	361.7	343.9	370.3	369.0	363.5	349.4
#8	370.3	369.3	364.7	353.0	370.4	369.8	367.4	361.0	370.4	370.0	368.3	363.9	370.4	370.1	368.9	365.5	370.4	370.2	369.2	366.6
#9	370.3	369.6	367.0	360.6	370.4	370.0	368.6	365.1	370.4	370.1	369.2	366.8	370.4	370.2	369.5	367.7	370.4	370.2	369.7	368.3
#10	370.4	369.9	367.9	362.7	370.4	370.1	369.1	366.3	370.4	370.2	369.5	367.6	370.4	370.3	369.7	368.3	370.4	370.3	369.9	368.7
#11	370.4	369.9	368.1	363.3	370.4	370.2	369.2	366.6	370.4	370.2	369.6	367.8	370.4	370.3	369.8	368.5	370.4	370.3	369.9	368.9
#12	370.4	370.0	368.2	363.7	370.4	370.2	369.2	366.8	370.4	370.2	369.6	368.0	370.4	370.3	369.8	368.6	370.4	370.3	369.9	369.0
#13	369.4	355.7	306.8	224.9	369.9	362.5	333.6	274.3	370.0	365.0	344.5	299.0	370.1	366.3	350.7	314.3	370.2	367.2	354.8	325.1
#14	369.7	361.1	329.1	266.9	370.0	365.4	347.3	306.7	370.1	367.0	354.4	324.5	370.2	367.8	358.3	335.0	370.2	368.4	360.9	342.1
#15	370.1	365.4	346.5	305.6	370.2	367.7	357.4	332.8	370.3	368.6	361.4	344.0	370.3	369.0	363.6	350.3	370.3	369.3	365.1	354.5
#16	370.1	366.4	351.7	319.2	370.3	368.3	360.3	341.3	370.3	369.0	363.4	350.1	370.3	369.3	365.2	355.0	370.3	369.6	366.3	358.3
#17	370.2	366.8	353.5	324.4	370.3	368.5	361.3	344.5	370.3	369.1	364.1	352.4	370.3	369.4	365.7	356.7	370.3	369.6	366.7	359.6
	$\lambda=0.55$				$\lambda=0.65$				$\lambda=0.75$				$\lambda=0.85$				$\lambda=0.95$			
	$\kappa=0.05$	$\kappa=0.1$	$\kappa=0.15$	$\kappa=0.2$	$\kappa=0.05$	$\kappa=0.1$	$\kappa=0.15$	$\kappa=0.2$	$\kappa=0.05$	$\kappa=0.1$	$\kappa=0.15$	$\kappa=0.2$	$\kappa=0.05$	$\kappa=0.1$	$\kappa=0.15$	$\kappa=0.2$	$\kappa=0.05$	$\kappa=0.1$	$\kappa=0.15$	$\kappa=0.2$
#1	370.4	370.4	370.4	370.4	370.4	370.4	370.4	370.4	370.4	370.4	370.4	370.4	370.4	370.4	370.4	370.4	370.4	370.4	370.4	370.4
#2	370.4	370.4	370.4	370.4	370.4	370.4	370.4	370.4	370.4	370.4	370.4	370.4	370.4	370.4	370.4	370.4	370.4	370.4	370.4	370.4
#3	370.4	370.4	370.4	370.4	370.4	370.4	370.4	370.4	370.4	370.4	370.4	370.4	370.4	370.4	370.4	370.4	370.4	370.4	370.4	370.4
#4	370.4	370.4	370.4	370.4	370.4	370.4	370.4	370.4	370.4	370.4	370.4	370.4	370.4	370.4	370.4	370.4	370.4	370.4	370.4	370.4
#5	370.4	370.4	370.4	370.4	370.4	370.4	370.4	370.4	370.4	370.4	370.4	370.4	370.4	370.4	370.4	370.4	370.4	370.4	370.4	370.4
#6	370.4	370.4	370.4	370.4	370.4	370.4	370.4	370.4	370.4	370.4	370.4	370.4	370.4	370.4	370.4	370.4	370.4	370.4	370.4	370.4
#7	370.3	369.3	364.9	353.5	370.3	369.5	365.9	356.5	370.4	369.7	366.8	359.0	370.4	369.8	367.4	361.0	370.4	369.9	367.7	361.9
# 8	370.4	370.2	369.4	367.4	370.4	370.2	369.6	367.9	370.4	370.3	369.8	368.4	370.4	370.3	369.9	368.7	370.4	370.3	369.9	368.9
#9	370.4	370.3	369.8	368.7	370.4	370.3	369.9	369.0	370.4	370.3	370.0	369.3	370.4	370.3	370.1	369.5	370.4	370.3	370.1	369.6
#10	370.4	370.3	370.0	369.1	370.4	370.3	370.1	369.3	370.4	370.3	370.1	369.5	370.4	370.4	370.2	369.7	370.4	370.4	370.2	369.7
#11	370.4	370.3	370.0	369.2	370.4	370.3	370.1	369.4	370.4	370.3	370.1	369.6	370.4	370.4	370.2	369.7	370.4	370.4	370.2	369.8
#12	370.4	370.3	370.0	369.3	370.4	370.3	370.1	369.5	370.4	370.4	370.2	369.6	370.4	370.4	370.2	369.8	370.4	370.4	370.2	369.8
#13	370.2	367.8	357.9	333.5	370.3	368.3	360.2	339.8	370.3	368.7	362.0	345.1	370.3	369.0	363.5	349.5	370.3	369.1	364.1	351.3
#14	370.3	368.8	362.8	347.5	370.3	369.1	364.2	351.6	370.3	369.3	365.3	355.0	370.3	369.5	366.2	357.7	370.3	369.6	366.6	358.8
#15	370.3	369.5	366.2	357.6	370.4	369.7	366.9	359.9	370.4	369.8	367.6	361.8	370.4	369.9	368.1	363.4	370.4	370.0	368.3	364.0
#16	370.4	369.7	367.1	360.7	370.4	369.9	367.7	362.4	370.4	370.0	368.2	363.9	370.4	370.0	368.6	365.1	370.4	370.1	368.8	365.5
#17	370.4	369.8	367.4	361.8	370.4	369.9	368.0	363.4	370.4	370.0	368.4	364.6	370.4	370.1	368.8	365.7	370.4	370.1	368.9	366.1

Table A4: Phase II samples of $t = 1, 2, \ldots 20$ subgroups of size $n = 5$

	Subgroup																			
First 20 subgroups for both examples																				
X_{ij}	1	2	3	4	5	6	7	8	9	10	11	12	13	14	15	16	17	18	19	20
1	20.083	20.028	19.950	19.889	19.941	20.020	20.101	20.022	20.049	20.169	20.099	19.978	20.135	19.878	20.130	20.010	20.086	19.888	20.000	19.885
2	20.115	20.129	19.900	20.043	19.996	20.072	20.109	20.009	20.013	19.808	19.923	20.052	20.011	19.917	20.120	20.096	20.124	19.931	19.974	20.107
3	19.990	19.954	19.940	20.003	20.009	20.182	19.846	20.018	20.110	20.110	20.045	20.038	19.911	19.925	20.124	19.906	20.140	19.903	20.078	20.004
4	20.022	20.080	20.133	19.800	19.853	20.132	20.198	20.047	19.893	20.029	19.985	20.097	19.913	19.988	19.801	20.108	20.057	20.003	20.135	20.067
5	19.995	20.049	19.976	20.113	19.906	20.099	19.905	19.962	19.857	19.913	19.852	20.031	19.781	20.058	19.962	19.891	20.111	19.878	19.885	20.197

Last 10 subgroups for example 1 (Figure 5.1)

X_{ij}	21	22	23	24	25	26	27	28	29	30
1	19.843	20.038	20.077	20.031	19.650	20.265	20.028	20.162	20.000	20.544
2	20.142	19.709	20.046	20.190	19.396	20.085	20.139	19.949	20.093	19.865
3	19.757	19.872	20.154	19.903	19.969	20.201	19.824	19.859	19.901	19.857
4	20.184	20.016	20.083	19.669	19.955	20.238	19.779	20.395	19.836	20.262
5	20.178	20.205	20.248	20.049	20.102	20.048	19.824	19.615	19.918	19.838

Last 10 subgroups for example 2 (Figure 5.2)

X_{ij}	21	22	23	24	25	26	27	28	29	30
1	20.044	20.044	20.097	20.049	20.018	19.994	19.957	20.044	20.047	19.942
2	20.046	20.037	19.859	20.001	20.003	20.038	20.009	19.969	20.051	19.975
3	20.058	19.966	19.983	20.085	20.076	20.001	20.018	20.009	19.931	20.041
4	20.104	20.046	19.944	19.986	20.087	20.016	20.071	20.090	19.974	20.008
5	19.969	19.998	19.979	20.018	20.070	19.996	19.939	20.055	20.015	19.973

Table A5: ARL values of the two-sided 2C-WSR EWMA chart for fixed values of $h = \{0.1, 0.15, \ldots, 0.3\}$ and different combinations of (n, λ, K).

	$(n,\lambda,K)=(5,0.2,2.763)$					$(n,\lambda,K)=(7,0.2,2.799)$					$(n,\lambda,K)=(11,0.2,2.814)$				
	h					h					h				
$2m+1$	0.1	0.15	0.2	0.25	0.3	0.1	0.15	0.2	0.25	0.3	0.1	0.15	0.2	0.25	0.3
51	350.0	355.1	359.1	362.0	364.1	376.9	376.8	376.4	375.9	375.1	366.6	367.2	367.6	367.8	367.9
61	371.9	371.1	370.3	369.5	368.9	365.9	366.4	366.6	366.8	367.0	369.4	369.5	369.4	369.4	369.3
71	364.8	366.7	367.9	368.5	368.7	371.3	370.0	369.5	369.4	369.3	370.3	370.1	369.9	369.8	369.7
81	383.6	378.3	373.6	370.9	369.6	365.0	367.0	368.4	369.2	369.4	371.8	371.7	371.5	371.3	371.1
91	369.0	369.6	369.6	369.6	369.4	370.6	370.5	370.3	370.1	370.0	368.4	368.5	368.7	368.8	369.0
101	372.8	371.2	370.3	369.8	369.6	369.4	369.6	369.7	369.8	369.8	369.1	369.2	369.3	369.3	369.4
111	367.8	369.3	369.8	369.8	369.7	371.2	371.0	370.7	370.4	370.2	369.7	369.7	369.7	369.8	369.8
121	370.7	370.4	370.1	370.0	369.8	369.4	369.5	369.7	369.9	370.0	369.9	369.9	369.9	370.0	370.0
131	369.4	370.1	370.2	370.0	369.8	369.5	369.8	370.0	370.1	370.1	370.1	370.1	370.0	370.0	370.0
141	370.0	370.3	370.2	370.1	369.9	370.5	370.3	370.3	370.2	370.2	370.9	370.2	370.1	370.1	370.1
151	370.2	370.4	370.3	370.1	369.9	370.5	370.5	370.4	370.3	370.3	370.2	370.2	370.2	370.2	370.2
161	371.7	370.6	370.3	370.1	370.0	374.5	373.0	371.5	370.8	370.4	370.0	370.0	370.1	370.1	370.2
171	370.5	370.5	370.3	370.2	370.0	371.0	370.7	370.5	370.4	370.3	374.3	373.5	372.6	371.7	371.1
181	370.8	370.5	370.4	370.2	370.0	370.7	370.5	370.4	370.4	370.4	370.4	370.4	370.4	370.3	370.3
191	370.1	370.5	370.4	370.2	370.0	370.1	370.3	370.4	370.4	370.4	370.4	370.4	370.3	370.3	370.3
201	370.5	370.5	370.4	370.2	370.0	370.3	370.4	370.4	370.4	370.4	370.5	370.4	370.4	370.4	370.3

Table A6: Comparison of in control ARL values for the two-sided 2-WSR EWMA (without "continuousify") and two-sided 2C-WSR EWMA (with "continuousify" and $h = 0.2$) for several desired $\text{ARL})_0$ values

(In-control ARL values for the 2-WSR EWMA and 2C-WSR EWMA charts for desired $\text{ARL}_0 = 200$)

	$(n, \lambda, K) = (5, 0.2, 2.568)$		$(n, \lambda, K) = (7, 0.2, 2.586)$		$(n, \lambda, K) = (9, 0.2, 2.597)$		$(n, \lambda, K) = (11, 0.2, 2.604)$	
$2m+1$	2-WSR EWMA	2C-WSR EWMA	2-WSR EWMA	2C-WSR EWMA	2-WSR EWMA	2C-WSR EWMA	2-WSR EWMA	2C-WSR EWMA
51	190.2	192.3	200.6	200.2	195.0	199.1	199.7	199.7
61	205.2	200.2	199.4	200.5	198.0	199.0	200.1	199.5
71	197.0	200.0	196.3	199.6	199.8	199.9	200.4	199.5
81	197.4	199.4	192.0	195.7	199.0	199.6	197.5	198.2
91	191.7	199.6	200.8	199.7	199.1	199.7	199.2	199.8
101	202.0	200.0	196.7	199.8	199.5	200.0	200.0	199.9
111	196.7	199.8	202.2	200.1	199.9	200.0	200.2	199.9
121	194.8	199.9	200.6	199.8	200.1	199.7	199.4	200.0
131	201.5	199.9	198.5	199.9	200.9	199.9	200.3	200.0
141	201.8	199.9	200.8	199.9	199.7	199.9	200.3	200.0
151	198.1	199.9	200.5	199.9	202.1	200.0	200.4	200.1
161	204.5	200.0	205.4	200.1	196.7	200.0	200.2	199.8
171	202.8	200.0	199.9	200.0	200.4	200.0	199.8	199.9
181	199.2	200.0	201.9	200.0	199.5	199.9	199.7	200.0
191	199.8	200.0	198.9	200.0	199.3	200.0	200.4	200.0
201	204.0	200.0	201.4	200.0	200.3	200.0	200.4	200.0
211	199.1	200.0	199.1	200.0	199.5	200.0	200.1	200.0

(In-control ARL values for the 2-WSR EWMA and 2C-WSR EWMA charts for desired $\text{ARL}_0 = 370.4$)

	$(n, \lambda, K) = (5, 0.2, 2.76)$		$(n, \lambda, K) = (7, 0.2, 2.790)$		$(n, \lambda, K) = (9, 0.2, 2.805)$		$(n, \lambda, K) = (11, 0.2, 2.814$	
$2m+1$	2-WSR EWMA	2C-WSR EWMA	2-WSR EWMA	2C-WSR EWMA	2-WSR EWMA	2C-WSR EWMA	2-WSR EWMA	2C-WSR EWMA
51	338.5	359.1	379.1	363.7	370.6	368.4	366.6	367.6
61	382.4	370.3	363.0	366.1	372.2	381.2	370.5	369.4
71	359.0	367.9	373.2	367.0	370.8	369.9	368.9	369.9
81	389.3	373.6	362.3	367.3	371.0	368.6	370.1	371.5
91	362.2	369.6	371.3	373.3	370.8	369.2	368.4	368.7
101	376.7	370.3	370.7	370.2	371.0	369.8	369.9	369.3
111	354.6	369.8	369.9	370.1	369.6	369.5	369.4	369.7
121	369.6	370.1	371.0	370.4	368.4	369.9	369.2	369.9
131	363.3	370.2	372.5	371.5	369.6	369.8	369.3	370.0
141	365.4	370.2	372.8	370.3	374.6	370.1	369.8	370.1
151	363.5	370.3	371.5	370.3	370.4	370.1	370.1	370.2
161	377.8	370.3	376.2	370.4	370.2	370.3	370.8	370.1
171	359.1	370.3	368.3	370.4	374.8	370.2	369.8	372.6
181	371.9	370.4	367.1	370.3	369.8	370.3	371.8	370.4
191	354.2	370.4	369.8	370.4	370.4	370.4	368.3	370.3
201	369.0	370.4	370.4	370.4	371.1	370.4	370.2	370.4
211	364.1	370.4	372.4	370.4	366.5	370.3	371.8	370.4

(In-control ARL values for the 2-WSR EWMA and 2C-WSR EWMA charts for desired $\text{ARL}_0 = 500$)

	$(n, \lambda, K) = (5, 0.2, 2.85)$		$(n, \lambda, K) = (7, 0.2, 2.882)$		$((n, \lambda, K) = (9, 0.2, 2.89)$		$(n, \lambda, K) = (11, 0.2, 2.910)$	
$2m+1$	2-WSR EWMA	2C-WSR EWMA	2-WSR EWMA	2C-WSR EWMA	2-WSR EWMA	2C-WSR EWMA	2-WSR EWMA	2C-WSR EWMA
51	503.8	503.8	515.8	499.1	495.7	498.7	501.6	496.0
61	491.2	498.5	508.5	498.7	492.7	493.8	496.5	497.6
71	526.2	498.9	511.5	499.5	494.6	497.1	490.7	497.6
81	493.8	497.7	504.8	497.8	500.4	497.2	493.6	497.0
91	495.9	498.2	477.5	488.7	500.4	498.3	496.0	498.9
101	514.9	499.8	505.3	499.6	497.3	499.3	497.0	499.6
111	468.9	498.0	497.9	499.7	503.4	499.8	500.3	499.9
121	506.8	499.6	502.9	499.9	499.5	499.0	497.7	499.7
131	507.8	499.6	497.0	499.6	495.1	491.6	494.3	498.2
141	490.3	499.6	502.5	499.5	499.9	499.3	498.2	499.6
151	501.7	499.7	496.2	499.5	500.9	500.0	498.9	499.9
161	495.8	499.7	504.2	499.7	497.9	499.9	497.8	499.7
171	500.2	499.8	504.4	499.8	498.1	499.6	494.2	498.2
181	487.2	499.8	511.5	500.3	501.3	499.7	500.5	500.0
191	497.6	499.8	498.2	499.8	501.2	499.9	497.1	500.2
201	509.0	499.9	503.2	499.8	499.5	500.0	498.5	500.0
211	498.4	499.9	499.3	499.8	502.7	500.1	500.8	500.1

Table A7: Comparison of in control ARL values for the two-sided WSR EWMA (without "continuousify") and two-sided C-WSR EWMA (with "continuousify" and $h = 0.2$) using $(\lambda, K) = (0.2, 2.85)$ for different (n, p_1) combinations.

	$(n,p_1)=(5,0.52)$		$(n,p_1)=(5,0.53)$		$(n,p_1)=(5,0.54)$		$(n,p_1)=(5,0.55)$	
$2m+1$	2-WSR EWMA	2C-WSR EWMA	2-WSR EWMA	2C-WSR EWMA	2-WSR EWMA	2C-WSR EWMA	2-WSR EWMA	2C-WSR EWMA
51	406.8	403.9	326.0	324.1	253.2	251.9	195.0	194.1
61	397.3	399.7	319.0	321.0	248.1	249.7	191.3	192.6
71	399.1	400.5	320.7	321.6	249.8	250.1	192.7	192.8
81	399.3	399.2	320.5	320.5	249.3	249.3	192.2	192.2
91	401.1	399.8	322.0	321.0	250.5	249.6	193.1	192.4
101	392.7	401.0	315.5	321.8	245.6	250.2	189.5	192.9
111	380.6	399.6	306.6	320.8	239.3	249.5	185.0	192.3
121	409.1	400.8	327.9	321.7	254.6	250.1	196.0	192.8
131	409.9	400.8	328.5	321.6	255.1	250.1	196.4	192.7
141	396.7	400.8	318.6	321.6	247.9	250.1	191.2	192.7
151	405.1	400.9	324.8	321.7	252.3	250.1	194.2	192.8
161	397.7	400.9	319.2	321.7	248.3	250.1	191.4	192.8
171	404.0	400.9	324.0	321.7	251.7	250.2	193.9	192.8
181	394.2	400.9	316.6	321.7	246.4	250.2	190.1	192.8
191	402.0	401.0	322.5	321.8	250.6	250.2	193.1	192.8
201	410.6	401.0	328.9	321.8	255.3	250.2	196.4	192.8
211	398.3	401.0	319.6	321.8	248.6	250.2	191.6	192.8

	$(n,p_1)=(7,0.52)$		$(n,p_1)=(7,0.53)$		$(n,p_1)=(7,0.54)$		$(n,p_1)=(7,0.55)$	
$2m+1$	2-WSR EWMA	2C-WSR EWMA	2-WSR EWMA	2C-WSR EWMA	2-WSR EWMA	2C-WSR EWMA	2-WSR EWMA	2C-WSR EWMA
51	333.0	341.1	255.5	261.3	190.9	195.0	142.5	145.3
61	339.9	343.5	260.5	263.1	194.4	196.3	145.0	146.2
71	346.9	342.6	265.5	262.5	197.8	195.9	147.3	146.0
81	349.3	343.1	267.2	262.8	199.1	196.1	148.2	146.1
91	334.5	337.9	256.7	259.1	191.8	193.5	143.2	144.3
101	336.7	341.9	258.3	261.9	192.9	195.5	143.9	145.7
111	345.4	342.4	264.5	262.3	197.2	195.7	146.9	145.8
121	342.2	342.2	262.1	262.2	195.5	195.6	145.7	145.8
131	336.4	342.0	258.1	262.0	192.8	195.5	143.9	145.7
141	344.3	342.9	263.6	262.6	196.5	195.9	146.4	146.0
151	344.2	342.8	263.6	262.6	196.5	195.9	146.4	145.9
161	341.6	342.8	261.7	262.6	195.2	195.9	145.5	145.9
171	346.5	342.8	265.2	262.6	197.6	195.9	147.2	145.9
181	335.1	342.5	257.0	262.4	192.0	195.7	143.2	145.8
191	340.6	342.8	261.0	262.6	194.7	195.8	145.1	145.9
201	342.0	342.8	262.0	262.6	195.4	195.9	145.6	145.9
211	343.6	342.8	263.2	262.6	196.3	195.9	146.2	145.9

	$(n,p_1)=(9,0.52)$		$(n,p_1)=(9,0.53)$		$(n,p_1)=(9,0.54)$		$(n,p_1)=(9,0.55)$	
$2m+1$	2-WSR EWMA	2C-WSR EWMA	2-WSR EWMA	2C-WSR EWMA	2-WSR EWMA	2C-WSR EWMA	2-WSR EWMA	2C-WSR EWMA
51	302.3	306.4	222.9	225.5	161.0	162.7	117.1	118.2
61	312.9	313.1	230.0	230.1	165.7	165.7	120.2	120.2
71	308.2	305.9	226.6	225.1	163.2	162.3	118.5	117.9
81	310.6	307.3	228.1	226.0	164.2	162.9	119.0	118.2
91	303.6	307.4	223.5	226.1	161.2	162.9	117.1	118.3
101	306.8	307.5	225.7	226.1	162.7	162.9	118.1	118.3
111	308.6	307.8	226.9	226.3	163.5	163.1	118.6	118.4
121	308.6	307.8	226.9	226.3	163.4	163.1	118.6	118.4
131	313.4	310.3	230.1	228.0	165.5	164.2	120.0	119.1
141	309.1	308.0	227.2	226.5	163.7	163.2	118.8	118.5
151	307.4	308.1	226.1	226.5	162.9	163.2	118.3	118.5
161	309.8	308.1	227.7	226.6	164.0	163.3	119.0	118.5
171	305.0	308.0	224.4	226.5	161.8	163.2	117.6	118.5
181	308.1	308.2	226.5	226.5	163.2	163.2	118.5	118.5
191	313.8	309.1	230.3	227.2	165.7	163.7	120.1	118.8
201	307.9	308.1	226.3	226.5	163.1	163.2	118.4	118.5
211	307.9	308.1	226.4	226.5	163.1	163.2	118.4	118.5

Table A8: ARL values of the C-WSR EWMA chart for $h = 0.2$, $n \in \{5, 7, 9\}$ for the standardised kernels listed in Table 3.7

(In-control ARL values for the 2-WSR EWMA and 2C-WSR EWMA charts for desired $\text{ARL}_0 = 370.4$)

	$(n, \lambda, K) = (5, 0.2, 2.76)$					$(n, \lambda, K) = (7, 0.2, 2.790)$					$(n, \lambda, K) = (9, 0.2, 2.805)$				
$2m+1$	Parabolic	Biweight	Cosine	Triweight	Normal	Parabolic	Biweight	Cosine	Triweight	Normal	Parabolic	Biweight	Cosine	Triweight	Normal
51	360.8	360.3	360.6	360.0	359.1	363.6	363.7	363.6	363.7	363.7	368.9	368.7	368.9	368.6	368.4
61	370.2	370.3	370.2	370.3	370.3	365.9	365.9	365.9	366.0	366.1	381.0	381.0	381.0	381.1	381.2
71	368.4	368.2	368.4	368.2	367.9	367.1	367.1	367.1	367.1	367.0	369.9	369.9	369.9	369.9	369.9
81	370.7	371.6	370.9	372.1	373.6	367.6	367.5	367.6	367.5	367.3	368.5	368.6	368.5	368.6	368.6
91	369.6	369.6	369.6	369.7	369.6	372.9	373.0	372.9	373.0	373.3	369.2	369.2	369.2	369.2	369.2
101	369.6	369.8	369.7	369.9	370.3	370.2	370.2	370.2	370.2	370.2	369.8	369.8	369.9	369.8	369.8
111	370.3	370.2	370.3	370.1	369.8	369.9	370.0	369.9	370.0	370.1	369.5	369.6	369.5	369.6	369.5
121	370.1	370.1	370.1	370.1	370.1	370.2	370.3	370.2	370.3	370.4	370.0	370.0	370.0	369.9	369.9
131	370.4	370.3	370.3	370.2	370.2	370.6	370.8	370.6	370.9	371.5	369.8	369.8	369.8	369.8	369.8
141	370.3	370.3	370.3	370.2	370.2	370.2	370.2	370.2	370.2	370.3	370.1	370.1	370.1	370.1	370.1
151	370.3	370.3	370.3	370.3	370.3	370.2	370.3	370.2	370.3	370.3	370.1	370.1	370.1	370.1	370.1
161	370.4	370.4	370.4	370.3	370.3	370.3	370.3	370.3	370.3	370.4	370.3	370.3	370.3	370.3	370.3
171	370.3	370.3	370.3	370.3	370.3	370.3	370.3	370.3	370.3	370.4	370.2	370.2	370.2	370.2	370.2
181	370.4	370.4	370.4	370.4	370.4	370.4	370.4	370.4	370.4	370.3	370.3	370.3	370.3	370.3	370.3
191	370.3	370.3	370.3	370.4	370.4	370.5	370.4	370.4	370.4	370.4	370.4	370.4	370.4	370.4	370.4
201	370.4	370.4	370.4	370.4	370.4	370.4	370.4	370.4	370.4	370.4	370.4	370.4	370.4	370.4	370.4

(In-control ARL values for the 2-WSR EWMA and 2C-WSR EWMA charts for desired $\text{ARL}_0 = 370.4$)

	$(n, \lambda, K) = (5, 0.2, 2.85)$					$(n, \lambda, K) = (7, 0.2, 2.882)$					$(n, \lambda, K) = (9, 0.2, 2.89)$				
$2m+1$	Parabolic	Biweight	Cosine	Triweight	Normal	Parabolic	Biweight	Cosine	Triweight	Normal	Parabolic	Biweight	Cosine	Triweight	Normal
51	503.8	503.6	503.7	503.6	503.8	498.9	499.1	498.9	499.1	499.1	498.5	498.6	498.5	498.6	498.7
61	498.9	498.7	498.8	498.6	498.5	497.9	498.2	498.0	498.4	498.7	493.8	493.8	493.8	493.8	493.8
71	498.9	498.9	498.9	498.9	498.9	499.3	499.3	499.3	499.4	499.5	497.2	497.2	497.2	497.1	497.1
81	498.1	498.0	498.1	497.9	497.7	497.6	497.7	497.7	497.8	497.8	497.0	497.0	497.0	497.1	497.2
91	499.2	498.9	499.1	498.7	498.2	490.5	490.0	490.3	489.7	488.7	498.5	498.4	498.4	498.4	498.3
101	498.6	499.1	498.8	499.3	499.8	499.4	499.5	499.5	499.5	499.6	499.5	499.4	499.5	499.4	499.3
111	501.9	500.4	501.4	499.8	498.0	499.5	499.6	499.6	499.6	499.7	499.7	499.8	499.7	499.8	499.8
121	499.2	499.4	499.3	499.4	499.6	499.7	499.7	499.7	499.8	499.9	499.1	499.1	499.1	499.1	499.0
131	499.5	499.6	499.6	499.6	499.6	499.5	499.5	499.5	499.5	499.6	492.5	492.2	492.4	492.1	491.6
141	500.1	499.9	500.0	499.8	499.6	499.5	499.5	499.5	499.5	499.5	499.4	499.4	499.4	499.3	499.3
151	499.5	499.6	499.6	499.6	499.7	499.6	499.6	499.6	499.6	499.5	499.9	499.9	499.9	500.0	500.0
161	499.6	499.7	499.6	499.7	499.7	499.7	499.7	499.7	499.7	499.7	499.9	499.9	499.9	499.9	499.9
171	499.7	499.8	499.7	499.8	499.8	499.6	499.7	499.7	499.7	499.8	499.7	499.7	499.7	499.7	499.6
181	499.8	499.8	499.8	499.8	499.8	498.9	499.4	499.1	499.6	500.3	499.8	499.8	499.8	499.8	499.7
191	499.8	499.8	499.8	499.8	499.8	499.9	499.9	499.9	499.8	499.8	499.9	499.9	499.9	499.9	499.9
201	500.0	499.9	499.9	499.9	499.9	499.9	499.9	499.9	499.9	499.8	499.9	500.0	499.9	500.0	500.0

Table A9: ARL_0 values of the upper-sided C-WSR EWMA chart for $\lambda = 0.2, K_1 = 2.75$ and fixed values of $h = \{0.1, 0.15, \ldots, 0.3\}$ under different values of n.

	$n=5$					$n=8$					$n=11$				
	h					h					h				
m	0.1	0.15	0.2	0.25	0.3	0.1	0.15	0.2	0.25	0.3	0.1	0.15	0.2	0.25	0.3
50	456.3	455.8	455.7	455.7	455.6	413.6	413.5	413.4	413.4	413.4	397.7	397.6	397.4	397.2	397.0
60	457.2	456.7	456.4	456.2	455.9	414.9	414.5	414.1	413.9	413.7	396.3	396.2	396.1	396.1	396.1
70	456.7	456.7	456.5	456.3	456.1	412.6	413.2	413.5	413.6	413.7	396.3	396.4	396.4	396.4	396.4
80	458.2	456.9	456.6	456.4	456.2	410.7	412.0	413.0	413.5	413.7	396.5	396.6	396.6	396.5	396.5
90	457.2	456.8	456.6	456.5	456.2	414.2	414.1	414.0	413.9	413.9	396.4	396.4	396.5	396.5	396.5
100	457.0	456.8	456.7	456.5	456.3	413.6	413.8	413.9	413.9	413.9	396.5	396.6	396.6	396.6	396.6
110	457.2	456.9	456.7	456.6	456.3	414.1	414.0	414.0	414.0	414.0	396.4	396.5	396.5	396.6	396.6
120	457.2	456.9	456.8	456.6	456.4	414.0	414.0	414.1	414.0	414.0	396.5	396.6	396.6	396.6	396.6
130	457.0	456.9	456.8	456.6	456.4	415.2	414.4	414.1	414.1	414.1	396.8	396.7	396.7	396.7	396.7
140	457.0	456.9	456.8	456.6	456.4	414.2	414.1	414.1	414.1	414.1	396.7	396.7	396.7	396.7	396.7
150	457.1	457.0	456.8	456.6	456.4	414.1	414.1	414.1	414.1	414.1	396.7	396.7	396.7	396.7	396.7
160	457.1	457.0	456.8	456.6	456.4	414.1	414.1	414.1	414.1	414.1	396.7	396.7	396.7	396.7	396.7
170	457.1	457.0	456.8	456.6	456.4	414.1	414.1	414.1	414.1	414.1	396.8	396.7	396.7	396.7	396.7
180	457.1	457.0	456.9	456.6	456.4	414.1	414.1	414.1	414.1	414.1	396.8	396.7	396.7	396.7	396.7
190	457.1	457.0	456.9	456.7	456.4	414.2	414.2	414.1	414.1	414.1	396.7	396.7	396.7	396.7	396.7
200	457.1	457.0	456.9	456.7	456.4	414.2	414.2	414.2	414.1	414.1	396.8	396.8	396.7	396.7	396.7

	$n=13$					$n=15$					$n=20$				
	h					h					h				
m	0.1	0.15	0.2	0.25	0.3	0.1	0.15	0.2	0.25	0.3	0.1	0.15	0.2	0.25	0.3
50	389.6	389.6	389.6	389.6	389.6	384.6	384.6	384.6	384.5	384.6	378.3	378.3	378.2	378.1	378.0
60	389.2	389.2	389.2	389.2	389.3	384.6	384.6	384.6	384.6	384.6	377.6	377.6	377.6	377.6	377.5
70	389.0	389.5	389.7	389.8	389.8	385.3	385.3	385.3	385.2	385.2	377.6	377.6	377.6	377.5	377.5
80	389.7	389.7	389.7	389.7	389.7	387.7	387.4	387.1	386.8	386.6	377.7	377.7	377.7	377.6	377.6
90	389.8	389.8	389.8	389.8	389.8	385.0	385.0	385.0	385.0	385.0	377.8	377.8	377.8	377.8	377.7
100	389.9	389.9	389.9	389.8	389.8	385.2	385.1	385.1	385.1	385.1	376.2	376.3	376.4	376.6	376.8
110	390.0	389.9	389.9	389.9	389.9	385.1	385.1	385.1	385.1	385.1	377.6	377.6	377.6	377.6	377.6
120	389.9	389.9	389.9	389.9	389.9	385.2	385.2	385.2	385.2	385.1	377.8	377.8	377.8	377.8	377.8
130	390.7	390.5	390.3	390.2	390.1	384.3	384.4	384.6	384.8	384.9	377.6	377.6	377.6	377.6	377.6
140	389.9	389.9	389.9	389.9	389.9	385.2	385.2	385.2	385.2	385.2	377.6	377.6	377.6	377.7	377.7
150	389.8	389.9	389.9	389.9	389.9	385.2	385.2	385.2	385.2	385.2	377.7	377.7	377.7	377.7	377.7
160	389.9	389.9	389.9	389.9	389.9	385.7	385.5	385.4	385.3	385.3	377.7	377.7	377.7	377.7	377.7
170	389.9	389.9	389.9	389.9	389.9	385.2	385.2	385.2	385.2	385.2	377.7	377.7	377.7	377.7	377.7
180	389.9	389.9	389.9	389.9	389.9	385.2	385.2	385.2	385.2	385.2	377.7	377.7	377.7	377.7	377.7
190	389.9	389.9	389.9	389.9	389.9	385.4	385.3	385.2	385.2	385.2	377.7	377.7	377.7	377.7	377.7
200	390.0	390.0	390.0	390.0	390.0	385.2	385.2	385.2	385.2	385.2	377.9	377.9	377.8	377.8	377.8

Table A10: Comparison of in control ARL values for the upper-sided WSR EWMA (without "continuousify") and upper-sided C-WSR EWMA (with "continuousify" and $h = 0.2$) for several desired ARL_0 values

(In-control ARL values for the WSR EWMA and C-WSR EWMA charts for desired $\text{ARL}_0 = 200$)

	$(n, \lambda, K_1) = (5, 0.2, 2.477)$		$(n, \lambda, K_1) = (8, 0.2, 2.491)$		$(n, \lambda, K_1) = (9, 0.2, 2.500)$		$(n, \lambda, K_1) = (11, 0.2, 2.505)$	
m	WSR EWMA	C-WSR EWMA	WSR EWMA	C-WSR EWMA	WSR EWMA	C-WSR EWMA	WSR EWMA	C-WSR EWMA
50	200.4	199.9	299.8	200.1	201.1	199.7	193.7	199.8
60	199.3	199.9	275.8	199.2	199.7	199.9	221.6	199.8
70	202.6	199.9	294.2	199.6	200.8	200.4	189.8	200.0
80	202.8	200.0	281.1	200.0	200.1	200.0	204.4	200.0
90	197.6	200.0	186.5	199.8	201.2	200.0	206.8	200.0
100	200.9	200.0	192.7	200.0	199.9	200.0	191.1	200.0
110	199.8	200.0	199.5	200.0	199.8	200.0	214.4	200.0
120	201.8	200.0	164.9	200.0	199.9	200.0	210.5	200.1
130	200.9	200.0	187.2	200.0	200.1	200.0	187.5	200.0
140	201.2	200.0	250.7	200.0	202.0	200.1	189.3	200.2
150	199.6	200.0	296.6	200.0	201.6	200.0	177.3	200.1
160	198.9	200.0	229.5	200.0	199.8	200.0	196.9	200.1
170	198.7	200.0	167.9	200.0	200.7	200.0	209.9	200.1
180	200.7	200.0	295.4	200.0	199.8	200.0	207.5	200.1
190	199.3	200.0	212.0	200.0	200.6	200.0	217.4	200.1
200	202.7	200.0	243.5	200.0	200.1	200.1	203.4	200.1

(In-control ARL values for the WSR EWMA and C-WSR EWMA charts for desired $\text{ARL}_0 = 370.4$)

	$(n, \lambda, K_1) = (5, 0.2, 2.684)$		$(n, \lambda, K_1) = (8, 0.2, 2.713)$		$(n, \lambda, K_1) = (9, 0.2, 2.719)$		$(n, \lambda, K_1) = (11, 0.2, 2.727)$	
m	WSR EWMA	C-WSR EWMA	WSR EWMA	C-WSR EWMA	WSR EWMA	C-WSR EWMA	WSR EWMA	C-WSR EWMA
50	375.2	369.9	366.6	367.8	370.8	370.5	289.3	372.2
60	369.9	370.1	294.9	369.8	373.9	372.0	371.2	370.1
70	368.7	370.2	286.2	370.5	369.5	370.6	404.8	370.2
80	377.2	370.3	391.8	370.3	370.1	370.3	417.8	371.1
90	370.5	370.4	1012.1	370.4	371.7	370.7	303.8	370.2
100	373.9	370.4	400.8	370.4	370.7	370.4	308.0	370.4
110	367.1	370.4	367.5	370.5	371.4	370.4	450.6	370.3
120	364.4	370.4	720.5	370.5	371.2	370.5	371.0	370.3
130	370.4	370.5	275.9	370.4	369.5	370.5	370.2	370.4
140	369.8	370.5	339.4	370.5	371.7	370.5	326.8	370.4
150	373.3	370.5	303.7	370.6	371.0	370.5	402.0	370.4
160	372.9	370.5	825.1	370.6	369.9	370.5	356.3	370.4
170	367.7	370.5	1220.6	370.6	369.2	370.5	469.8	370.4
180	368.8	370.5	634.7	370.6	370.2	370.5	435.5	370.4
190	367.9	370.5	275.2	370.6	369.5	370.5	421.9	370.4
200	369.0	370.5	1160.3	370.6	370.9	370.5	462.1	370.4

(In-control ARL values for the WSR EWMA and C-WSR EWMA charts for desired $\text{ARL}_0 = 500$)

	$(n, \lambda, K_1) = (5, 0.2, 2.778)$		$(n, \lambda, K_1) = (8, 0.2, 2.811)$		$(n, \lambda, K_1) = (9, 0.2, 2.818)$		$(n, \lambda, K_1) = (11, 0.2, 2.827)$	
m	WSR EWMA	C-WSR EWMA	WSR EWMA	C-WSR EWMA	WSR EWMA	C-WSR EWMA	WSR EWMA	C-WSR EWMA
50	483.7	498.4	264.1	500.7	500.8	499.6	366.9	499.6
60	494.6	499.4	515.3	499.7	496.8	499.0	502.7	499.2
70	491.4	499.6	529.8	499.0	497.1	500.0	495.5	499.7
80	498.5	499.8	354.6	497.9	493.8	498.6	596.9	499.6
90	495.4	499.8	2391.4	499.7	501.0	500.0	659.0	500.1
100	498.0	499.9	322.9	500.2	501.3	500.0	431.3	500.0
110	476.1	499.9	408.1	499.9	500.3	500.2	444.2	500.0
120	490.8	499.9	1631.4	499.9	501.4	500.5	648.6	500.1
130	503.4	500.0	475.1	500.0	501.4	500.2	503.9	500.1
140	504.4	500.0	2002.3	500.0	499.2	500.3	370.5	500.1
150	504.1	500.0	469.1	500.0	500.5	500.2	555.4	500.2
160	506.5	500.0	838.1	500.0	503.1	500.3	593.3	500.0
170	503.3	500.0	397.4	500.0	499.2	500.3	580.4	500.0
180	503.6	500.0	369.8	500.0	499.8	500.3	395.2	500.2
190	501.1	500.0	329.9	500.1	506.7	500.3	498.8	500.2
200	500.2	500.0	363.0	500.1	500.1	500.3	472.9	500.2

Table A11: Comparison of in control ARL values for the upper-sided WSR EWMA (without "continuousify") and upper-sided C-WSR EWMA (with "continuousify" and $h = 0.2$) using $\lambda = 0.2, K_1 = 2.75$ for different (n, p_1) combinations when $p_1 < 0.6$.

	$(n, p_1) = (5, 0.52)$		$(n, p_1) = (5, 0.53)$		$(n, p_1) = (5, 0.54)$		$(n, p_1) = (5, 0.55)$	
m	WSR EWMA	C-WSR EWMA	WSR EWMA	C-WSR EWMA	WSR EWMA	C-WSR EWMA	WSR EWMA	C-WSR EWMA
50	356.3	263.9	271.3	204.2	208.9	159.8	162.8	126.4
60	360.6	264.2	274.4	204.4	211.1	159.9	164.4	126.5
70	350.4	264.3	266.8	204.4	205.5	159.9	160.2	126.5
80	349.9	264.3	266.6	204.5	205.5	159.9	160.2	126.5
90	364.0	264.4	276.6	204.5	212.7	160.0	165.5	126.6
100	364.3	264.4	276.7	204.5	212.7	160.0	165.4	126.6
110	359.1	264.4	273.1	204.5	210.1	160.0	163.6	126.6
120	357.0	264.4	271.6	204.5	209.1	160.0	162.8	126.6
130	358.8	264.4	272.9	204.5	210.0	160.0	163.5	126.6
140	350.2	264.4	266.7	204.5	205.4	160.0	160.1	126.6
150	359.8	264.4	273.7	204.5	210.6	160.0	163.9	126.6
160	360.3	264.4	274.0	204.5	210.8	160.0	164.1	126.6
170	354.8	264.4	270.1	204.5	207.9	160.0	162.0	126.6
180	359.1	264.4	273.2	204.6	210.2	160.0	163.7	126.6
190	357.7	264.4	272.1	204.6	209.4	160.0	163.1	126.6
200	362.8	264.4	275.8	204.6	212.0	160.0	165.0	126.6

	$(n, p_1) = (15, 0.52)$		$(n, p_1) = (15, 0.53)$		$(n, p_1) = (15, 0.54)$		$(n, p_1) = (15, 0.55)$	
m	WSR EWMA	C-WSR EWMA	WSR EWMA	C-WSR EWMA	WSR EWMA	C-WSR EWMA	WSR EWMA	C-WSR EWMA
50	164.5	164.6	112.3	204.2	79.0	79.0	57.3	57.3
60	145.5	164.6	102.9	204.4	74.3	79.0	54.8	57.3
70	174.2	164.8	117.8	204.4	82.2	79.1	59.2	57.4
80	195.2	165.3	127.6	204.5	87.0	79.3	61.6	57.5
90	156.9	164.7	107.9	204.5	76.4	79.1	55.7	57.3
100	164.8	164.7	112.5	204.5	79.1	79.1	57.3	57.3
110	165.5	164.7	112.5	204.5	78.9	79.1	57.1	57.3
120	195.5	164.8	127.6	204.5	86.9	79.1	61.5	57.3
130	174.7	164.5	117.3	204.5	81.6	79.0	58.6	57.3
140	185.3	164.8	121.4	204.5	83.1	79.1	59.2	57.3
150	157.2	164.8	109.1	204.5	77.6	79.1	56.7	57.3
160	178.3	164.8	118.6	204.5	82.0	79.1	58.8	57.3
170	140.3	164.8	99.5	204.5	72.0	79.1	53.4	57.3
180	149.1	164.8	105.1	204.6	75.6	79.1	55.6	57.3
190	143.3	164.8	101.2	204.6	73.1	79.1	54.0	57.3
200	174.3	164.8	117.8	204.6	82.2	79.1	59.2	57.3

	$(n, p_1) = (20, 0.52)$		$(n, p_1) = (20, 0.53)$		$(n, p_1) = (20, 0.54)$		$(n, p_1) = (20, 0.55)$	
m	WSR EWMA	C-WSR EWMA	WSR EWMA	C-WSR EWMA	WSR EWMA	C-WSR EWMA	WSR EWMA	C-WSR EWMA
50	137.9	144.7	91.3	94.7	62.7	64.5	44.7	45.6
60	148.6	144.4	96.6	94.5	65.5	64.3	46.2	45.6
70	146.0	144.4	95.4	94.5	64.8	64.3	45.8	45.6
80	138.2	144.5	91.5	94.5	62.8	64.3	44.8	45.6
90	141.1	144.5	93.0	94.5	63.6	64.4	45.2	45.6
100	144.7	144.0	94.6	94.2	64.4	64.2	45.6	45.4
110	146.0	144.4	95.4	94.5	64.8	64.3	45.9	45.5
120	149.1	144.5	96.7	94.5	65.4	64.3	46.1	45.6
130	146.2	144.4	95.3	94.5	64.7	64.3	45.7	45.5
140	155.9	144.4	100.1	94.5	67.2	64.3	47.0	45.5
150	145.6	144.5	95.1	94.5	64.6	64.3	45.7	45.6
160	155.3	144.5	99.7	94.5	66.9	64.3	46.9	45.6
170	136.3	144.5	90.4	94.5	62.2	64.3	44.4	45.6
180	154.5	144.5	99.2	94.5	66.6	64.3	46.7	45.6
190	155.7	144.4	99.8	94.5	67.0	64.3	46.9	45.5
200	155.2	144.5	99.4	94.5	66.7	64.3	46.8	45.6

Table A12: ARL values for the WSR EWMA chart for large shifts

	$(n=5)$				$(n=8)$				$(n=11)$				$(n=12)$			
m	$p_1=0.55$	$p_1=0.6$	$p_1=0.65$	$p_1=0.7$	$p_1=0.55$	$p_1=0.6$	$p_1=0.65$	$p_1=0.7$	$p_1=0.55$	$p_1=0.6$	$p_1=0.65$	$p_1=0.7$	$p_1=0.55$	$p_1=0.6$	$p_1=0.65$	$p_1=0.7$
50	128.1	46.9	22.3	13.1	75.7	28.5	14.2	8.8	76.0	23.2	11.2	7.0	72.6	21.6	10.4	6.6
60	126.4	46.4	22.2	13.0	103.7	31.7	14.8	8.9	79.1	23.6	11.3	7.0	67.7	21.1	10.3	6.5
70	125.9	46.3	22.1	13.0	90.4	30.3	14.5	8.8	70.9	22.7	11.1	6.9	64.2	20.9	10.3	6
80	128.8	47.0	22.4	13.1	90.9	30.4	14.5	8.9	65.4	22.0	10.9	6.9	66.1	21.0	10.3	6.5
90	125.9	46.3	22.1	13.0	81.8	29.2	14.3	8.8	71.3	22.8	11.1	7.0	65.3	20.9	10.3	6.5
100	127.1	46.6	22.3	13.1	112.9	32.9	15.0	9.0	73.5	23.0	11.1	7.0	66.5	21.0	10.3	6.5
110	128.0	46.8	22.3	13.1	125.1	33.3	15.0	9.0	78.0	23.4	11.2	7.0	63.7	20.8	10.3	6.5
120	127.4	46.6	22.2	13.1	84.7	29.7	14.5	8.9	68.9	22.5	11.0	6.9	64.5	20.8	10.3	6.5
130	126.2	46.4	22.2	13.0	91.5	30.5	14.6	8.9	69.5	22.6	11.1	7.0	64.9	20.9	10.3	6.5
140	127.1	46.6	22.2	13.1	91.3	30.5	14.6	8.9	79.6	23.6	11.2	7.0	75.9	21.9	10.5	6.6
150	128.1	46.9	22.3	13.1	89.5	30.5	14.6	8.9	76.1	23.3	11.2	7.0	76.1	21.9	10.5	6.6
160	127.7	46.7	22.3	13.1	90.2	30.3	14.5	8.9	76.1	23.3	11.2	7.0	73.1	21.6	10.4	6.6
170	125.2	46.1	22.1	13.0	104.4	32.4	15.0	9.0	77.7	23.5	11.2	7.0	71.0	21.4	10.4	6.5
180	126.2	46.4	22.2	13.0	79.7	29.0	14.3	8.8	77.6	23.5	11.2	7.0	73.2	21.7	10.4	6.6
190	127.3	46.6	22.2	13.1	83.2	29.5	14.4	8.8	75.7	23.3	11.2	7.0	74.0	21.7	10.4	6.6
200	127.2	46.6	22.2	13.1	99.2	31.2	14.7	8.9	74.3	23.1	11.1	7.0	71.1	21.6	10.4	6.6

	$(n=15)$				$(n=16)$				$(n=19)$				$(n=20)$			
m	$p_1=0.55$	$p_1=0.6$	$p_1=0.65$	$p_1=0.7$	$p_1=0.55$	$p_1=0.6$	$p_1=0.65$	$p_1=0.7$	$p_1=0.55$	$p_1=0.6$	$p_1=0.65$	$p_1=0.7$	$p_1=0.55$	$p_1=0.6$	$p_1=0.65$	$p_1=0.7$
50	57.3	17.4	8.7	5.6	56.3	16.6	8.3	5.4	46.0	14.0	7.2	4.8	44.7	13.5	7.0	4.6
60	54.8	17.2	8.6	5.6	54.6	16.4	8.2	5.4	47.4	14.1	7.2	4.8	46.2	13.6	7.0	4.6
70	59.2	17.6	8.7	5.6	53.9	16.4	8.2	5.3	46.5	14.0	7.2	4.8	45.8	13.6	7.0	4.6
80	61.6	17.7	8.7	5.6	56.8	16.6	8.3	5.4	48.9	14.2	7.2	4.8	44.8	13.5	6.9	4.6
90	55.7	17.2	8.6	5.6	54.5	16.4	8.2	5.4	45.6	14.0	7.2	4.8	45.2	13.5	7.0	4.6
100	57.3	17.4	8.7	5.6	53.7	16.3	8.2	5.3	46.4	14.1	7.2	4.8	45.6	13.5	7.0	4.6
110	57.1	17.3	8.6	5.6	53.2	16.3	8.2	5.3	47.7	14.1	7.2	4.8	45.9	13.6	7.0	4.6
120	61.5	17.7	8.7	5.6	56.6	16.6	8.3	5.4	45.8	14.0	7.2	4.8	46.1	13.6	7.0	4.6
130	58.6	17.5	8.7	5.6	55.5	16.5	8.3	5.4	48.1	14.2	7.2	4.8	45.7	13.5	7.0	4.6
140	59.2	17.4	8.7	5.6	55.5	16.5	8.3	5.4	47.8	14.2	7.2	4.8	47.0	13.6	7.0	4.6
150	56.7	17.4	8.7	5.6	56.5	16.6	8.3	5.4	46.4	14.0	7.2	4.8	45.7	13.5	7.0	4.6
160	58.8	17.4	8.7	5.6	54.9	16.5	8.2	5.4	46.6	14.1	7.2	4.8	46.9	13.6	7.0	4.6
170	53.4	17.0	8.6	5.6	55.2	16.5	8.2	5.4	45.7	14.0	7.2	4.8	44.4	13.4	6.9	4.6
180	55.6	17.3	8.7	5.6	54.5	16.4	8.2	5.3	46.5	14.0	7.2	4.8	46.7	13.6	7.0	4.6
190	54.0	17.1	8.6	5.6	53.5	16.3	8.2	5.3	47.3	14.1	7.2	4.8	46.9	13.6	7.0	4.6
200	59.2	17.6	8.7	5.6	55.0	16.5	8.2	5.4	48.8	14.2	7.2	4.8	46.8	13.6	7.0	4.6

Table A13: ARL values of the C-WSR EWMA chart for $h = 0.2$, $n \in \{5, 8, 9\}$ for the kernels listed in Table 3.7

(In-control ARL values for the WSR EWMA and C-WSR EWMA charts for desired $ARL_0 = 370.4$)

	$(n, \lambda, K_1) = (5, 0.2, 2.686)$					$(n, \lambda, K_1) = (8, 0.2, 2.713)$					$(n, \lambda, K_1) = (9, 0.2, 2.719)$				
m	Parabolic	Biweight	Cosine	Triweight	Normal	Parabolic	Biweight	Cosine	Triweight	Normal	Parabolic	Biweight	Cosine	Triweight	Normal
50	369.8	370.1	369.9	370.3	369.9	387.4	387.6	387.5	387.7	367.8	369.1	369.1	369.1	369.1	370.5
60	371.4	371.8	371.5	371.9	370.1	370.6	370.6	370.6	370.6	369.8	351.1	351.1	351.1	351.1	372.0
70	370.0	370.1	370.0	370.1	370.2	367.7	367.6	367.7	367.6	370.5	369.2	369.2	369.2	369.2	370.6
80	368.5	368.1	368.4	367.8	370.3	369.1	369.1	369.1	369.1	370.3	370.7	370.7	370.7	370.7	370.3
90	369.3	369.4	369.4	369.4	370.4	370.1	370.0	370.1	369.9	370.4	369.9	369.8	369.9	369.8	370.7
100	370.5	370.3	370.4	370.2	370.4	367.9	367.9	367.9	367.9	370.4	370.5	370.5	370.5	370.5	370.4
110	369.4	369.8	369.6	369.9	370.4	370.5	370.5	370.5	370.5	370.5	370.0	370.0	370.0	369.9	370.4
120	370.2	370.2	370.2	370.2	370.4	369.8	369.9	369.8	369.9	370.5	371.8	371.8	371.8	371.9	370.5
130	370.4	370.3	370.3	370.2	370.5	369.4	369.4	369.4	369.3	370.4	370.3	370.4	370.4	370.4	370.5
140	370.2	370.2	370.2	370.2	370.5	370.4	370.5	370.4	370.5	370.5	370.6	370.6	370.6	370.6	370.5
150	370.2	370.3	370.2	370.3	370.5	370.4	370.4	370.4	370.4	370.6	370.8	370.8	370.8	370.8	370.5
160	370.6	370.4	370.6	370.4	370.5	370.3	370.3	370.3	370.3	370.6	370.3	370.3	370.3	370.3	370.5
170	370.3	370.3	370.3	370.3	370.5	370.4	370.3	370.4	370.3	370.6	370.4	370.4	370.4	370.4	370.5
180	370.4	370.4	370.4	370.4	370.5	370.5	370.4	370.4	370.4	370.6	370.5	370.6	370.5	370.6	370.5
190	370.3	370.4	370.4	370.4	370.5	370.5	370.5	370.5	370.5	370.6	370.4	370.4	370.4	370.4	370.5
200	370.4	370.4	370.4	370.4	370.5	370.5	370.5	370.5	370.5	370.6	370.4	370.4	370.4	370.4	370.5

(In-control ARL values for the WSR EWMA and C-WSR EWMA charts for desired $ARL_0 = 500$)

	$(n, \lambda, K_1) = (5, 0.2, 2.778)$					$(n, \lambda, K_1) = (8, 0.2, 2.812)$					$(n, \lambda, K_1) = (9, 0.2, 2.827)$				
m	Parabolic	Biweight	Cosine	Triweight	Normal	Parabolic	Biweight	Cosine	Triweight	Normal	Parabolic	Biweight	Cosine	Triweight	Normal
50	495.7	495.8	495.7	495.9	498.4	488.5	488.4	488.5	488.4	500.7	496.8	496.7	496.8	496.7	499.6
60	494.7	494.8	494.8	494.8	499.4	495.4	495.5	495.4	495.5	499.7	507.9	508.0	507.9	508.0	499.0
70	496.3	496.3	496.3	496.4	499.6	494.5	494.4	494.4	494.4	499.0	496.7	496.7	496.7	496.7	500.0
80	498.7	498.5	498.7	498.3	499.8	498.9	499.0	498.9	499.1	497.9	501.9	501.9	501.9	501.8	498.6
90	498.8	499.0	498.9	499.2	499.8	499.4	499.2	499.3	499.2	499.7	498.7	498.7	498.7	498.6	500.0
100	499.6	499.2	499.5	499.0	499.9	500.5	500.5	500.5	500.6	500.2	499.5	499.6	499.5	499.6	500.0
110	496.6	498.2	497.1	498.9	499.9	498.4	498.4	498.4	498.3	499.9	499.7	499.7	499.7	499.7	500.2
120	499.9	499.7	499.8	499.6	499.9	499.5	499.7	499.6	499.7	499.9	499.0	499.0	499.0	499.0	500.5
130	499.3	499.4	499.3	499.5	500.0	499.8	499.8	499.8	499.8	500.0	499.4	499.4	499.4	499.4	500.2
140	500.1	499.9	500.0	499.8	500.0	499.2	499.1	499.1	499.1	500.0	500.0	500.0	500.0	500.0	500.3
150	499.7	499.7	499.7	499.7	500.0	499.4	499.4	499.4	499.3	500.0	500.3	500.3	500.3	500.3	500.2
160	499.7	499.7	499.7	499.8	500.0	499.4	498.9	499.3	498.6	500.0	499.0	498.9	498.9	498.8	500.3
170	500.1	499.9	500.0	499.9	500.0	499.8	499.7	499.7	499.7	500.0	500.0	500.0	500.0	500.0	500.3
180	499.8	499.8	499.8	499.8	500.0	499.8	499.8	499.8	499.8	500.0	500.0	500.0	500.0	500.0	500.3
190	500.1	499.9	500.1	499.9	500.0	499.8	499.8	499.8	499.8	500.1	499.4	499.0	499.3	498.9	500.3
200	499.9	499.9	499.9	499.9	500.0	499.9	499.9	499.9	500.0	500.1	500.1	500.1	500.1	500.0	500.3

Bibliography

R.W Amin and A.J Searcy. A Nonparametric Exponentially Weighted Moving Average Control Scheme. *Communications in Statistics-Simulation and Computation*, 20(4):1049–1072, 1991.

R.W Amin, M.R Reynolds Jr, and S Bakir. Nonparametric Quality Control Charts Based on the Sign Statistic. *Communications in Statistics-Theory and Methods*, 24(6):1597–1623, 1995.

S. Bakir. A Distribution-free Shewhart Quality Control Chart based on Signed-Ranks. *Quality Engineering*, 16(4):613–623, 2004.

B.M. Bennett. On the Non-Null Distribution of Wilcoxon's Signed Rank Test. *Metrika*, 19 (1):36–38, 1972.

S. Bersimis, S. Psarakis, and J. Panaretos. Multivariate Statistical Process Control Charts: An Overview. *Quality and Reliability engineering international*, 23(5):517–543, 2007.

D. Brook and D.A. Evans. An Approach to the Probability Distribution of CUSUM Run Length. *Biometrika*, 59(3):539–549, 1972.

P. Castagliola. A New s^2-EWMA ControlChart for Monitoring the Process Variance. *Quality and Reliability Engineering International*, 21(8):781–794, 2005.

P. Castagliola, G. Celano, and S. Fichera. *Handbook of Engineering Statistics*, chapter Monitoring Process Variability using EWMA, pages 291–325. Series in Reliability Engineering. Springer, 2006. ISBN:1-85233-806-7.

P. Castagliola, G. Celano, and S. Psarakis. Monitoring the Coefficient of Variation Using EWMA Charts. *Journal of Quality Technology*, 43(3):249–265, 2011.

P. Castagliola, K.P. Tran, G. Celano, A.C. Rakitzis, and P.E. Maravelakis. An EWMA-Type Sign Chart With Exact Run Length Properties. *Journal of Quality Technology*, 51 (1):51–63, 2019.

P. Castagliola, K.P. Tran, G. Celano, and P.E Maravelakis. The Shewhart Sign Chart with Ties: Performance and Alternatives. In *Distribution-Free Methods for Statistical Process Monitoring and Control*, pages 107–136. Springer, 2020.

G. Celano, P. Castagliola, S. Chakraborti, and G. Nenes. On the Implementation of the Shewhart Sign Control Chart for Low-volume Production. *International Journal of Production Research*, 54(19):5886–5900, 2016.

S. Chakraborti and M.A. Graham. Nonparametric (Distribution-Free) Control Charts: An Updated Overview and Some Results. *Quality Engineering*, 31(4):523–544, 2019.

S. Chakraborti, P. Van der Laan, and S.T. Bakir. Nonparametric Control Charts: an Overview and Some Results. *Journal of Quality Technology*, 33(3):304–315, 2001.

J.D. Gibson and J.L. Melsa. *Introduction to Nonparametric Detection with Applications*. Academic press, 1976.

M.A. Graham, S. Chakraborti, and S.W. Human. A Nonparametric EWMA Sign Chart for Location Based on Individual Measurements. *Quality Engineering*, 23(3):227–241, 2011a.

M.A. Graham, S. Chakraborti, and S.W. Human. A Nonparametric Exponentially Weighted Moving Average Signed-Rank Chart for Monitoring Location. *Computational Statistics & Data Analysis*, 55(8):2490–2503, 2011b.

P. Hackl and J. Ledolter. A Control Chart Based on Ranks. *Journal of Quality Technology*, 23(2):117–124, 1991.

P. Hackl and J. Ledolter. A New Nonparametric Quality Control Technique. *Communications in Statistics-Simulation and Computation*, 21(2):423–443, 1992.

N.L Johnson. Systems of Frequency Curves Generated by Methods of Translation. *Biometrika*, 36(1/2):149–176, 1949.

M.BC Khoo and EG Lim. An Improved R (Range) Control Chart for Monitoring the Process Variance. *Quality and Reliability Engineering International*, 21(1):43–50, 2005.

G. Latouche and V. Ramaswami. *Introduction to Matrix Analytic Methods in Stochastic Modeling*. ASA-SIAM, Philadelphia, 1999.

K.W Linna and W.H Woodall. Effect of Measurement Error on Shewhart Control Charts. *Journal of Quality technology*, 33(2):213–222, 2001.

S.L. Lu. An Extended Nonparametric Exponentially Weighted Moving Average Sign Control Chart. *Quality and Reliability Engineering International*, 31(1):3–13, 2015.

M.R. Maleki, A. Amiri, and P. Castagliola. Measurement Errors in Statistical Process Monitoring: A Literature Review. *Computers & Industrial Engineering*, 103:316–329, 2017.

R.L. McCornack. Extended Tables of the Wilcoxon Matched Pair Signed Rank Statistic. *Journal of the American Statistical Association*, 60(311):864–871, 1965.

D.C Montgomery. *Introduction to Statistical Quality Control*. John Wiley & Sons, 2020.

M.F. Neuts. *Matrix-Geometric Solutions in Stochastic Models: An Algorithmic Approach*. Dover Publications Inc, New York, 1981.

P. Nomikos and J.F MacGregor. Multivariate spc charts for Monitoring Batch Processes. *Technometrics*, 37(1):41–59, 1995.

E.S. Page. Continuous Inspection Schemes. *Biometrika*, 41(1/2):100–115, 1954.

E. Parzen. On Estimation of a Probability Density Function and Mode. *The Annals of Mathematical Statistics*, 33(3):1065–1076, 1962.

V.Y Pawar, D.T. Shirke, and S.K Khilare. A nonparametric Control Chart for Process Variability Based on Quantiles. *International Journal of Statistics and Economics*, 19(3): 55–64, 2018.

T. Perdikis and S. Psarakis. A Survey on Multivariate Adaptive Control Charts: Recent Developments and Extensions. *Quality and Reliability Engineering International*, 35(5): 1342–1362, 2019.

T. Perdikis, S. Psarakis, P. Castagliola, and G. Celano. An Ewma-Type Chart Based on Signed Ranks With Exact Run Length Properties. *Journal of Statistical Computation and Simulation*, 91(4):732–751, 2021a.

T. Perdikis, S. Psarakis, P. Castagliola, and P.E Maravelakis. An Ewma Signed Ranks Control Chart With Reliable Run Length Performances. *Quality and Reliability Engineering International*, 37(3):1266–1284, 2021b.

T. Perdikis, S. Psarakis, P. Castagliola, A.C Rakitzis, and P.E Maravelakis. The Ewma Sign Chart Revisited: Performance and Alternatives without and with ties. *Journal of Applied Statistics*, 0(0):1–25, 2021c. doi: 10.1080/02664763.2021.1982879.

J. Putter. The Treatment of Ties in Some Sonparametric Tests. *The Annals of Mathematical Statistics*, 26(3):368–386, 1955.

M. Rahman, B.C Arnold, DV Gokhale, and .n Ullah. Data-based Selection of the Smoothing Parameter in Kernel Density Estimation Using Exact and Approximate mise. Technical report, Technical Report No, 1995.

A.C. Rakitzis, P. Castagliola, and P.E. Maravelakis. A New Memory-type Monitoring Technique for Count Data. *Computers & Industrial Engineering*, 85:235–247, 2015.

SW Roberts. Control Chart Tests Based on Geometric Moving Averages. *Technometrics*, 1: 239–250, 1959.

W.A Shewhart. Quality Control Charts. *The Bell System Technical Journal*, 5(4):593–603, 1926.

D.T Shirke and M.S Barale. A Nonparametric CUSUM Chart for Process Dispersion. *Quality and Reliability Engineering International*, 34(5):858–866, 2018.

B.W Silverman. *Density Estimation for Statistics and Data Analysis*, volume 26. CRC press, 1986.

I.S Triantafyllou and M. Ram. Distribution-Free CUSUM-Type Control Charts for Monitoring Industrial Processes: An Overview. 2021a.

I.S Triantafyllou and M. Ram. Nonparametric EWMA-Type Control Charts for Monitoring Industrial Processes: An Overview. 2021b.

M.P Wand and M.C Jones. *Kernel Smoothing*. CRC press, 1994.

F. Wilcoxon. Probability Tables for Individual Comparisons by Ranking Methods. *Biometrics*, 3(3):119–122, 1947.

W.H Woodall. Current Research on Profile Monitoring. *Production*, 17:420–425, 2007.

S. Wu, P. Castagliola, and G. Celano. A Distribution-free EWMA Control Chart for Monitoring Time-Between-Events-and-Amplitude Data. *Journal of Applied Statistics*, pages 1–21, 2020.

S.F. Yang and S.W. Cheng. A New Non-Parametric CUSUM Mean Chart. *Quality and Reliability Engineering International*, 27(7):867–875, 2011.

S.F. Yang, J.S. Lin, and S.W. Cheng. A New Nonparametric EWMA Sign Control Chart. *Expert Systems with Applications*, 38(5):6239–6243, 2011.

G. Zhang. Improved R and S Control Charts for Monitoring the Process Variance. *Journal of Applied Statistics*, 41(6):1260–1273, 2014.